

TENSION PILE STUDY
VOLUME IV
TESTING OF A 30-INCH DIAMETER
INSTRUMENTED PILE IN
SOFT CLAY

Report Number 82-200-4

*** * ***

Report
to
CONOCO NORWAY, INC.
through
A.S Veritec
Oslo, Norway

*** * ***

by
THE EARTH TECHNOLOGY CORPORATION
Houston, Texas

June, 1985

7020 Portwest Drive, Suite 150, Houston, Texas 77024
Telephone: (713) 869-0000 • Telex: 499-3065

November 7, 1985

Conoco, Inc.
600 N. Dairy Ashford Rd.
Dubai Bldg, Rm 2080

Attention: Mr. Jack Chan


Re: CNRD 13-3 Tension Pile Study; Volume IV - Testing of a 30-Inch
Diameter Instrumented Pile in Soft Clay

Gentlemen:

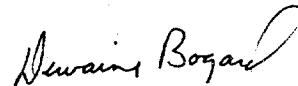
We are pleased to submit herewith 20 copies of our Final report entitled "Tension Pile Study; Volume IV - Testing of a 30-Inch Diameter Instrumented Pile in Soft Clay". Please forward the necessary copies to Conoco's staff, A.S. Veritec and your project participants, as you see appropriate.

We have enjoyed working on this project and look forward to be of further service to Conoco.

Very truly yours,



Jean M. E. Audibert, P.E.
General Manager
Gulf States Division



Dewaine Bogard
Senior Engineer

JMEA/plm

cc: Rune Dahlberg, A.S. Veritec
Hudson Matlock

PREFACE

This report contains the results of experiments performed on a 30-inch-diameter (76.2 cm) instrumented pipe pile at a decommissioned production platform in the West Delta Area, Gulf of Mexico. This work is a part of a larger research project sponsored by Conoco through Conoco Norway Research and Development for the purpose of developing a better understanding of pile-soil interaction associated with foundation piles for tension leg platforms. The project is identified as CNRD 13-3. Also participating in support of the project were Chevron Oil Company, the American Bureau of Shipping, and the Minerals Management Service of the United States Department of the Interior. Long-term retesting of the pile was subsequently done in 1985 under CNRD 13-4 and will be reported separately.

The work was performed by the Earth Technology Corporation, acting as a designated subcontractor to A.S Veritec (formerly Det Norske Veritas). The Earth Technology project team was composed of the following staff members:

- * Hudson Matlock, Vice President for Research and Development, provided overall technical direction for the project.
- * Dewaine Bogard was responsible for project planning and administration, instrumentation concepts and design, supervision of data collection and reduction, and the production of this report.
- * Tom Hamilton provided assistance in planning and administration during the early stages of the project.
- * Ronald Boggess and Neil Dwyer designed and assembled the data acquisition system and participated in transducer design and fabrication.
- * Leon Holloway planned and supervised the fabrication and installation of the test pile.

- * Chairat Suddhiprakarn performed most of the data reduction and the preparation of figures for this report.
- * Jean Audibert, Manager of the Houston office, provided assistance in administrative matters and in the production of this report.

Other staff members who contributed to the success of the project included Lino Cheang, W.C.V. Ping, and Fleet Brown.

A number of subcontractors made significant contributions to the work, including Mr. Wayne Kerr of Wayne Kerr and Associates, who assisted in design and production of the instrument cables; Mr. Dick Loudermilk of Brantner and Associates, who fabricated the special connections of cables to instruments; Mr. Agustin Chin, of Delta Marine Structures, who designed the load frame; Mr. Bryan Fisher of Small Systems Solutions, who developed the data acquisition software; and Mr. Norman Peterson of Electronic Measurements, who strain-gaged the total pressure transducers and assisted with the strain modules.

Portions of the work were handled directly by Conoco through parallel contracts. Assembly of the pile and installation of instruments were done by Vemar, Inc. of Houston, who also subcontracted the field installation operation to Laredo Marine Services. Comet Construction Company of Venice, Louisiana, provided field and operational support.

Various representatives from Norway observed and assisted in the field tests. These included Tore Kvalstad, Kjell Hauge, and Rune Dahlberg of Veritec; Lars Grande of the Norwegian Institute of Technology, Trondheim; and Kjell Karlsrud of the Norwegian Geotechnical Institute. Jack H. C. Chan, assisted by Jeff Mueller, served as Project Manager for Conoco, under the general direction of N. D. Birrell. George Santos and Tom Gautreaux of the New Orleans Division of Conoco were responsible for field construction and support.

The first draft of this report was reviewed by Jean Audibert and Donald Anderson. The final review was performed by Hudson Matlock.

TABLE OF CONTENTS

	<u>Page</u>
PREFACE	
EXECUTIVE SUMMARY	
1. INTRODUCTION	
1.1 Background.....	1
1.2 Contents of This Report.....	1
1.3 Report Organization.....	2
2. SITE DESCRIPTION	
2.1 General.....	4
3. TEST EQUIPMENT AND INSTRUMENTATION	
3.1 Introduction.....	5
3.2 Pressure Measurements.....	5
3.3 Strain Measurements.....	7
3.4 Data Acquisition System.....	9
3.5 Displacement Measurements.....	10
3.6 Effects of Wave Loading on Load Measurements.....	11
4. TEST METHODS	
4.1 Introduction.....	13
4.2 Planned Procedures for Obtaining Instrument Zero Readings.....	13
4.3 Strain Module and Extensometer Zero Voltages.....	15
4.4 Total and Pore Pressure Transducer Zero Voltages.....	17
4.5 Summary and Evaluation of Instrument Zero Readings.....	19
4.6 The Loading and Control System.....	20
4.7 Data Reduction Procedures.....	22
4.8 Chronological Record of the Experiment.....	22

5. RESULTS OF THE EXPERIMENTS

5.1	Introduction.....	26
5.2	Soil Pressures During Installation and Consolidation.....	26
5.3	Results of the Load Test Performed Immediately After Driving....	31
5.4	Load Tests After Partial Consolidation.....	33
5.5	Initial Load Tests to Failure in Tension and Compression.....	33
5.6	Effects of Pile Loading on At-Rest Soil Pressures.....	35
5.7	Results of the Short-Term Creep Test.....	37
5.8	Results of the Repeated-Load Cyclic Tension Tests.....	39
5.9	Soil Pressure Variations During the One-Way Cyclic Tests.....	41
5.10	Results of the Two-Way Cyclic Tests.....	42
5.11	Soil Pressure Variations During the Two-Way Cyclic Tests.....	44
5.12	Effects of Repeated and Reversed Loading on Axial Pile Capacity.	45
5.13	Effects of Repeated and Reversed Loading on Shear Transfer.....	47

6. SUMMARY AND CONCLUSIONS

6.1	Objectives of the Experiment.....	49
6.2	Summary of Instrument Performance.....	50
6.3	Summary of Pressure Measurements.....	51
6.4	Summary of Static and Cyclic Load Test Results.....	54
6.5	Conclusions.....	57

REFERENCES

APPENDICES

- Appendix 1 - Illustrations for Chapter 1
- Appendix 2 - Illustrations for Chapter 2
- Appendix 3 - Illustrations for Chapter 3
- Appendix 4 - Illustrations for Chapter 5
- Appendix 5 - Illustrations for Chapter 6
- Appendix 6 - Illustrations for Chapter 7
- Appendix 7 - Dynamic Pile Measurements

EXECUTIVE SUMMARY

Conoco, Inc., through Conoco Norway Research and Development (CNRD), has sponsored a comprehensive program of research aimed to improve the understanding of the pile-soil interaction along driven piles subjected to static and cyclic tension loading. The final goal of the research is the development of guidelines and procedures for the design and analysis of foundation piles for Tension Leg Platforms.

The research was performed by A.S Veritec (formerly Det Norske Veritas) and by The Earth Technology Corporation, acting as a designated contractor to Conoco Norway through Veritec.

The research has been performed in four interrelated phases.

The first, under CNRD Research Project 13-1, was the planning study for the remainder of the work.

The second, under CNRD 13-2, consisted of a site characterization study and in situ 3-inch-diameter (7.62 cm) pile segment model tests at the West Delta 58A platform site by The Earth Technology Corporation, and a program of laboratory experiments using 1-inch-diameter (2.54 cm) pile segment models by A.S Veritec.

The third, under CNRD 13-2 and 13-3, consisted of additional in situ experiments using 3-inch-diameter (7.62 cm) and 1.72-inch-diameter (4.37 cm) pile segment models and load tests on a 30-inch-diameter (76.2 cm) instrumented test pile at the West Delta 58A platform site, further development of analytical models of pile-soil interaction, and the development of guidelines for the design of tension piles in soft clays by The Earth Technology Corporation.

The fourth, under CNRD 13-4, consisted of a number of static and cyclic load tests performed by The Earth Technology Corporation on the 30-inch-diameter (76.2) pile sixteen months after the pile was driven.

This report contains the results of the experiments on the 30-inch-diameter (76.2 cm) instrumented pile performed under CNRD 13-3. Additional reports will be issued which document the remainder of the work performed under the 13-3 and 13-4 research projects.

The primary goal of the portion of the work reported herein was the determination of the tensile capacity of a thin-wall pile driven open-ended into soft, normally-consolidated clays. The pile was therefore instrumented to measure the load distribution with depth along the pile, with displacements also being measured at three elevations, in order to develop shear transfer-displacement relationships for the soil along the pile.

In order to obtain the most information possible from the experiment, the pile instrumentation included pressure transducers to measure the total radial pressure exerted on the pile by the soil, with companion measurements of the pore water pressure at the same depths.

The instruments performed extremely well throughout the course of the research program. With the exception of two of the strain modules, which were damaged prior to pile installation, the success rate of the instruments was 100 percent. All the instruments survived the impact stresses during pile driving with no zero-shift, and showed no evidence of moisture leakage, long-term drift, or short-term instability during a sixteen month period after installation.

The redundant drop-in electro-mechanical extensometers were used successfully to replace one level of strain modules, and also provided an independent check of the loads and the shear transfer calculated using the strain modules.

The load tests which were performed during the work reported herein included

- 1) a slow loading to failure in tension and compression shortly after driving,
- 2) a slow loading to failure in tension and compression after four months of consolidation,

- 3) a series of one-way cyclic tension tests, with the cyclic component of load being increased until progressive pullout of the pile was observed, and
- 4) a static loading to failure in tension, followed by fully-reversed cyclic loading to failure, resulting in the maximum degree of cyclic degradation in the shearing resistance of the soil.

The effect of consolidation and set-up on the capacity of the pile was an approximate doubling of the capacity, from a value of 443 kips (1971 kN) immediately after driving to a value of 963 kips (4285 kN) after four months of consolidation.

Due to the elastic stretch in the pile, the peak shear transfer was not reached simultaneously at all depths along the pile; the summation of maximum shear transfer yields an ultimate pile capacity of 1070 kips (4761 kN), approximately 10 percent larger than the maximum measured pile head load.

The one-way cyclic tension tests, as expected, reduced the pile capacity, with progressive pullout of the pile occurring at load levels of 720 (3204 kN) to 740 kips (3293 kN). During these tests, the progressive migration of load down the pile as the cyclic component of load was increased was clearly evident.

As expected, the cyclic degradation in shearing resistance was greater during the two-way cyclic tests than during those in which the plastic slip in the soil was not reversed along the full length of the pile.

The average alpha-value (ratio of shear transfer to shear strength) based on the peak values of shear transfer measured during the load test performed four months after installation was 0.88. The values of peak shear transfer measured during the load test immediately after driving yield an average alpha-value of 0.36.

Since the peak values of shear transfer were not reached simultaneously along the length of the pile, due to elastic axial deformation, an average alpha-value of 0.79 would be calculated, based solely on the peak pile-head load.

The average degree of consolidation in the soil along the pile after four months of consolidation was 83 percent. If it is assumed that the increase in the peak shear transfer after driving is directly related to the degree of consolidation, then the projected alpha value at the end of consolidation would be 0.98, near the value of 1.0 which is currently used for axial pile design in clay soils in the Gulf of Mexico.

The results of the experiments also indicate that the present practice of calculating ultimate pile capacity, while ignoring both consolidation time and the reductions in mobilized pile capacity due to progressive yielding of the soil along the pile, may lead to somewhat unconservative foundation pile designs. For pile foundations subjected to cyclic loads, the design methods must also include consideration of progressive cyclic degradation under repeated loadings.

The effects of time on pile capacity are obvious; however, if sufficient time is not allowed for the development of axial capacity between the times of pile driving and of loading the foundation, the actual capacity may be significantly less than that required for the design loads, especially in the case of large-diameter piles. For such piles, the design methods should consider the long set-up time in estimating the axial capacity of the piles at the time the service loads are to be experienced.

An additional consideration for design is the load-deformation behavior of the foundation. The actual peak load measured during the static load test was only 90 percent of the ultimate load which would be calculated based solely on the peak values of shear transfer. For this particular site, the reduction of 10 percent is not a large decrease; however, the effects may be greater in more sensitive soils, and those soils which exhibit more pronounced peak-residual stress-strain behavior.

For piles subjected to cyclic loads, a design based on a constant (and probably too-large) alpha value will have even more significant consequences. During the cyclic tension tests reported herein, the pullout capacity of the pile was reduced to 720 kips (3204 kN), only 75 percent of the measured static pile capacity, and

59 percent of that calculated using an alpha value of 1.0, which is the standard practice for Gulf of Mexico clays.

The successful completion of the experiments on the near-full-scale instrumented pile has resulted in the collection of a unique set of pile-soil interaction information. The collection of data from the instruments along the pile for an extended period of time, with load tests performed at three stages in the consolidation process (only two of which are reported in this volume), has added greatly to the knowledge of the behavior of axially loaded piles, whether the nature of the loading be tensile or compressive.

The data provide a sound basis for the development of design methods for axial pile design in normally consolidated clays, and will furnish much needed information to be used to evaluate or develop existing and future total stress and effective stress approaches to the methods of design.

The results of these experiments, coupled with the other data from the program and the analytical procedures now under development, will serve to broaden the range of application of the results of the experiments.

1. INTRODUCTION

1.1 Background

This report presents the results of experiments performed on a 30-inch-diameter pipe (76.2 cm) pile installed at decommissioned CAGC platform 58A of the West Delta area, Gulf of Mexico. The soil stratigraphy at the platform location was found to be comparable to that existing at the proposed site of a Tension Leg Platform in the Green Canyon area, also in the Gulf of Mexico (Ref 2).

The experiments were a part of a comprehensive program of investigation of the behavior of axially loaded piles driven into normally-consolidated clays and subjected to static and cyclic loading, with primary emphasis on foundations for tension-leg platforms.

The overall project organization is shown in Plate 1.1. The primary sponsorship was by Conoco, Inc., through Conoco Norway Research and Development Company, with participation by Chevron Oil Company, the American Bureau of Shipping, and the Minerals Management Service of the United States Department of the Interior.

1.2 Contents of this Report

This report contains the experimental results obtained during CNRD Research Project 13-3 with the 30-inch-diameter (76.2 cm) instrumented pipe pile. Long-term testing was subsequently performed under CNRD Project 13-4 and will be reported separately.

The pile was 359 ft (109.5 m) in length, with a wall thickness of 0.75 inch (19.1 mm). The pile was driven open-ended to a final penetration of 234 ft (71.3 m) below the mudline. The absence of end-plugging was verified by measurements made of the elevation of the soil plug inside the pile after each pile driving operation, which showed a final soil plug elevation which was slightly above the mudline, as would be expected due to the internal volume of the pile occupied by the instruments and the access tubes.

The pile was made up of three sections, one slightly less than 180 ft (54.9 m) in length and two which were slightly less than 90 ft (27.4 m) in length. One 90-ft (27.4-m) section contained a specially-designed loading head which allowed the pile to be loaded in both tension and compression and was instrumented to measure the pile head load. The 180-ft (54.9 m) section was instrumented to measure the axial strain in the pile at six depths below the mudline and radial total and pore pressures at the pile wall at depths approximately midway between the locations of the strain measurements. The displacement of the pile was measured at three locations: the pile head and two depths below the mudline.

The load test program in CNRD 13-3 was designed to (1) obtain the static capacity immediately after driving, (2) obtain the static capacity after approximately 50 to 60 percent of the excess pore pressures generated by the pile installation had dissipated, (3) investigate the effects of repeated tensile loading on the frictional resistance, and (4) investigate the effects of fully-reversed large-displacement cyclic loading on the frictional resistance.

Continuous measurements of lateral soil pressures were made to observe the process of consolidation and to obtain the soil parameters necessary to evaluate effective stress analyses of axial pile capacity.

The results of these experiments are intended to be combined with the results of laboratory studies performed by Veritec using 1-inch-diameter (25.4 mm) pile models (Ref 6) and tests performed by The Earth Technology Corporation using in situ 3-inch-diameter (76.2 mm) pile segment models (Ref 8). The purpose is to develop procedures for the design and analysis of axially loaded piles in soft clays with particular emphasis on performance of piles for tension leg platforms.

1.3 Report Organization

A brief description of the site is given in Chapter 2 of this report. For a more complete characterization of the soils, see Ref 2.

Chapter 3 contains a summary of the instruments and their placement along the pile. Detailed design drawings and specifications for the test pile and the instruments are given in Ref 5.

Chapter 4 contains a brief description of the methods used to perform the tests and to obtain and evaluate the data.

The results of the experiments are presented in Chapter 5.

Chapter 6 contains a summary of the results, and concluding remarks. Appendices 1 through 6 contain the Plates corresponding to Chapters 1 through 6, respectively.

Appendix 7 consists of a copy of a report submitted to The Earth Technology Corporation by Pile Dynamics, Inc. (Goble and Associates, Inc.), which contains the results of dynamic measurements made during pile driving along with the results of CAPWAP analyses of selected hammer blows.

This report contains only the data and results obtained from the 30-inch-diameter (76.2 cm) pile, intended to present and explain the observations. Interpretation and correlation of the results with soil properties and the results of the parallel experiments will be presented in a subsequent report.

2. SITE DESCRIPTION

2.1 General

A map showing the location of the offshore test site is given in Plate 2.1. The water depth at the site is approximately 49 ft (14.9 m). A homogeneous clay stratum, having no sand or silt layers in the zone of interest, extends from the seafloor to a depth of 253 ft (77.1 m).

The stratigraphy of interest (above the 234 ft (71.3 m) depth) can be described as a very soft clay at the seafloor, increasing in strength to a stiff olive gray clay at a depth of 234 ft (71.3 m). The stratigraphy is given in more detail on the boring logs, Plates 2.2, 2.3, and 2.4, which were taken from Ref 2.

The interpreted shear strength profile, given in Plate 2.4, is bilinear in nature. The plate shows a linear increase in the average undrained shear strength from 0.1 ksf (4.8 kPa) at the mudline to 0.75 ksf (35.9 kPa) at a depth of 160 ft (48.8 m), followed by a linear increase in strength to 1.80 ksf (86.2 kPa) at a depth of 250 ft (76.2 m).

The interpreted unit weight profile shown in Plate 2.5 was derived from the results of both field and laboratory test results (Ref 2).

The results of the Atterberg limit tests on samples taken from the site are given in Plate 2.6 and confirm that the clays have a high activity.

Based on the results of the laboratory and field tests, the clay deposit at the site has been divided into three strata (Ref 2), with the three strata being approximately bounded by the depths of 0 to 80 feet (0 to 24.4 m), 80 to 160 feet (24.4 to 48.8 m), and 160 to 253 feet (48.8 to 77.1 m) below the mudline.

3. TEST EQUIPMENT AND INSTRUMENTATION

3.1 Introduction

A brief description of the instruments which were installed in the pile will be given here. For a more detailed description of the instruments and their exact locations along the pile, see Ref 5.

The distribution of the instruments along the test pile is given schematically in Plate 3.1. A vertical spacing of 30 ft (9.1 m) was chosen for the strain measurements, in order to obtain adequate discrimination of the variation in shear transfer along the pile. In order to avoid the circumferential welds at the joints of the 10-ft (3.0 m) cans which made up the pile, the strain modules were placed 2 ft (0.6 m) above each joint, with the bottom pair of strain modules being located 22 ft (6.7 m) above the pile tip, at a final depth of 212 ft (64.6 m) below the mudline.

The nominal depth of each set of four pressure transducers was at the midpoint of the middle 10-ft (3.0 m) can in each 30-foot (9.1 m) module and therefore fell 2 feet (0.6 m) below the midpoint between adjacent strain module stations.

All instruments were duplicated on both sides of the pile to cancel effects of crookedness and bending of the pile. When the instrumented section arrived at the offshore site, two of the strain modules (one each at the 122 (37.2 m) and 152-ft (46.3 m) depths) were found to be inoperable. In each of the strain gage circuits, one arm of the full bridge was shorted. Since the resistance-to-ground remained essentially infinite, the failure must have been due to damage in fabrication or transport of the pile.

3.2 Pressure Measurements

The total radial pressure and the pore water pressure were measured at six depths along the embedded length of the pile. The nominal depths of pressure measurement

were 79, 109, 139, 169, 199, and 224 ft (24.1, 33.2, 42.4, 51.5, 60.7, and 68.3 m) below the mudline.

The pressure transducers were bolted into mating fixtures which were welded into holes cut in the pile wall, as shown in Plates 3.2 and 3.3. At each level of pressure instrumentation, two total and two pore pressure transducers were used, both for redundancy and to cancel any bent-pile effects (i.e., pressure variations around the circumference of the pile). The total and pore pressure transducers alternated in position on each side of the pile, one foot (0.3 m) above and below the nominal depths. The pressure measurements were later averaged, with the values being reported as those at the elevation midway within each pair.

After assembly of the pressure transducers, the units were pressure-tested in a 30-inch-diameter (76.2 cm), 10-ft (3.0 m) long chamber. The instruments and the attached cables were placed inside the chamber, with the free ends of the cables passed through packing glands welded to one end of the pressure chamber. The chamber was then filled with water and pressurized. The instruments were monitored during the pressure test for stability, drift, and for resistance to ground. No instability or leakage was observed during the pressure tests.

The transducers were calibrated using a Bourdon gage during the pressure tests. The pressure inside the chamber was increased from atmospheric to 100 psi (689 kPa) in steps of 20 psi (138 kPa), and then decreased in the same increments. The variation in transducer output was recorded using the digital data acquisition system and, in the case of the total pressure transducers, a precise strain-gage bridge-balance box. Calibration factors for the instruments were then calculated in units of ksf/volt.

The values of the calibration factors for the total and the pore pressure transducers varied from approximately 3200 to 3900 ksf (153280 to 186810 kPa) per volt. The repeatability in the voltage readings during the calibration, and during the experiments under hydrostatic pressure conditions, was better than 0.000010 volts, yielding an expected resolution in the measured pressures of approximately 0.03 ksf (1.4 kPa), which was sufficient to resolve the pressures within the degree of accuracy of the calibration, which was approximately 1 percent.

While they were in sea water, both types of pressure transducers showed only hydrostatic pressure differences corresponding to the 2-ft (0.6 m) difference in elevation. The pore pressure transducers also showed only the normal hydrostatic difference in pressure during steady-state consolidation. A slightly wider variation in the soil pressures was measured by some, but not all, of the pairs of total pressure transducers; however, the differences were not large, and probably reflect real differences in the radial effective pressure due to a slight degree of crookedness.

3.3 Strain Measurements

The axial strain in the pile was measured at the pile head and at six depths along the embedded length of the pile. Two independent methods were used to measure the axial strain. The first system consisted of prefabricated strain modules which utilized foil strain gages mounted on the inner of two concentric steel tubes, as shown in Plate 3.4. The second system consisted of electro-mechanical extensometers which used DC LVDTs to measure the changes in length of a 60-in. (1.52 m) gage length of the pile, as shown in Plate 3.5.

As reported in Refs 1 and 5, it had been planned to calibrate each of the 30-ft (9.1 m) long cans during fabrication. The strain modules and the extensometers were to be calibrated simultaneously under a series of known loads.

In order to perform the calibration to the planned precision, it was necessary for the pile and the calibration frame to remain at a constant temperature during the calibration process. One of the requirements for the fabrication contractor, as specified in Conoco, Inc. Bid Tender 4397-1, was, therefore, that sufficient vertical clearance must be provided in the fabrication shop so that the calibration frame and the pile could remain indoors, with the expectation that they would come to a reasonably constant and uniform temperature during the night or early morning hours.

The contractor selected did not have such a facility. Since it was not possible to perform the calibration indoors, it was therefore attempted to calibrate the cans outdoors, with the calibration loading being performed at night. Both the calibration frame and the pile were in the sunlight for several hours prior to the calibration. With variations in air flow and radiation cooling, the temperatures of the pile and the four steel bars used to apply the loads did not reach thermal equilibrium, even after waiting until 3 am to perform the calibration.

As a result, the calibration readings all showed considerable time-dependent drift. Linear corrections to the raw data were attempted, but the corrections did not satisfactorily remove the transient variations. The calibration data thus could not be used to determine the axial stiffness AE of the pile to the required accuracy.

The calibration factors used to convert strain to load were therefore based on ultrasonic measurements of wall thickness. Four ultrasonic measurements were made on each of six cross-sections in each 30-ft (9.1 m) can in the instrumented section (two cross-sections on each 10-ft (3.0 m) section), and showed very consistent wall thicknesses. It was thus decided to use the measured wall thicknesses of the pile material, the nominal cross sections of the added members at each station, and an assumed value of 30,000,000 pounds per square inch (206,800,000 kPa) for Young's modulus to calculate the values of axial stiffness AE for the conversion of axial strain to load.

The calculated cross-sectional areas included all the added appurtenances, such as the internal and external cover plates, the extensometer access tubes, the tell-tale access tubes, the extensometer gage sections, and the strain modules.

By performing a careful and precise calibration of the test pile during fabrication, it had been expected that static load measurements, performed manually with a precise bridge-balancing instrument, could be made to a precision of less than one kip (4.45 kN), with automatically-recorded data being made to a precision of approximately 10 kips (44.5 kN). In the absence of an adequate calibration, the expected precision in the load measurements is determined by the uncertainties in the cross-sectional area of the pile and in the modulus of elasticity of the pile

material, which are in the order of 5 to 6 percent, with an uncertainty in the reported values of shear transfer being twice the uncertainty in the loads, or in the range of 10 to 12 percent.

3.4 Data Acquisition System

The data acquisition system used to record the raw voltages from the instruments is shown schematically in Plate 3.6. The system is designed to utilize a Hewlett-Packard 3497A Scanning Digital Voltmeter as an analog-to-digital voltage converter. The HP3497A, with 6-1/2 digit accuracy, was selected so that the absolute strain gage bridge output could be recorded directly, eliminating the need for intermediate signal-conditioning equipment.

The output voltages from the instruments were sequentially sampled, digitized, and passed from the HP3497A to the Digital Equipment Corp. MINC 11/23 computer for visual display and for storage on 8-inch (20.3 cm) floppy discs. The order in which the instruments were sampled is shown in Plate 3.7. The calibrations are in engineering units per volt: inches, kips, and kips per square foot, as appropriate.

The digital records stored on the floppy discs were transferred to the 9-track magnetic tape as each floppy disc was filled. The magtape was used both for redundancy and for transferring the data to non-DEC computers for post-processing.

After each scan, or sample of data from all instruments, the records were printed as raw voltages, with stored values of zero-voltage being subtracted before printing. Optionally, the voltages were multiplied by a calibration factor before printing, to reduce the data to engineering units.

The computer program which controlled the acquisition of raw voltages obtained data in three modes, one automatic and two manual. The first mode collected data at fixed time intervals; the intervals could be changed easily by the computer operator. The other two modes were sample-on-demand, with the results being printed in either voltages or engineering units.

The data from selected transducers were also recorded on analog x-y-y recorders. The analog records were used for visualization of the progress of a test and for test control. The analog recordings normally included the pile-head load and displacement on one recorder, with the second recorder being used to display either load or displacement or pressure, depending on the particular test sequence being performed.

Manual reading of the strain modules and the total pressure transducers was performed during quiescent periods using a precise and stable bridge-balance instrument. The instrument has variable sensitivity; the ranges used during the tests were chosen to have a sensitivity of approximately 1 kip (4.45 kN) per division for the strain modules and 0.01 ksf (0.48 kPa) per division for the total pressure transducers.

3.5 Displacement Measurements

It was desired to run a load test as quickly as possible after completion of driving, to provide an initial datum condition. Because of the time required, the displacement reference frame and the electro-mechanical extensometers were not in place during the load test which was performed immediately after driving. The only displacement measured was at the pile head and was made with respect to the load frame. A reference frame was then installed, which was supported on two 8-inch-diameter (20.3 cm) pipes driven into the seafloor.

During the later testing, the displacement of both the test pile and the load frame were measured with respect to the reference frame. The pile head displacements measured during the immediate load test were later corrected by subtracting the estimated elastic deflections of the load frame and supporting platform structure.

The displacement of the pile head and of two tell-tales were measured with DC LVDTs and mechanical dial indicators. The telltales employed cylindrical steel weights which were lowered onto prepared seats inside square mechanical tubing welded inside the pile. A spring-steel wire having a flat cross-section was attached to the weights and was passed over two pulleys, mounted on the reference

beam. A second, smaller weight was attached to the free end of the wire to maintain constant tension.

The dial indicators and the LVDT's were then used to measure the relative displacement between the constant-tension steel wire and the reference beam.

The pile-head displacements were measured by dial indicators and LVDT's which were attached to a length of steel angle which was welded to the pile.

The validity of the displacements which were measured with the tell-tales was verified by calculating a change in displacement at each tell-tale location under a known change in load, assuming the measured pile head displacements were correct. The calculated displacements agreed with those measured within 5 percent, which is approximately the expected error in the calculated axial stiffness, AE.

Once the measured displacements were verified under these loads, the measurements by the tell-tales were assumed to be correct, and were used for calculating the displacements along the pile in developing curves of shear transfer versus displacement.

3.6 Effects of Wave Loading on Load Measurements

An analog recording of the output of three pairs of strain modules with time is shown in Plate 3.8. The topmost pair of strain modules was at the 62-foot (18.9 m) depth, the middle pair at the 92-foot (28.0 m) depth, and the bottom pair at the 182-foot (55.5 m) depth.

The vertical scale is approximately 7 kips per inch; the pen was moving horizontally at a nominal rate of 33 seconds per inch.

The digital data acquisition system, which sampled the instruments at fixed time intervals, sampled each instrument at random points in the analog record. Two effects will be noted in the digital records: First, the records for individual instruments will reflect the spread of the analog variations shown in Plate 3.8.

Secondly, since the two strain modules at each level were sampled 0.05 seconds apart, the effects of bending are not perfectly cancelled, especially during the periods of rapid change in bending moment. The effects of wave loading on the shear transfer were greater than for the load at any single level, since the effects are compounded by taking differences in the loads.

Similar effects observed during testing of the 3-inch-diameter (7.62 cm) pile segment probes (Ref 4) were investigated and found to be due to the slight upward and downward movement of the platform associated with lateral tilting. The effects were observed with waves only 3 to 5 feet (0.9 to 1.5 m) in height. With the 30-inch-diameter (76.2 cm) pile, additional effects were caused by lateral wave forces directly against the exposed pile, producing bending strains in the axial strain measurements and direct pressure effects on exposed pressure cells.

Although some of the plots of data show the time-variant load effects, all such effects are small and have no significant effects on the interpretation of results.

4. TEST METHODS

4.1 Introduction

This section of the report contains a description of the methods used to perform the experiments and to evaluate the quality of the data.

A chronological log of the significant events occurring during the field activities is also included.

4.2 Planned Procedures for Obtaining Instrument Zero Readings

In order to evaluate the results of an instrumented pile test, it is essential to obtain a set of initial voltage and balance box readings for the instruments with the pile under known conditions of axial load and lateral pressure. After the pile is in place, the ideally stable temperature environment is of great benefit in making precise measurements; the principal difficulties are associated with establishing accurate zero readings before the pile is driven.

For the strain-sensing elements, the ideal condition under which the initial readings should be made is one with zero soil reactions along the pile, accompanied by negligible values of bending moment. Such a condition occurs only when the pile is suspended in tension, with the pile not having contact with another support anywhere along its length. Any later change from this condition at any level will reflect the total soil reaction below that level. By subtracting the changes at any level from those at any other level, the load transferred to the soil between the two levels may be determined.

For zeroing the pressure transducers while the pile is suspended in the water, it is necessary to obtain sets of readings under two or more known pressures, and then to extrapolate the changes in the readings to the conditions existing at atmospheric pressure. Due to the design of the total pressure transducers, the

output at atmospheric pressure (in air) is affected by changes in temperature, especially when the transducers are exposed to direct sunlight. Only when the transducers are in a constant-temperature environment is the output stable, without any temperature-induced drift.

For the test pile, this meant that the pressure transducers must be read at several depths below the water surface, and the change in output voltage for each transducer extrapolated to mean sea level in order to calculate a value of voltage equivalent to that which would be recorded at atmospheric pressure, without any significant effects of temperature on the bridge output.

For the pressure transducers at the two lowest levels, readings at only one depth (and therefore only one pressure) were available, since the pile was lowered into position with the tip 5 ft (1.5 m) above the mudline before the instruments were attached to the data acquisition system. The readings taken with the transducers at this depth were to be corrected by using the hydrostatic pressure gradient measured by the pressure transducers in the four upper cans to establish the initial pressure conditions.

As reported in Refs 1 and 5, it had been planned to monitor each instrument closely during the overnight period while the pile was hanging from the crane or from the clamping device at the pile guide on the load frame, to evaluate the stability of the instruments, and to obtain several sets of data under known load and pressure conditions prior to releasing the pile.

At the time the pile was in position for the zero readings, the installation contractor became quite concerned about the need to leave the crane and the test pile fixed in position during an overnight period, even though the contractor had been aware of the need to do so for months in advance. At their urgent request, the pile was lowered into the seafloor under its own weight, and the crane was unhooked.

The data which had been taken during the short period of time in which the pile was suspended were later carefully reviewed, in order to deduce the zero-load and zero-pressure voltage and balance box readings. It was found, however, that the

instrument readings taken during this period were not sufficiently stable, and that only minimal checks of the resistance-to-ground had been made.

Due to the prolonged exposure to weather and to seawater from spray during transport to the site, the connectors at the upper ends of the instrument cables were either damp, or contained liquid water. The connectors were cleaned and dried but some were not done satisfactorily until after the pile had been lowered into the seafloor. As a result, the data which had been taken during the crucial period of zero soil reactions and bending moment, and of known hydrostatic pressures on the two lower levels of pressure transducers, could not be used, since the presence of moisture in the connectors resulted in instability in the output of the strain gage circuits. In addition, the temperatures of the pile and the instruments had not stabilized, which also contributed to the uncertainties in establishing the zero-load conditions with confidence.

Once the connectors at the ends of the cables had been satisfactorily cleaned and dried, the resistance to ground was found to be essentially infinite, and no drift or unstable behavior was noted. Even after returning to the platform on 14 Dec 1984 and on 26 Mar 1985, fifteen months after the installation of the pile, all of the strain gage circuits were still extremely stable, and showed no evidence of moisture intrusion or drift.

The best possible zero-reading values have been deduced by methods explained in following sections and appear to be adequate for reconstructing all significant results. Additional checks on pore pressures at ambient conditions will be available from long-term tests performed in April, 1985.

4.3 Strain Module and Extensometer Zero Voltages

In order to establish zero-voltage readings for the strain modules and the extensometers, it was necessary to assume a load distribution in the pile for the conditions existing after the pile had penetrated into the seafloor to a depth of 46 ft (14.0 m).

As noted earlier, the desired condition was one of zero soil reactions along the pile length; such a condition requires that any cross-section of the pile support in tension the weight of the pile below that cross section. Once the pile is lowered vertically until the pile is supported at the tip, the change in load at any cross-section above the point of support is equal to the total weight of the pile (from tension equal to the weight of the pile below the cross-section to compression equal to the weight of the pile above the cross-section).

For those strain modules which were above the mudline, such a condition (with no bending moment) was assumed.

For the two bottom pairs of strain modules, which were below the mudline, it was assumed that a triangular distribution of soil resistance existed along the embedded length of pile, with the magnitude of the total soil resistance being equal to the weight of the pile. Values of axial load which were consistent with this distribution of soil resistance were calculated for the elevations of the two embedded levels of strain measurement.

Although the method described above was used to estimate the average load at the two embedded cross-sections with an adequate degree of accuracy, the method can not be used to calculate individual zero-voltage or balance box readings for the strain modules or the extensometers on each side of the pile, since the value of bending moment which existed could not be ascertained, and was therefore assumed to be zero.

The zero voltage readings calculated using this method were then used to calculate the load distribution in the pile during two later conditions, (1) at the ultimate load during plastic slip in tension and compression during the immediate load test and (2) during the last cycle of two-way loading after the long-term test. It was found that, for the two bottom levels of strain modules, the loads during plastic slip in tension and compression were essentially equal, differing by only 20 kips (433 kPa). The zero-voltage readings for the two lower levels of strain modules were thus assumed to be correct. The zero-load conditions for the remaining strain modules and extensometers were then defined to be one-half the peak-to-peak voltages under the same two loading conditions.

This procedure does not affect the magnitude nor the precision of the loads calculated at each level; it merely removes the effects of bending moment from the zero-load readings which were calculated for the individual instruments, allowing comparisons to be made more easily among the several instruments. It should be noted that, since the magnitude of bending moment that existed at the time the connectors were cleaned is not known, any later changes in the absolute strain across the pile diameter included changes in bending moment from the initial, unknown condition. As a result, the magnitudes of the absolute values of strain were therefore felt to be inconsequential.

Once the zero-load voltages had been established using the above procedures, the relative changes in total axial thrust during the tests could be calculated.

For the two levels at which only one strain module survived, it was found that the static bending moment changed during the course of the load tests, since the values of zero voltage (taken as one-half the peak-to-peak voltage) varied from cycle to cycle, and differed between the two tests. The values of load calculated using the strain modules at these two levels could therefore not be used to calculate values of shear transfer.

In calculating the distribution of shear transfer along the pile during the 1984 load tests, the loads measured by the extensometers were substituted for the strain modules at the 122-ft (37.2 m) depth; the single strain module at the 152-ft (46.3 m) depth was ignored. For the immediate (1983) test, before the extensometers were installed, the single strain modules at both the 122-ft (37.2 m) and the 152-ft (46.3 m) depths were ignored. Thus, the shear transfer was computed over a longer (90 ft, 27.4 m) section of pile in that vicinity.

4.4 Total and Pore Pressure Transducer Zero Voltages

In order to estimate the zero-pressure voltage readings for the total and pore pressure transducers, the voltage readings obtained with each instrument at known elevations (a minimum of two, and up to four) were plotted versus depth below mean

sea level. A line was then drawn through the points, and the intersection of the line with the elevation of the water surface was used to determine the zero-voltage reading. Since some of the readings were affected by currents, minor adjustments to the values were necessary in order to obtain the best agreement among the four transducers at each of the depths at which hydrostatic pressure measurements were made.

For the pressure transducers in the two bottom cans, such a procedure could not be followed, since the first stable readings were taken when the instruments were already below the mudline. For these instruments, the following procedures were used.

For the pressure transducers in Can 2 (final penetration depth of 199 ft, or 60.7 m), a pressure profile with depth below the mudline was established using values of total and pore pressure measured during pile installation with the instruments in the four upper cans. Then, the values of total pressure and pore pressure for Can 2 were forced to fit this pressure profile. The data from the pressure transducers were then reduced to engineering units.

A similar procedure was used for the pressure transducers in Can 1 (final penetration depth of 224 ft, or 68.3 m); however, the initial zero-voltage readings taken prior to lowering the pile were used, with values of hydrostatic pressure assigned to the instruments being equal to those measured by the transducers in the upper cans at a similar depth in the seawater.

The pore pressure profile with depth established using the pressure measurements made on 14 Dec 1984 was compared with similar profiles established with the NGI piezometers and with the small-diameter in situ tools. The values of pore pressure at the 199 and 224-ft (60.7 and 68.3 m) depths were then corrected to fit the near-ambient pore pressure distribution, with the total pressures being corrected by an equal amount, in order to maintain consistent values of radial effective pressure.

The relative changes in total and pore pressure reported for the pressure transducers in the two bottom cans are thus correct; however, the absolute values of

pressure remain slightly uncertain. The magnitudes of these errors, however, are less than 1 ksf (48 kPa), or a maximum of 3 percent of the measured pressures at the final depth of penetration of the pressure transducers.

At the final depths of Cans 1 and 2, 199 and 224 feet (60.7 and 68.3 m) below the mudline, the radial effective pressures were quite small in relation to the ambient total and pore pressures. The values of radial effective pressure, being deduced by taking the differences between the measured pressures, are quite sensitive to small errors or offsets in the zero readings for the pressure transducers. The consistency among the values of radial effective pressure obtained at these depths, as compared with those obtained at the shallower depths, where no uncertainty exists, was generally quite good. The magnitudes of the calculated effective pressures also appear quite reasonable; thus, the methods used to establish the values of total and pore pressure are felt to be quite satisfactory.

4.5 Summary and Evaluation of Instrument Zero Readings

The voltage readings for the strain modules which were to be used to calculate the changes in axial load from a condition of zero soil reaction and negligible bending moment were not obtained.

Using deduced values of load for the two lower levels of strain modules with the pile tip at a penetration of 46 ft (14.0 m) below the mudline, a set of zero-load voltage readings were calculated. The voltages recorded during plastic slip in tension and compression during the load test performed immediately after driving, and during the last cycle of two-way loading after consolidation, were found to be symmetric above and below these values of zero-voltage, within the degree of precision in the measurements.

The calculated values of zero-load voltages for the strain modules at the 182-foot and 212-foot (55.5 and 64.6 m) depths were thus assumed to be correct. Values of zero-load voltage readings for all the other strain-sensing instruments were then calculated as being one-half the peak-to-peak voltages recorded for the instruments during the same cyclic load tests.

Although the procedures used to establish the zero-load readings could not be used to deduce the absolute strain values for each transducer, the procedures will permit values of average strain, or axial load at each station, to be deduced.

Values of zero-voltage corresponding to atmospheric pressure were not obtained with absolute certainty for the pressure transducers in Cans 1 and 2. Values of zero-pressure voltage were therefore assigned to the instruments in Can 1 based on readings taken before the connectors were proven by resistance-to-ground measurements to be cleaned and dried satisfactorily. For the instruments in Can 2, a set of initial pressure conditions were deduced from the pressures later measured at the same depth with the pressure transducers in Cans 3 and 4, and the data was processed.

The values of pore pressure were later corrected by adjusting the values to fit the ambient pore pressure profile established using the remaining pressure transducers of the large pile, the NGI piezometers, and the pore pressures measured with the small-diameter in situ tools. In order to maintain consistent values of radial effective pressure, the values of total pressure were also corrected, by an equal amount.

It will later be shown that the values of pore pressure reported for Can 1 (the 224-ft (68.3 m) depth) and Can 2 (the 199-ft (60.7 m) depth) are reasonably correct; the values of total radial pressure are estimated to be offset by less than 1 ksf (48 kPa) from the actual values (at most 3 percent of the measured pressures). The variation with depth of the calculated radial effective pressures, on the other hand, are very consistent, indicating that the reported values of total pressure are also reasonably correct.

4.6 The Loading and Control System

The loads were applied to the pile using eight hydraulic rams, each with a capacity of 340 kips (1513 kN) at 3000 psi (20700 kPa). The hydraulic pump had a pumping rate of 30 gpm (114 l/min) at a pressure of 1500 psi (10300 kPa), which reduced to 15 gpm (57 l/min) at the maximum rated pressure of 3000 psi (20700

kPa). The rated capacity of the loading system was thus 2720 kips (12104 kN), with a nominal maximum calculated pile-head displacement rate of 9.6 inch/min (24.4 cm/min) for loads up to 1360 kips (6052 kN), which decreased to 4.8 inch/min (12.2 cm/min) at the maximum load, excluding losses.

A schematic diagram of the hydraulic system is shown in Plate 4.1. Control of the direction of travel of the hydraulic rams was accomplished using an electrical four-way solenoid valve. Control of the rate of loading was accomplished using variable-rate flow-control valves arranged to restrict the outflow from either end of the rams. This was done to prevent the dumping of pressure and subsequent rapid unloading of the pile during load reversals and during the repeated tension loading, since the low-pressure and high-pressure lines become reversed during such loading.

A dual set of controls were used, one for control of the cyclic loading, which was actuated by limit switches mounted on an x-y-y recorder, and one for manual control of the static tests.

The circuit which automatically controlled the reversal of ram movement had a 13-second delay between stopping the movement and starting in the opposite direction. In terms of the pile-head load, the effect was one of load-pause-unload or unload-pause-load. This was arranged so that at least one scan of all data was taken at the maximum and minimum loads during the repeated-tension tests, which may not have been possible had the data merely been sampled at a constant rate with no delay in the load reversal.

The fastest possible sampling rate for all 48 channels of data using the HP3497A voltmeter on the most sensitive range was approximately 2.4 seconds. Including the additional overhead involved in printing and storing the results on the floppy discs, the time was increased to approximately 5 seconds per scan.

In order to ensure that a sample was taken at the peak load, a sampling interval of 10 to 15 seconds was selected, with two "demand" scans taken during the 13-second pause at each load reversal.

4.7 Data Reduction Methods

During the course of the experiment, the raw voltages were stored on the floppy discs in files which contained 100 (or fewer) scans each. The identification of the data within each file was based on alphanumeric data strings which contained the date and time of each scan.

In order to facilitate the reduction and the plotting of the data, the raw voltages were copied into new data files which were reorganized to contain related portions of the data. For example, the raw voltages from each set of four pressure transducers at each depth were placed in six files which contained all the data collected during the experiment.

The data were reduced to engineering units by subtracting an initial voltage and multiplying the difference by a calibration factor. The results were then placed in a new data file. During this process, alphanumeric data strings which contained the time and date of the scan were transferred with the data; each record from any instrument could later be correlated with corresponding records from any other instruments.

The pressure data from the balance box and the voltmeter which were recorded manually during the period of consolidation were also entered into the reduced data files manually. The data were plotted, and then edited manually to remove unnecessary data points. The data were not smoothed nor altered by this process; excess data points were simply removed so that the points were spaced more equally on the graphs.

For the load tests, little editing of the data was done. All the data points which were recorded are shown in the figures.

4.8 Chronological Record of the Experiment

The chronological log of events in Table 4.1 details the consolidation history of the soil and the times at which the load tests were performed. Since the pile was

driven in four stages, during four different time intervals, the early portion of consolidation began at different times for each depth. As shown in the table, the initial time for calculating the consolidation times at any depth can be determined by the times given for successive pile tip penetrations.

As shown in Table 4.1, a series of static and cyclic load tests were performed on the test pile in April 1985, sixteen months after the pile was driven. At this time, the process of consolidation was essentially complete. The results of the load tests performed in 1985, under CNRD Research Project 13-4, will be presented in a subsequent volume.

The loading rates at which the static pile capacities were obtained may be determined by subtracting the times given for the initiation of loading from those given for the failure loads, which correspond to the time at which the peak pile head loads were recorded.

Due to impact stress and vibration during pile driving, the pressure measurements made during the process were not anticipated to be useful. The pile driving was therefore stopped for short periods of time to enable sets of static pressure measurements to be made. It was planned that stops would be scheduled so the pressure transducers in the bottom can, 10 ft (3.0 m) above the pile tip would be positioned near the final depths of each of the other five sets of pressure transducers. Thus, the pressure transducers in the bottom can could be used to record the maximum total and pore pressures created by pile driving at each of the other locations. In addition, the variations in pressure along the length of the pile could be used to estimate the effects during pile driving of axial shearing on the excess pressures.

TABLE 4.1 CHRONOLOGICAL RECORD OF PILE INSTALLATION AND TESTING

<u>DATE</u>	<u>TIME</u>	<u>EVENT</u>
2 Dec 1983	21:12	Initial readings after first connecting the instruments to the data acquisition system. Pile tip 5 ft (1.5 m) above mudline.
	23:23	Pile tip resting on seafloor, reducing the load on the crane.
	23:58	Pile tip at a penetration of 46 ft (14 m); all pile weight on bottom.
4 Dec	10:10	Pile tip at a penetration of 56 ft (17 m); top of instrumented section driven to a convenient working height. First add-on section being welded to the instrumented section
6 Dec	11:13	Pause for static pressure measurements; pile tip penetration 83 ft (25.3 m)
	11:20	Pause for static pressure measurements; pile tip penetration 91 ft (27.7 m)
	12:26	Pause for static pressure measurements; pile tip penetration 93 ft (28.4 m)
	13:14	Pause for static pressure measurements; pile tip penetration 121 ft (36.9 m)
	13:37	End of driving, pile tip penetration 145 ft (44.2 m). Second add-on section being welded to the pile
8 Dec	18:59	Pause for static pressure measurements; pile tip penetration 181 ft (55.2 m)
	19:54	Pause for static pressure measurements; pile tip penetration 211 ft (64.3 m)

	20:44	Pile tip at a penetration of 233.5 ft (71.2 m) (End of Driving)
	21:38	Began loading pile in tension
	23:50	Failure load, in tension
9 Dec	00:28	Began loading pile in compression
	00:37	Failure load, in compression
	02:46	Using diesel hammer, pile driven to a tip penetration of 234 ft (71.3 m)
28 Mar 1984	16:34	Initial data taken after return to platform
2 Apr 1984	13:42	Began loading pile in tension
	14:57	Failure load, in tension
	16:14	Began loading pile in compression
	17:18	Failure load, in compression
3 Apr 1984	12:27	At creep load, beginning test
	14:23	At creep load, at end of test
	17:22	Beginning one-way cyclic tension tests
4 Apr 1984	01:03	End of one-way cyclic tension tests
	01:32	Beginning two-way cyclic tests
	02:24	End of two-way cyclic tests
14 Dec 1984	-----	Return to check instrument stability and take bridge readings
26 Mar 1985	-----	Return to make bridge readings
15-22 Apr 1985	-----	Perform series of static and cyclic load tests after the completion of consolida- tion (to be covered in a subsequent report under CNRD Research Project 13-4).

5. RESULTS OF THE EXPERIMENTS

5.1 Introduction

The results of the experiments on the 30-inch-diameter (76.2 cm) pile will be presented in this section of the report. The results are in chronological sequence of occurrence, and will be summarized in the following section.

In the discussion of results, the following sign convention is used:

- (1) Positive thrust (internal axial force in the pile) is tensile.
- (2) Positive shear transfer resists upward movement of the pile.
- (3) Positive pile displacement is upward.

The elevations given for the instruments are those measured with respect to the mudline.

The reported values of axial pile capacity include only the net soil reactions; values of total pile-head load capacity, which include the effects of pile self-weight, will be larger (tension) or smaller (compression) than those reported. It is the purpose of this report to establish only that portion of axial pile capacity which is due to the shear transfer capacity of the soil; the effects of gravity have thus been ignored.

5.2 Soil Pressures During Installation and Consolidation

The profiles of the maximum total and pore pressures measured by the transducers in Can 1 during pile installation are shown in Plate 5.1.

During each pile driving operation, pile driving was interrupted when the pressure transducers in Can 1 were near the final elevation which the pressure transducers in the upper cans would occupy when the pile was fully driven, and a number of sets of data were taken. It was intended to use the Can 1 pressure transducers to measure the initial values of maximum total and pore pressure at each elevation, so that the complete consolidation history at each level of pressure transducers could be established.

The upper segments of the curves are the values measured during the initial installation of the 180-foot (54.9 m) long instrumented section; the lower pair are taken from the data recorded during the short pauses during driving, with the instruments in Can 1 near the final elevation the pressure transducers in the upper cans would occupy at the end of driving.

The instantaneous pressure profiles obtained in the soil by the pressure transducers along the pile at each pause during the various pile installation operations are shown in Plates 5.2 and 5.3, and enumerated in Table 5.1. At each time, the maximum values of total radial pressure shown in Plate 5.2 and pore pressure shown in Plate 5.3 are those given in Plate 5.1 for Can 1. As shown in the two plates, excellent agreement was obtained for the values of pressure at each depth obtained by the transducers at the four upper levels as the pile progressively moved downward, with higher initiating values being recorded by the pressure transducers in Can 1.

The greatest effect of continued pile driving on the excess pressures seems to have occurred early in the redrive (or continuation of driving). This is indicated by the fact that all pressure transducers, except for those in Cans 1 and 2, yielded nearly equal values of pressure at any depth. Thus, the excess pressures generated by the initial passage of the pile tip (as measured by the transducers in Can 1) dissipated to reasonably constant values during the process of advancing the pile.

The values of total and pore pressure which are shown in Plates 5.1, 5.2, and 5.3 are given in Table 5.1. The elevations shown in Table 5.1 are those at which the pressure transducers were located at the time the measurements were made, during

periods of various lengths of time during which the pile driving operation was stopped.

TABLE 5.1 SOIL PRESSURE PROFILES RECORDED DURING PILE INSTALLATION

10:10 04 Dec 1983, Pile Tip Penetration 56 ft (17.1 m)

Depth		Total Pressure		Pore Pressure		Effective Pressure	
<u>ft</u>	<u>m</u>	<u>ksf</u>	<u>kPa</u>	<u>ksf</u>	<u>kPa</u>	<u>ksf</u>	<u>kPa</u>
21	6.4	5.7	273	5.7	273	0.0	0
46	14.0	9.5	455	9.0	431	0.5	24

11:26 06 Dec 1983, Pile Tip Penetration 91 ft (27.7 m)

Depth		Total Pressure		Pore Pressure		Effective Pressure	
<u>ft</u>	<u>m</u>	<u>ksf</u>	<u>kPa</u>	<u>ksf</u>	<u>kPa</u>	<u>ksf</u>	<u>kPa</u>
26	7.9	5.2	249	5.1	244	0.1	5
56	17.1	9.7	464	9.4	450	0.3	14
81	24.7	13.6	651	12.8	613	0.8	38

13:14 06 Dec 1983, Pile Tip Penetration 121 ft (36.9 m)

Depth		Total Pressure		Pore Pressure		Effective Pressure	
<u>ft</u>	<u>m</u>	<u>ksf</u>	<u>kPa</u>	<u>ksf</u>	<u>kPa</u>	<u>ksf</u>	<u>kPa</u>
26	7.9	5.3	254	5.4	259	- 0.1	- 5
56	17.1	9.0	431	8.8	421	0.2	10
86	26.2	13.1	627	12.1	579	1.0	48
111	33.8	17.5	838	16.6	795	0.9	43

06 Dec 1983 13:37, Pile Tip Penetration 145 ft (44.2 m)

Depth		Total Pressure		Pore Pressure		Effective Pressure	
<u>ft</u>	<u>m</u>	<u>ksf</u>	<u>kPa</u>	<u>ksf</u>	<u>kPa</u>	<u>ksf</u>	<u>kPa</u>
20	6.1	4.7	225	4.7	225	0.0	0
50	15.2	7.9	378	8.0	383	- 0.1	-5
80	24.3	11.5	551	11.3	541	0.2	10
110	33.5	15.8	757	15.3	733	0.5	24
135	41.2	20.6	986	19.6	938	1.0	48

08 Dec 1983 18:59, Pile Tip Penetration 181 ft (55.2 m)

Depth		Total Pressure		Pore Pressure		Effective Pressure	
<u>ft</u>	<u>m</u>	<u>ksf</u>	<u>kPa</u>	<u>ksf</u>	<u>kPa</u>	<u>ksf</u>	<u>kPa</u>
26	7.9	5.4	259	5.4	259	0.0	0
56	17.1	8.9	426	8.8	421	0.1	5
86	26.2	11.8	565	12.0	575	- 0.2	- 10
116	35.4	15.4	737	14.9	713	0.5	24
146	44.5	20.1	962	19.6	938	0.5	24
171	52.1	25.7	1231	24.7	1183	1.0	48

08 Dec 1983 19:55, Pile Tip Penetration 221 ft (67.4 m)

Depth		Total Pressure		Pore Pressure		Effective Pressure	
<u>ft</u>	<u>m</u>	<u>ksf</u>	<u>kPa</u>	<u>ksf</u>	<u>kPa</u>	<u>ksf</u>	<u>kPa</u>
56	17.1	9.1	436	9.1	436	0.0	0
86	26.2	12.0	575	12.0	575	0.0	0
116	35.4	15.1	723	15.1	723	0.0	0
146	44.5	19.4	929	18.8	900	0.6	29
176	53.7	24.8	1187	24.1	1154	0.7	33
201	61.3	30.1	1441	28.3	1355	1.8	86

08 Dec 1983 20:45, Pile Tip Penetration 233.5 ft (71.2 m)

Depth		Total Pressure		Pore Pressure		Effective Pressure	
<u>ft</u>	<u>m</u>	<u>ksf</u>	<u>kPa</u>	<u>ksf</u>	<u>kPa</u>	<u>ksf</u>	<u>kPa</u>
78.5	23.9	11.7	560	11.7	560	0.0	0
108.5	33.1	14.3	685	14.1	675	0.2	10
138.5	42.2	18.6	891	18.6	891	0.0	0
168.5	51.4	22.0	1053	21.1	1010	0.9	43
198.5	60.5	27.5	1317	27.1	1298	0.4	19
223.5	68.1	33.2	1590	32.4	1551	0.8	39

09 Dec 1983 03:09, Pile Tip Penetration 234 ft (71.3 m)

Depth		Total Pressure		Pore Pressure		Effective Pressure	
<u>ft</u>	<u>m</u>	<u>ksf</u>	<u>kPa</u>	<u>ksf</u>	<u>kPa</u>	<u>ksf</u>	<u>kPa</u>
79	24.1	11.7	560	11.6	555	0.1	5
109	33.2	14.5	695	14.3	685	0.2	10
139	42.4	18.7	895	18.5	886	0.2	9
169	51.5	22.3	1068	21.3	1020	1.0	48
199	60.7	27.7	1326	26.5	1269	1.2	57
224	68.3	32.7	1566	31.0	1484	1.7	82

The variations in radial pressure during consolidation at the six embedded depths are given in Plates 5.4 through 5.9. In each of the six plates, the total radial pressure and the pore pressure are shown in the upper graph; the radial effective pressure, calculated as the difference in the two measured variables, is shown in the lower graph, expanded in scale. Zero time for each plot corresponds to the time at which the earliest pressure data are available, i.e., when the pile tip was approximately 10 feet (3.0 m) deeper than the elevation shown.

The variations in pressure shown in the plates are consistent with those observed during the experiments with the 3-inch-diameter (7.62 cm) probes (Ref 4), with a greater decrease being observed in the pore pressure than in the total radial pressure, resulting in a net increase with time in the calculated radial effective pressure. The discontinuity in the curves shown in Plates 5.4 through 5.7 corres-

ponds to the time of the driving of the last add-on section, prior to the immediate load test. Since the pile tip was advanced rapidly to the final elevation, no such delay occurred for the depths of 199 and 224 feet (60.7 and 68.3 m), shown in Plates 5.8 and 5.9.

The profiles of total, pore, and radial effective pressure which were obtained immediately after driving, immediately after the redrive, and on 28 March, 1984, after 111 days of consolidation, are given in Plates 5.10, 5.11, and 5.12. As seen in the plates, the pressure profile recorded after the redrive was very close to that obtained after the initial driving, except for the reduced values of pore pressure recorded at the depths of 199 and 224 ft (60.7 and 68.3 m) below the mudline.

The load test performed immediately after driving can thus be seen to have had little permanent effect on the soil pressures, except possibly in the soil below the 179-ft (54.6 m) depth. After 111 days of consolidation, both the total and pore pressures at each level had decreased, with significant increases in the radial effective pressure being observed.

Although the radial effective pressures increased significantly during consolidation, the values were still small, as compared with the measured total and pore pressures. Immediately after driving, the magnitudes of the radial effective pressures ranged from 2 to 5 percent of the measured pressures; at the end of consolidation, the magnitudes of the radial effective pressure were on the order of 10 to 15 percent of the measured pressures.

5.3 Results of the Load Test Performed Immediately After Driving

The load-displacement behavior recorded during the load test performed immediately after driving is shown in Plate 5.13. The displacements are those calculated for the pile at the mudline; the forces are those measured with the strain modules at the pile head and at depths of 62, 92, 182, and 212 ft (18.9, 28.0, 47.9, and 64.6 m) below the mudline. The peak load at the pile head was 443 kips (1971 kN), with a reduced post-failure load, during plastic slip, of 410 kips (1825 kN).

The total, pore, and effective radial pressures shown in Plate 5.47 were recorded at the conclusion of the initial compression loading. The values of soil pressure are tabulated below.

TABLE 5.3 PRESSURE PROFILE AFTER INITIAL LOAD TESTS

Depth		Total Pressure		Pore Pressure		Effective Pressure	
<u>ft</u>	<u>(m)</u>	<u>ksf</u>	<u>(kPa)</u>	<u>ksf</u>	<u>(kPa)</u>	<u>ksf</u>	<u>(kPa)</u>
79	24.1	11.09	531	10.55	505	0.54	26
109	33.2	13.28	636	13.22	633	0.06	3
139	42.4	16.82	805	16.27	779	0.55	26
169	51.5	19.90	953	18.58	890	1.32	63
199	60.7	24.65	1180	22.36	1071	2.29	109
224	68.3	28.39	1359	25.12	1203	3.27	157

Following the initial load tests to failure, an 18-hour period was allowed for the soil pressures to equilibrate. At the end of this period, the total, pore, and effective radial pressures, shown in Plate 5.48, are tabulated below.

TABLE 5.4 PRESSURE PROFILE AFTER PRESSURE EQUILIBRATION

Depth		Total Pressure		Pore Pressure		Effective Pressure	
<u>ft</u>	<u>(m)</u>	<u>ksf</u>	<u>(kPa)</u>	<u>ksf</u>	<u>(kPa)</u>	<u>ksf</u>	<u>(kPa)</u>
79	24.1	11.15	534	10.28	492	0.87	42
109	33.2	13.50	646	13.06	625	0.46	21
139	42.4	16.85	807	15.94	763	0.94	44
169	51.5	20.02	959	18.59	890	1.43	68
199	60.7	24.70	1183	22.21	1063	2.49	119
224	68.3	28.39	1359	25.12	1203	3.27	157

An examination of Plates 5.46, 5.47, and 5.48, along with Tables 5.2, 5.3, and 5.4, shows that the reductions in radial effective pressure are predominantly due

to increases in the pore pressure, and that the increased pore pressure did not fully dissipate during the 18-hour quiescent period.

5.7 Results of the Short-Term Creep Test

At the request of one of the observers an abbreviated creep test was performed prior to performing the one-way, or repeated tension load tests.

The creep tests consisted of placing a load of 250 kips (1113 kN) on the pile, then holding the load constant (as closely as possible) for a period of two hours. The loads were applied manually, using a pressure gauge to maintain the load. The variations in the load applied are due to manual adjustments in the hydraulic pressure plus the effects of wave loading on the platform.

The results of the creep test are given in Plates 5.49 through 5.56. Plates 5.49 and 5.50 show the variation with time in the loads measured along the pile, with the variation with time in the soil pressures shown in Plates 5.51 through 5.56. As shown in the plates, the loads were adjusted twice, then remained reasonably constant.

As seen in Plate 5.49, the loads in the pile at the 182 and 212-ft (55.5 and 64.6 m) depths were essentially equal, indicating a very small value of shear stress in the soil between these depths. At the 122-ft (37.2 m) depth, only small values of tension were recorded; at a slightly greater depth, the thrust in the pile remained compressive throughout the test.

As shown in the plates, the soil pressures fluctuated during the application of the bias load, (during the period between 15 and 20 minutes on the graph) then remained reasonably constant. The total, pore, and effective radial pressures at each depth prior to loading are shown in Plate 5.48. The values of pressure measured immediately after the creep load of approximately 250 kips (1113 kN) was applied, shown in Plate 5.57, are tabulated below.

TABLE 5.5 PRESSURE PROFILE AT THE BEGINNING OF CREEP TEST

Depth		Total Pressure		Pore Pressure		Effective Pressure	
<u>ft</u>	<u>(m)</u>	<u>ksf</u>	<u>(kPa)</u>	<u>ksf</u>	<u>(kPa)</u>	<u>ksf</u>	<u>(kPa)</u>
79	24.1	10.99	526	10.31	494	0.68	33
109	33.2	13.41	642	13.11	628	0.30	14
139	42.4	16.63	796	16.09	770	0.54	26
169	51.5	20.02	959	18.67	894	1.35	65
199	60.7	24.55	1175	22.25	1065	2.30	110
224	68.3	28.37	1358	25.18	1206	3.19	153

After one hour and 56 minutes, the total, pore, and effective radial pressures, shown in Plate 5.58, are tabulated below.

TABLE 5.6 PRESSURE PROFILE AT THE END OF CREEP TEST

Depth		Total Pressure		Pore Pressure		Effective Pressure	
<u>ft</u>	<u>(m)</u>	<u>ksf</u>	<u>(kPa)</u>	<u>ksf</u>	<u>(kPa)</u>	<u>ksf</u>	<u>(kPa)</u>
79	24.1	10.98	526	10.29	493	0.69	33
109	33.2	13.38	641	13.09	627	0.29	14
139	42.4	16.59	794	16.06	769	0.53	25
169	51.5	20.05	960	18.68	894	1.37	66
199	60.7	24.53	1174	22.29	1067	2.24	107
224	68.3	28.36	1358	25.19	1206	3.17	152

Thus, after the initial fluctuation during the application of the bias load, the pressures remained constant, within the degree of precision in the measurements. It had been speculated that, due to the application of shear stress, the radial effective pressure would decrease; no such reduction was observed.

The results of the tests indicate that, at least during a 2-hour period, no significant creep and relaxation occurred. Had creep and relaxation occurred in the soil above the 122-ft (37.2 m) depth, the axial thrust in the pile below this depth would have increased significantly. Since the thrust in the pile at the lower depths showed only slight increases, and remained compressive at the 182 and

212-ft (55.5 and 64.6 m) depths, it can be inferred that significant creep did not occur.

5.8 Results of the Repeated-Load Cyclic Tension Tests

Upon completion of the creep test, the pile was subjected to a series of repeated tension loads in which a constant bias load was maintained, and the cyclic component of load above and below the bias load was progressively increased. The maximum, minimum, and bias loads during each sequence of loading are given below.

TABLE 5.7 PILE-HEAD LOADS DURING ONE-WAY CYCLIC TENSION TESTS

MAXIMUM THRUST		MINIMUM THRUST		BIAS LOAD		NUMBER OF CYCLES
<u>kips</u>	<u>kN</u>	<u>kips</u>	<u>kN</u>	<u>kips</u>	<u>kN</u>	
446	1985	271	1206	359	1598	8
325	1446	163	725	244	1086	10
362	1611	124	552	243	1081	6
345	1535	132	587	239	1064	4
422	1878	63	280	243	1081	10
501	2229	- 2	- 9	250	1113	9
572	2545	- 33	- 147	270	1202	10
605	2692	- 102	- 454	252	1121	5
666	2964	- 127	- 565	270	1202	5
693	3084	- 156	- 694	269	1197	5
737	3280*	- 225	- 1001**	256	1139	25

* Average of all cycles; Max Peak = 760 kips (3382 kN), Min Peak = 723 kips (3217 kN), with progressive upward movement greatest with largest loads, as shown in Plate 5.61.

** The net internal thrust in the pile above the mudline was -180 kips (-801 kN), which is equal to the weight of pile, load frame, cables, and all other appurtenances. This value is the weight of the 359-ft (109.5 m) length of pile, as driven, suspended in air. The net external force applied to the pile was thus approximately 45 kips (200 kN).

The results of the one-way, repeated tension load test are given in Plates 5.59 through 5.73.

Plates 5.59 and 5.60 show the peak tension load on each cycle, from the strain modules and the extensometers, respectively. To show the precision in the control of the test, only the peak tension loads are given. Had more precise control of the loads been possible, and had more cycles of loading been applied, cyclic degradation in shear transfer during the test would be apparent in the figure by the convergence of loads at adjacent levels near the top of the pile as the soil between the two levels lost the ability to absorb load, plus a divergence in the loads at lower levels, as the loads were transferred deeper in the soil.

The variations in the displacements measured at the pile head and at depths of 62 and 212 ft (18.9 and 64.6 m) below the mudline during the application of the maximum tension loads are given in Plate 5.61. A comparison of Plates 5.59 and 5.61 shows that the accumulation of permanent displacement began to occur when the peak load equalled values which fluctuated between 723 and 740 kips (3217 and 3293 kN), approximately 12 percent less than the reduced post-peak load of 822 kips (3658 kN) recorded during the test to failure in compression.

The cycle-by-cycle variation in the maximum and minimum shear transfer along the pile is shown in Plates 5.62 through 5.67. The values shown are those which were calculated at the maximum and minimum loads on each cycle, when the pile was temporarily motionless for 13 second pauses.

As noted in Section 4.6, fast-rate scanning (and thus continuous digital recording) was deliberately sacrificed during these tests in order to ensure that peak data could be taken during the 13-second pause. This was done for two reasons. First, the rate of displacement of the pile head was increased during these tests, in order to approximate the time-rate of application of loads by wave action. Due to the limitations of the HP 3497A voltmeter, the last instrument was sampled 2.5 seconds after the first. Therefore, only those data points taken during the 13-second pause could be directly related to each other without interpolating with respect to time. Secondly, it was felt that the peak-load data were of greater importance than was the actual loading path; thus, the acquisition of data was

aimed toward obtaining the most useful information, rather than merely obtaining the largest possible quantity of data, which also would later require arduous post-processing.

The progressive downward migration of load along the pile, as the peak pile head load is increased, results in increased positive shear transfer at the greater depths, and in the evolution from positive to negative shear transfer at the minimum load at depths less than 122 feet (37.2 m).

The reversal in shear transfer at the upper depths during purely tensile loading is due to the recovery of elastic deformation of the pile during the reduction in load. Although the shear transfer does reverse in sign, only at the shallow depths (less than 62 ft (18.9 m)) is the shear transfer fully reversed (i.e., equal in both directions).

5.9 Soil Pressure Variations During the One-Way Cyclic Tests

The variation in the soil pressures during this sequence of loadings are given in Plates 5.68 through 5.73. With the exception of the 224-ft (68.3 m) depth, the soil pressures showed a general decrease in the radial effective pressure, with the decreases in pressure accompanying the larger values of shear.

The responses of the soil pressures at the 224-ft (68.3 m) depth, shown in Plate 5.73, are unlike those recorded at the other levels, in that an increase in the radial effective pressure accompanies the application of successive plastic slip. The peak (temporary) effective pressure, reached during plastic slip, was near the value of radial effective pressure at the end of the consolidation period.

The effects of the one-way loading on the soil pressures can be seen in Plates 5.74 and 5.75, which show the pressure profiles immediately before loading the pile and after the conclusion of the tests.

Prior to beginning the tests, the total, pore, and effective radial pressures, shown in Plate 5.74, were as tabulated below.

TABLE 5.8 PRESSURE PROFILE PRIOR TO ONE-WAY CYCLIC TESTS

Depth		Total Pressure		Pore Pressure		Effective Pressure	
<u>ft</u>	<u>(m)</u>	<u>ksf</u>	<u>(kPa)</u>	<u>ksf</u>	<u>(kPa)</u>	<u>ksf</u>	<u>(kPa)</u>
79	24.1	10.97	525	10.28	492	0.69	33
109	33.2	13.33	638	13.07	626	0.26	12
139	42.4	16.60	795	16.00	766	0.60	29
169	51.5	20.04	960	18.61	891	1.43	68
199	60.7	24.50	1173	22.21	1063	2.29	110
224	68.3	28.32	1356	25.12	1203	3.20	153

After completion of the load tests, the total, pore, and effective radial pressures, shown in Plate 5.75, were as tabulated below.

TABLE 5.9 PRESSURE PROFILE FOLLOWING THE ONE-WAY CYCLIC TESTS

Depth		Total Pressure		Pore Pressure		Effective Pressure	
<u>ft</u>	<u>(m)</u>	<u>ksf</u>	<u>(kPa)</u>	<u>ksf</u>	<u>(kPa)</u>	<u>ksf</u>	<u>(kPa)</u>
79	24.1	11.16	534	10.45	500	0.71	34
109	33.2	13.26	635	13.20	632	0.06	3
139	42.4	16.36	783	16.10	771	0.26	12
169	51.5	19.59	938	19.27	923	0.32	15
199	60.7	23.18	1110	23.34	1118	-0.16	-8
224	68.3	27.89	1335	24.09	1153	3.80	182

5.10 Results of the Two-Way Cyclic Tests

At the end of the one-way, or repeated-load, tension test, the pile was subjected to 5 cycles of fully-reversed cyclic loading. The results of the cyclic load tests are given in Plates 5.76 through 5.92.

Plate 5.76 shows the load-displacement behavior at the mudline during the two-way cyclic test. On the first cycle, the maximum load was 760 kips (3382 kN), slightly larger than that recorded during the progressive pullout during the preceding series of cyclic tension loadings. During the second cycle of loading, the test was stopped, the flow control valves reset for faster loading, and the test resumed. The effects of this sequence can be seen in the plates, with the load decreasing during the pause, and the loads on the following cycles being increased slightly.

During the first cycle, the rate of pile-head displacement was 0.006 in./sec (0.152 mm/sec); during the later cycles, the rate was 0.020 in./sec (0.508 mm/sec).

The hysteretic shear transfer-displacement, or t - z , relationships calculated for the two-way cyclic tests using the strain modules are given in Plates 5.77 through 5.82. Plates 5.83 through 5.86 contain similar relationships, calculated from the extensometer data.

For the portion of the pile above the 122-ft (37.2 m) depth, the shear transfer shows a slight increase during the two-way cyclic loading, with no cyclic degradation; this is primarily due to the effects of load rate on the shear transfer. Between the depths of 122 and 182 ft (37.2 and 55.5 m), the shear transfer remains almost constant, and only beyond the depth of 182 ft (55.5 m) does the shear transfer decrease during the cyclic loading.

The absence of further cyclic degradation during the two-way cyclic tests at the shallower depths should not be unexpected; the upper soils had been degraded due to reversed plastic slip during the one-way cyclic tests, while the deeper soils, where the plastic slip was one-directional, had not yet been fully degraded.

5.11 Soil Pressure Fluctuations During the Two-Way Cyclic Loading

The variation in soil pressure during the two-way cyclic tests are shown in Plates 5.87 through 5.92. The increases in radial effective pressure coincide with the plastic slip portion of the t-z curves, much the same as was reported for the 3-inch-diameter (7.62 cm) probes (Ref 4). During plastic slip in compression, no such increases were observed.

At the depths of 79 and 109 ft (24.1 and 33.2 m) below the mudline, the fluctuations in pressure were small. The magnitude of the fluctuations in pressure increased with depth, and with increasing magnitudes of shear transfer.

The lack of accurate zero-voltage readings for the pressure transducers at the 199-ft (60.7 m) depth can be noted in the small values of negative radial effective pressure, however, the fluctuations are properly displayed, with the actual values of pressure probably being near-zero.

At the 224-ft (68.3 m) depth, the cyclic shearing resulted in a decrease in the radial effective pressure, which had been observed to increase during one-way loading.

The effects of the two-way cyclic loading on the static soil pressures can be seen by comparing Plate 5.93, which shows the pressure profile at the end of the two-way cyclic tests, with Plate 5.75, which was taken before the tests. The total, pore, and radial effective pressures shown in Plate 5.93 are

TABLE 5.10 PRESSURE PROFILE AFTER TWO-WAY CYCLIC TESTS

Depth		Total Pressure		Pore Pressure		Effective Pressure	
<u>ft</u>	<u>(m)</u>	<u>ksf</u>	<u>(kPa)</u>	<u>ksf</u>	<u>(kPa)</u>	<u>ksf</u>	<u>(kPa)</u>
79	24.1	11.09	531	10.46	501	0.63	30
109	33.2	13.50	646	13.11	628	0.39	19
139	42.4	16.74	802	16.01	767	0.73	35
169	51.5	19.54	936	18.97	908	0.57	27
199	60.7	24.31	1164	22.80	1092	1.51	72
224	68.3	27.93	1337	25.14	1204	2.79	134

The instruments were then monitored for a period of 28.5 hours, while the hydraulic rams were removed, and the equipment was being demobilized. The total, pore, and effective radial pressures at the time the instruments were disconnected, shown in Plate 5.94, were

TABLE 5.11 PRESSURE PROFILE AFTER 28.8 HOUR EQUILIBRATION PERIOD

Depth		Total Pressure		Pore Pressure		Effective Pressure	
<u>ft</u>	<u>(m)</u>	<u>ksf</u>	<u>(kPa)</u>	<u>ksf</u>	<u>(kPa)</u>	<u>ksf</u>	<u>(kPa)</u>
79	24.1	11.13	533	10.48	502	0.65	31
109	33.2	13.54	648	13.29	636	0.25	12
139	42.4	16.71	800	16.19	775	0.52	25
169	51.5	19.74	945	19.05	912	0.69	33
199	60.7	24.21	1159	22.79	1091	1.42	68
224	68.3	27.94	1338	25.44	1218	2.50	120

A comparison of Tables 5.10 and 5.11 shows that, except for the 199-foot (60.7 m) depth, the measured pore pressures increased during the 28.8 hour quiescent period, with little change in the total pressures being observed.

Similarly, a comparison of Tables 5.1 and 5.11 shows that the pressure effects of the load tests were most noticable in pore pressure changes, although small decreases in the total radial pressure were also recorded.

5.12 Effects of Repeated and Reversed Loading on Axial Pile Capacity

The values of net axial pile capacity measured during the various sequences of load tests performed after the 115-day period allowed for partial consolidation are tabulated below. The tabulated values include only the net soil reactions, as recorded at the pile head, and do not include the effects of pile self-weight. As noted earlier, the pile capacity calculated as the summation of the measured values of peak unit shear transfer would be somewhat higher.

As also noted earlier, the values of total pile capacity, which include the effects of gravity, would indicate an increase in the tensile pile capacity and a decrease in the compressive pile capacity, as compared with the tabulated values, which include only the effects of the soil resistance.

TABLE 5.12 SUMMARY OF AXIAL PILE CAPACITY

<u>LOAD TEST SEQUENCE</u>	<u>AXIAL PILE CAPACITY, KIPS (kN)</u>	
Initial Loading in Tension, Peak	963	4285
Post-peak, During Plastic Slip	884	3934
Compression Loading After Tension Test, Peak	-860	-3827
Post-peak, During Plastic Slip	-822	-3658
Tensile Capacity Under Repeated Loading	720 to 740 (3204 to 3293)	
(Permanent displacement per cycle also varied with the magnitude of the load)		
Minimum Axial Capacity After Two-Way Cyclic Loading	760 to 780 (3382 to 3471)	
(At maximum displacement, not at yield; due to end-bearing forces, the load continued to increase with increasing displacement)		

It can thus be seen that the predominant portion of the losses in axial pile capacity occurred during the first reversal of loading, with the post-peak reductions in capacity being greater than the additional losses during the cyclic load tests. The post-peak capacity of 822 kips (3658 kN) during the compression test was only 85 percent of the initial peak tension capacity; at the end of the two-way cyclic tests, the capacity had been reduced to 760 kips (3382 kN), for a final capacity equal to 79 percent of the initial tension peak.

Although the behavior observed during these load tests was affected by the actual sequence of loading, the end result of the one-way and two-way cyclic tests would not be very different, had the pile not been loaded to failure prior to performing the cyclic tests. The one-way, or repeated-load, tension tests would possibly have required a larger number of cycles prior to pullout, but the magnitude of the failure load would not be expected to be greatly different.

5.13 Effects of Repeated and Reversed Loading of Shear Transfer

The effects of repeated-tension and two-way, fully reversed cyclic loading at the pile head on the shear transfer developed along the pile are given in Plates 5.95 through 5.104, with the pertinent values also given in Table 5.12.

The plates contain the positive-shear portion of the shear transfer-displacement relationships recorded during the initial tension loading, the final cycle of the repeated (one-way) tension tests, and the final quarter-cycle of the two-way cyclic tests. Because of the methods used to sample data during the one-way tension tests, the curves shown for this load cycle have fewer data points.

TABLE 5.13 SUMMARY OF MEASURED SHEAR TRANSFER

<u>DEPTH</u>		<u>INITIAL PEAK</u>		<u>POST-PEAK</u>		<u>AFTER ONE-WAY</u>		<u>AFTER TWO-WAY</u>	
<u>ft</u>	<u>(m)</u>	<u>ksf</u>	<u>kPa</u>	<u>ksf</u>	<u>kPa</u>	<u>ksf</u>	<u>kPa</u>	<u>ksf</u>	<u>kPa</u>
0-62	0-18.9	0.19	9	0.12	6	0.08	4	0.12	5
62-92	18.9-28.0	0.64	31	0.58	28	0.51	24	0.51	24
92-122	28.0-37.2	0.35	17	0.22	11	0.25	12	0.28	13
122-182	37.2-55.5	0.59	28	0.52	25	0.56	27	0.56	27
182-212	55.5-64.6	0.97	46	0.82	39	0.72	35	0.60	29
212-234	64.6-71.3	1.36	65	1.10	53	0.92	44	0.71	34

For the soils above the 182-ft (55.5 m) depth, little degradation was observed during the cyclic tests. Except for the soil layer between the depths of 62 and 92 ft (18.9 and 28.0 m) below the mudline, the shear transfer essentially stabilized at a minimum value during one-directional large-displacement slip on the first

loading to failure in tension, with no additional losses during the cyclic testing.

For the clay layer below the 160-ft (48.8 m) depth, however, a different pattern of behavior was observed. For this soil stratum, the shear transfer did not stabilize at the reduced post-peak value recorded on the initial loading, but continued to decrease during cyclic loading, finally stabilizing at a minimum value during the two-way cyclic tests.

It should be noted that, for the soil layer between the depths of 212 ft (64.6 m) and the pile tip (at 234 ft (71.3 m) below the mudline), the value shown for shear transfer includes an indeterminate amount of end-bearing, or tip resistance. A comparison of Plates 5.99 and 5.100 suggests that the increase in shear transfer after yield in Plate 5.100 (the sharp break-point in the curve) is due to end-bearing. The apparent increase in shear transfer is not observed in Plate 5.99, since any end-bearing is common to both sets of strain modules, and is thus subtracted from the calculated values of shear transfer in all except the bottom soil layer.

6. SUMMARY AND CONCLUSIONS

The results of the experiments, given in Section 5, show that the objectives of this portion of the research program have been fulfilled. A large quantity of high-quality data has been obtained over a sixteen-month period from a near-full-scale instrumented pile driven to a penetration of 234 ft (71.3 m) in an offshore deposit of soft-to-stiff under-to-normally consolidated clay.

In this section of this report, the major findings from the pile tests will be summarized. These results will later be combined with the in situ model pile experiments (Ref 4) and the results of the site characterization study (Ref 2) to provide a data base of in-situ testing. In turn, these will be combined with other information from the overall program to develop guidelines for the design of tension piles in normally consolidated clays.

6.1 Objectives of the Experiment

The primary goal of the experiment was the determination of the tensile capacity and behavior of an open-ended pile driven in soft, normally-consolidated clays. The pile was therefore instrumented to measure the load distribution with depth along the pile, with displacements also being measured at three elevations, in order to develop curves of shear transfer versus displacement for the soil along the pile.

The load tests which were performed included static loadings to failure in tension and compression shortly after driving and after four months of consolidation and set-up. During the load tests performed four months after installation, cyclic tension loadings were performed to investigate the progressive migration of load down the pile with increases in the cyclic load component, followed by fully-reversed cyclic loadings to failure in tension and compression to determine the minimum, fully degraded cyclic resistance of the soil.

Shear transfer-displacement (t - z) relationships were developed for both static and cyclic tension loading. The t - z relationships are not restricted to tensile loading only, but apply equally well to friction piles loaded in compression.

In order to obtain the most information possible from the experiment, the pile instrumentation included pressure transducers to measure the total radial pressure exerted on the pile by the soil, with companion measurements of the pore water pressure at the same depths. The pressure measurements were made in order to estimate the average intergranular, or effective, radial pressures. The values of radial effective pressure are useful in evaluating existing effective stress concepts of axial pile-soil interaction, and possibly to modify and extend theoretical concepts.

A second, and equally important, function of the pore pressure measurements was to monitor the consolidation of the soil after pile installation, in order to estimate the time required for set-up after driving. For the design of prototype piles, which are larger in diameter than the test pile, the service loads will likely be applied at an intermediate degree of consolidation; the time-rate of increase in pile capacity after driving must be considered in the design.

6.2 Summary of Instrument Performance

The instruments performed extremely well throughout the course of the research program. With the exception of two of the strain modules, which were damaged prior to pile installation, the success rate of the instruments was 100 percent. All the instruments survived the impact stresses during pile driving with no zero-shift, and showed no evidence of moisture leakage, long-term drift, or short-term instability during a sixteen month period after installation.

The provision for redundant strain measurements using drop-in electro-mechanical extensometers proved to be extremely valuable, since the instruments successfully replaced one level of strain modules, and also provided an independent check of the loads and the shear transfer calculated using the strain modules.

The stability of the strain-gage circuits in the strain modules can be seen in Plate 6.1, which shows the residual load distribution in the pile (with the loading system disconnected) on 20 Dec 1983, 28 Mar 1984, and 14 Dec 1984. Also shown in Plate 6.1 are the measured load distributions along the pile during the load test immediately after driving and during the initial tension test to failure after 115 days of consolidation.

It should be noted that, at each of the 122 and 152-ft (37.2 and 46.3 m) depths, only one strain module was operational. At these depths, the changes in axial force shown in Plate 6.1 also include changes in bending moment with time, which is most apparent at the 152-ft (46.3 m) depth during the period from 10 Dec 1983 until 30 Mar 1984. As seen in the plate, the residual thrust distribution did not change appreciably between the period from 10 Dec 1983 until 30 Mar 1984. On 4 April 1984, the residual load distribution (not shown) was essentially as shown for 30 Mar, even though the series of static and cyclic load tests were performed during the intervening period.

Prior to 30 Mar 1984, the residual pile force were only those required to support the weight of the pile; during the period from 04 Apr to 14 Dec 1984, an additional 100 kips (445 kN) of residual force was recorded for depths greater than 92 ft (28.0 m) below the mudline.

6.3 Summary of Pressure Measurements

The variation with depth of the total radial pressures measured at various stages of consolidation are shown in Plate 6.2. The pressure distributions are those measured on 8 Dec 1983, immediately after the pile was driven to grade, on 28 Mar 1984, after approximately 4 months of undisturbed consolidation, and on 14 Dec 1984, approximately 12 months after the pile was installed.

As seen in the plate, the total radial pressures decreased throughout the period of consolidation; however, any long-term effects of the static and cyclic loading performed in April 1984 on the pressures measured on 14 Dec 1984 are not known. As noted in Section 5, only minor short-term changes in the static total pressures were observed during the quiescent periods on 28 Mar and 9 Apr 1984, which

occurred before and after the series of load tests. However, the additional volume changes in the near-pile clay during reconsolidation and dissipation of shear-induced pore pressures may have resulted in some additional reductions in the radial total pressures beyond those which would occur under undisturbed conditions.

It may be noted that very similar behavior was observed at all depths, indicating that the instruments were very stable, with no long-term drift, and that the measurements therefore reflect the actual soil response.

The pore pressures that were measured at the same times as the total pressures are shown in Plate 6.3. Again, excellent stability was observed, with no obvious long-term drift or short-term instability noted for any of the instruments. Included in the plate are the values of ambient free-field pore pressure reported by the Norwegian Geotechnical Institute (Ref 7).

As shown in the plate, reasonable agreement was noted among the values of pore pressures measured by the instruments on the pile and by the free-field piezometers. Because of the agreement shown, the uncertainties suggested earlier for the zero readings for the pore pressure transducers must be small.

A comparison of the pore pressures measured on 28 Mar 1984 with those measured on 14 Dec 1984 indicates that the process of consolidation was almost complete at the time of the series of major load tests. If the pore pressures measured on 14 Dec 1984 are taken to be the ambient pore pressures in the soil, then the average degree of consolidation at the time the tests were performed was 83 percent. It should be noted that knowledge of the absolute values of pore pressure is not required to determine the degree of consolidation; a comparison of the relative values is sufficient.

It had earlier been estimated (Ref 1) that a period of 100 days after installation would be required for approximately 50 to 60 percent of the excess pore pressures to dissipate, based on the best knowledge of consolidation around driven piles at the time the planning study was performed. The rapidity of the consolidation of the soil around the large pile, which was also observed during the experiments

with the small-diameter pile segment models (to be presented in a subsequent report), indicates that not only the pile diameter, but also the wall thickness (therefore the extent of plastically strained soil), influence the time-rate of consolidation around a driven pile.

The variation with depth in the radial effective pressures, calculated from the pressures shown in Plates 6.2 and 6.3, are shown in Plate 6.4. Also included in the plate are the values of effective pressure given in Table 5.10, which were measured on 9 April 1984, after the completion of the series of static and cyclic load tests.

As seen in the plate, the radial effective pressures increased significantly during the four-month period of undisturbed consolidation from Dec 1983 until Apr 1984. The plate also shows that the radial effective pressures were considerably reduced by the static and cyclic loading of the pile (4 Apr 1984), but that the pressures were essentially recovered by reconsolidation during the long rest period following the load tests. Note that the changes in effective stress apparently do not result in proportionate changes in pile capacity.

The consistency of the calculated effective pressures, in terms of the variations with both depth and time, again serves to demonstrate the stability of the pressure transducers. Since the magnitudes of the radial effective pressures are a small fraction of the magnitudes of the total and the pore pressures, only slight drift or instability in either type of pressure transducer would be reflected as significant changes in the calculated values of radial effective pressure. Drift or instability of the pressure transducers in the range of 1 percent would result in a 10 percent effect on the calculated values of effective pressure; as seen in the plate, no such effects are evident.

The consistency in the variation in the calculated radial effective pressures with depth also lends a higher degree of confidence in the reported total and pore pressures at the 199 and 224-ft (60.7 and 68.3 m) depths.

6.4 Summary of Static and Cyclic Load Test Results

The load tests which were performed during the work reported herein included

- (1) a slow loading to failure in tension and compression shortly after driving,
- (2) a slow loading to failure in tension and compression after four months of consolidation,
- (3) a series of cyclic tension tests, with the cyclic component of load being increased until progressive pullout of the pile was observed, and
- (4) a static loading to failure in tension, followed by fully-reversed large-displacement cyclic loading, resulting in the maximum degree of cyclic degradation of the shearing resistance of the soil.

The results of selected load tests performed during the research are shown in Plate 6.5. Plate 6.5 contains the load-displacement behavior measured at the pile head during the test immediately after driving, during the static load test to failure after four months of consolidation, the last cycle of the one-way tension tests, and the tension-load portion of the first and fifth cycles of reversed large-displacement loading.

The effect of 115 days of consolidation and set-up on the capacity of the pile was an approximate doubling of the capacity, from a value of 443 kips (1971 kN) immediately after driving to a value of 963 kips (4285 kN) after four months of consolidation.

Due to the elastic stretch in the pile, the peak shear transfer was not reached simultaneously at all depths along the pile; the summation of maximum shear transfer yields an ultimate pile capacity of 1070 kips (4762 kN), approximately 10 percent larger than the peak load actually measured.

The cyclic tension tests, as expected, reduced the pile capacity, with progressive pullout of the pile occurring at load levels of 720 to 740 kips (3204 to 3293 kN) (approximately 75 percent of the static pile capacity). During these tests, the progressive migration of load down the pile as the cyclic component of load was increased was clearly evident.

The reversal of shear transfer at the shallow depths under cyclic (but not reversed) pile head loads was also observed. Such behavior had earlier been postulated to occur when the recovery of elastic pile deformation during the decrease in tensile load was sufficient to yield the soil; the experiments verified the concept. Had the upper soil layers been more susceptible to cyclic degradation, the loads at which the pile was progressively moved upward would have been smaller than those observed, since the upper soils would have provided less resistance, leading to an "unzippering" effect, and the progressive downward movement of cyclic degradation in resistance with additional applications of load.

As expected, the cyclic degradation in shearing resistance was greater during the two-way cyclic tests than during those in which the plastic slip in the soil was not reversed at all points along the full length of the pile.

The distribution with depth of the peak unit shear transfer measured during the static load test to failure after four months of consolidation (taken from Plates 5.24 through 5.33) is compared in Plate 6.6 with the interpreted shear strength profile given in Plate 2.4. As seen in the plate, the values generally follow the shear strength profile, as would be expected.

The average alpha-value (ratio of shear transfer to shear strength) based on the peak values of shear transfer shown in Plate 6.6 is 0.88. The values of peak shear transfer measured during the load test immediately after driving yield an average alpha-value of 0.36.

Since the peak values of shear transfer were not reached simultaneously along the length of the pile, due to elastic axial deformation, an average alpha-value of 0.79 would be calculated, based solely on the peak pile-head load.

As noted in Section 6.3, the average degree of consolidation in the soil along the pile at the time of the second test was 83 percent. If it is assumed that the increase in the peak shear transfer after driving is directly related to the degree of consolidation, then the projected alpha value at the end of consolidation would be $0.98 (= 0.36 + (100\% / 83\%)(0.88 - 0.36))$, near the value of 1.0 which is currently used for static axial pile design in clay soils in the Gulf of Mexico.

Since the same form of t-z relationship should be expected for the soil at the end of consolidation, similar behavior should also be expected for a prototype pile, resulting in an effective alpha-value somewhat less than the projected value of unity.

The results of the experiments also suggest that the present practice of calculating ultimate pile capacity, while ignoring both consolidation time and the reductions in capacity due to progressive yielding of the soil along the pile, may lead to unconservative foundation pile designs. For pile foundations subjected to cyclic loading, the progressive cyclic degradation of the shearing resistance of the soil along the pile must also be considered.

The effects of time on pile capacity are obvious; however, if sufficient time is not allowed for the development of axial capacity between the times of pile driving and of loading the foundation, the actual capacity may be significantly less than required for the design loads. The time-rate of development of pile capacity is most important for large-diameter piles, which will have a longer set-up time, as compared with the 30-inch-diameter (76.2 cm) pile which was tested.

The maximum measured static pile head load was 90 percent of the ultimate load which would be calculated for the pile using the peak values of shear transfer. Although the reduction of 10 percent noted at this site is not a large decrease, the effects may be greater in more sensitive soils, and for piles installed in soils which exhibit a more pronounced peak to residual reduction in shear resistance.

The pullout capacity of the pile under cyclic tension loading was 720 kips (3204 kN), only 75 percent of the measured static pile capacity, and 59 percent of that which would be predicted using standard design methods and an alpha value of 1.0. Again, this comparison indicates that the design of pile foundations subjected to cyclic loading must include consideration of the degree of consolidation (and pile capacity) at the time the piles are loaded, and must also consider the possible effects of progressive cyclic degradation. As noted above, the actual pile capacity may be significantly less than predicted using standard design practice, and the effect appears to be greater in more highly plastic and sensitive clays.

6.5 Conclusions

The successful completion of the experiments on the near-full-scale instrumented pile has resulted in the collection of a unique set of pile-soil interaction information. The collection of data from the instruments along the pile for an extended period of time, with load tests performed at three stages in the consolidation process (only two of which are reported in this volume), has added greatly to the knowledge of the behavior of axially loaded piles, whether the nature of the loading be tensile or compressive.

The data provide a sound basis for the development of design methods for axial pile design in normally consolidated clays, and will furnish much needed information to be used to evaluate or develop existing and future total stress and effective stress approaches to axial pile design.

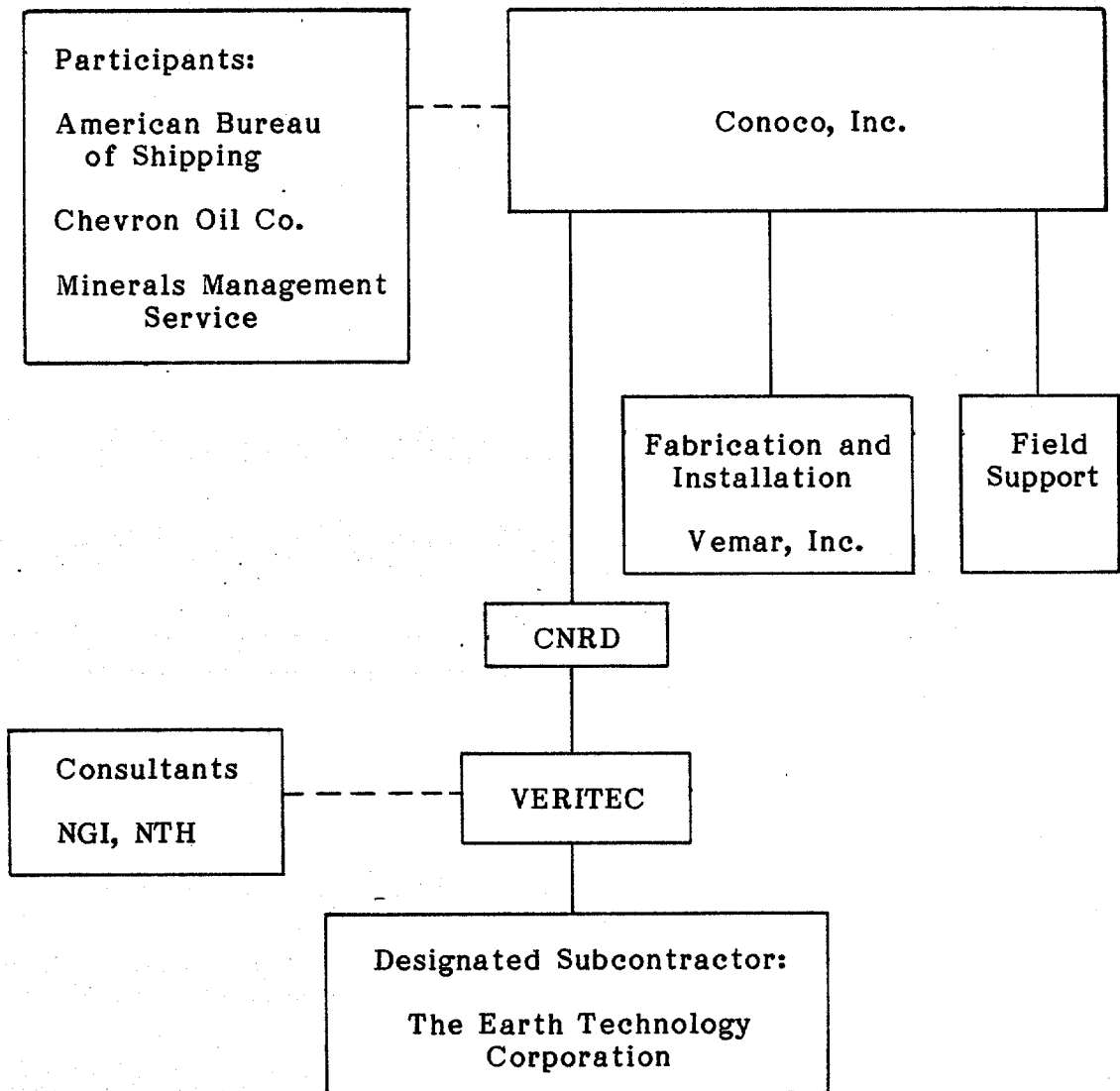
The results of these experiments, coupled with the results of the small diameter pile segment model experiments in borings at the same site, the long-term load tests performed sixteen months after driving, and the analytical procedures now under development, will serve to broaden the range of application of the results of the experiments.

REFERENCES

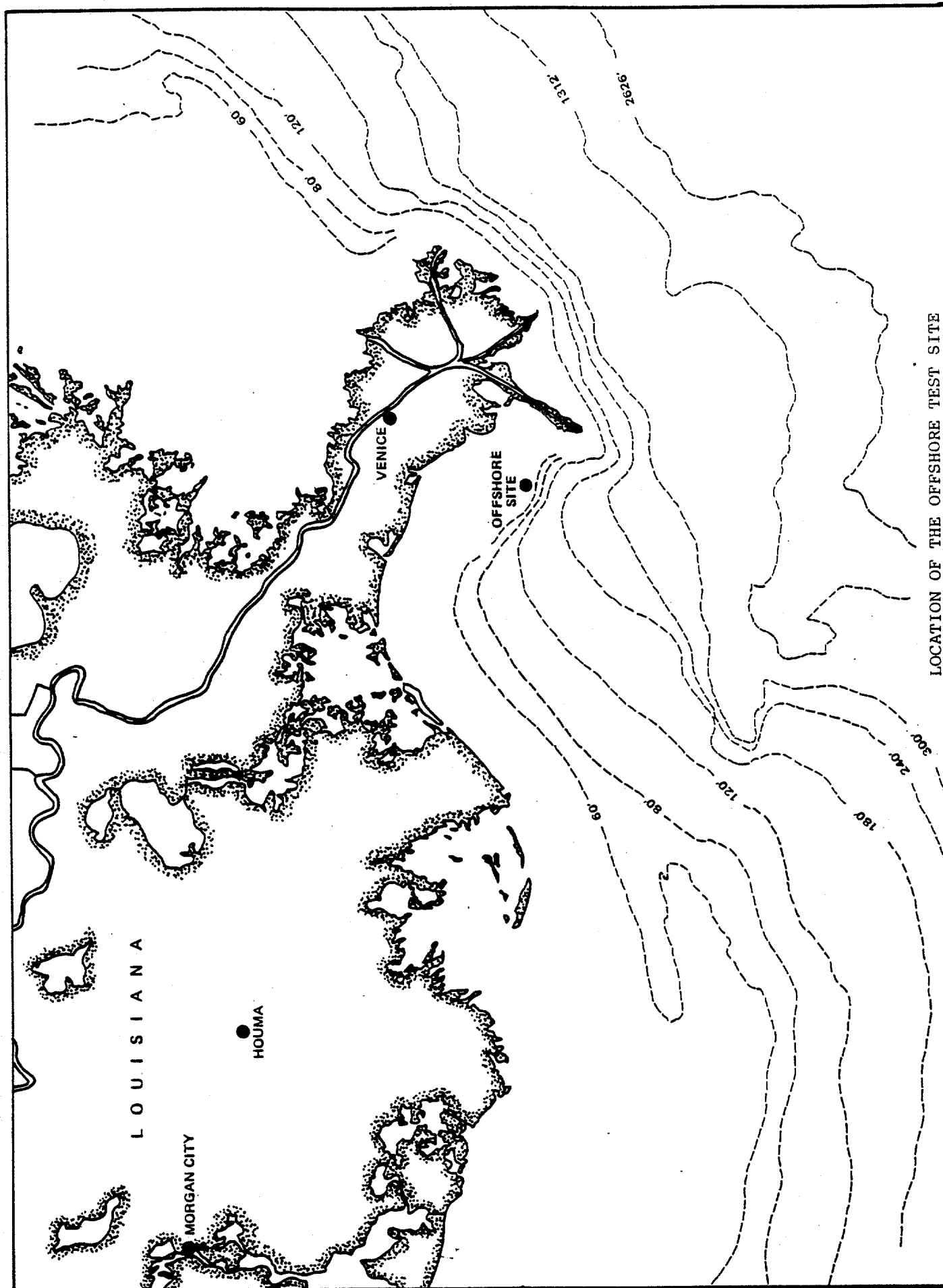
1. Final Technical Report, CNRD Subproject 13-1 Tension Pile Planning Study, Report No. 81-204, 28 August, 1981.
2. Volume I: Site Investigation and Soil Characterization Study at Block 58A, West Delta Area, Gulf of Mexico, CNRD Project 13-2 Tension Pile Study, Report No. 82-200-1, April 1982.
3. Volume II. Plan for Performing Offshore Small-Diameter Pile Segment Tests, CNRD Project 13-2 Tension Pile Study, Report No. 82-200-2, August, 1982.
4. Volume III: Final Report on Small-Diameter Pile Segment Tests, CNRD Project 13-2 Tension Pile Study, Interim Technical Report No. 82-200-01, August, 1983.
6. Final Report, CNRD 13-2: Tension Pile Study, Veritec Report No. 84-3361, June, 1984.
7. Norwegian Geotechnical Institute, "Piezometer Readings up to 3.10.83", CNRD 13-2, West Delta, Block 58A, Gulf of Mexico, 10 April 1984.

APPENDIX 1

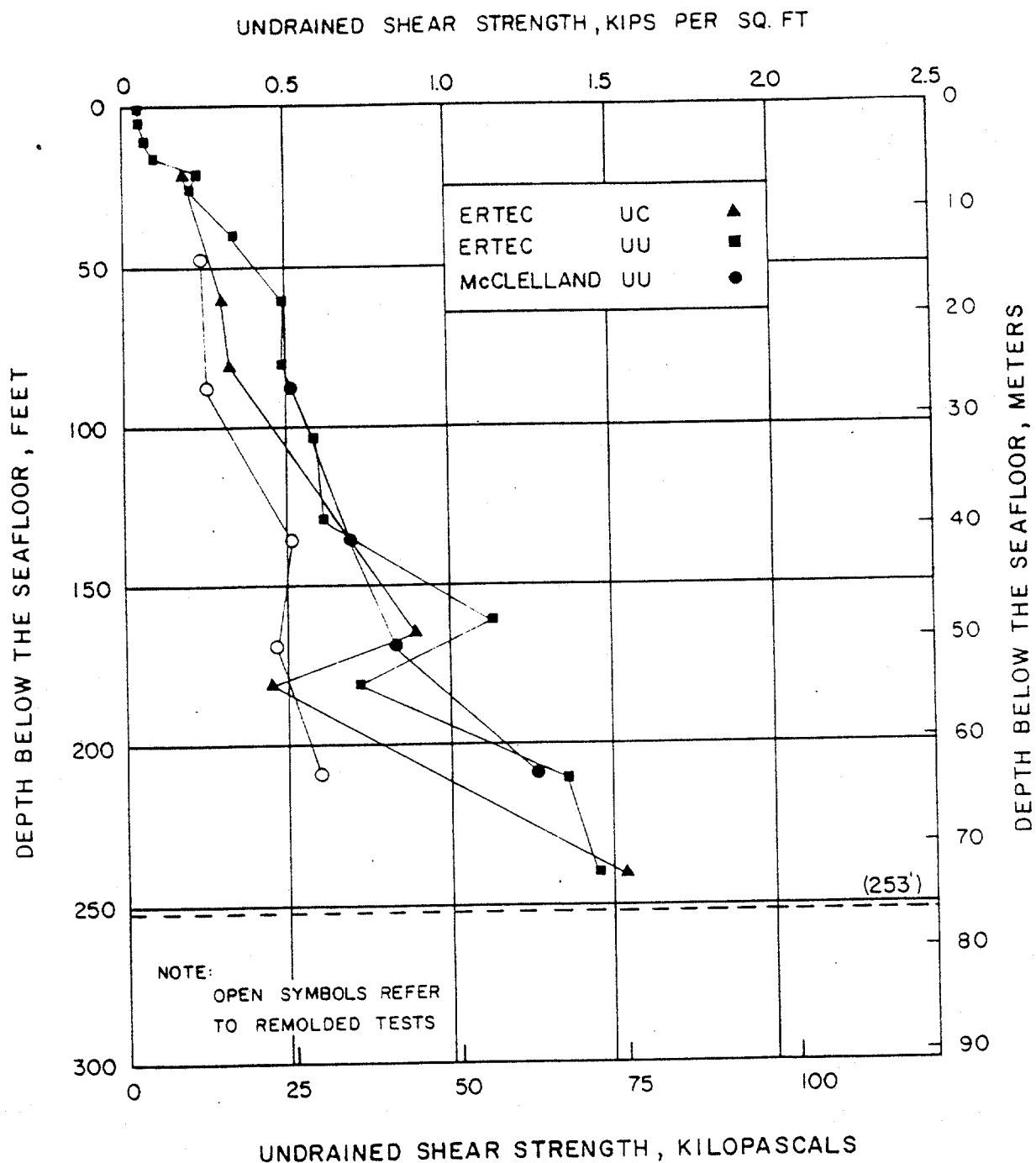
ILLUSTRATION FOR CHAPTER 1



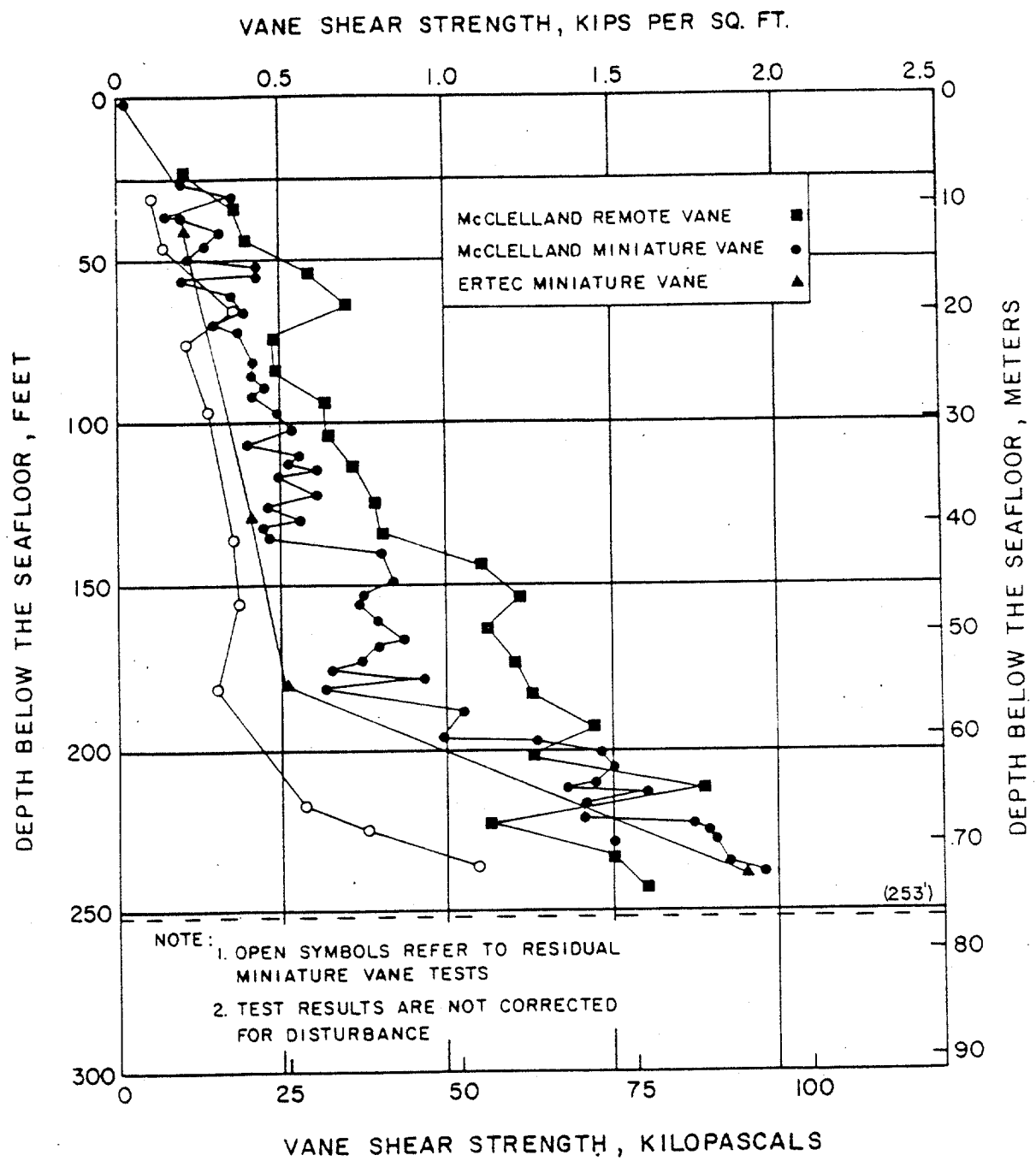
PROJECT ORGANIZATION CHART

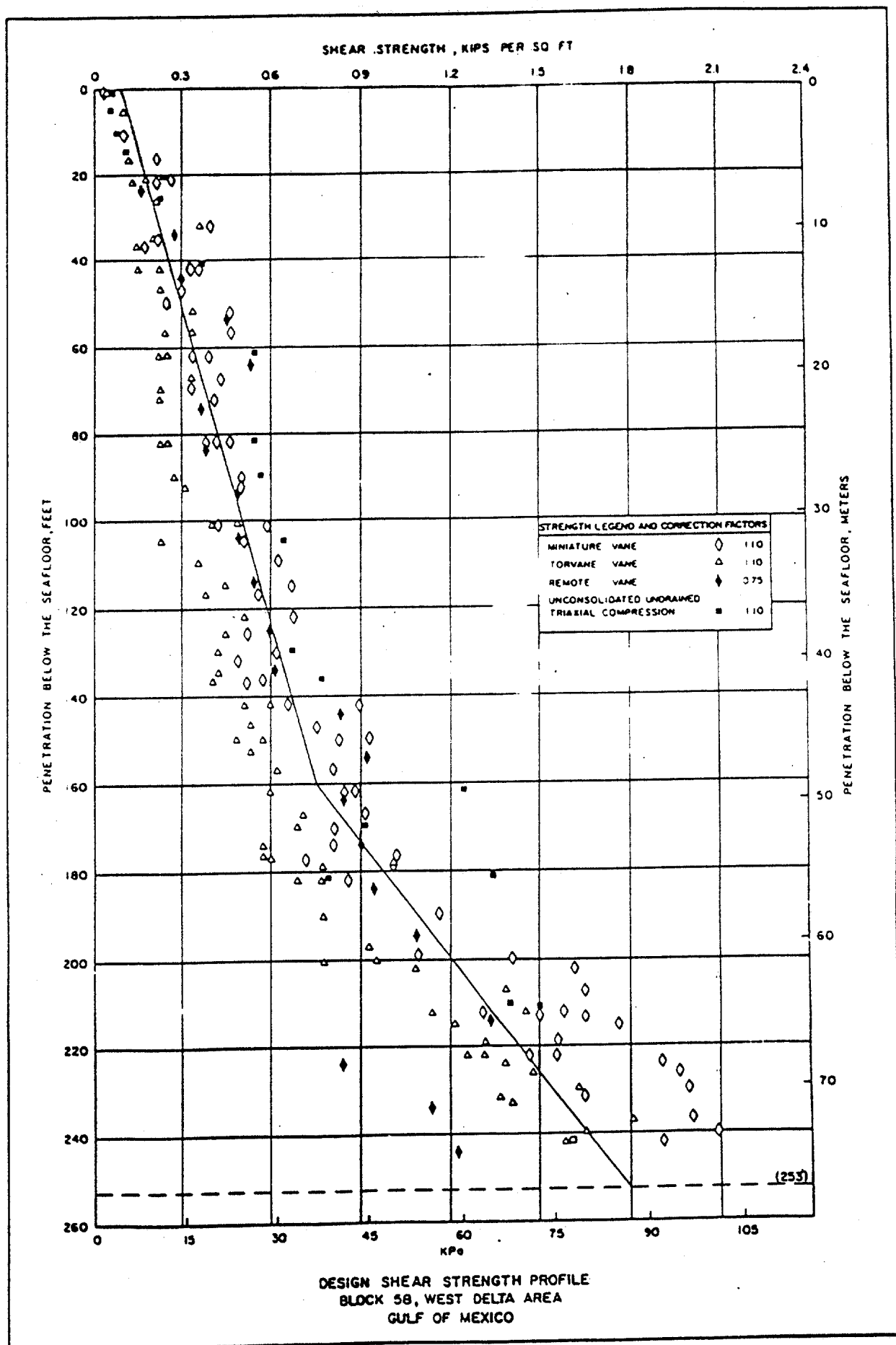


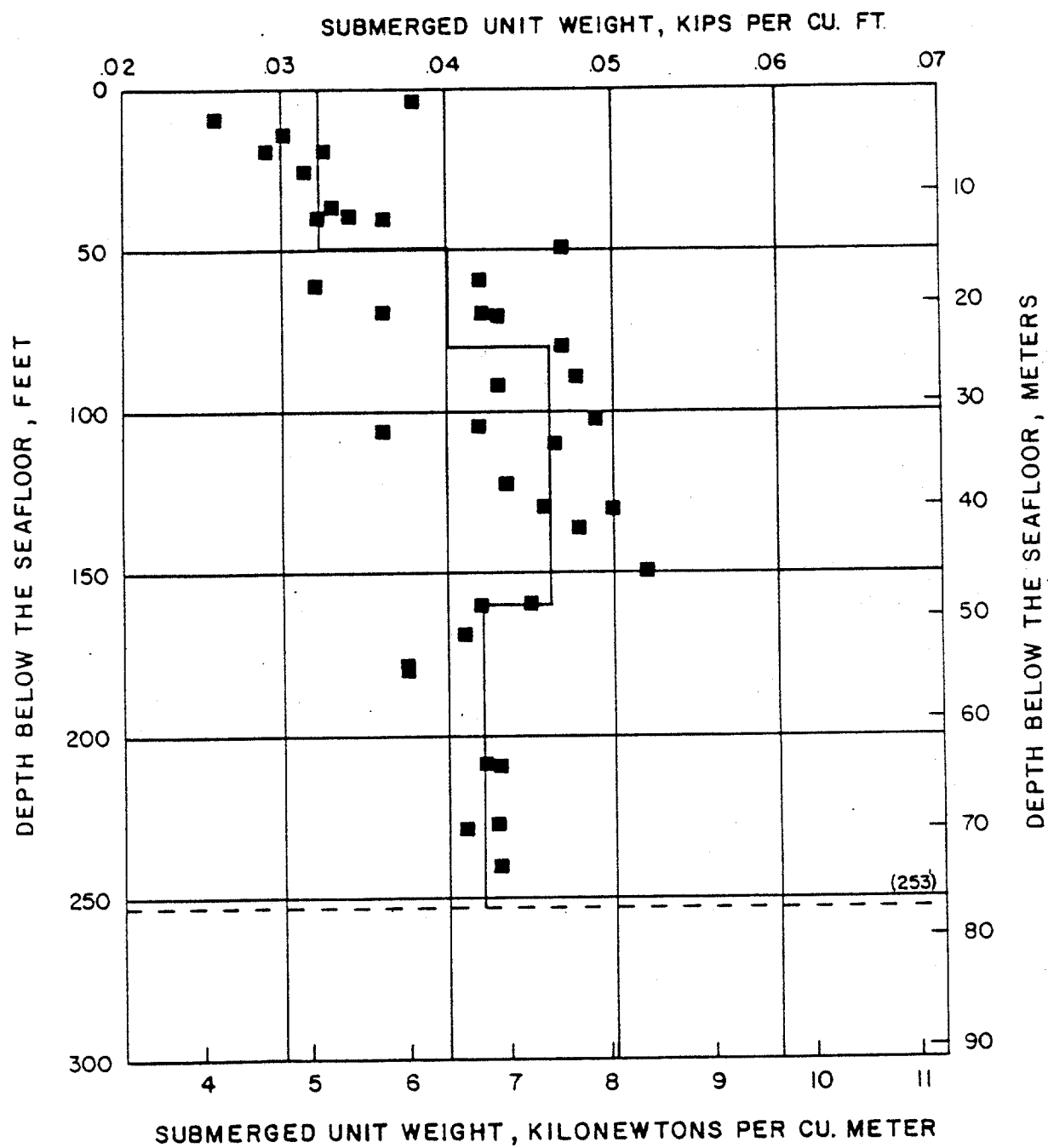
LOCATION OF THE OFFSHORE TEST SITE



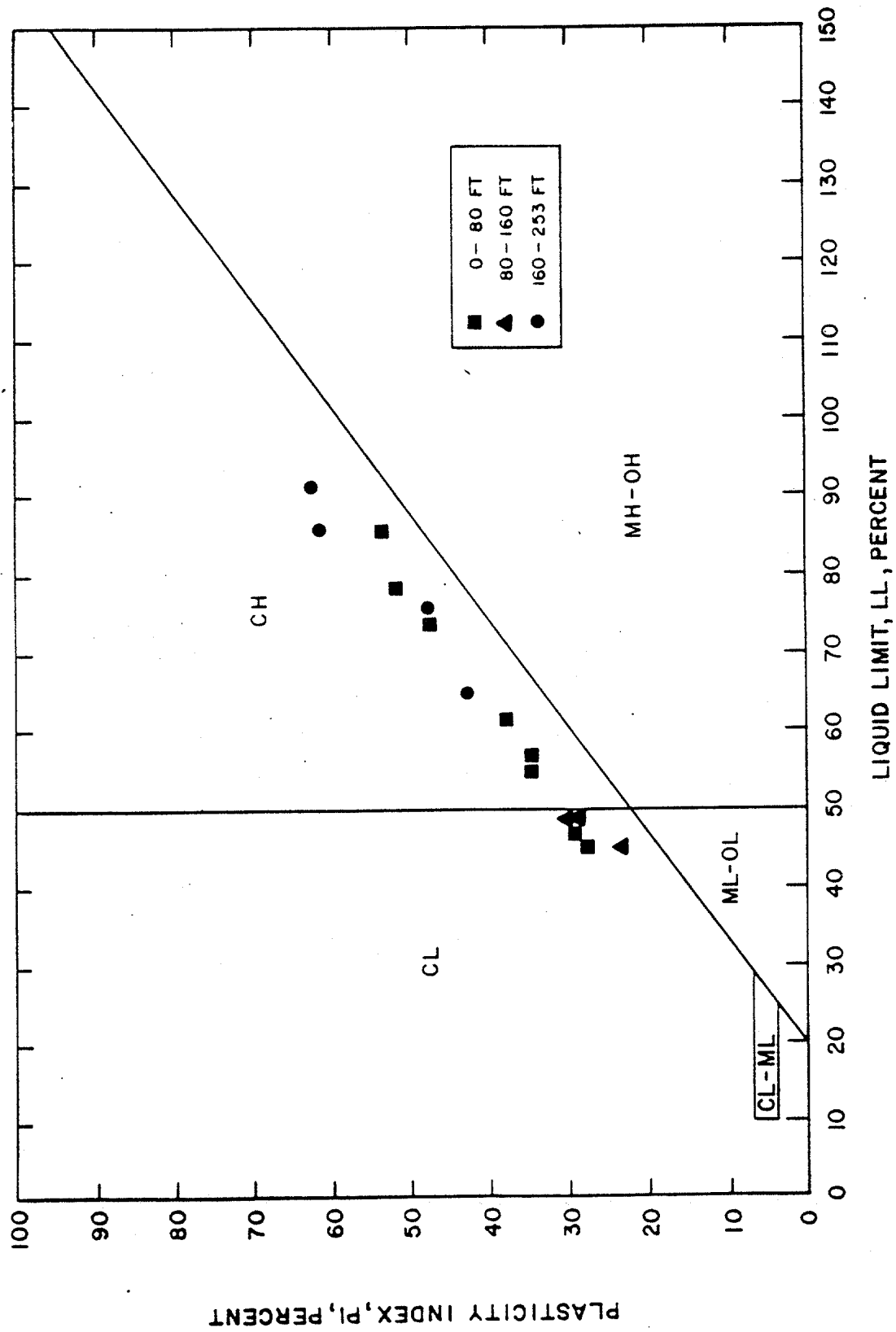
UNDRAINED SHEAR STRENGTH VERSUS PENETRATION
UU AND UC TESTS







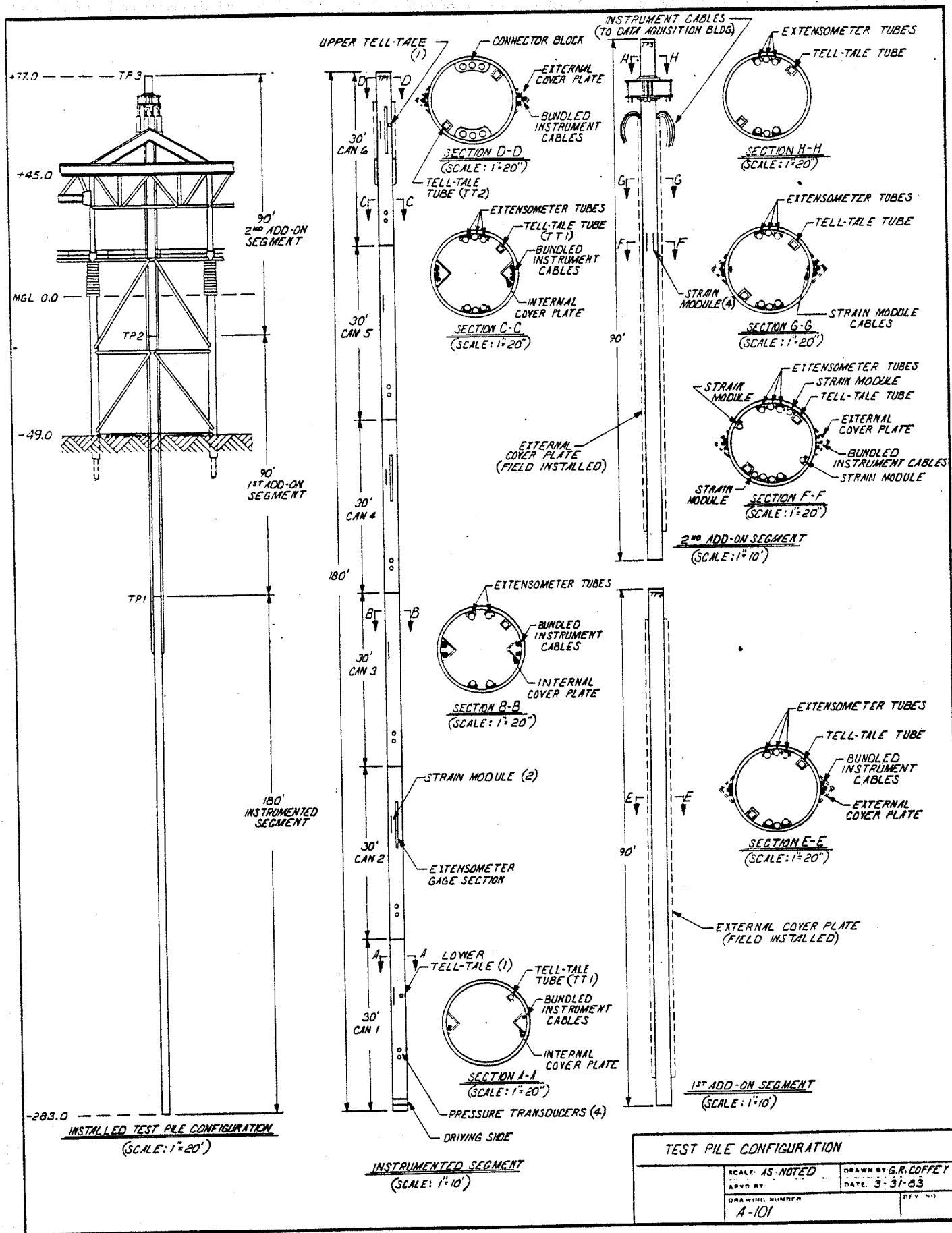
SUBMERGED UNIT WEIGHT PROFILE
BLOCK 58, WEST DELTA AREA
GULF OF MEXICO



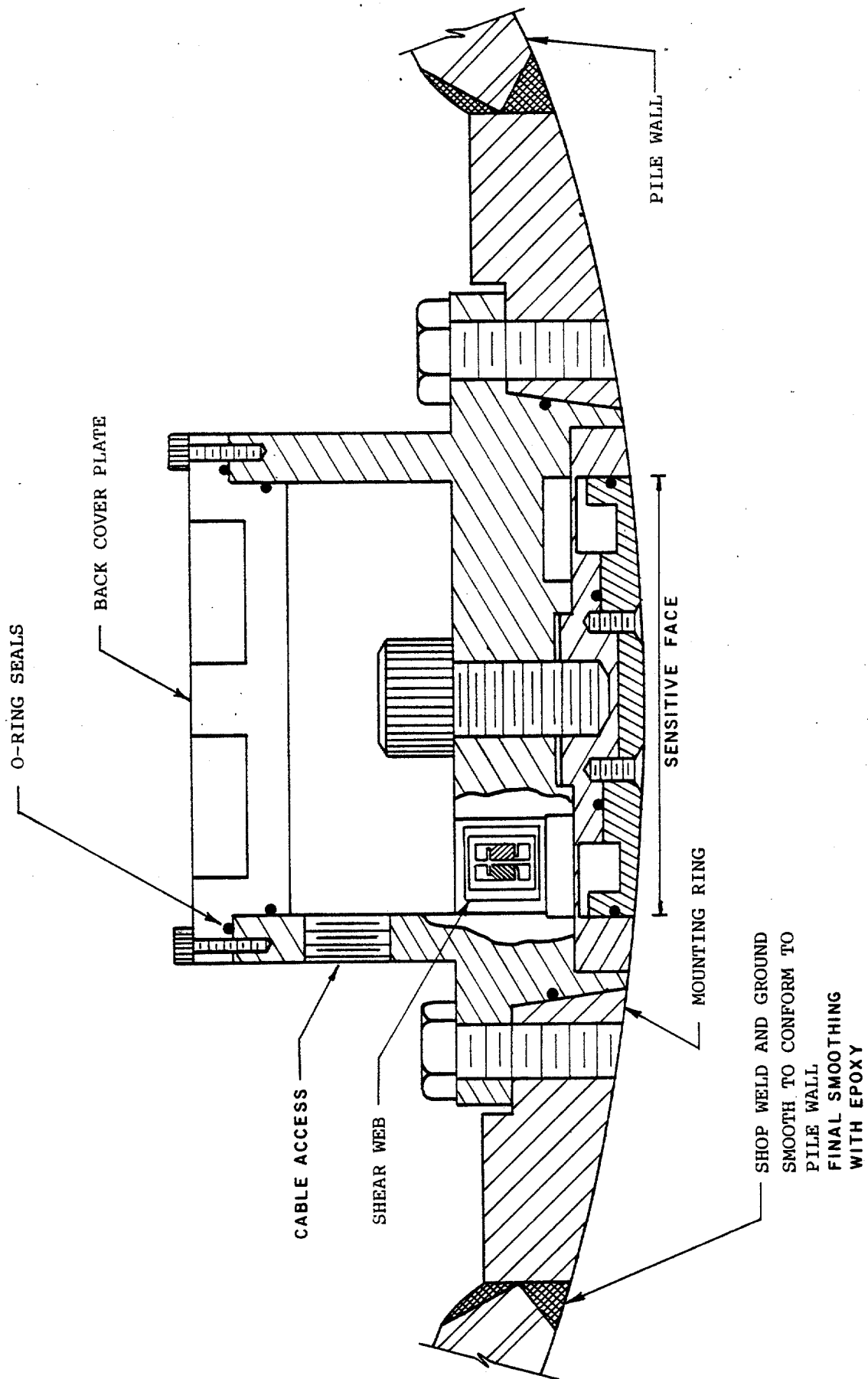
PLASTICITY CHART
BLOCK 58, WEST DELTA AREA

APPENDIX 3

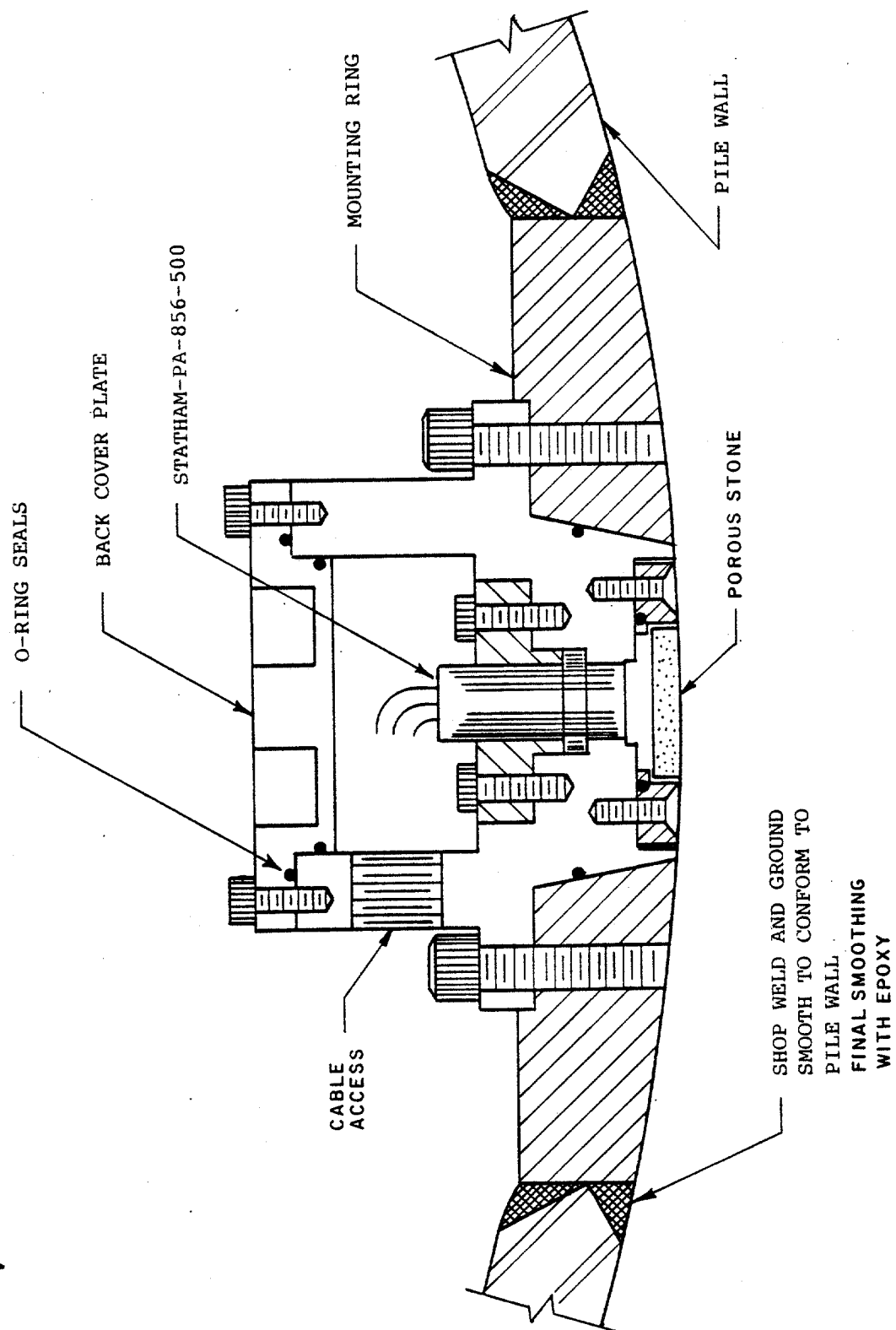
ILLUSTRATIONS FOR CHAPTER 3



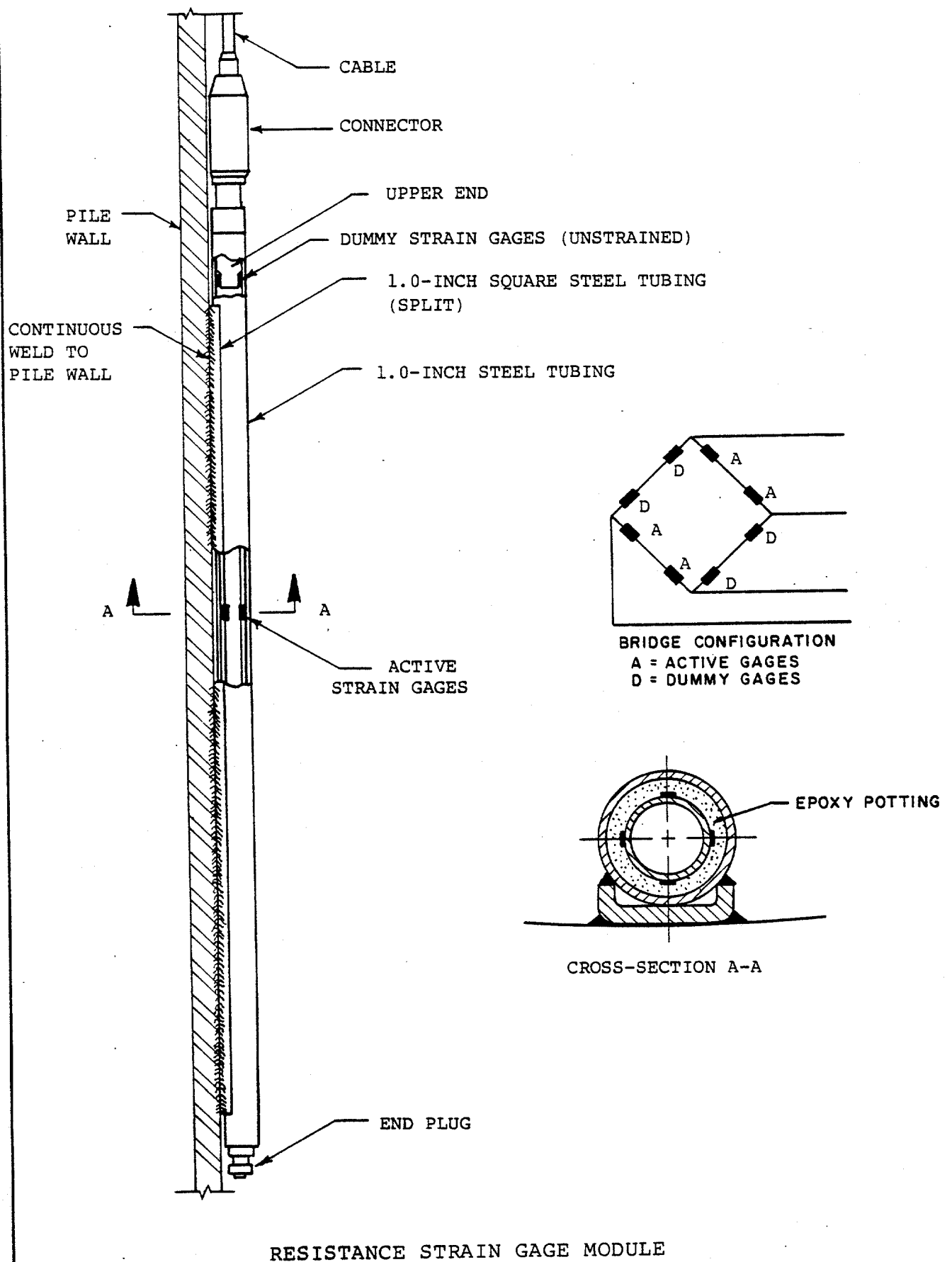
SCHEMATIC DIAGRAM OF INSTRUMENT PLACEMENT

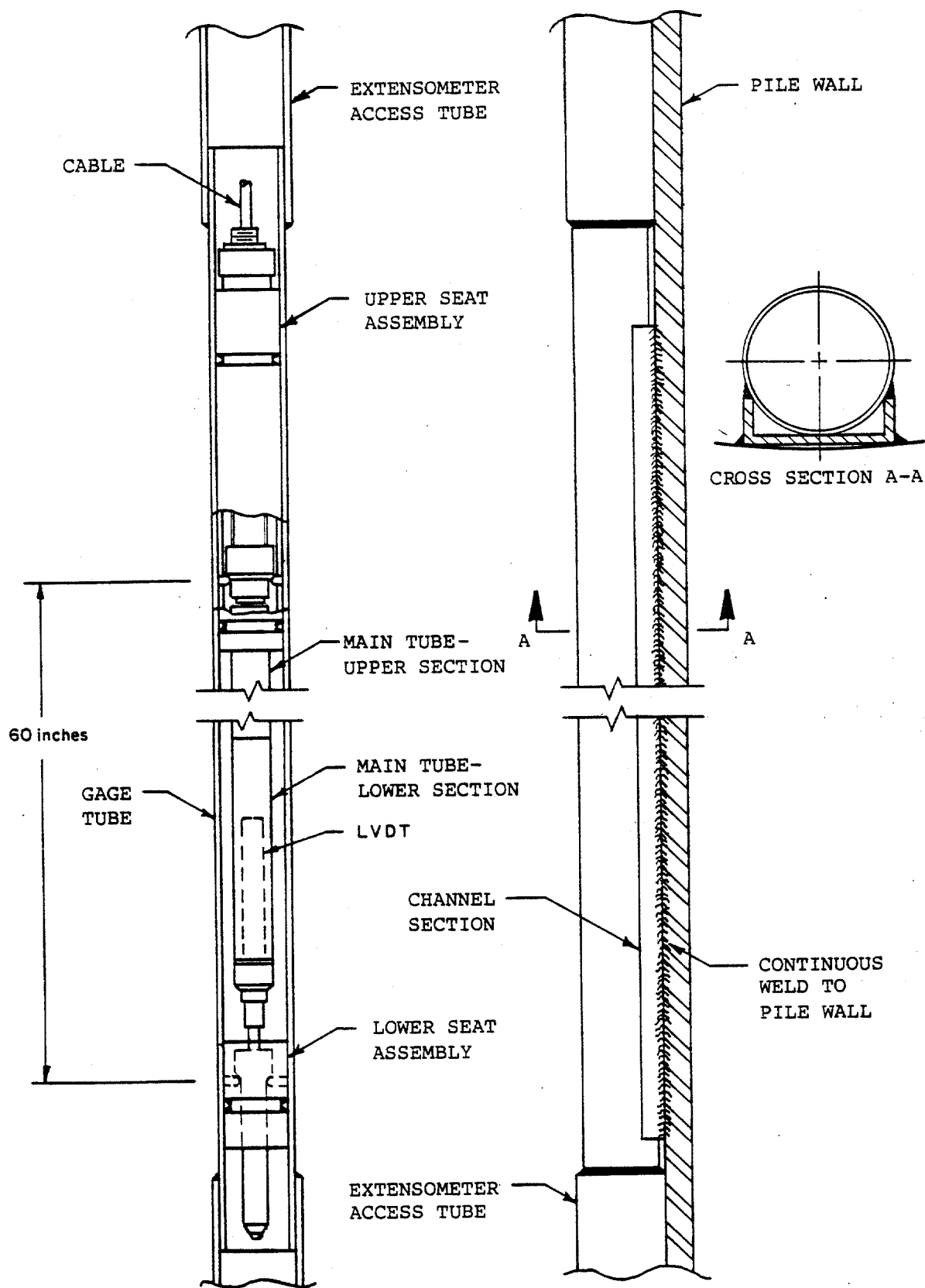


TOTAL PRESSURE TRANSDUCER



PORE PRESSURE TRANSDUCER

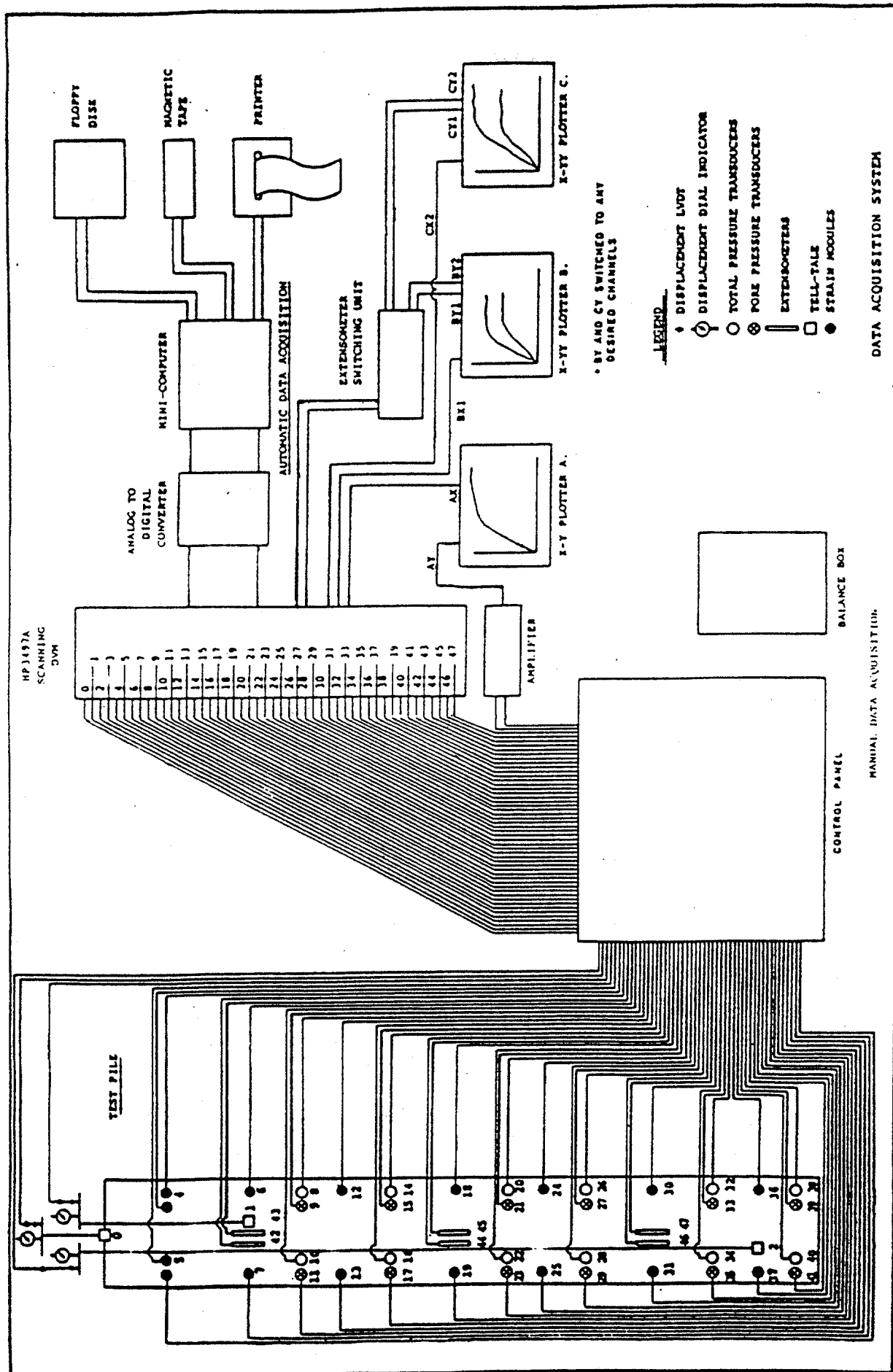




EXTENSOMETER UNIT

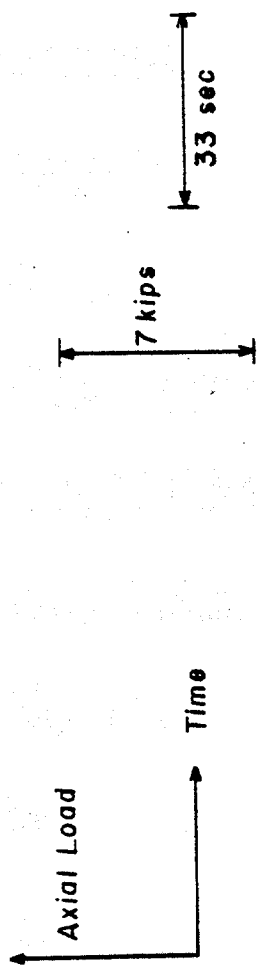
APPENDIX 2

ILLUSTRATIONS FOR CHAPTER 2



INSTRUMENT CHANNEL NUMBERING SYSTEM

CHANNEL NUMBER	ELEVATION, FT. (MUDLINE=0)	INSTRUMENT TYPE	CALIBRATION FACTORS
00	+105	LVDT	- 0.476
01	- 62	LVDT	- 0.294
02	-212	LVDT	- 0.294
03	N/A	SHORTED INPUT	
04	+ 90	STRAIN MODULE	127180
05	+ 90	STRAIN MODULE	127180
06	- 62	STRAIN MODULE	137970
07	- 62	STRAIN MODULE	137970
08	- 80	TOTAL PRESSURE	- 3439
09	- 78	PORE PRESSURE	3636
10	- 78	TOTAL PRESSURE	- 3439
11	- 80	PORE PRESSURE	3191
12	- 92	STRAIN MODULE	107750
13	- 92	STRAIN MODULE	107750
14	-110	TOTAL PRESSURE	- 3373
15	-108	PORE PRESSURE	3240
16	-110	TOTAL PRESSURE	- 3383
17	-108	PORE PRESSURE	3742
18	-122	STRAIN MODULE	110040
19	INOP		
20	-140	TOTAL PRESSURE	- 3395
21	-138	PORE PRESSURE	3751
22	-138	TOTAL PRESSURE	- 3377
23	-140	PORE PRESSURE	3804
24	-152	STRAIN MODULE	109920
25	INOP		
26	-170	TOTAL PRESSURE	- 3448
27	-168	PORE PRESSURE	3646
28	-168	TOTAL PRESSURE	- 3448
29	-170	PORE PRESSURE	3635
30	-182	STRAIN MODULE	112480
31	-182	STRAIN MODULE	112480
32	-200	TOTAL PRESSURE	- 3443
33	-198	PORE PRESSURE	3733
34	-198	TOTAL PRESSURE	- 3376
35	-200	PORE PRESSURE	3734
36	-212	STRAIN MODULE	106620
37	-212	STRAIN MODULE	106620
38	-225	TOTAL PRESSURE	- 3400
39	-223	PORE PRESSURE	3724
40	-223	TOTAL PRESSURE	- 3376
41	-225	PORE PRESSURE	3646
42	- 62	EXTENSOMETER	- 643.1
43	- 62	EXTENSOMETER	- 643.1
44	-122	EXTENSOMETER	- 531.9
45	-122	EXTENSOMETER	- 531.9
46	-182	EXTENSOMETER	- 545.5
47	-182	EXTENSOMETER	- 545.5



Channel

06

Depth = 62 ft

07

12

Depth = 92 ft

13

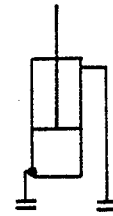
30

Depth = 182 ft

31

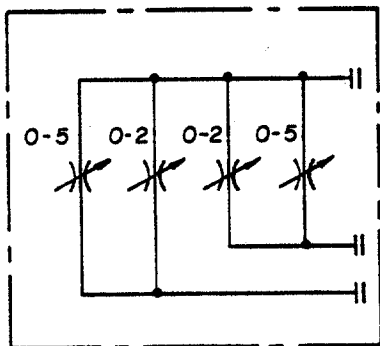
APPENDIX 4

ILLUSTRATIONS FOR CHAPTER 4

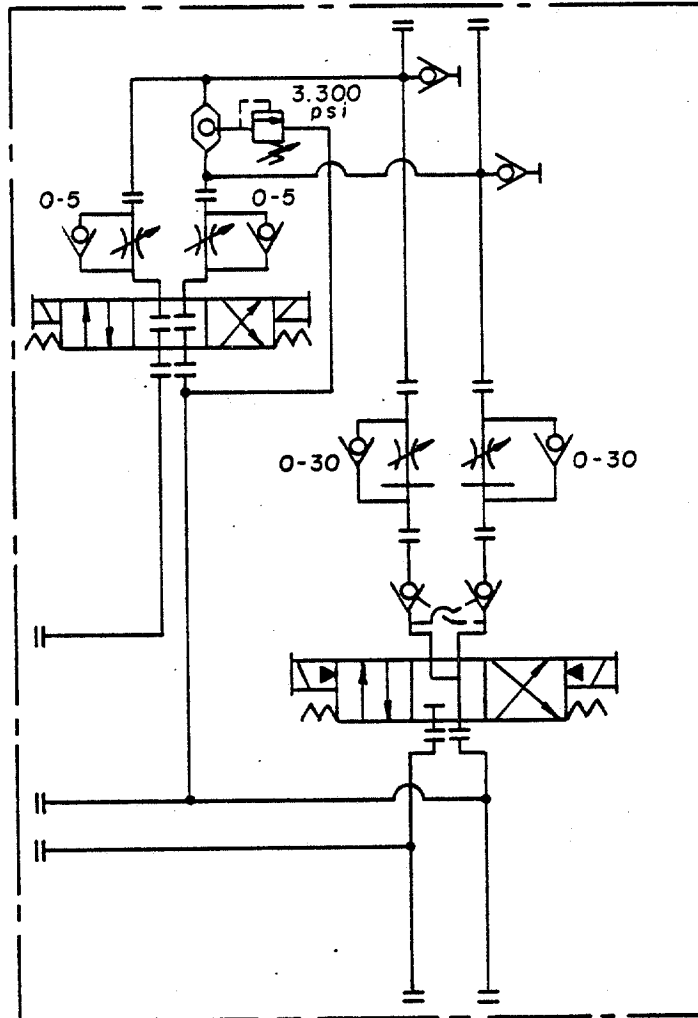


Hydraulic
Ram

0-5 gpm
Hydraulic
Circuit for
Static Tests



Manually - Operated
Hydraulic Control
Circuit for Static Tests

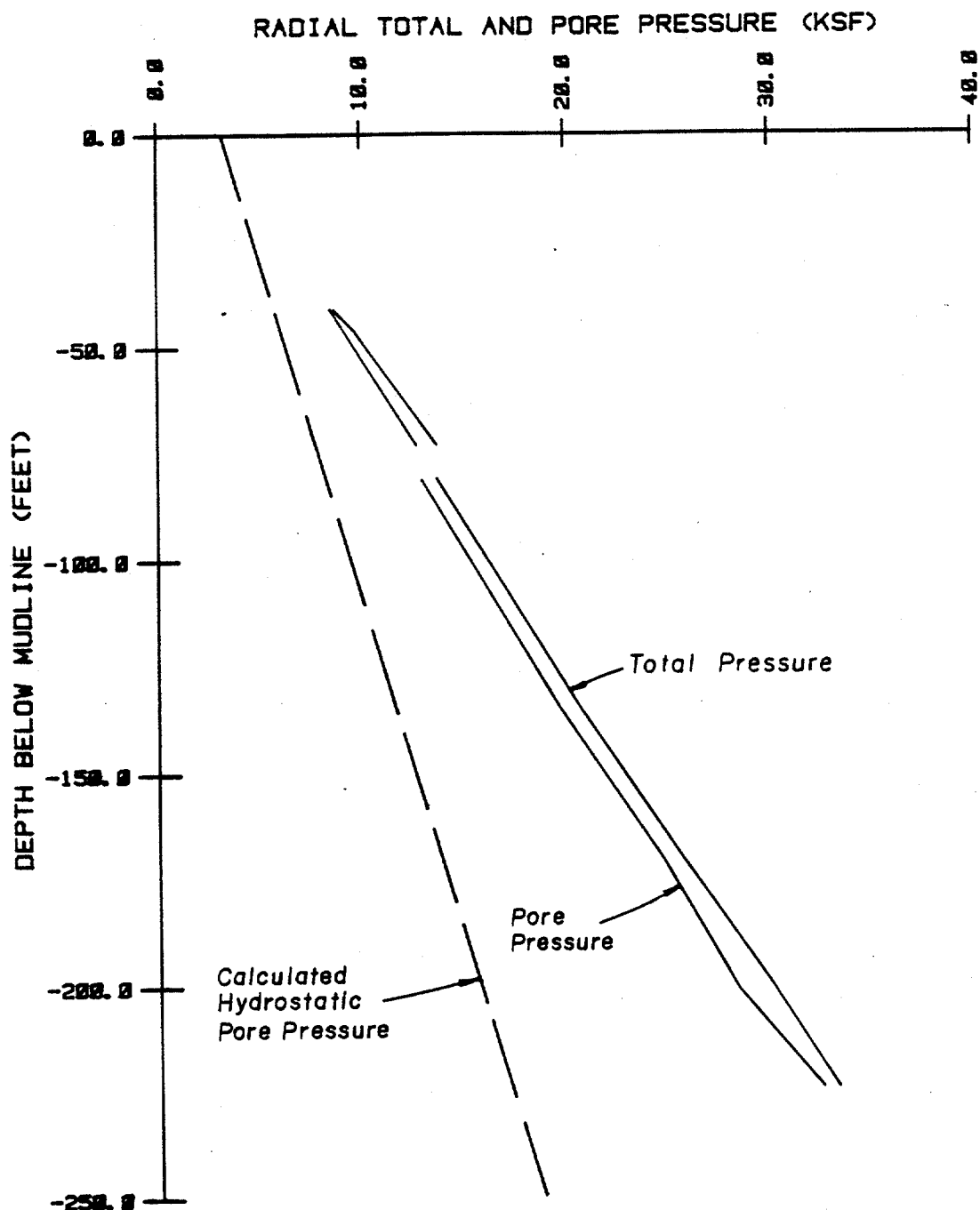


0-30 gpm
Hydraulic
Circuit for
Cyclic Tests

Pressure Return

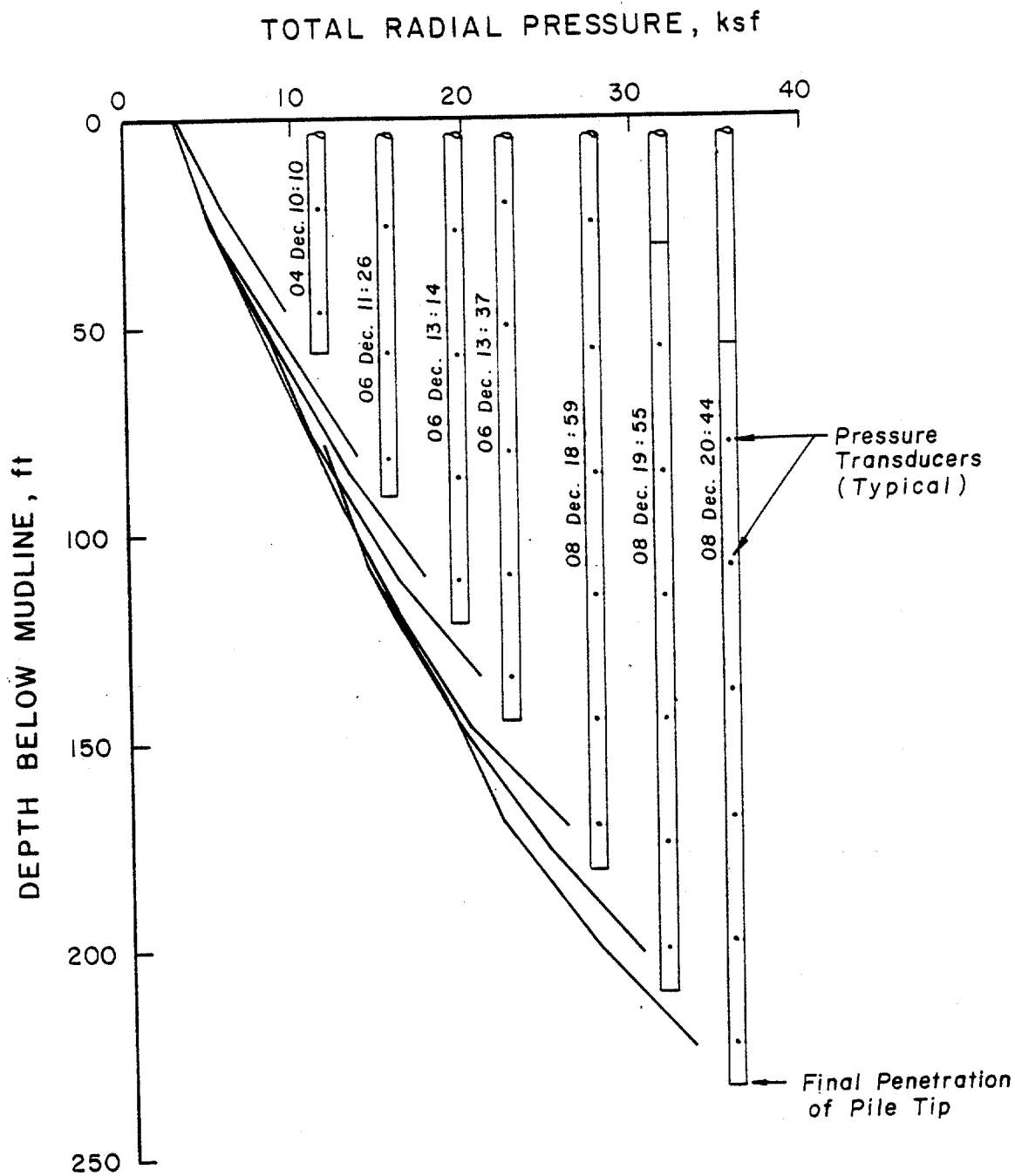
SCHEMATIC DIAGRAM OF HYDRAULIC SYSTEM

APPENDIX 5
ILLUSTRATIONS FOR CHAPTER 5



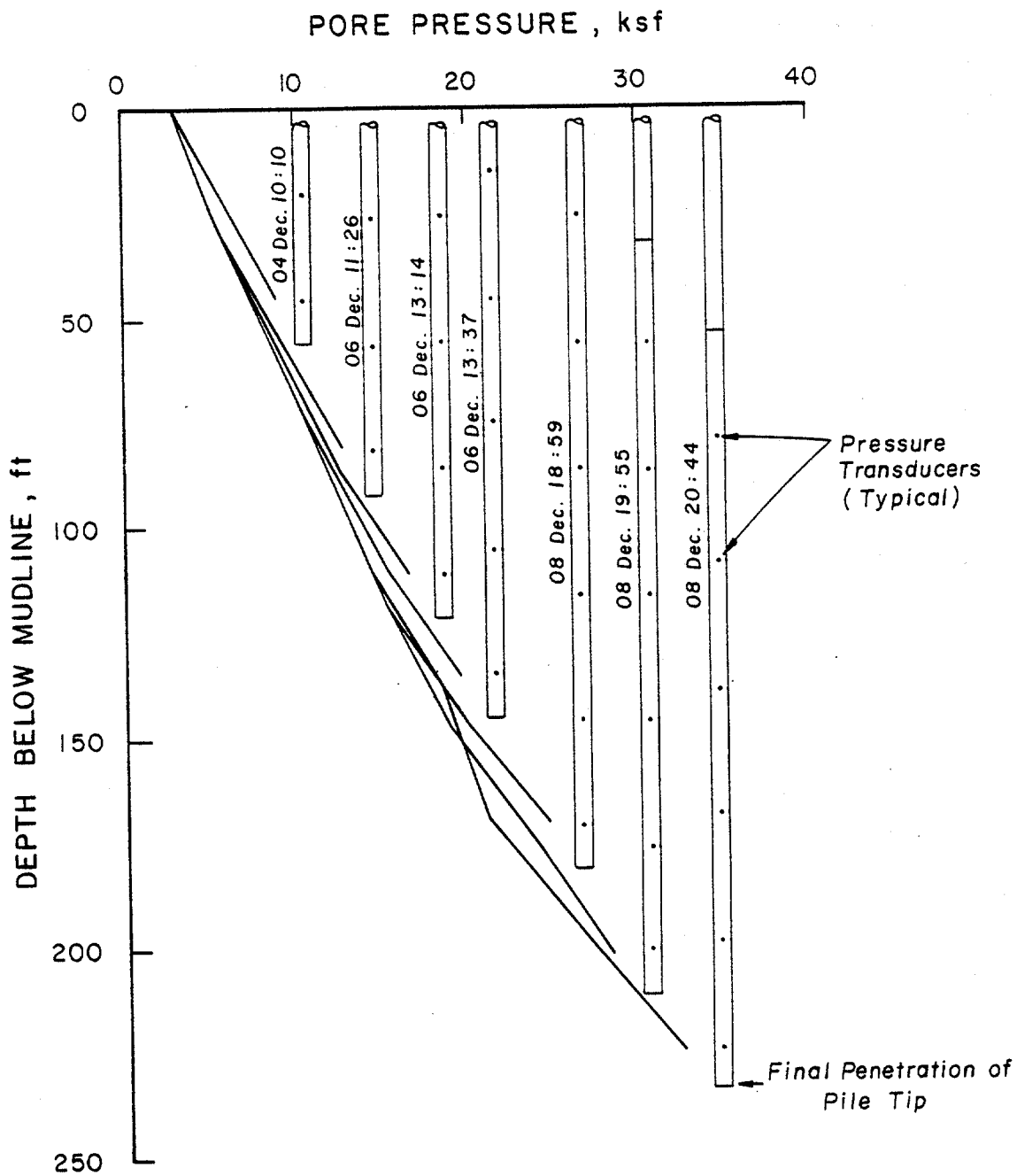
MAXIMUM TOTAL AND PORE PRESSURES RECORDED BY PRESSURE TRANSDUCERS
IN CAN 1 DURING INSTALLATION OF PILE

(1 inch = 25.4 mm, 1 ft = 0.305 m, 1 kip = 4.45 kN, 1 ksf = 47.9 kPa)



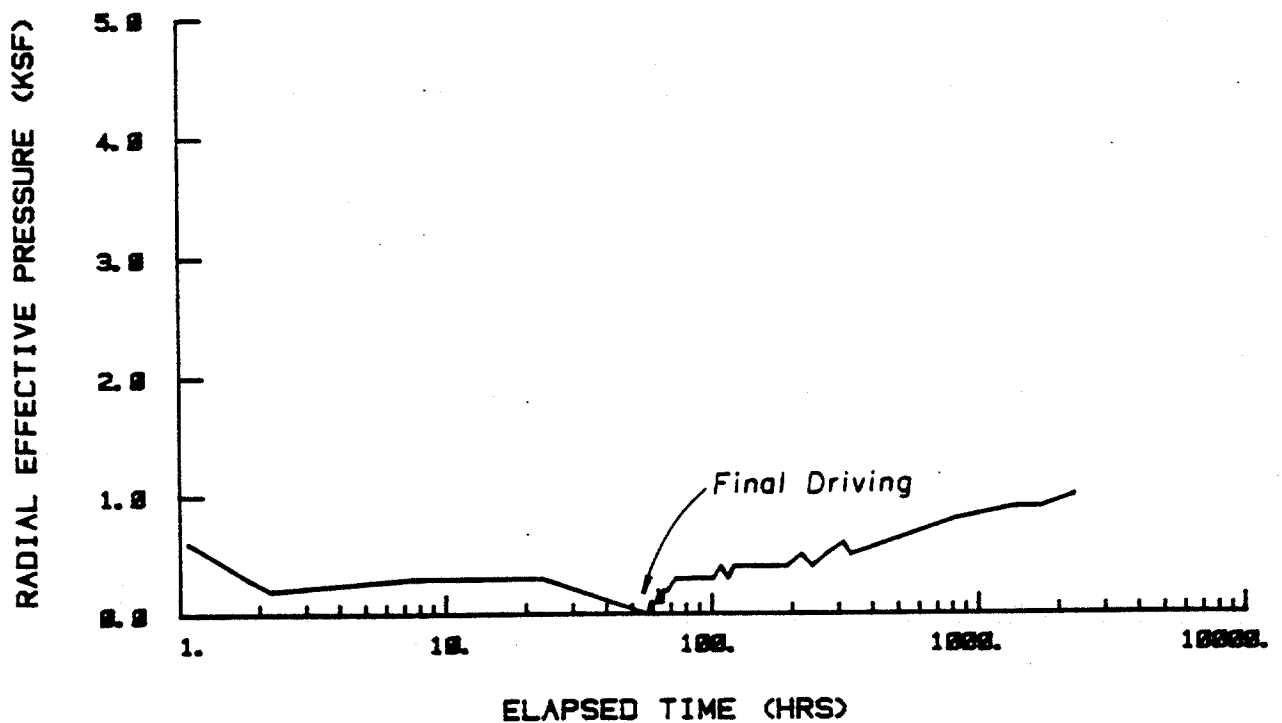
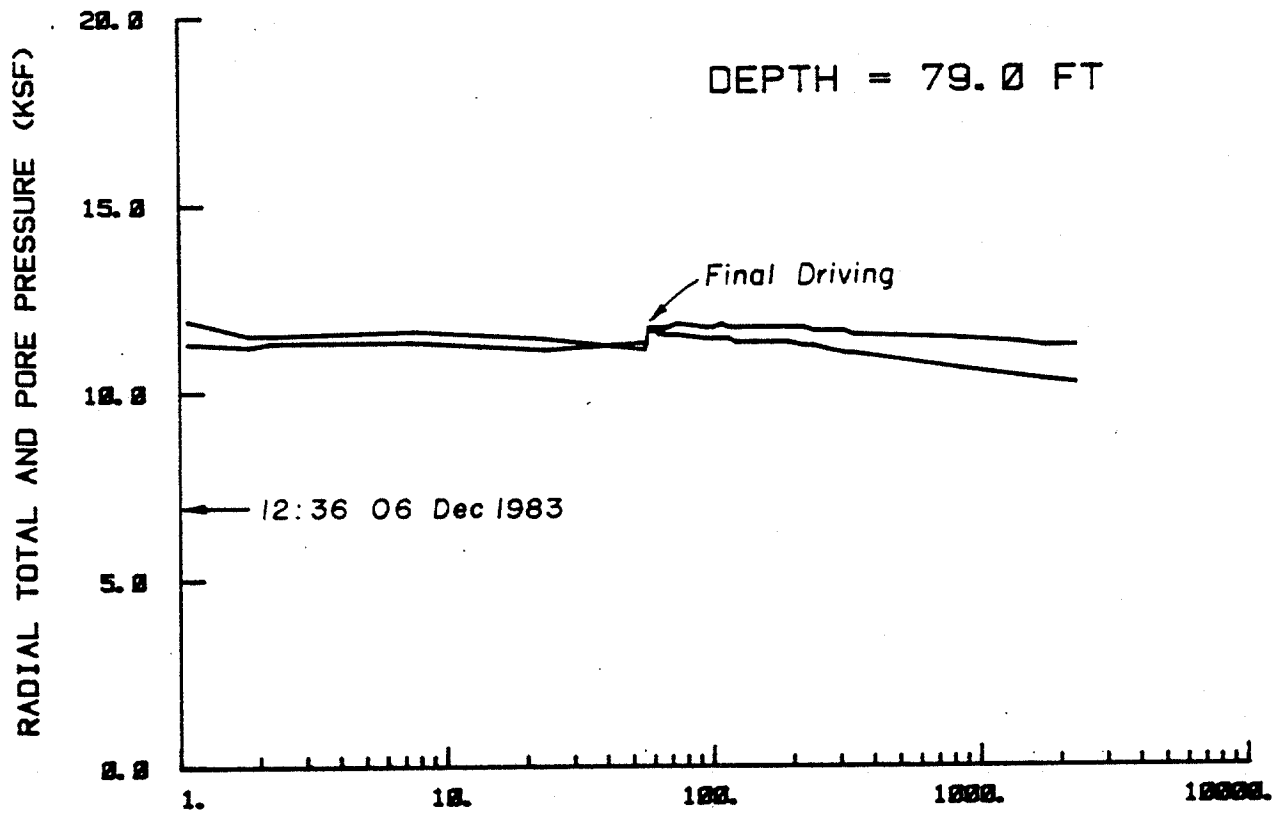
TOTAL RADIAL PRESSURES ALONG PILE AT VARIOUS TIMES DURING INSTALLATION

(1 inch = 25.4 mm, 1 ft = 0.305 m, 1 kip = 4.45 kN, 1 ksf = 47.9 kPa)

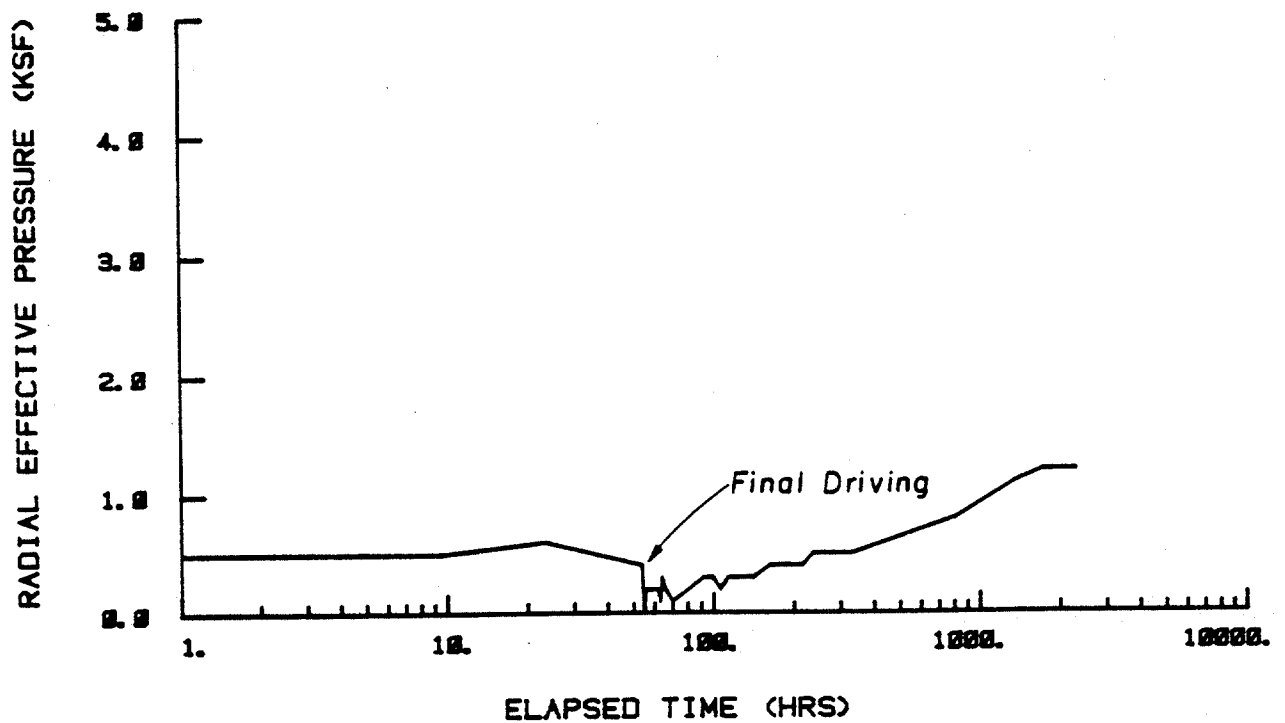
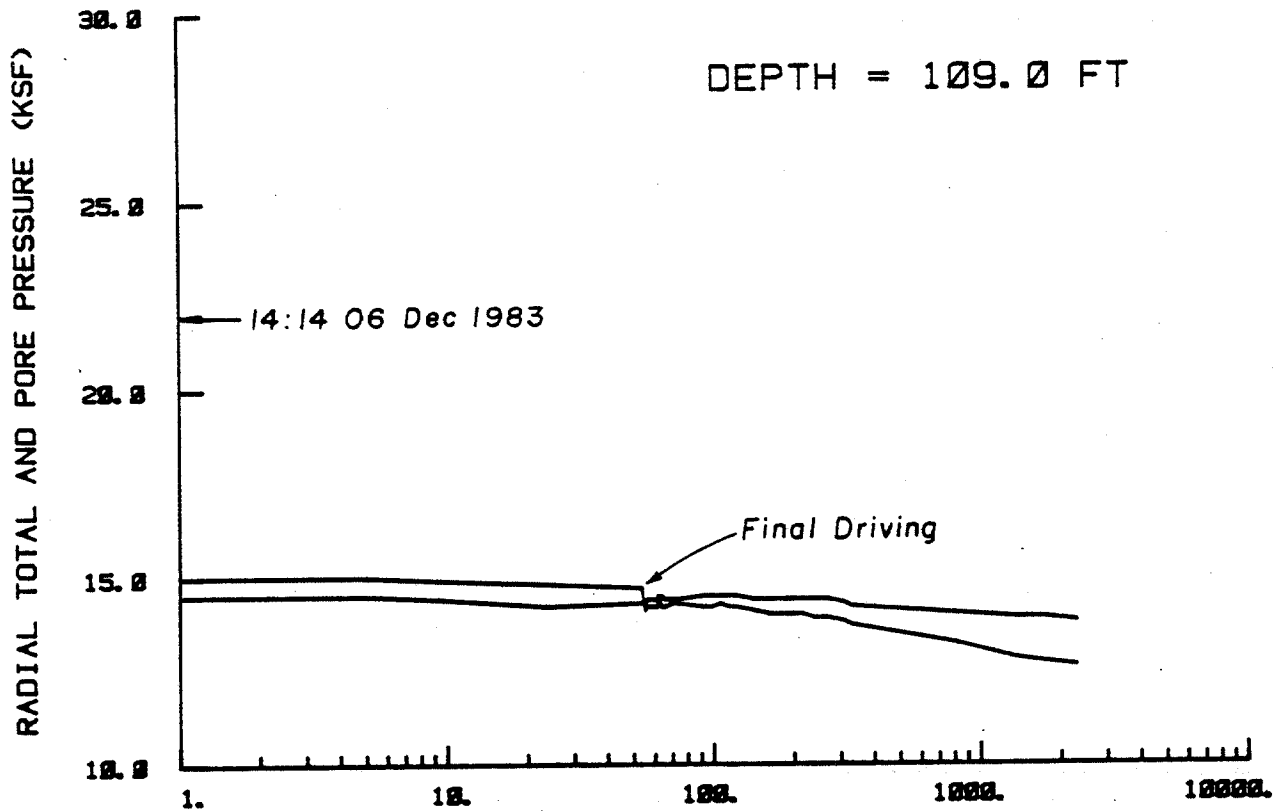


PORE PRESSURES ALONG PILE AT VARIOUS TIMES DURING INSTALLATION

(1 inch = 25.4 mm, 1 ft = 0.305 m, 1 kip = 4.45 kN, 1 ksf = 47.9 kPa)



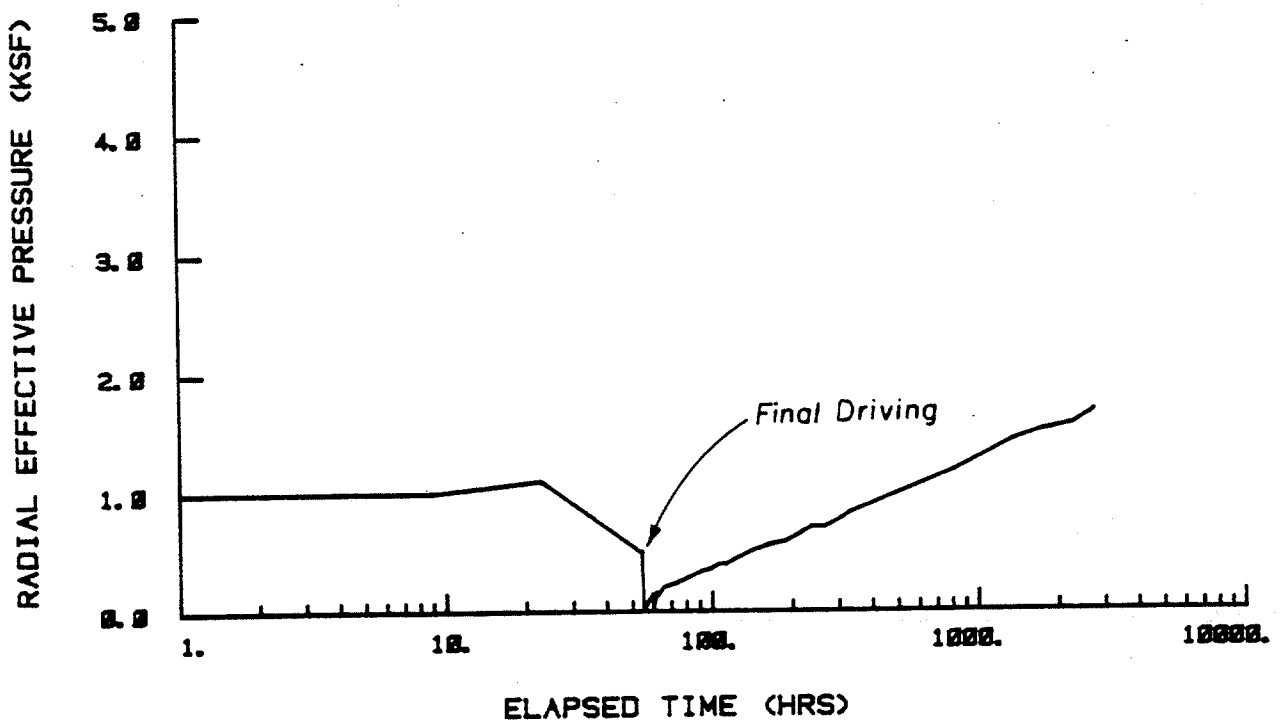
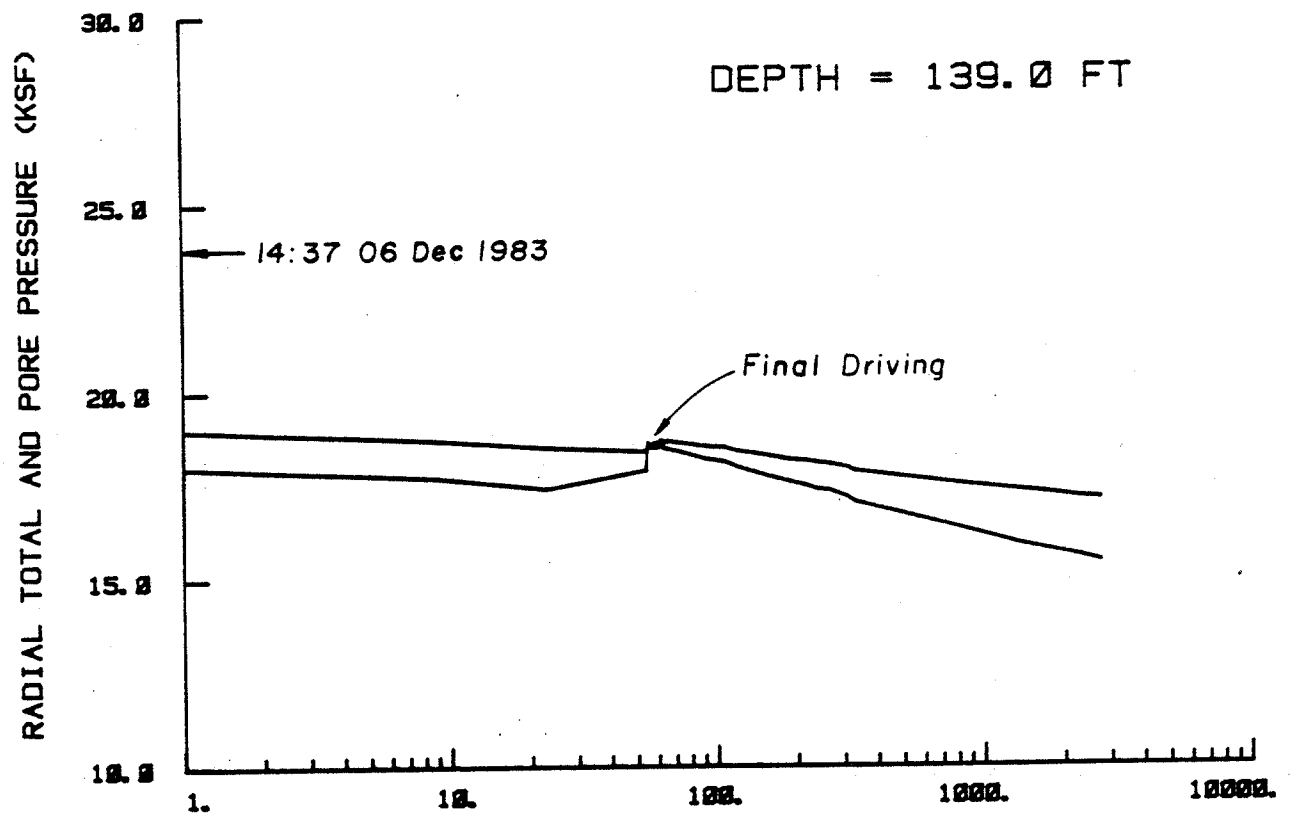
SOIL PRESSURES AT THE 79-FOOT DEPTH DURING CONSOLIDATION
 (1 inch = 25.4 mm, 1 ft = 0.305 m, 1 kip = 4.45 kN, 1 ksf = 47.9 kPa)



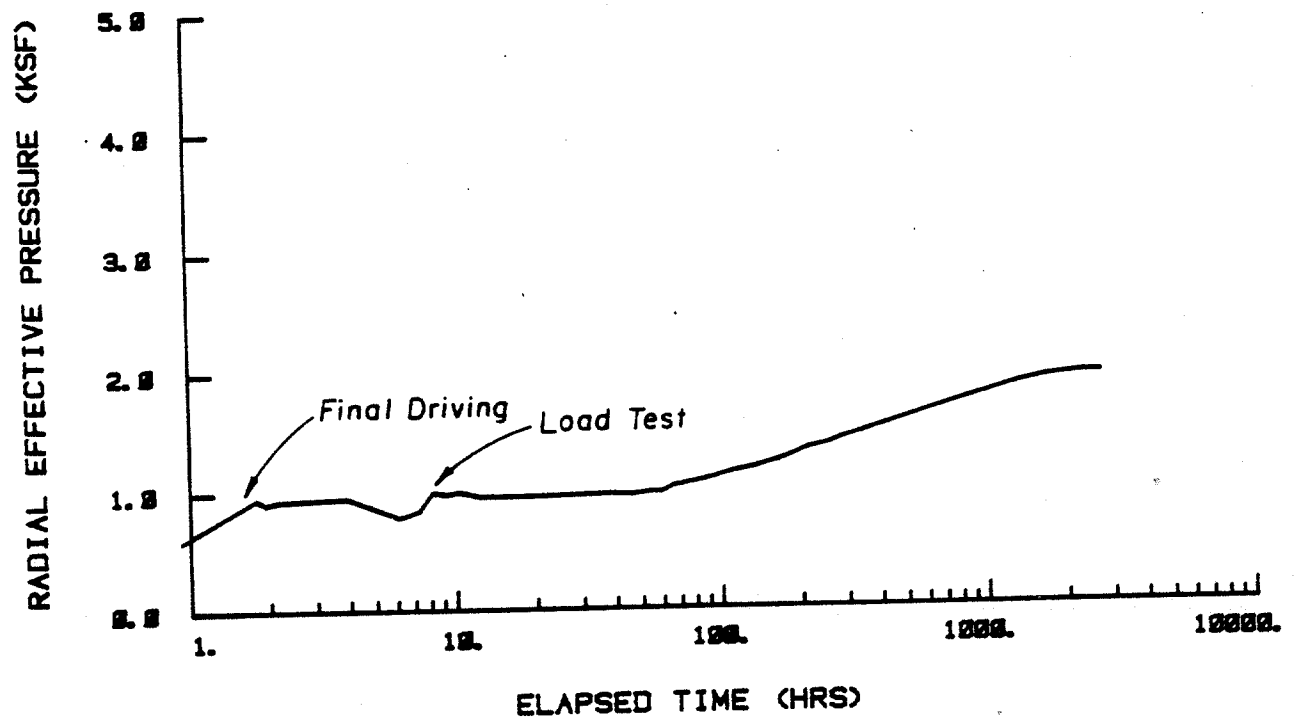
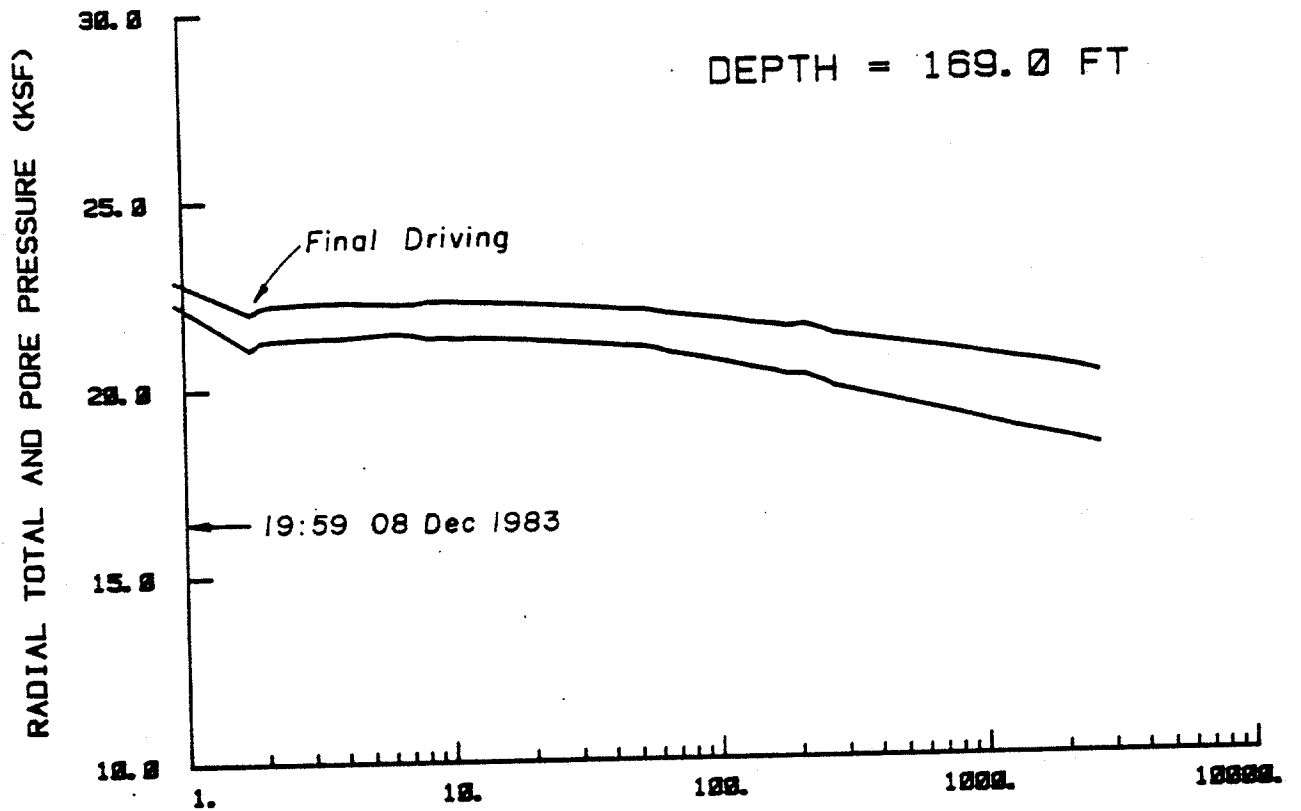
ELAPSED TIME (HRS)

SOIL PRESSURES AT THE 109-FOOT DEPTH DURING CONSOLIDATION

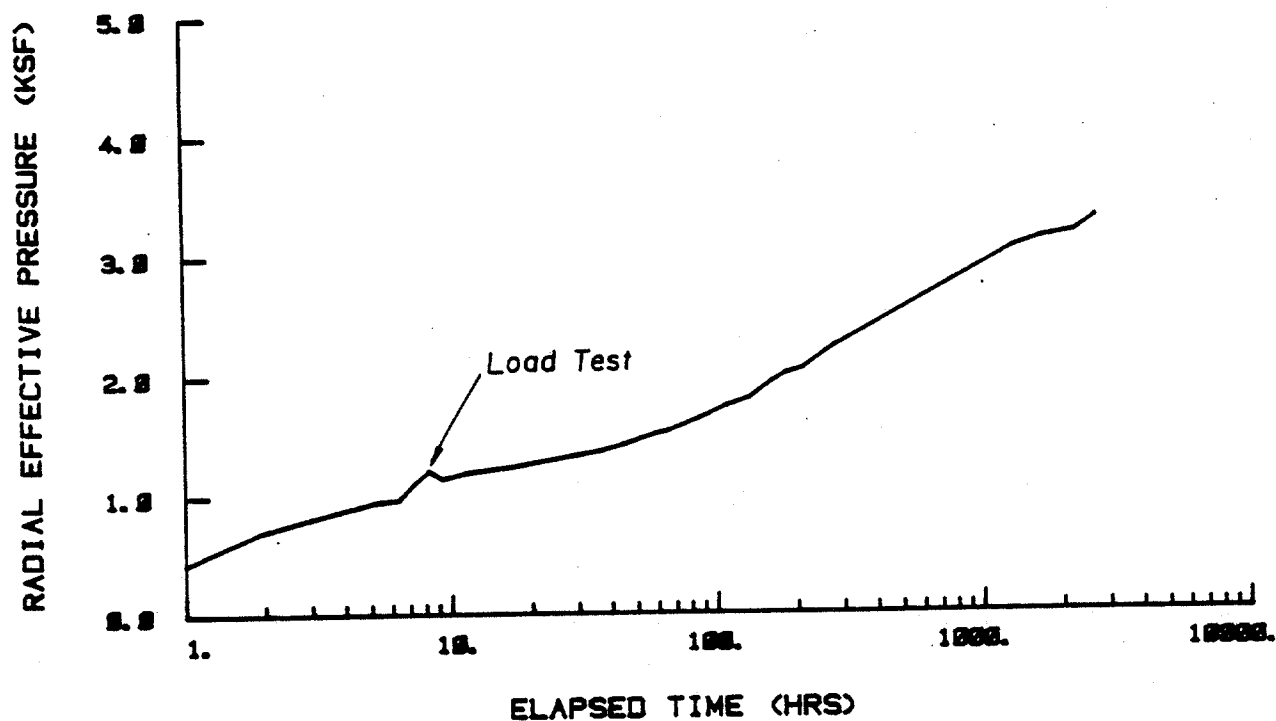
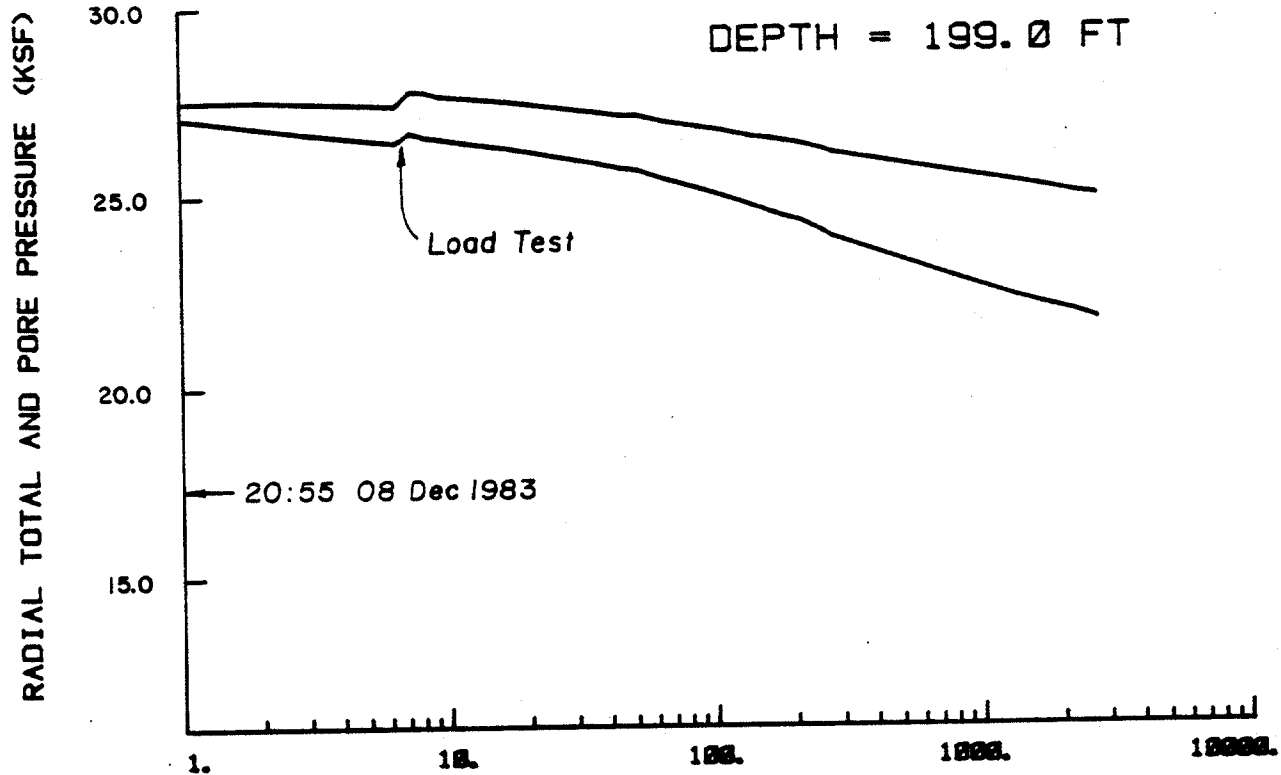
(1 inch = 25.4 mm, 1 ft = 0.305 m, 1 kip = 4.45 kN, 1 ksf = 47.9 kPa)



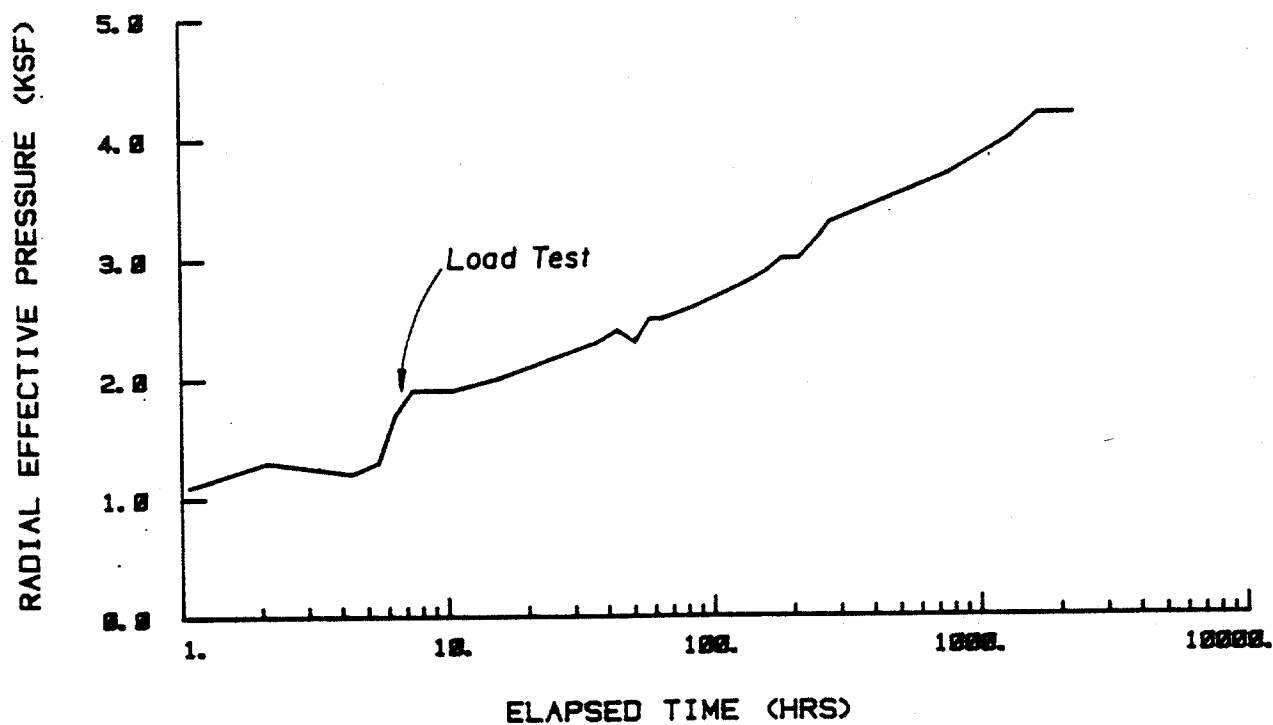
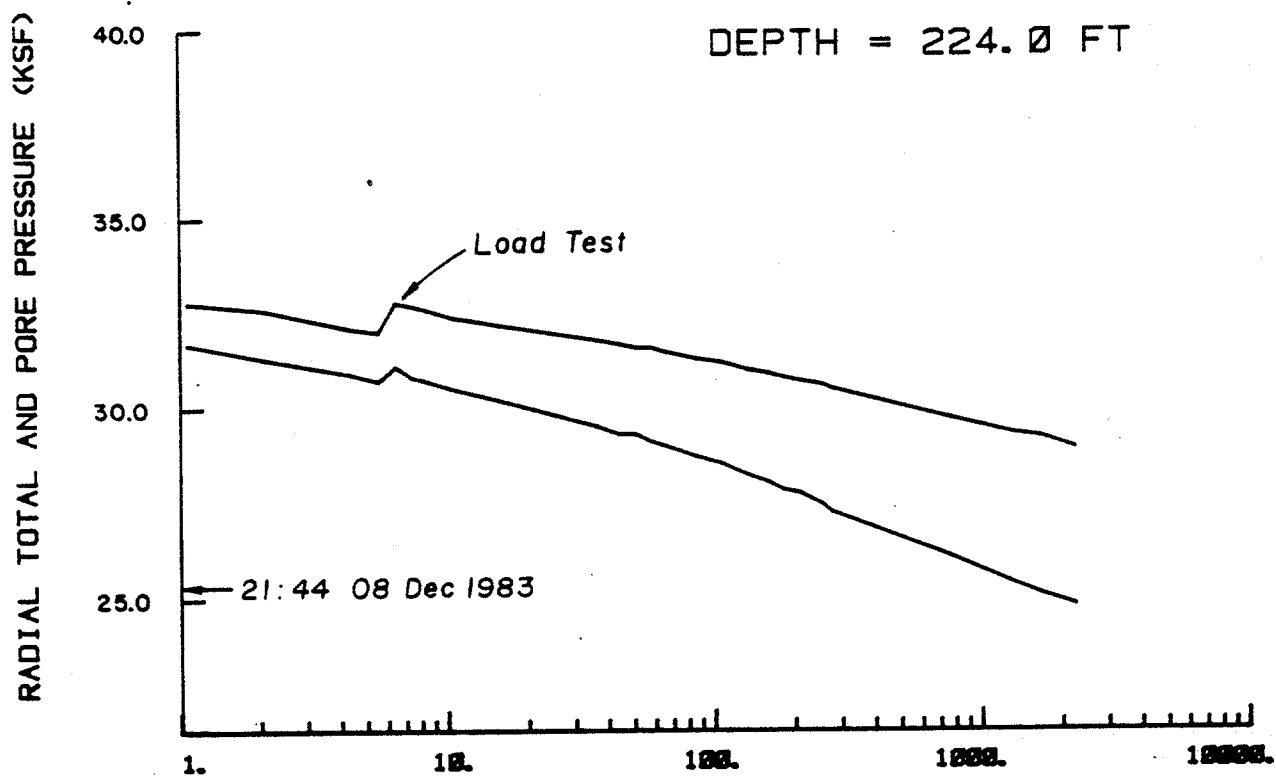
SOIL PRESSURES AT THE 139-FOOT DEPTH DURING CONSOLIDATION
(1 inch = 25.4 mm, 1 ft = 0.305 m, 1 kip = 4.45 kN, 1 ksf = 47.9 kPa)



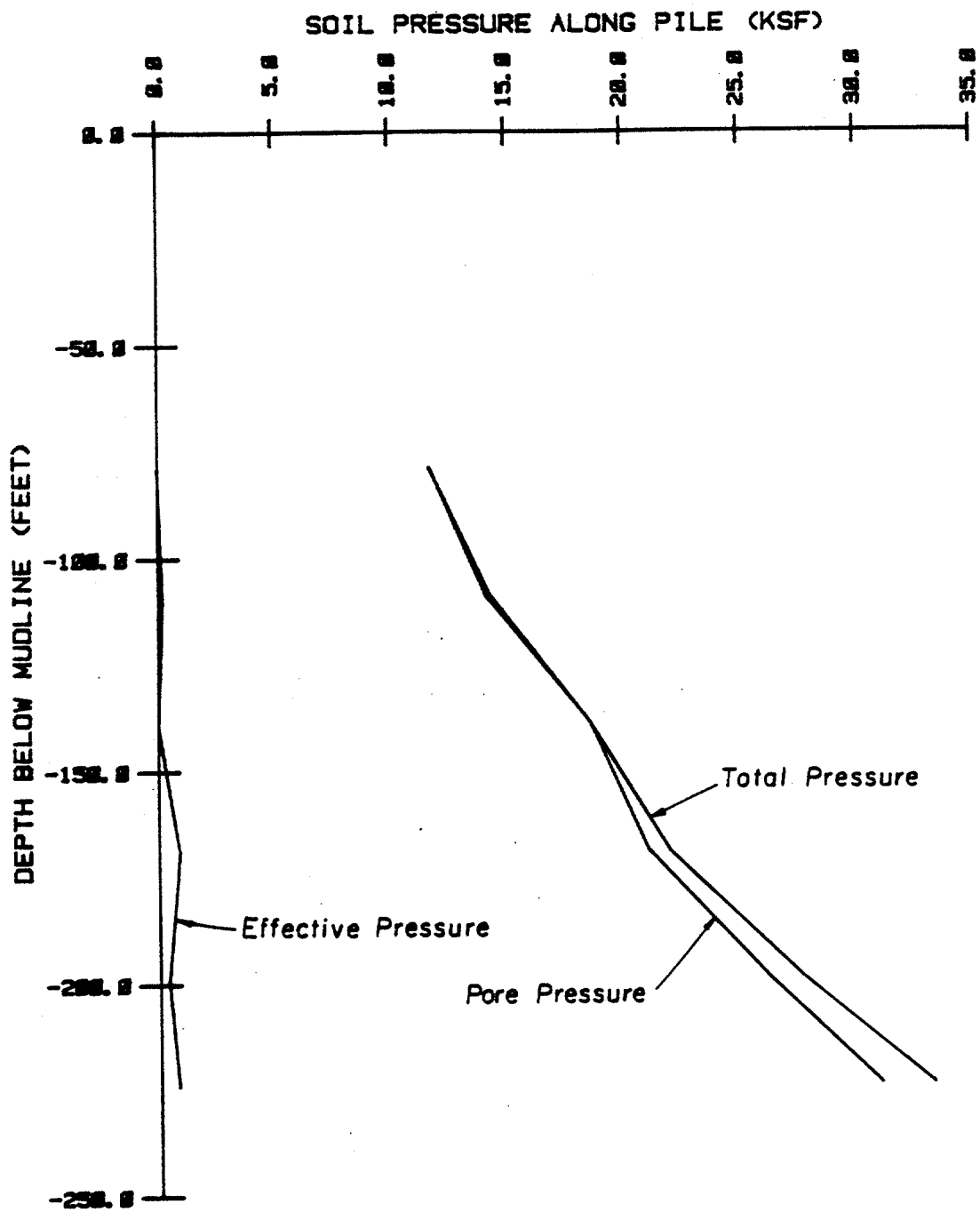
SOIL PRESSURES AT THE 169-FOOT DEPTH DURING CONSOLIDATION
 (1 inch = 25.4 mm, 1 ft = 0.305 m, 1 kip = 4.45 kN, 1 ksf = 47.9 kPa)



SOIL PRESSURES AT THE 199-FOOT DEPTH DURING CONSOLIDATION
 (1 inch = 25.4 mm, 1 ft = 0.305 m, 1 kip = 4.45 kN, 1 ksf = 47.9 kPa)

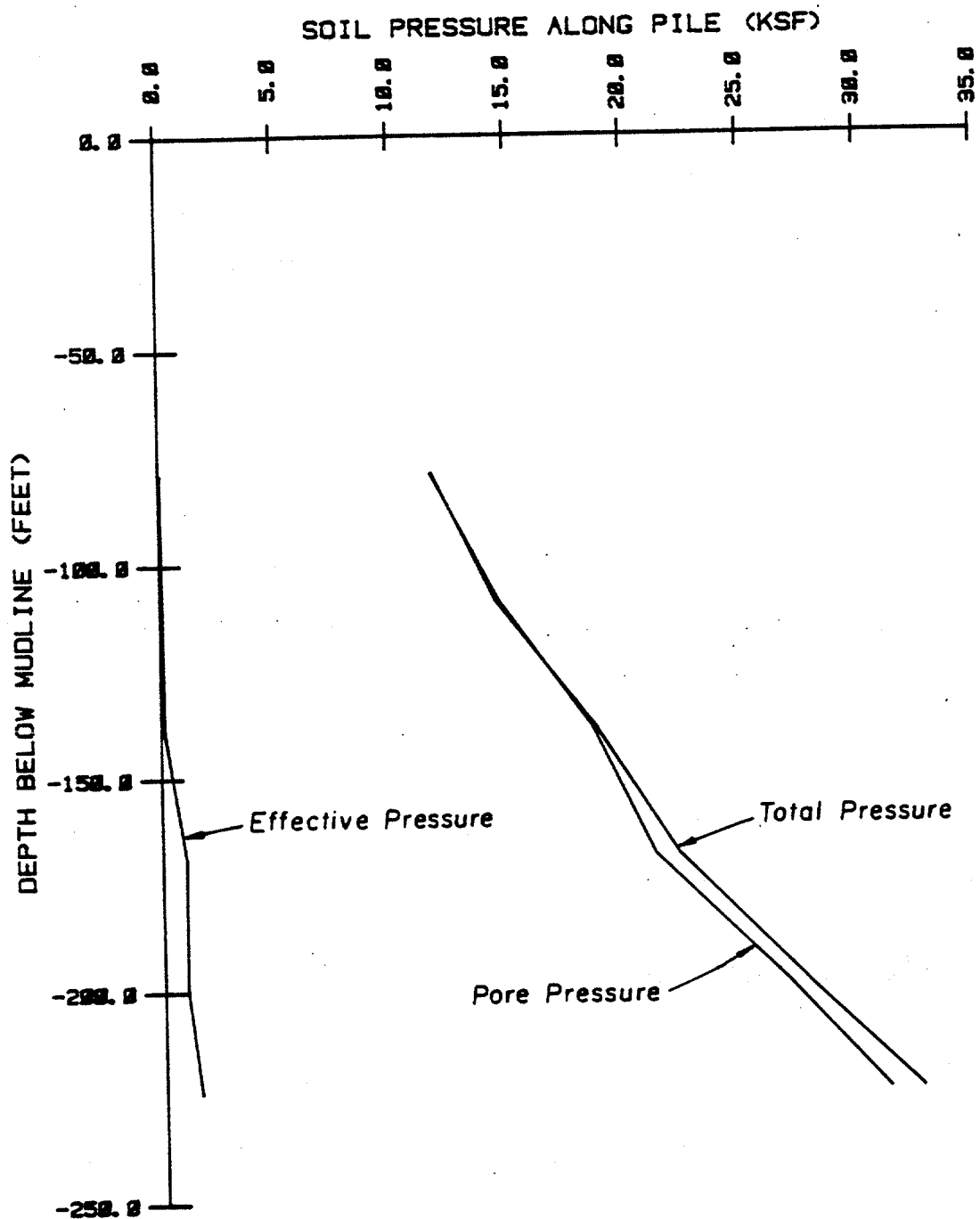


SOIL PRESSURES AT THE 224-FOOT DEPTH DURING CONSOLIDATION
 (1 inch = 25.4 mm, 1 ft = 0.305 m, 1 kip = 4.45 kN, 1 ksf = 47.9 kPa)



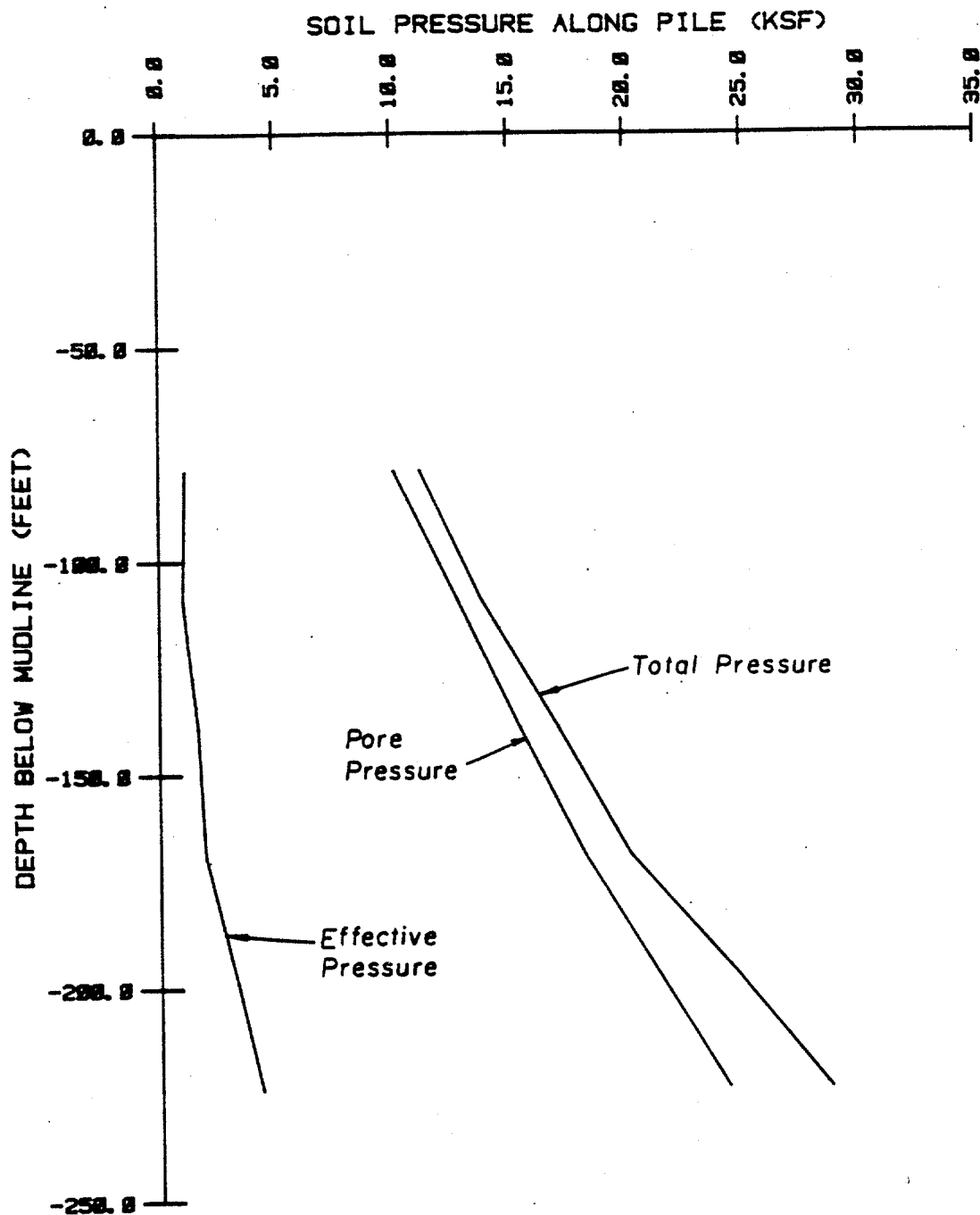
SOIL PRESSURE PROFILES AT THE END OF DRIVING

(1 inch = 25.4 mm, 1 ft = 0.305 m, 1 kip = 4.45 kN, 1 ksf = 47.9 kPa)



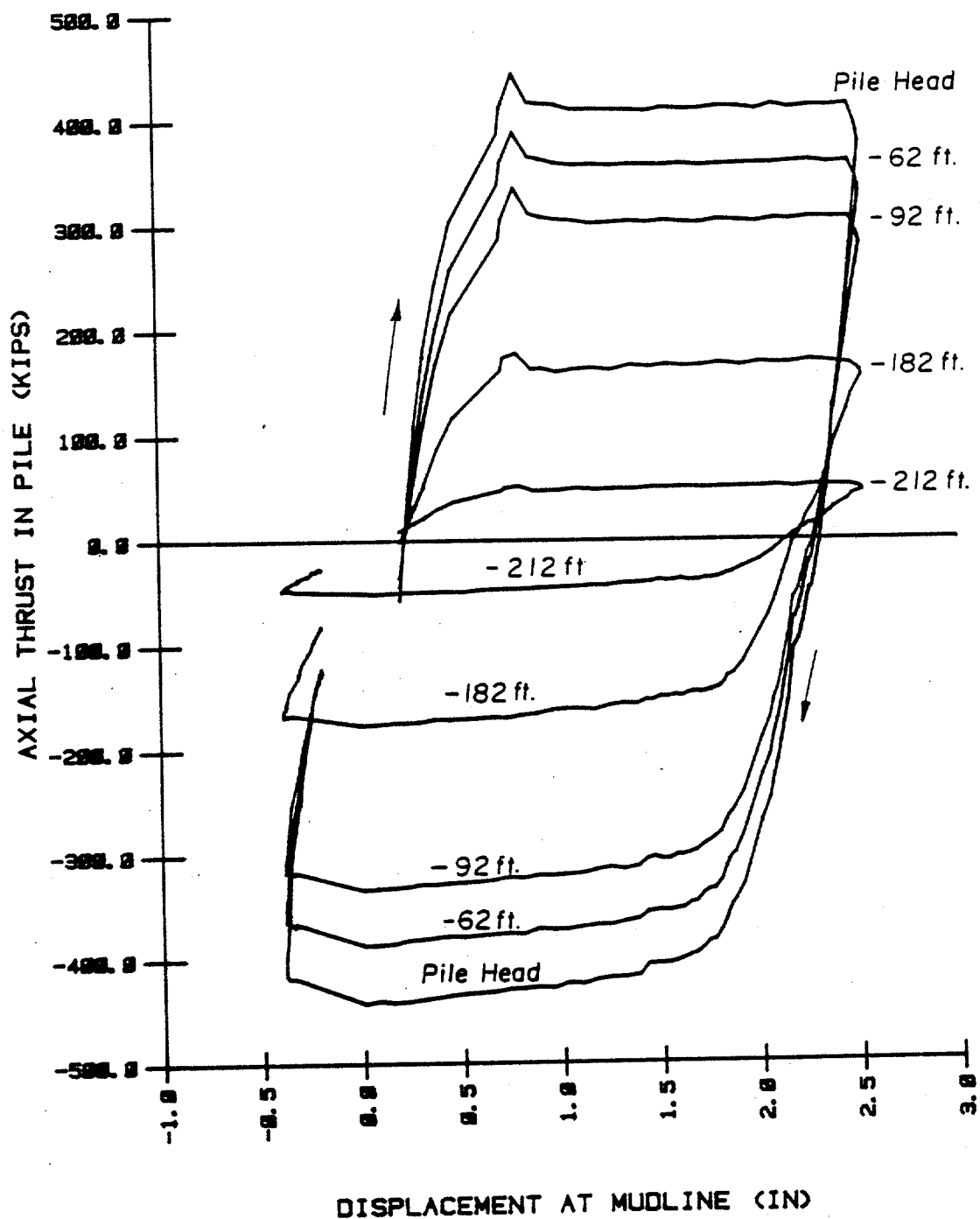
SOIL PRESSURE PROFILES AT THE END OF REDRIVING .

(1 inch = 25.4 mm, 1 ft = 0.305 m, 1 kip = 4.45 kN, 1 ksf = 47.9 kPa)



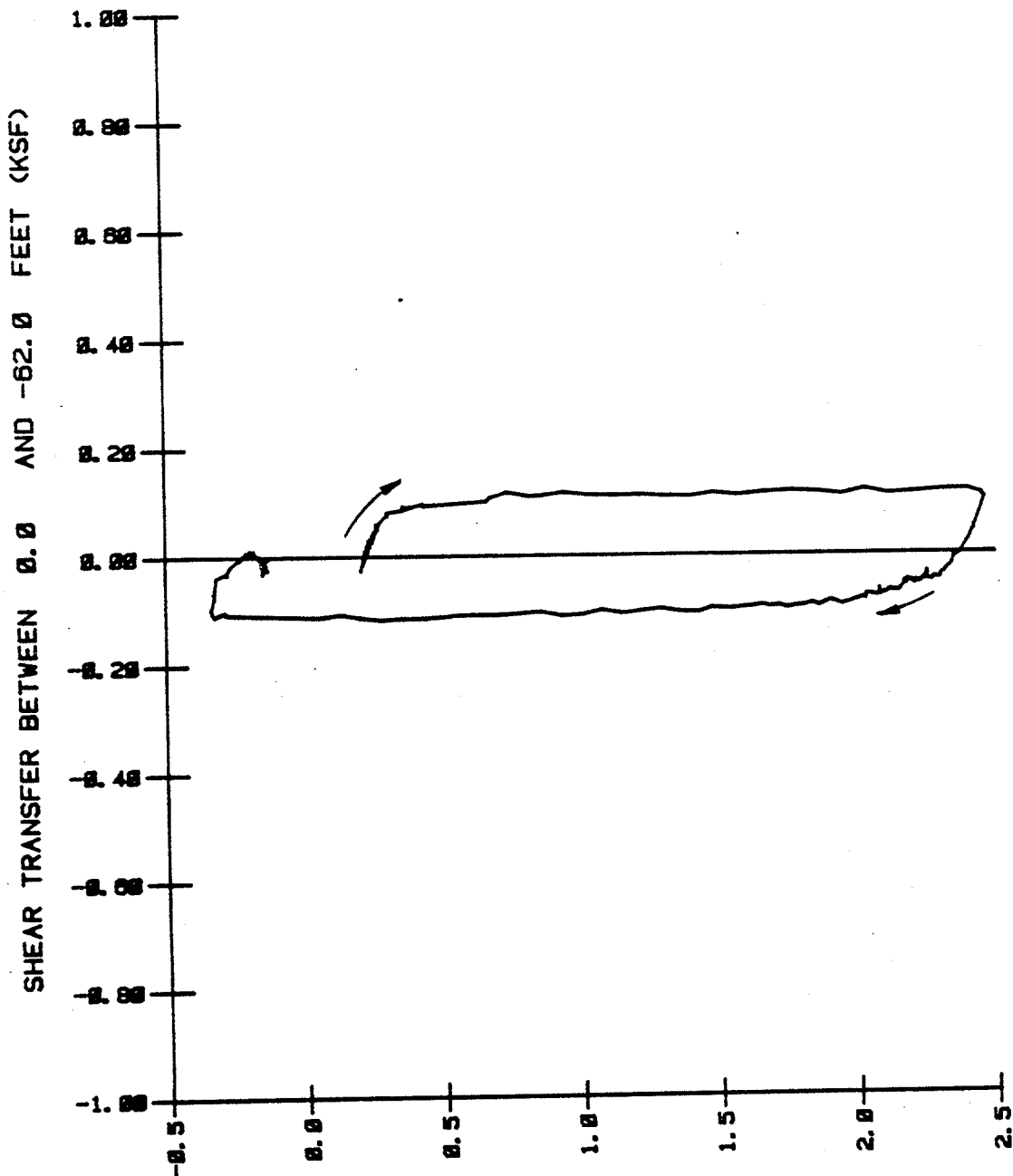
SOIL PRESSURE PROFILES AFTER 111 DAYS OF CONSOLIDATION

(1 inch = 25.4 mm, 1 ft = 0.305 m, 1 kip = 4.45 kN, 1 ksf = 47.9 kPa)



VARIATION IN AXIAL THRUST MEASURED WITH THE STRAIN MODULES
DURING THE LOAD TESTS IMMEDIATELY AFTER DRIVING

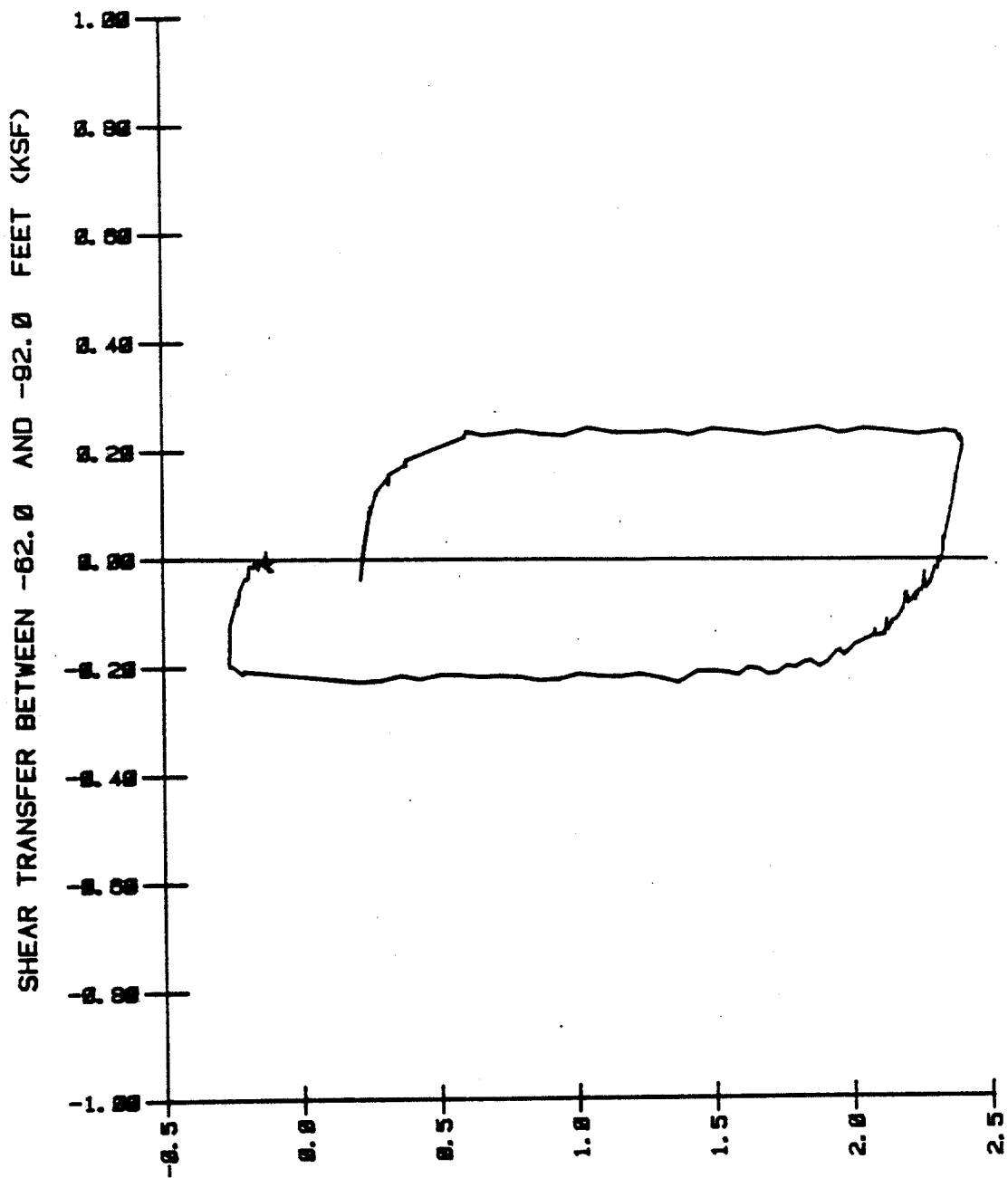
(1 inch = 25.4 mm, 1 ft = 0.305 m, 1 kip = 4.45 kN, 1 ksf = 47.9 kPa)



DISPLACEMENT AT -31.0 FEET (IN)

SHEAR TRANSFER VERSUS DISPLACEMENT BETWEEN THE DEPTHS OF 0 AND 62 FEET
DURING THE LOAD TESTS IMMEDIATELY AFTER DRIVING - STRAIN MODULES

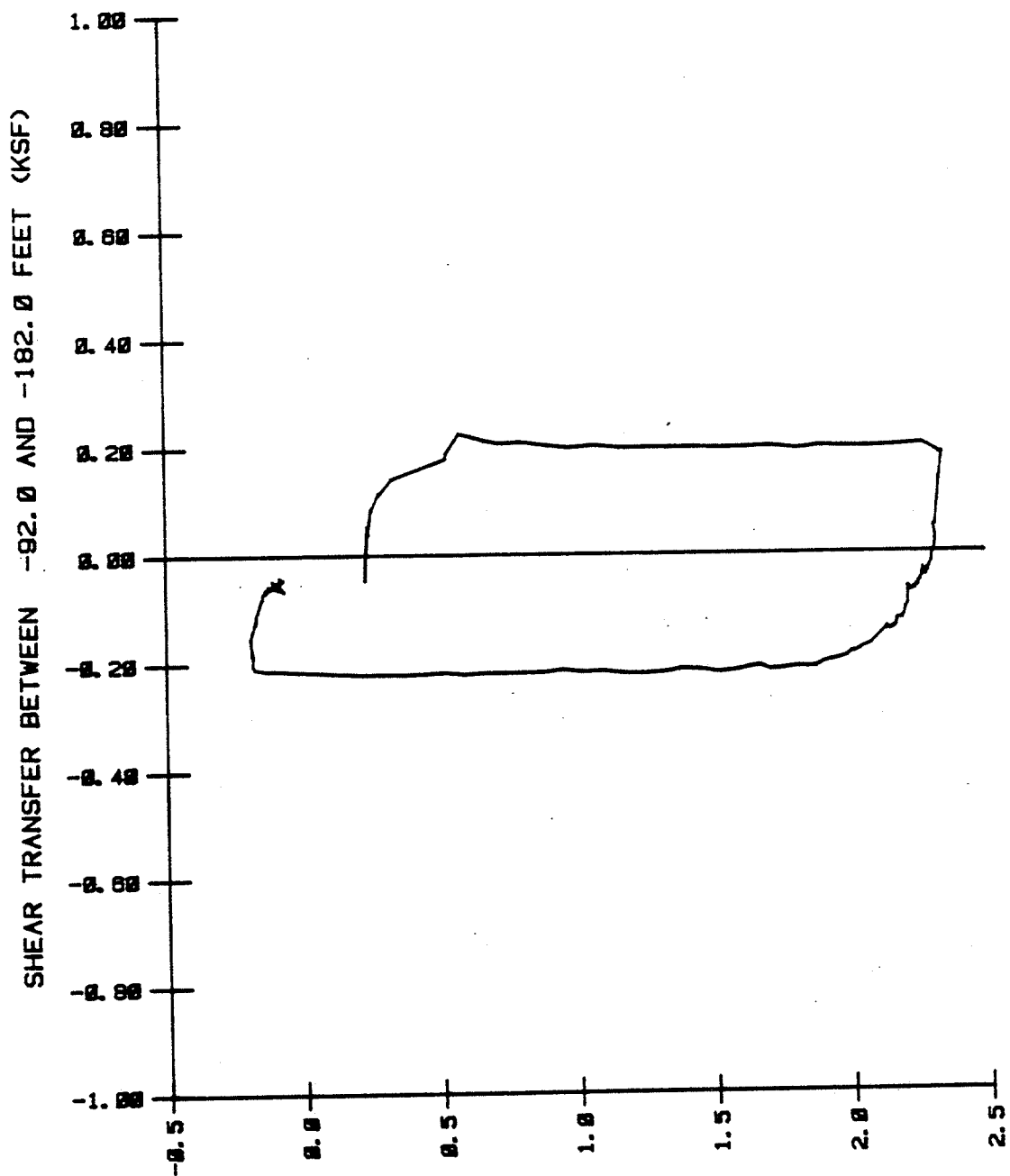
(1 inch = 25.4 mm, 1 ft = 0.305 m, 1 kip = 4.45 kN, 1 ksf = 47.9 kPa)



DISPLACEMENT AT -77.0 FEET (IN)

SHEAR TRANSFER VERSUS DISPLACEMENT BETWEEN THE DEPTHS OF 62 AND 92 FEET
DURING THE LOAD TESTS IMMEDIATELY AFTER DRIVING - STRAIN MODULES

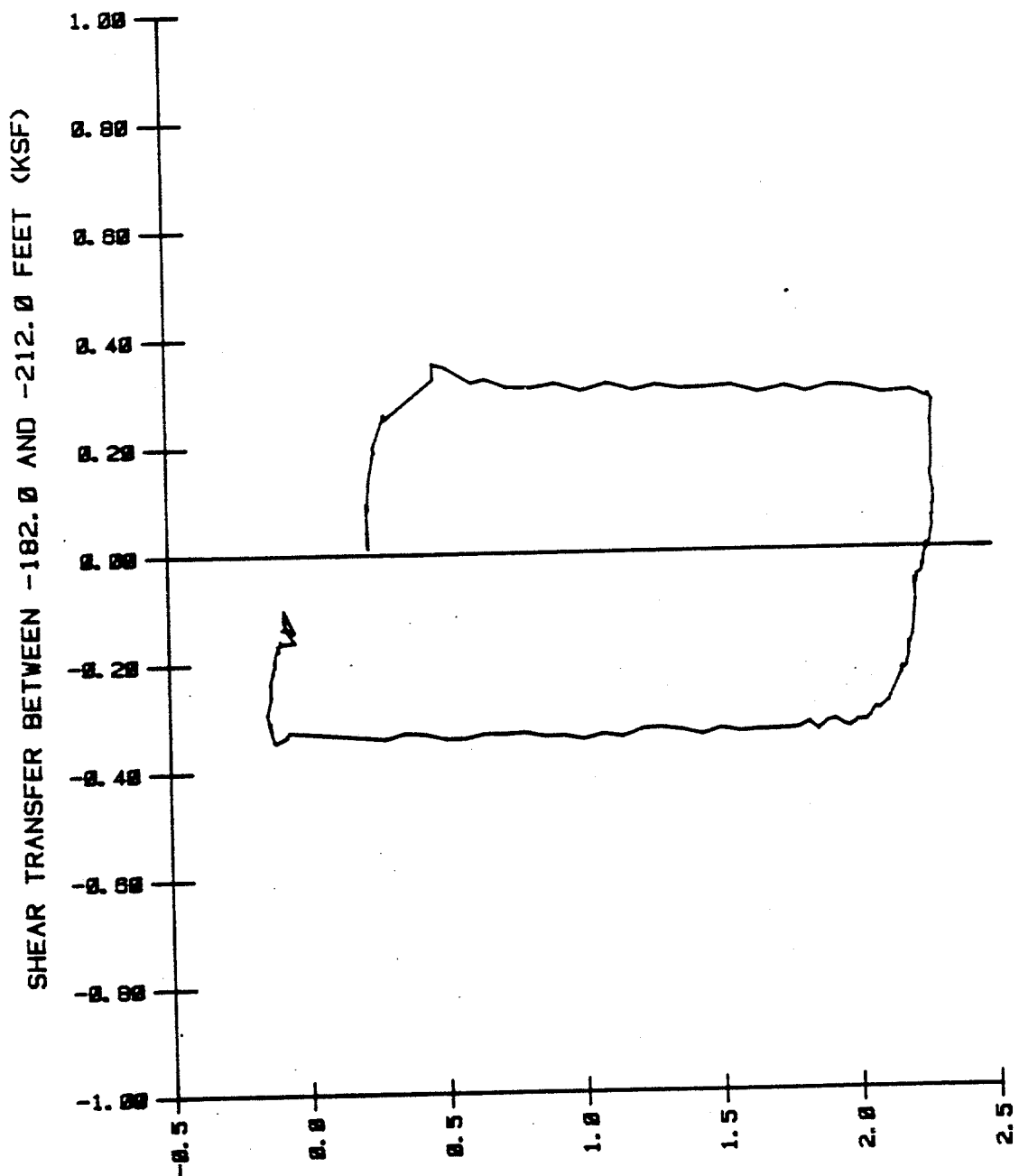
(1 inch = 25.4 mm, 1 ft = 0.305 m, 1 kip = 4.45 kN, 1 ksf = 47.9 kPa)



DISPLACEMENT AT -137.0 FEET (IN)

SHEAR TRANSFER VERSUS DISPLACEMENT BETWEEN THE DEPTHS OF 92 AND 182 FEET
DURING THE LOAD TESTS IMMEDIATELY AFTER DRIVING - STRAIN MODULES

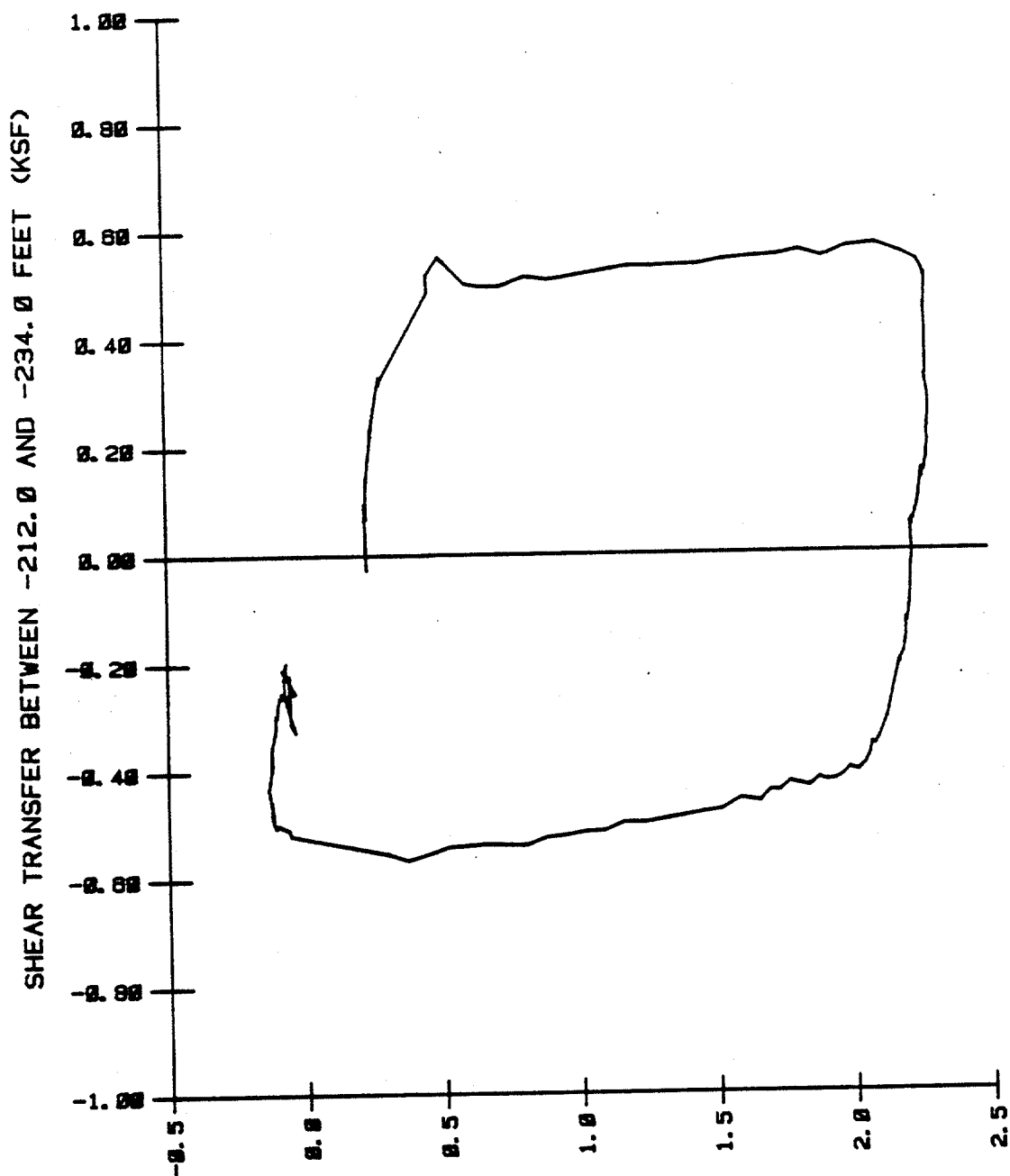
(1 inch = 25.4 mm, 1 ft = 0.305 m, 1 kip = 4.45 kN, 1 ksf = 47.9 kPa)



DISPLACEMENT AT -197.0 FEET (IN)

SHEAR TRANSFER VERSUS DISPLACEMENT BETWEEN THE DEPTHS OF 182 AND 212 FEET
DURING THE LOAD TESTS IMMEDIATELY AFTER DRIVING - STRAIN MODULES

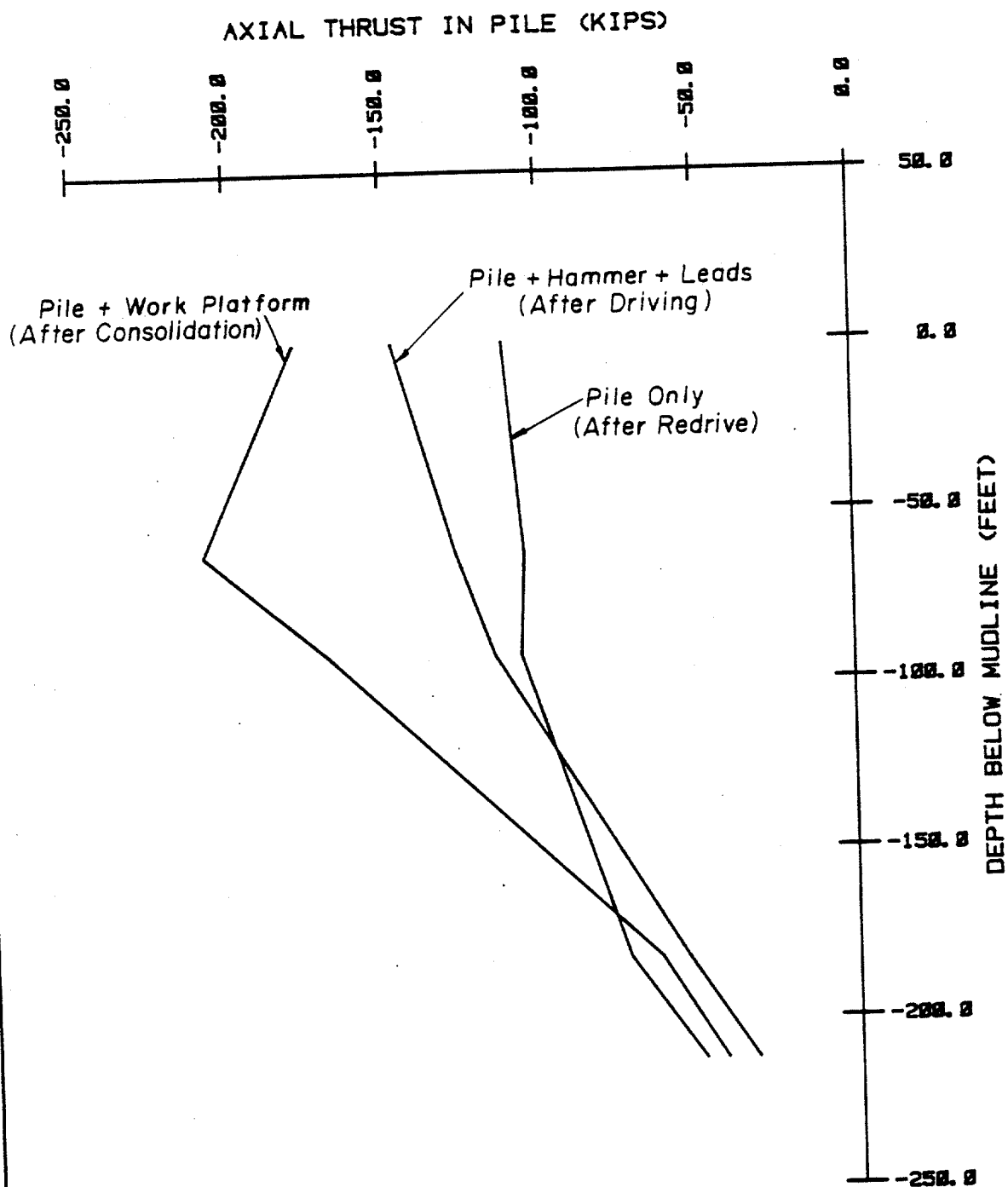
(1 inch = 25.4 mm, 1 ft = 0.305 m, 1 kip = 4.45 kN, 1 ksf = 47.9 kPa)



DISPLACEMENT AT -223.0 FEET (IN)

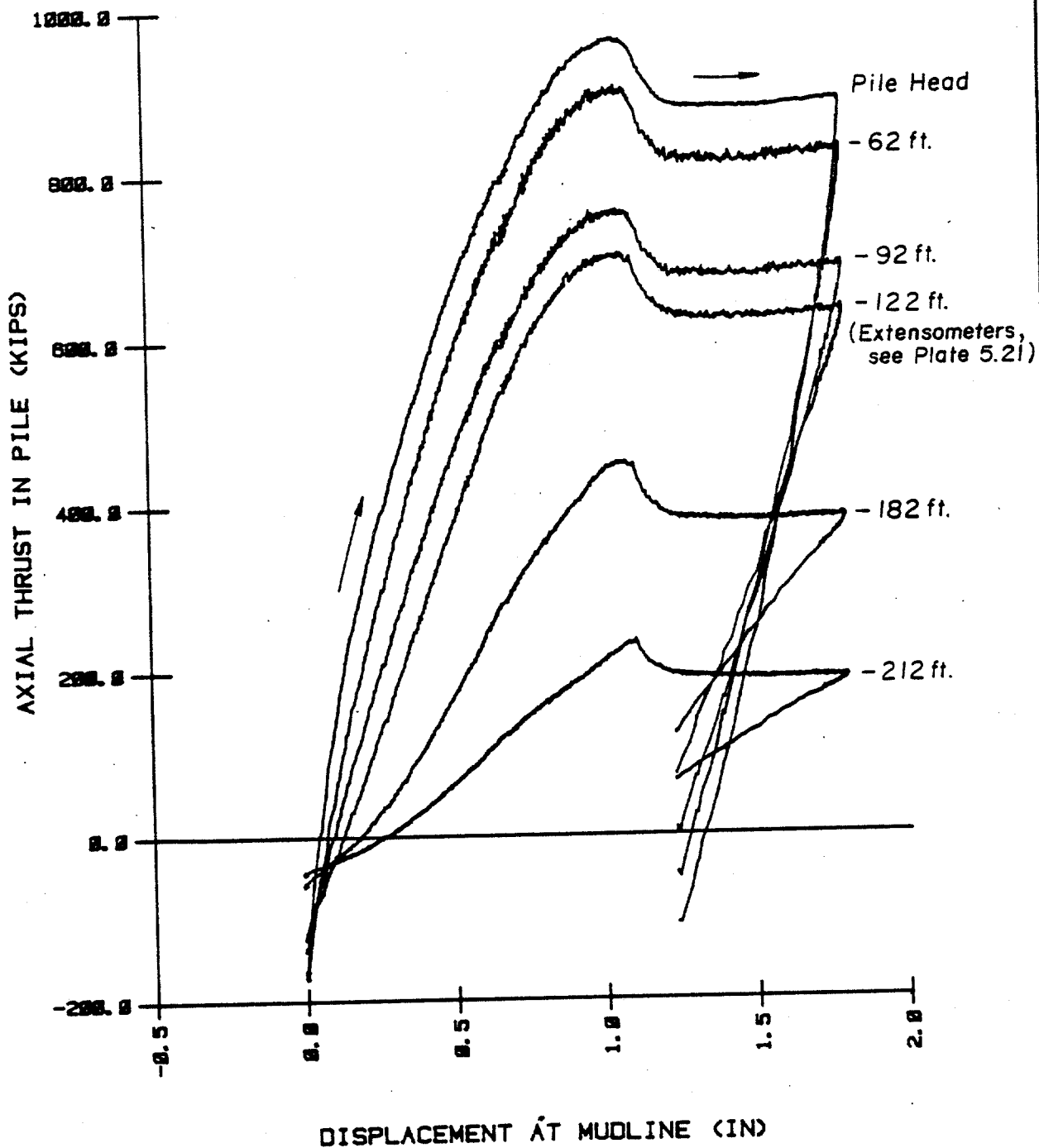
SHEAR TRANSFER VERSUS DISPLACEMENT BETWEEN THE DEPTHS OF 212 AND 234 FEET
DURING THE LOAD TESTS IMMEDIATELY AFTER DRIVING - STRAIN MODULES

(1 inch = 25.4 mm, 1 ft = 0.305 m, 1 kip = 4.45 kN, 1 ksf = 47.9 kPa)



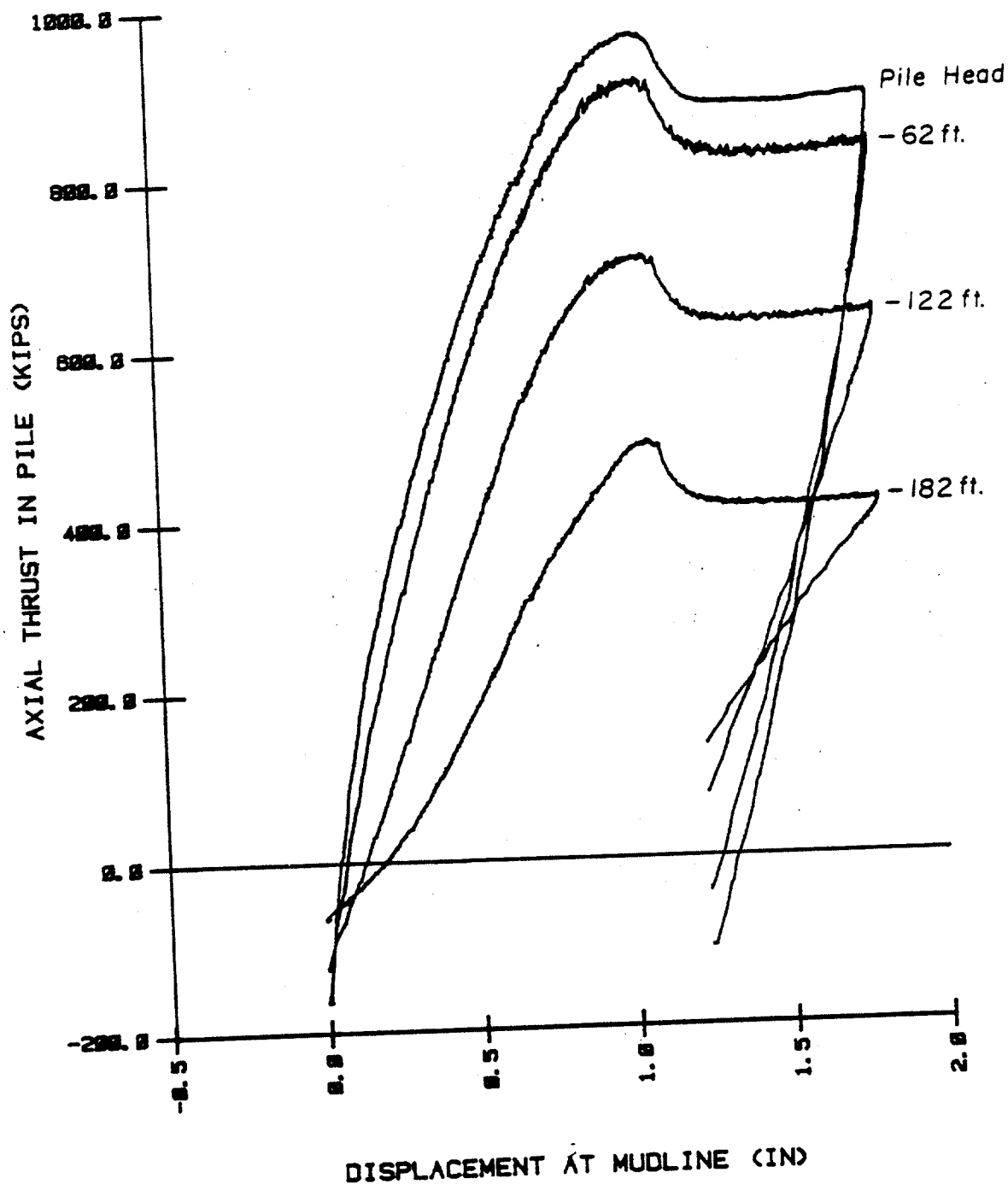
RESIDUAL AXIAL THRUST IN PILE MEASURED WITH THE
STRAIN MODULES AT VARIOUS TIMES AFTER DRIVING

(1 inch = 25.4 mm, 1 ft = 0.305 m, 1 kip = 4.45 kN, 1 ksf = 47.9 kPa)



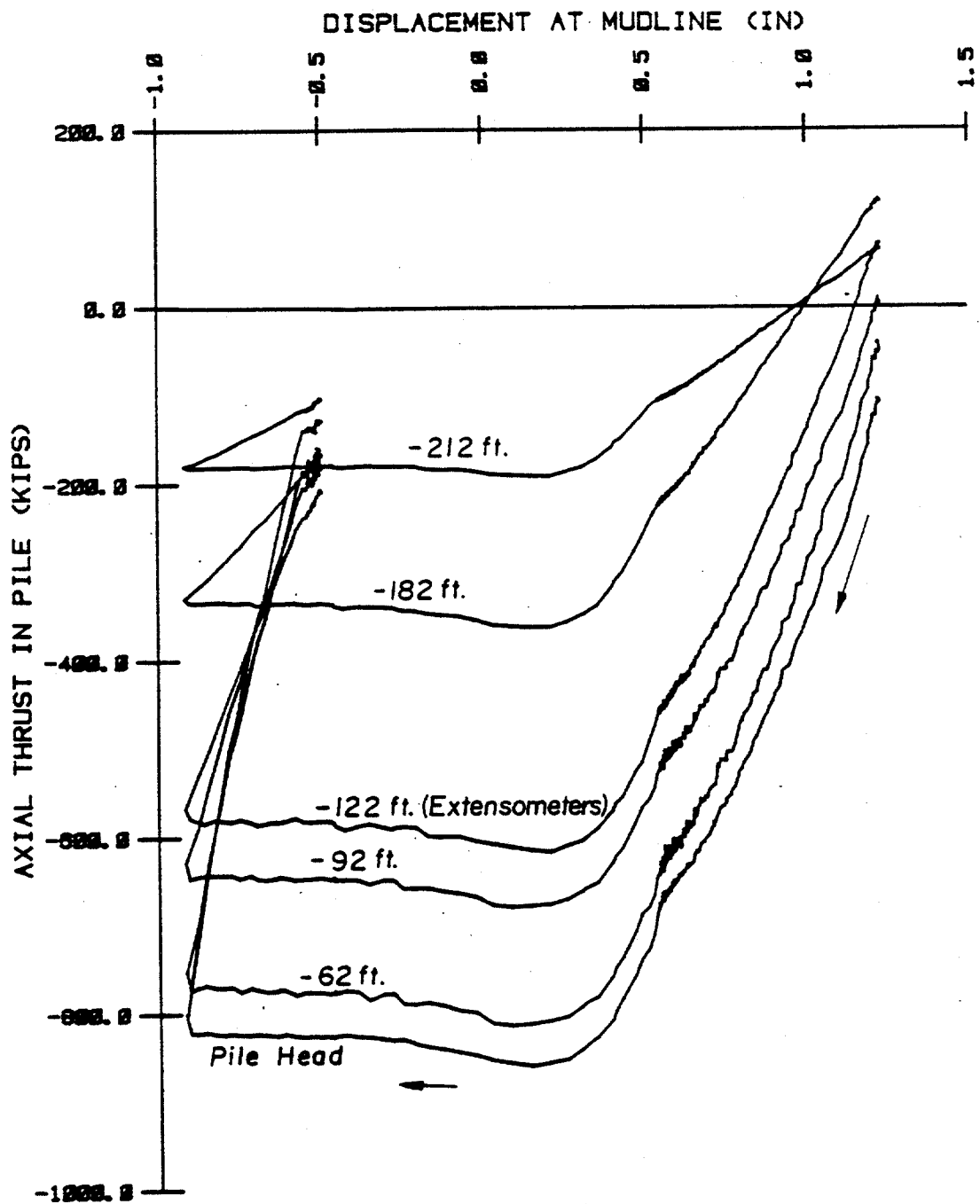
VARIATION IN AXIAL THRUST MEASURED WITH THE STRAIN MODULES
DURING THE TENSION TEST AFTER PARTIAL CONSOLIDATION

(1 inch = 25.4 mm, 1 ft = 0.305 m, 1 kip = 4.45 kN, 1 ksf = 47.9 kPa)



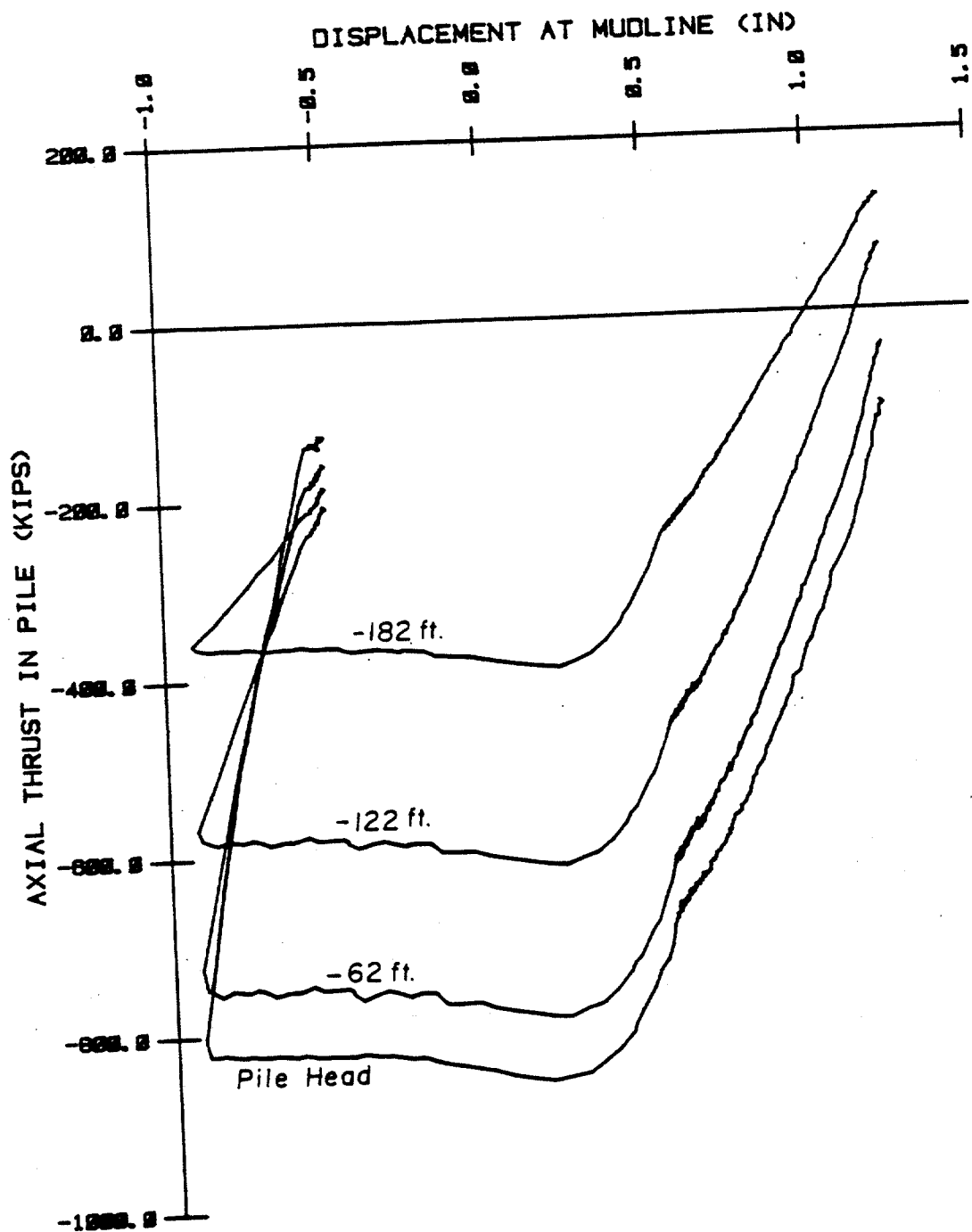
VARIATION IN AXIAL THRUST MEASURED WITH THE EXTENSOMETERS
DURING THE TENSION TEST AFTER PARTIAL CONSOLIDATION

(1 inch = 25.4 mm, 1 ft = 0.305 m, 1 kip = 4.45 kN, 1 ksf = 47.9 kPa)



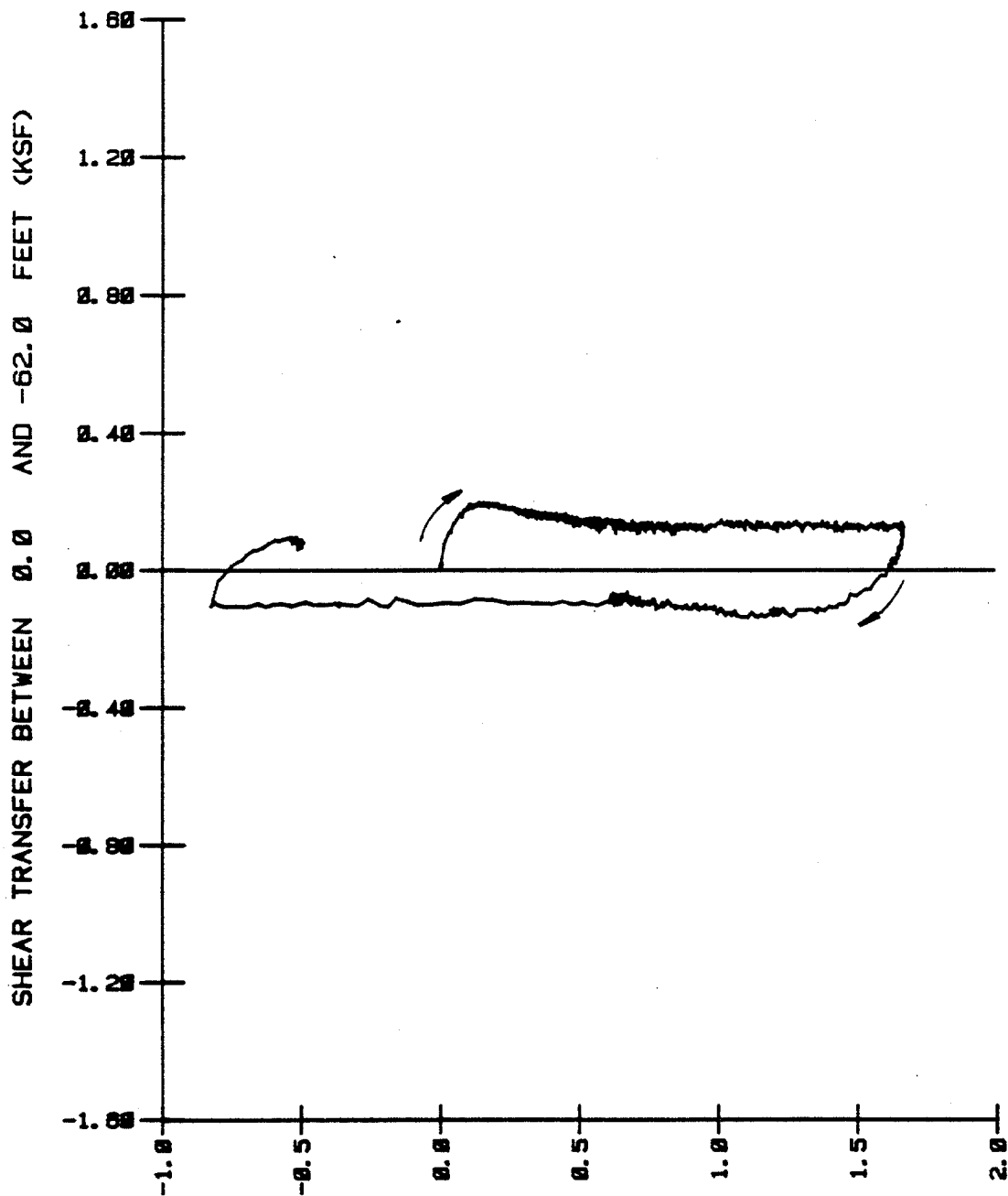
VARIATION IN AXIAL THRUST MEASURED WITH THE STRAIN-MODULES
DURING THE COMPRESSION TEST AFTER PARTIAL CONSOLIDATION

(1 inch = 25.4 mm, 1 ft = 0.305 m, 1 kip = 4.45 kN, 1 ksf = 47.9 kPa)



VARIATION IN AXIAL THRUST MEASURED WITH THE EXTENSOMETERS
DURING THE COMPRESSION TEST AFTER PARTIAL CONSOLIDATION

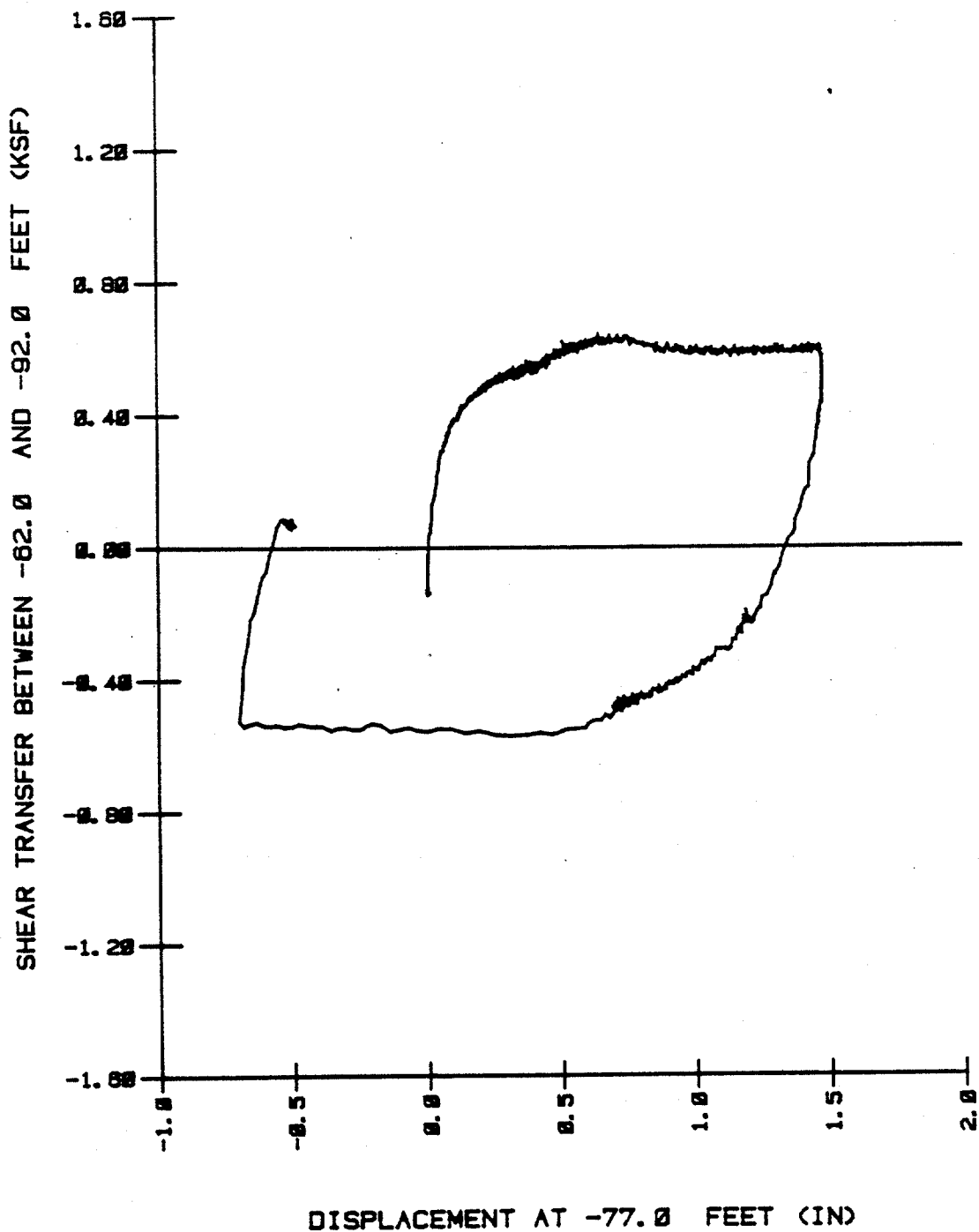
(1 inch = 25.4 mm, 1 ft = 0.305 m, 1 kip = 4.45 kN, 1 ksf = 47.9 kPa)



DISPLACEMENT AT -31.0 FEET (IN)

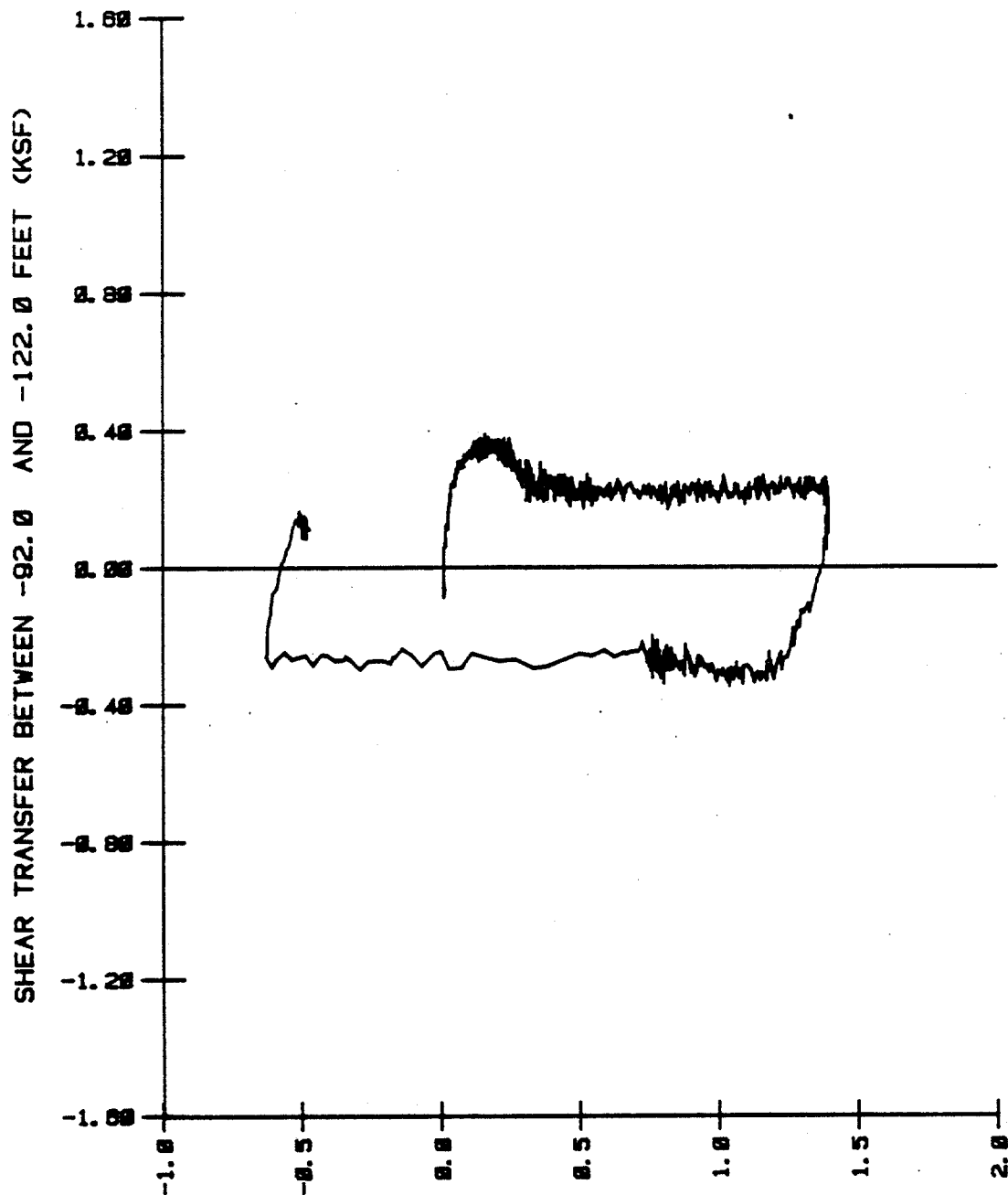
SHEAR TRANSFER VERSUS DISPLACEMENT BETWEEN THE DEPTHS OF 0 AND 62 FEET
DURING STATIC LOAD TESTS AFTER PARTIAL CONSOLIDATION - STRAIN MODULES

(1 inch = 25.4 mm, 1 ft = 0.305 m, 1 kip = 4.45 kN, 1 ksf = 47.9 kPa)



SHEAR TRANSFER VERSUS DISPLACEMENT BETWEEN THE DEPTHS OF 62 AND 92 FEET
DURING STATIC LOAD TESTS AFTER PARTIAL CONSOLIDATION - STRAIN MODULES

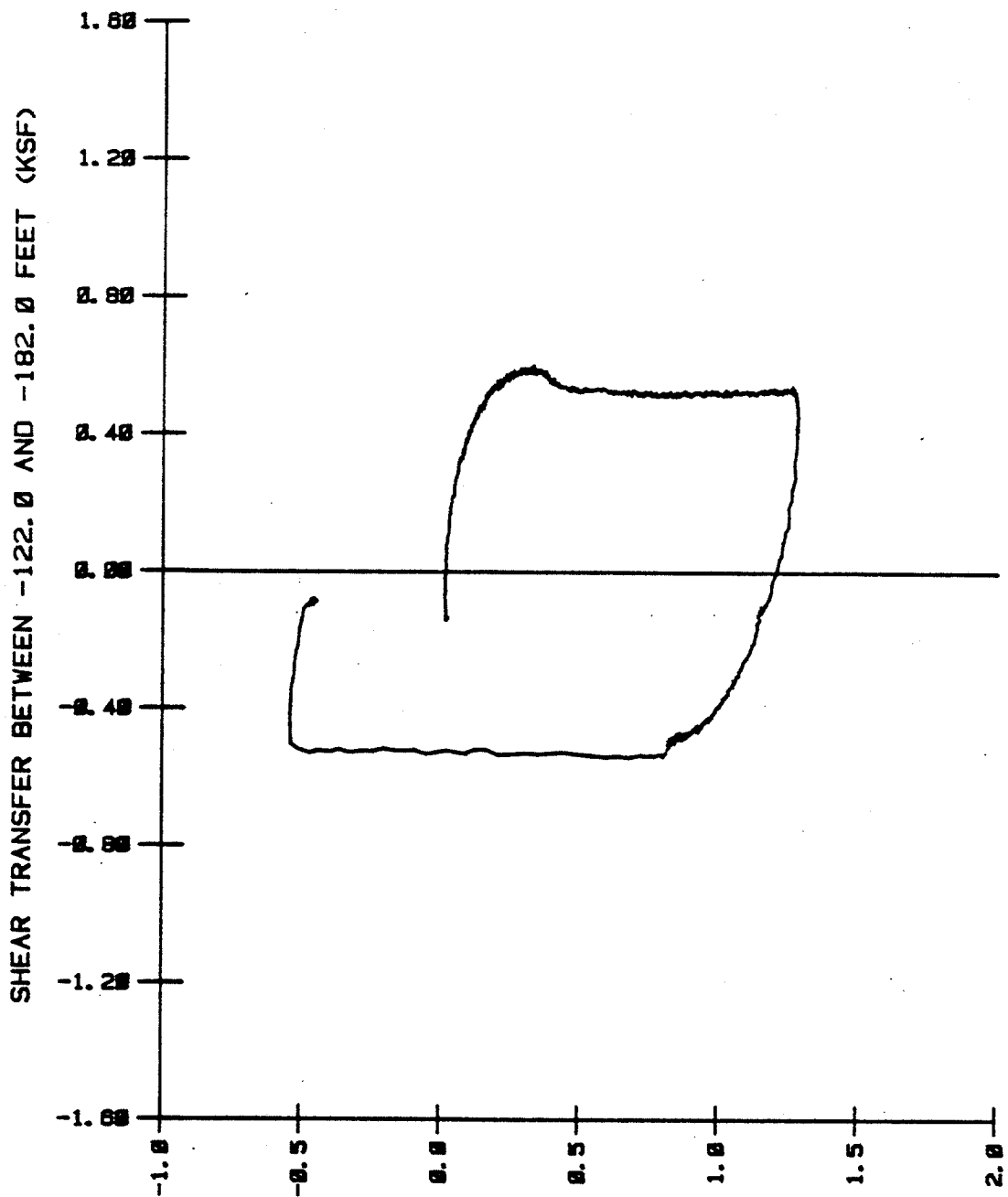
(1 inch = 25.4 mm, 1 ft = 0.305 m, 1 kip = 4.45 kN, 1 ksf = 47.9 kPa)



DISPLACEMENT AT -107.0 FEET (IN)

SHEAR TRANSFER VERSUS DISPLACEMENT BETWEEN THE DEPTHS OF 92 AND 122 FEET
DURING STATIC LOAD TESTS AFTER PARTIAL CONSOLIDATION - STRAIN MODULES

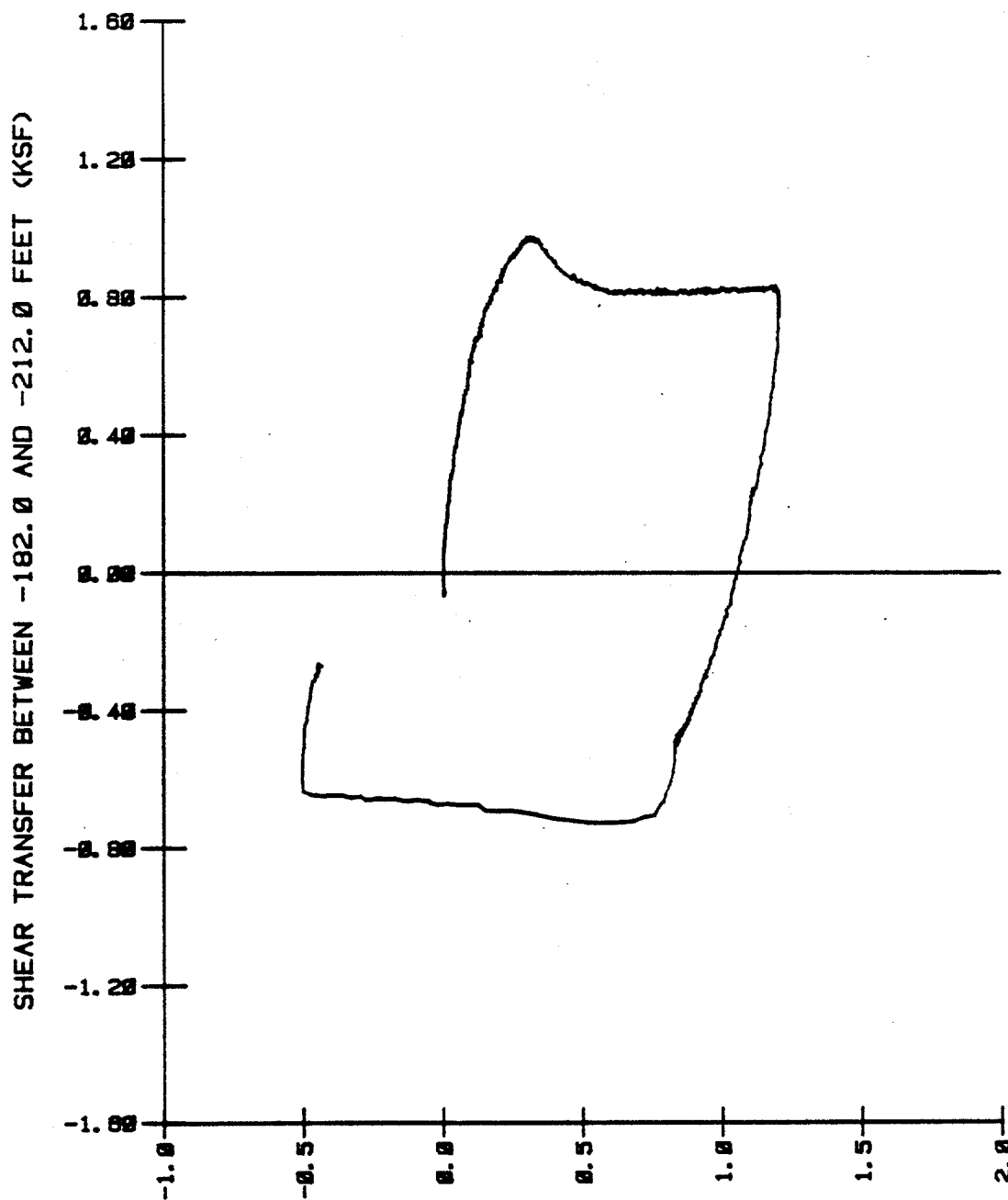
(1 inch = 25.4 mm, 1 ft = 0.305 m, 1 kip = 4.45 kN, 1 ksf = 47.9 kPa)



DISPLACEMENT AT -152.0 FEET (IN)

SHEAR TRANSFER VERSUS DISPLACEMENT BETWEEN THE DEPTHS OF 122 AND 182 FEET
DURING STATIC LOAD TESTS AFTER PARTIAL CONSOLIDATION - STRAIN MODULES

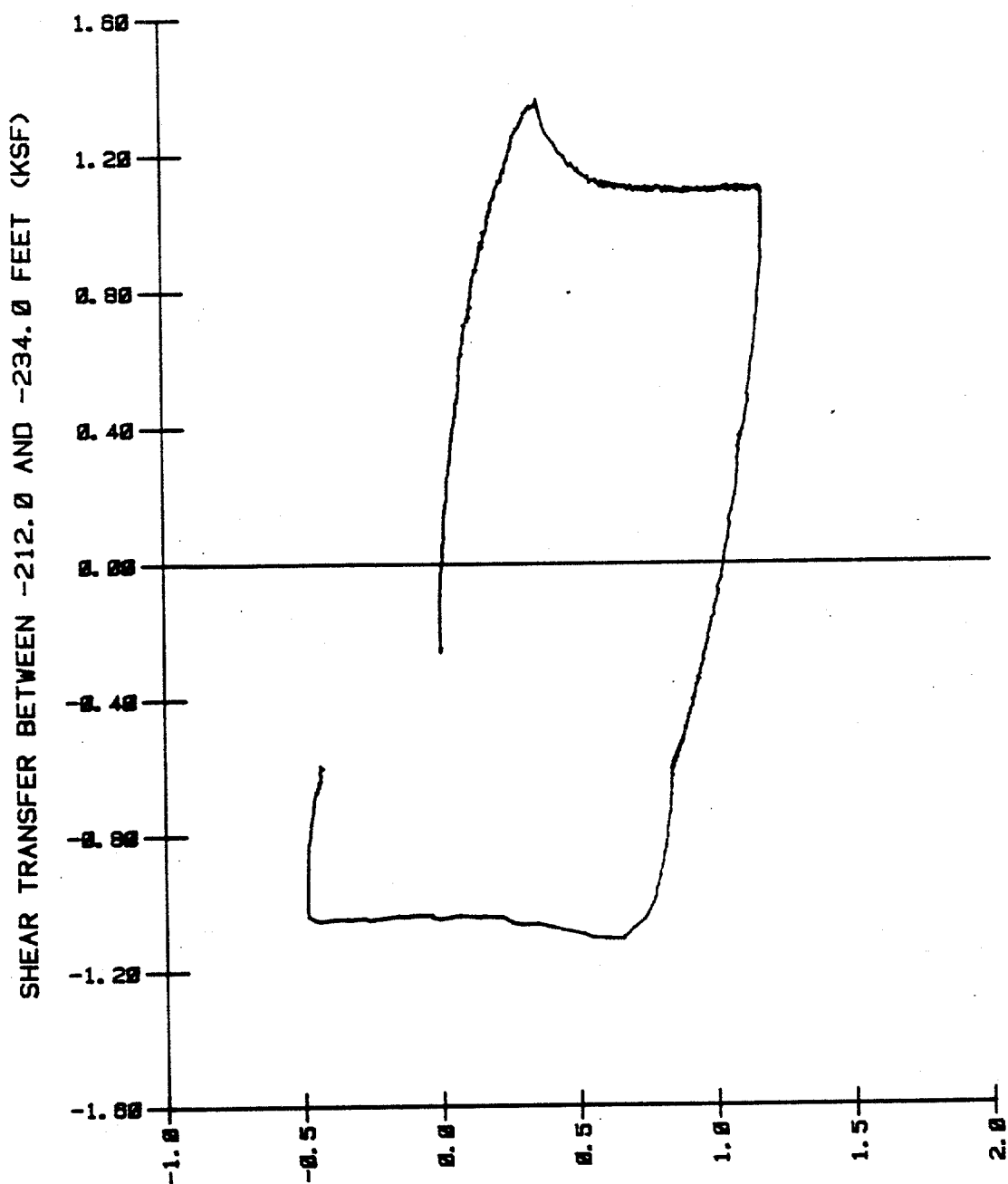
(1 inch = 25.4 mm, 1 ft = 0.305 m, 1 kip = 4.45 kN, 1 ksf = 47.9 kPa)



DISPLACEMENT AT -197.0 FEET (IN)

SHEAR TRANSFER VERSUS DISPLACEMENT BETWEEN THE DEPTHS OF 182 AND 212 FEET
DURING STATIC LOAD TESTS AFTER PARTIAL CONSOLIDATION - STRAIN MODULES

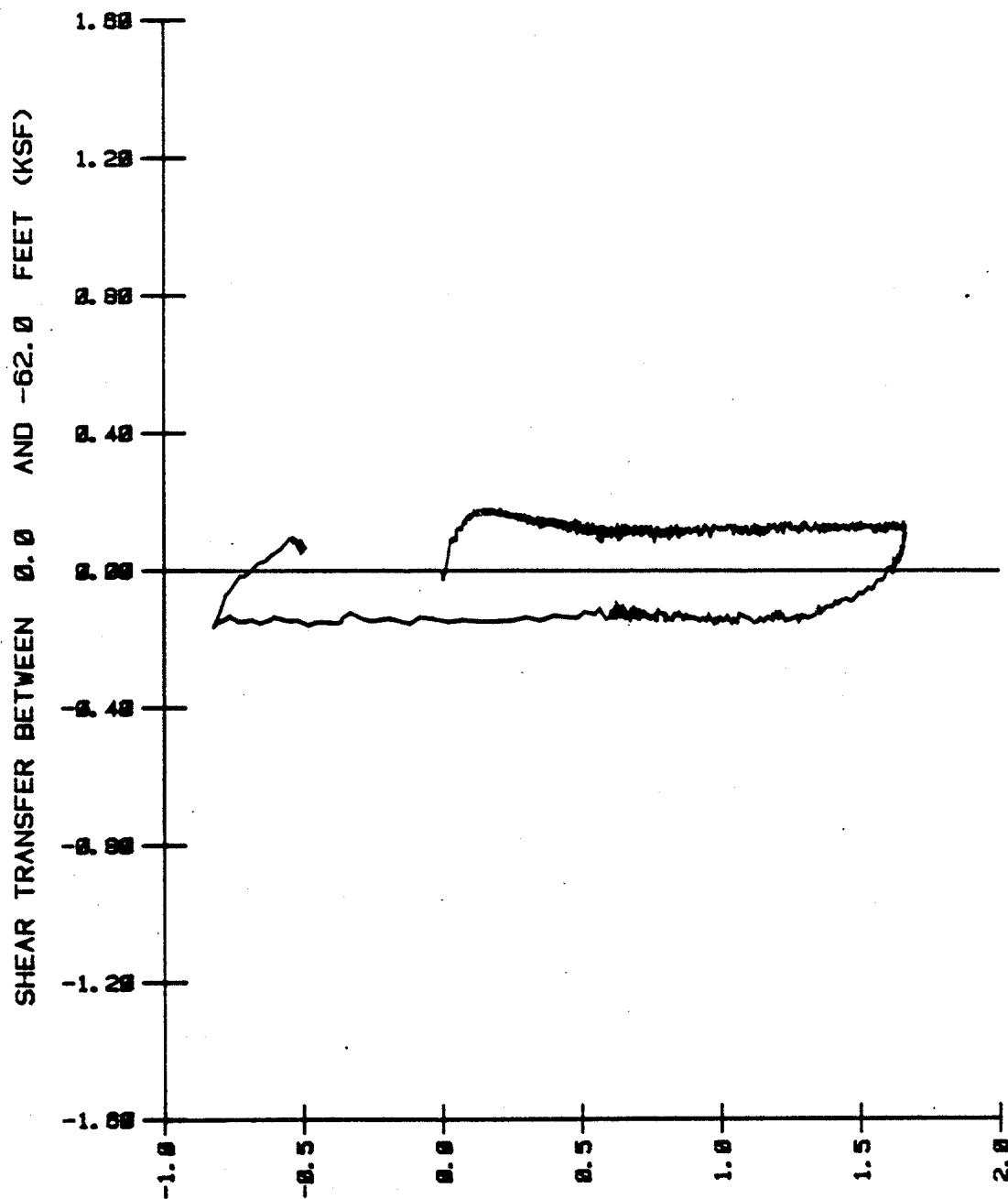
(1 inch = 25.4 mm, 1 ft = 0.305 m, 1 kip = 4.45 kN, 1 ksf = 47.9 kPa)



DISPLACEMENT AT -223.0 FEET (IN)

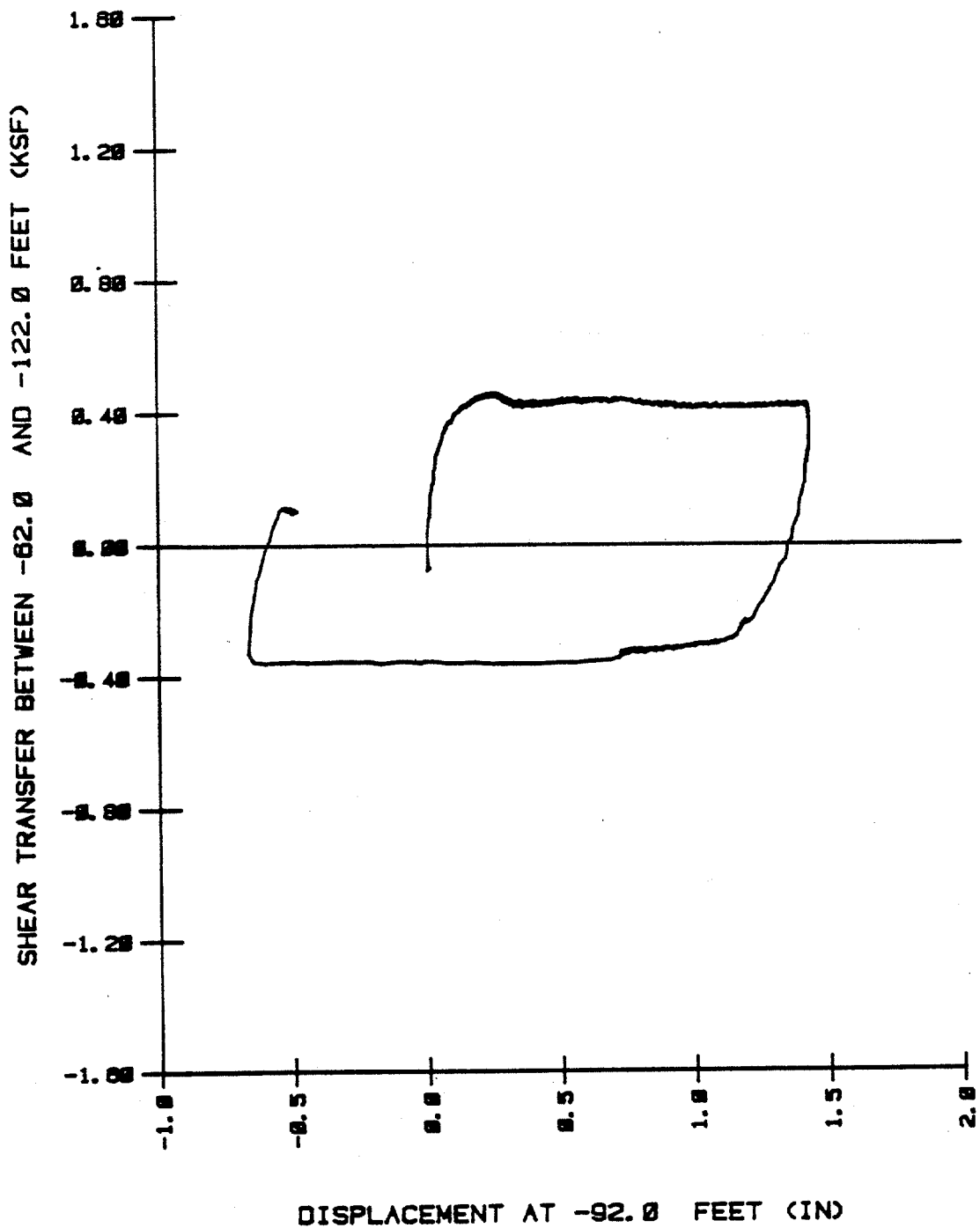
SHEAR TRANSFER VERSUS DISPLACEMENT BETWEEN THE DEPTHS OF 212 AND 234 FEET
DURING STATIC LOAD TESTS AFTER PARTIAL CONSOLIDATION - STRAIN MODULES

(1 inch = 25.4 mm, 1 ft = 0.305 m, 1 kip = 4.45 kN, 1 ksf = 47.9 kPa)



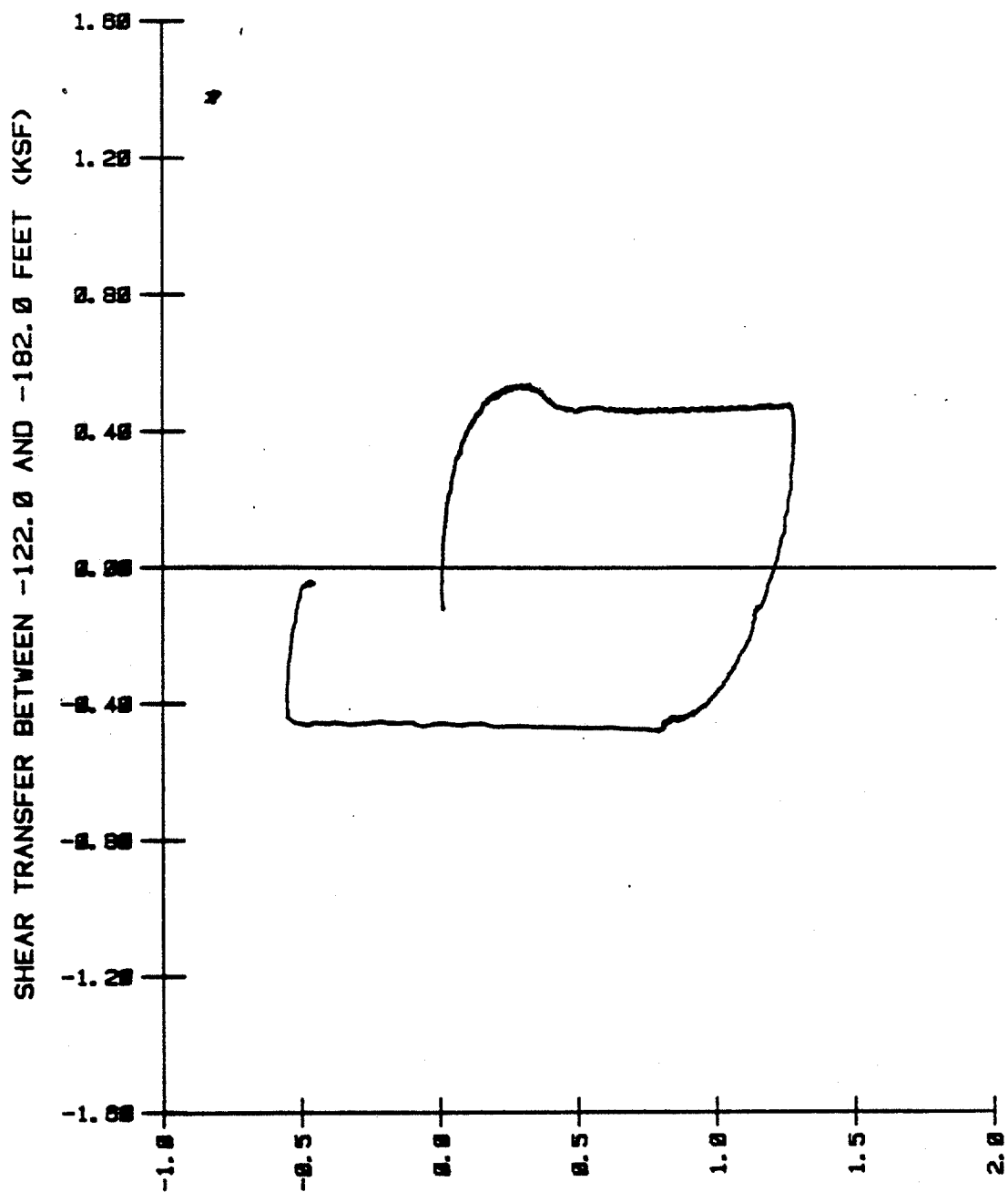
SHEAR TRANSFER VERSUS DISPLACEMENT BETWEEN THE DEPTHS OF 0 AND 62 FEET
DURING STATIC LOAD TESTS AFTER PARTIAL CONSOLIDATION - EXTENSOMETERS

(1 inch = 25.4 mm, 1 ft = 0.305 m, 1 kip = 4.45 kN, 1 ksf = 47.9 kPa)



SHEAR TRANSFER VERSUS DISPLACEMENT BETWEEN THE DEPTHS OF 62 AND 122 FEET
DURING STATIC LOAD TESTS AFTER PARTIAL CONSOLIDATION - EXTENSOMETERS

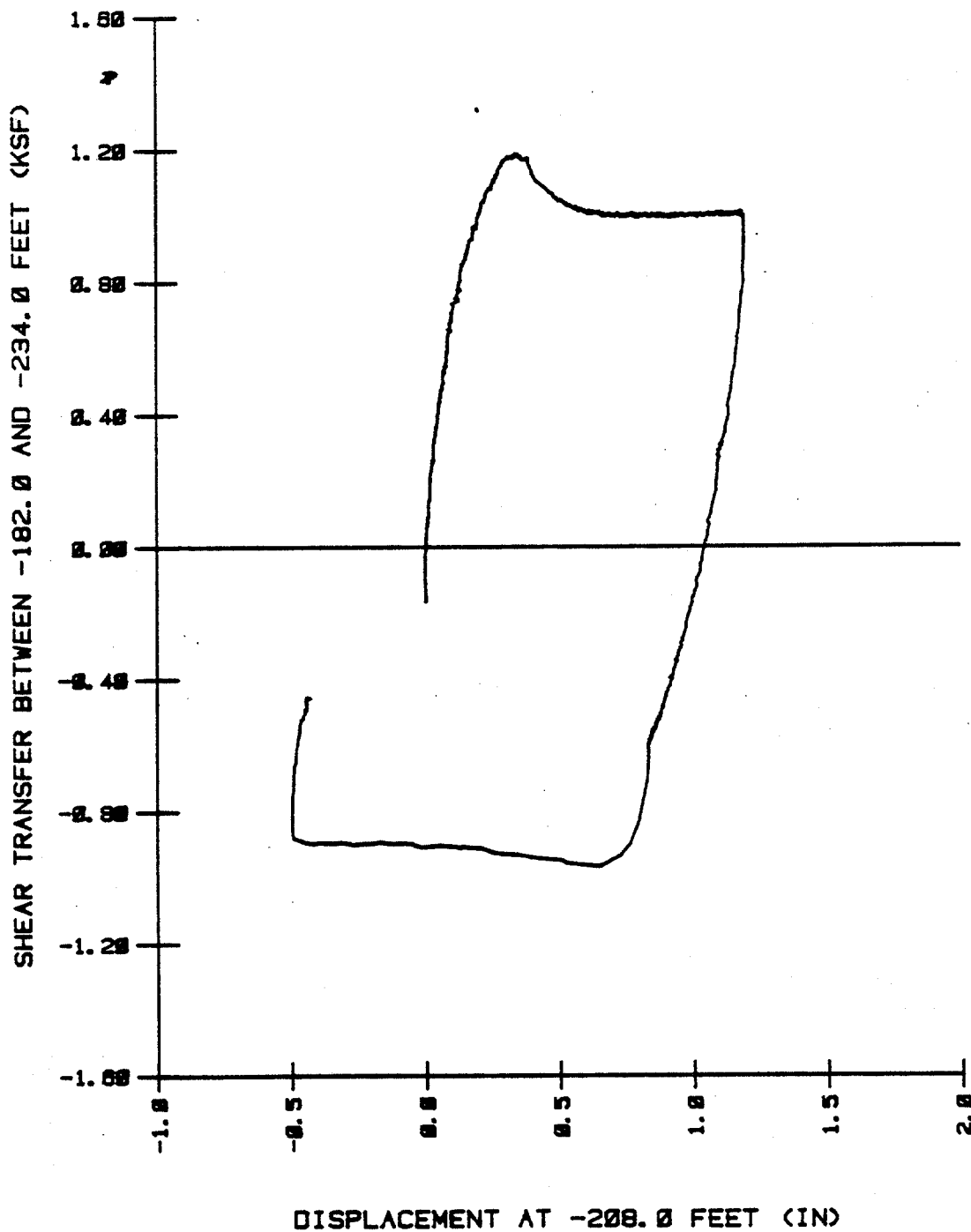
(1 inch = 25.4 mm, 1 ft = 0.305 m, 1 kip = 4.45 kN, 1 ksf = 47.9 kPa)



DISPLACEMENT AT -152.0 FEET (IN)

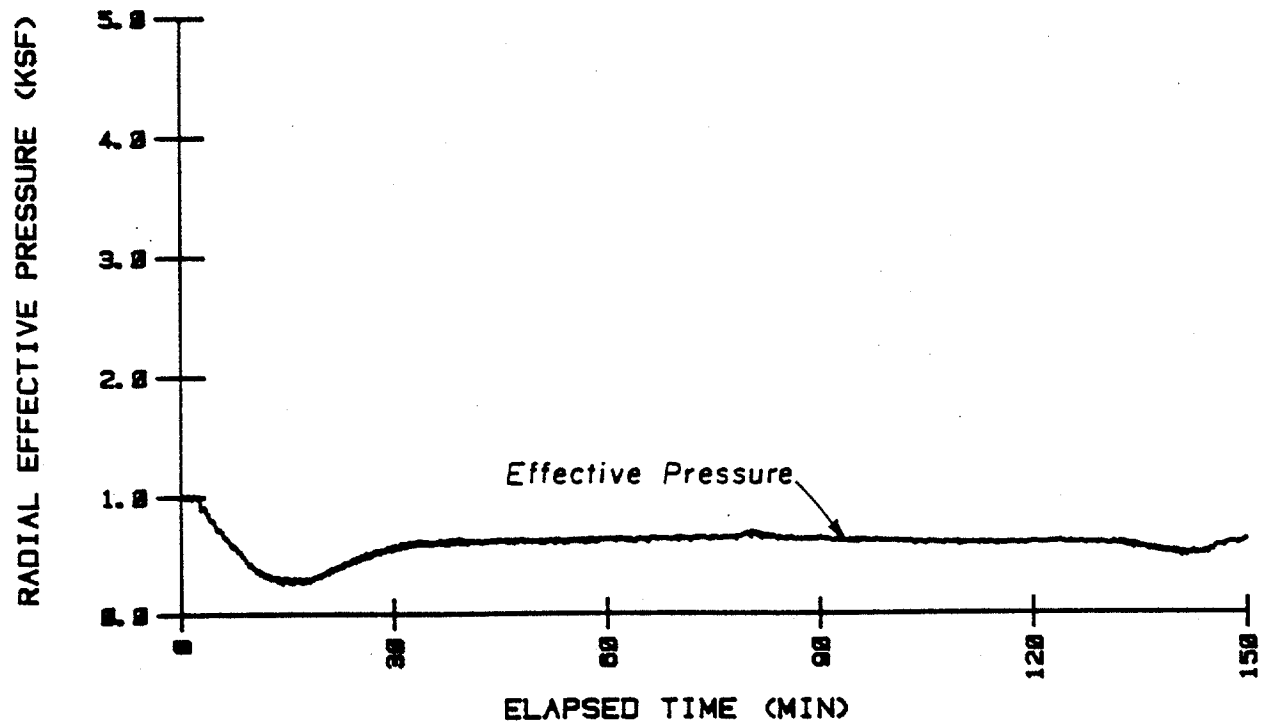
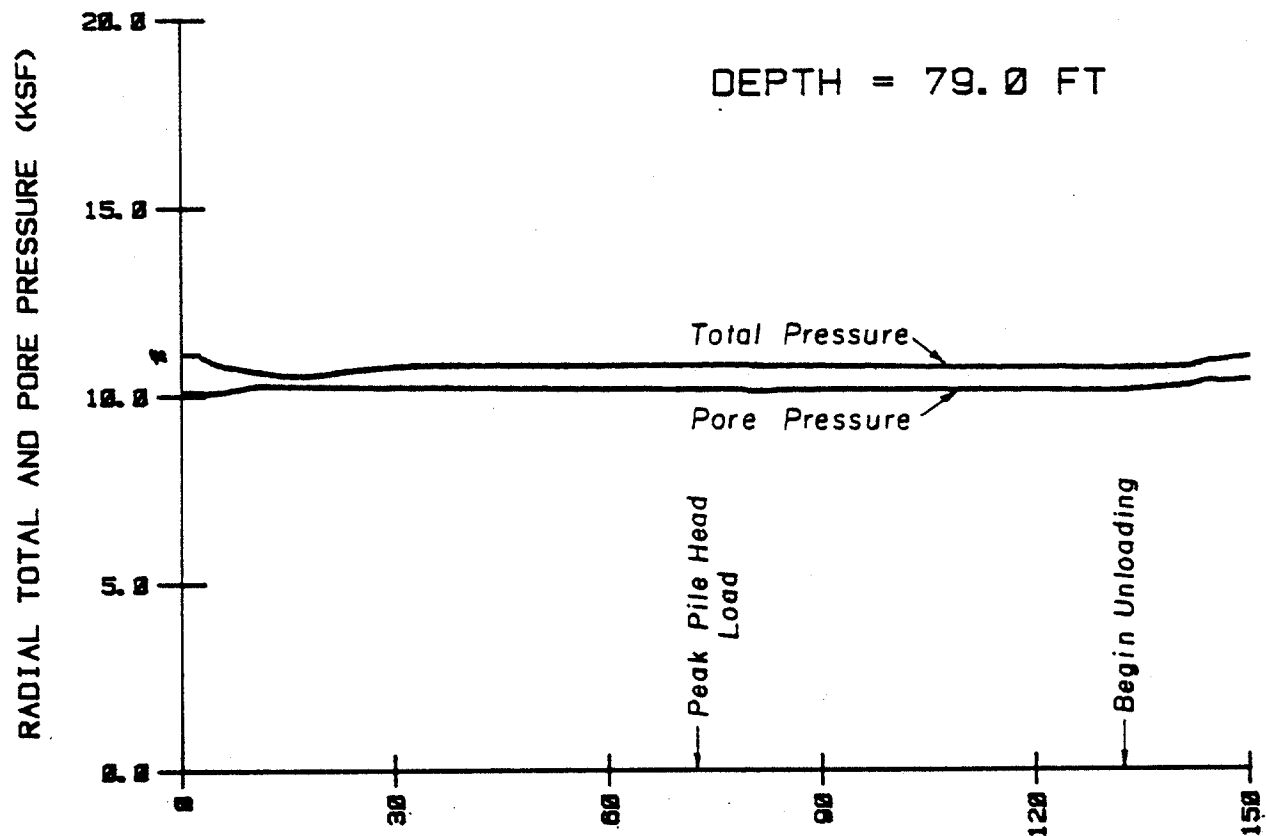
SHEAR TRANSFER VERSUS DISPLACEMENT BETWEEN THE DEPTHS OF 122 AND 182 FEET
DURING STATIC LOAD TESTS AFTER PARTIAL CONSOLIDATION - EXTENSOMETERS

(1 inch = 25.4 mm, 1 ft = 0.305 m, 1 kip = 4.45 kN, 1 ksf = 47.9 kPa)

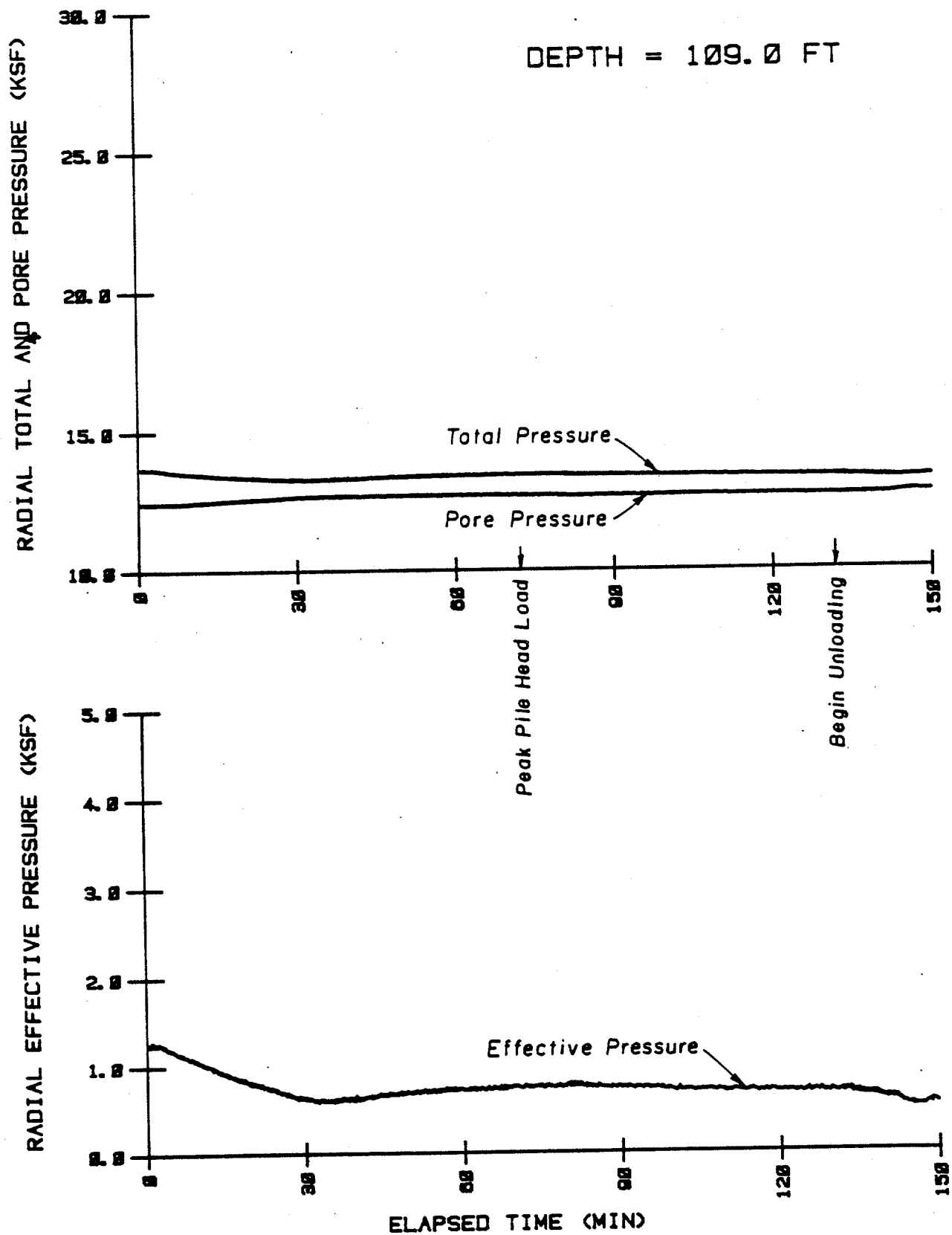


SHEAR TRANSFER VERSUS DISPLACEMENT BETWEEN THE DEPTHS OF 182 AND 234 FEET
DURING STATIC LOAD TESTS AFTER PARTIAL CONSOLIDATION - EXTENSOMETERS

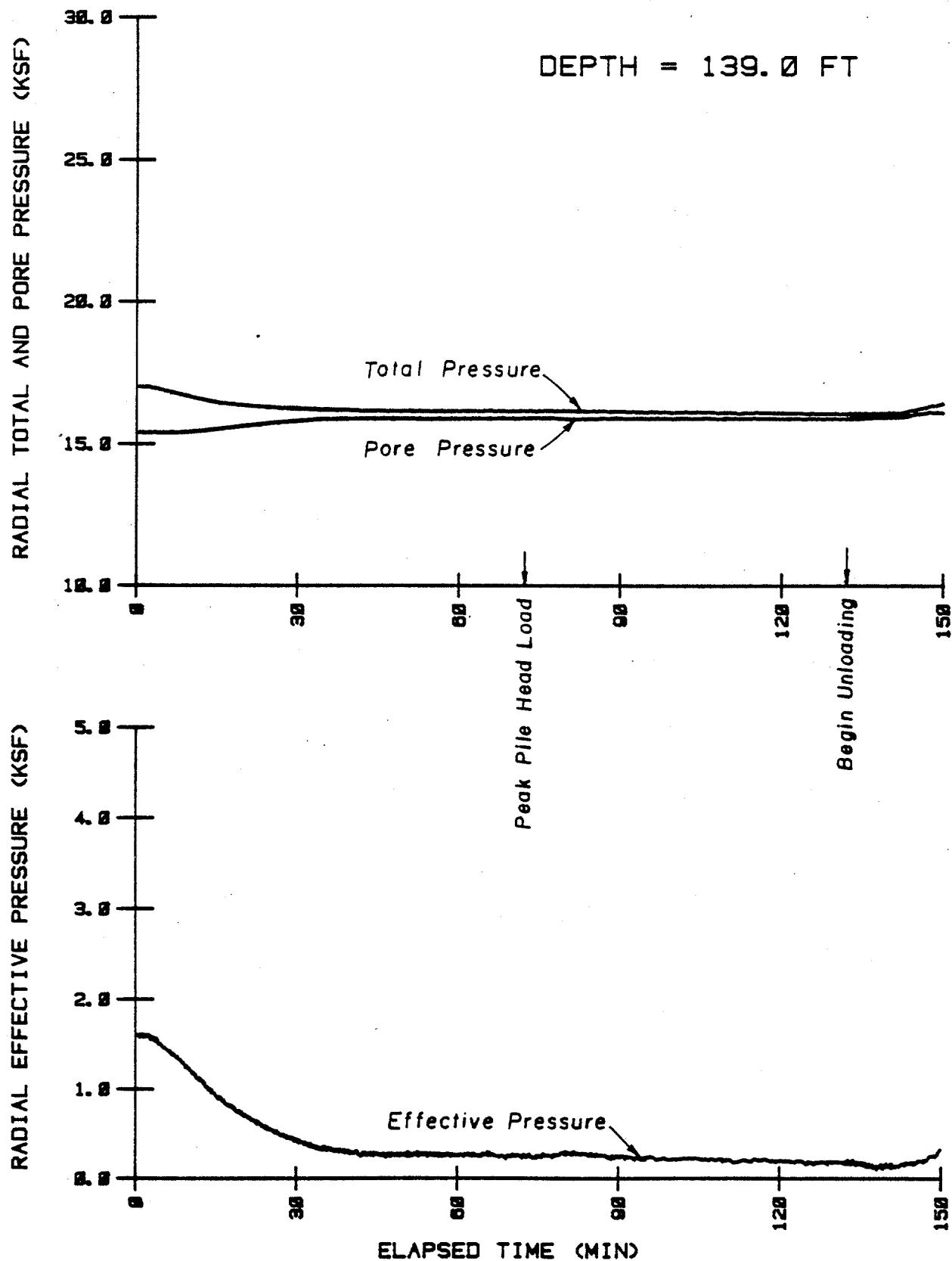
(1 inch = 25.4 mm, 1 ft = 0.305 m, 1 kip = 4.45 kN, 1 ksf = 47.9 kPa)



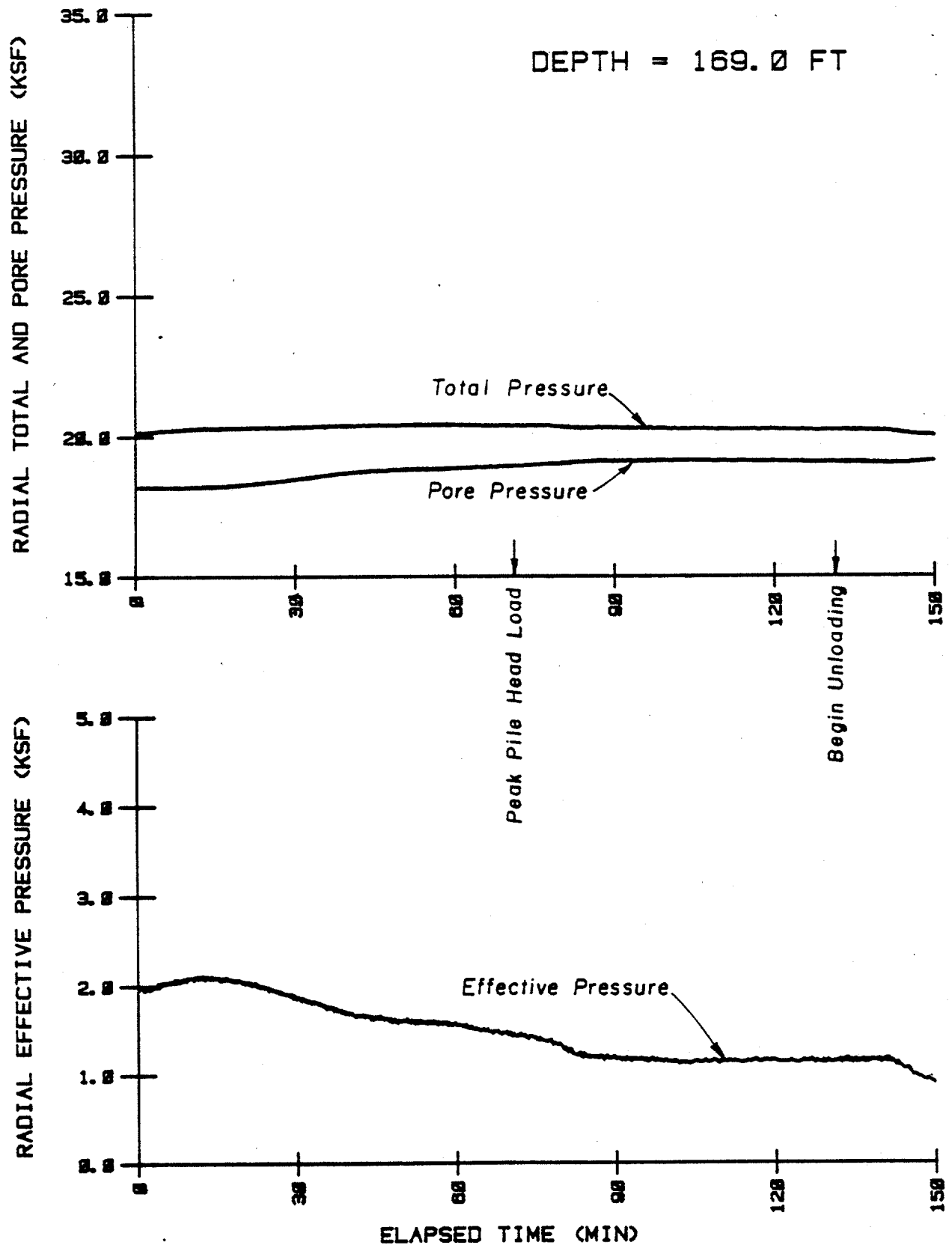
SOIL PRESSURE VARIATIONS AT THE 79-FOOT DEPTH DURING THE STATIC TENSION TEST
 (1 inch = 25.4 mm, 1 ft = 0.305 m, 1 kip = 4.45 kN, 1 ksf = 47.9 kPa)



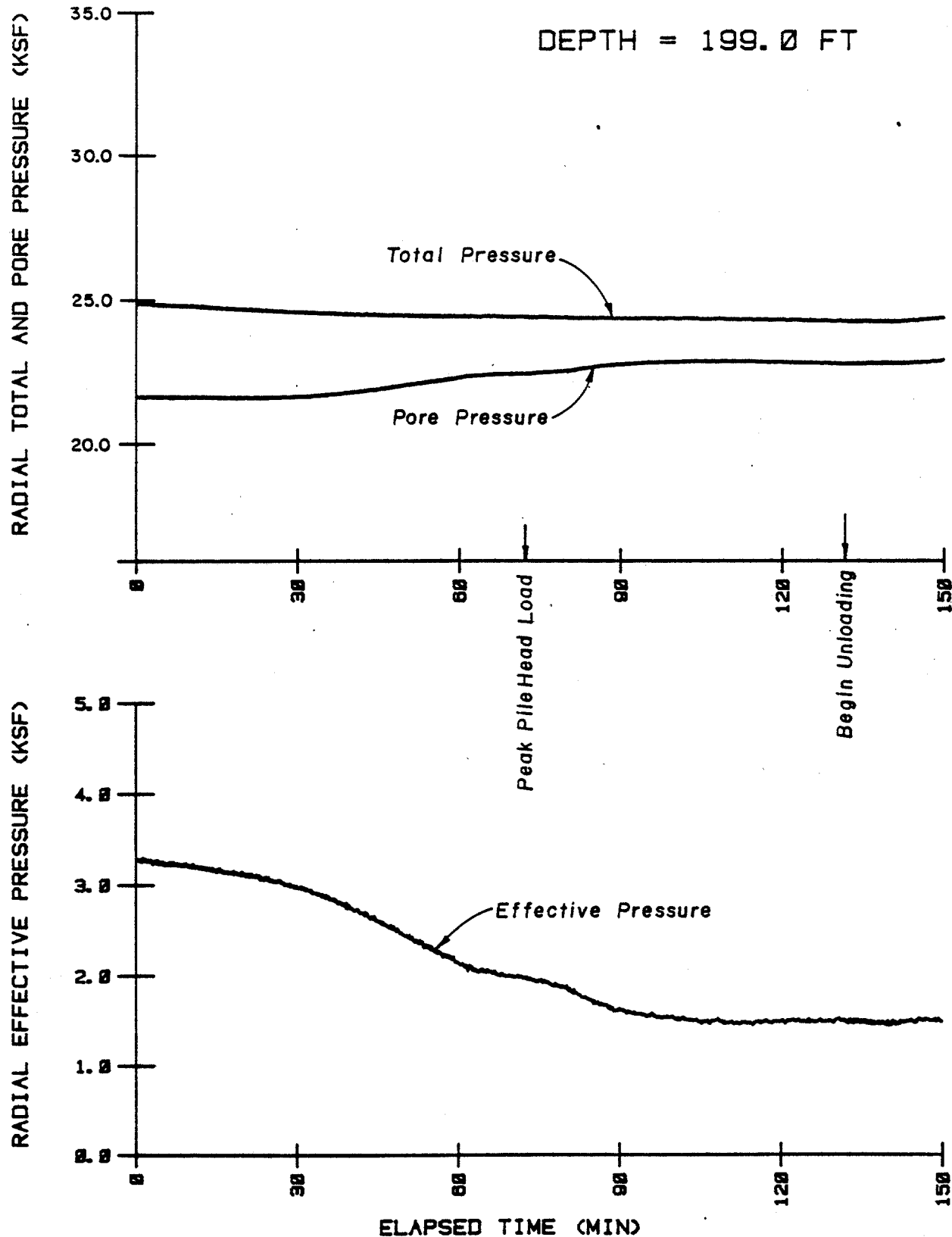
SOIL PRESSURE VARIATIONS AT THE 109-FOOT DEPTH DURING THE STATIC TENSION TEST
(1 inch = 25.4 mm, 1 ft = 0.305 m, 1 kip = 4.45 kN, 1 ksf = 47.9 kPa)



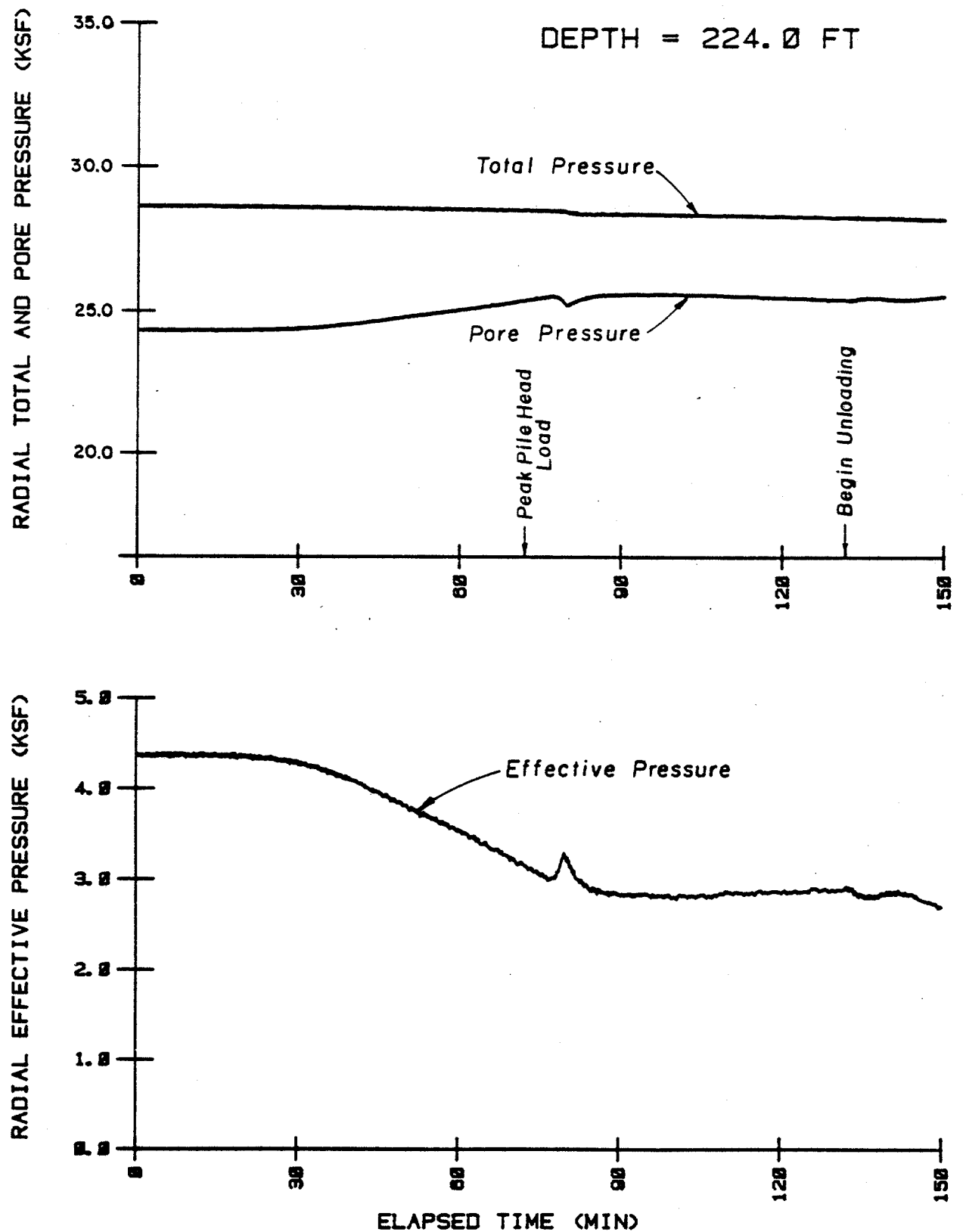
SOIL PRESSURE VARIATIONS AT THE 139-FOOT DEPTH DURING THE STATIC TENSION TEST
(1 inch = 25.4 mm, 1 ft = 0.305 m, 1 kip = 4.45 kN, 1 ksf = 47.9 kPa)



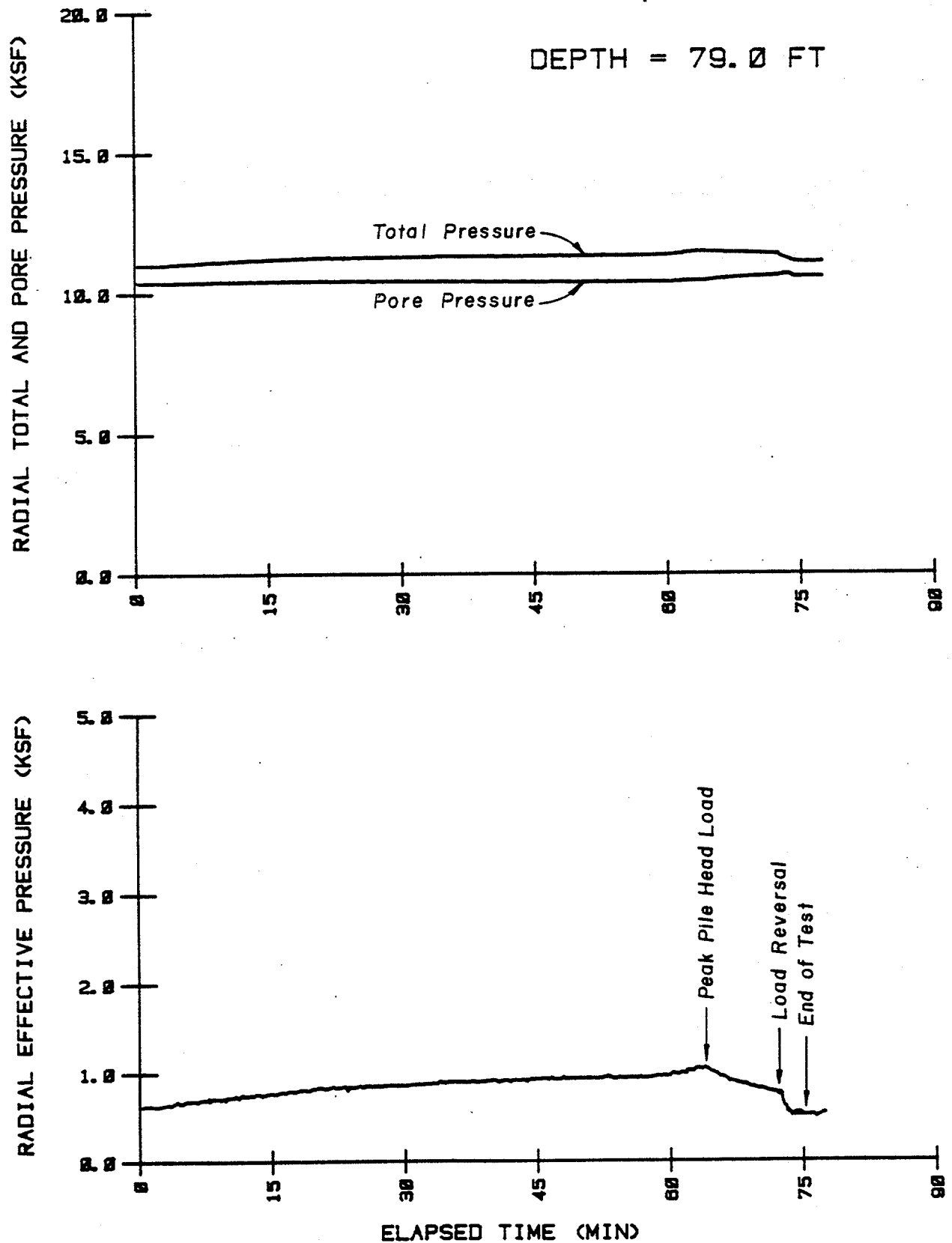
SOIL PRESSURE VARIATIONS AT THE 169-FOOT DEPTH DURING THE STATIC TENSION TEST
(1 inch = 25.4 mm, 1 ft = 0.305 m, 1 kip = 4.45 kN, 1 ksf = 47.9 kPa)



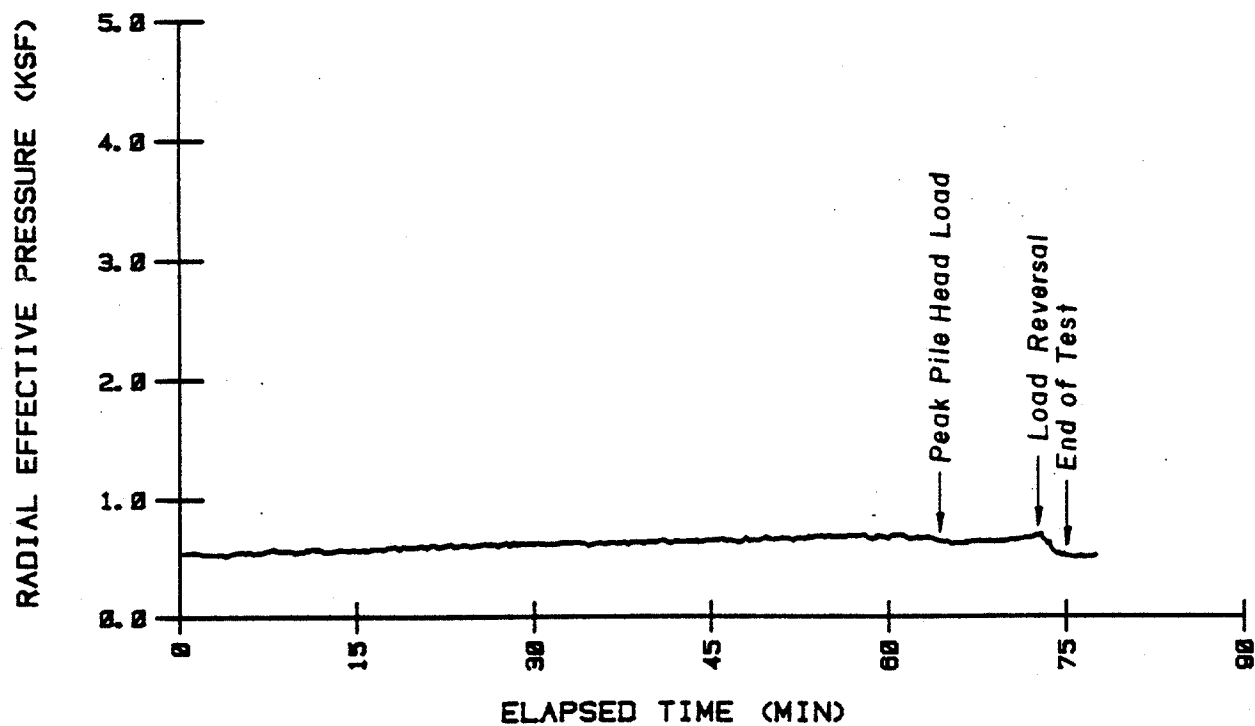
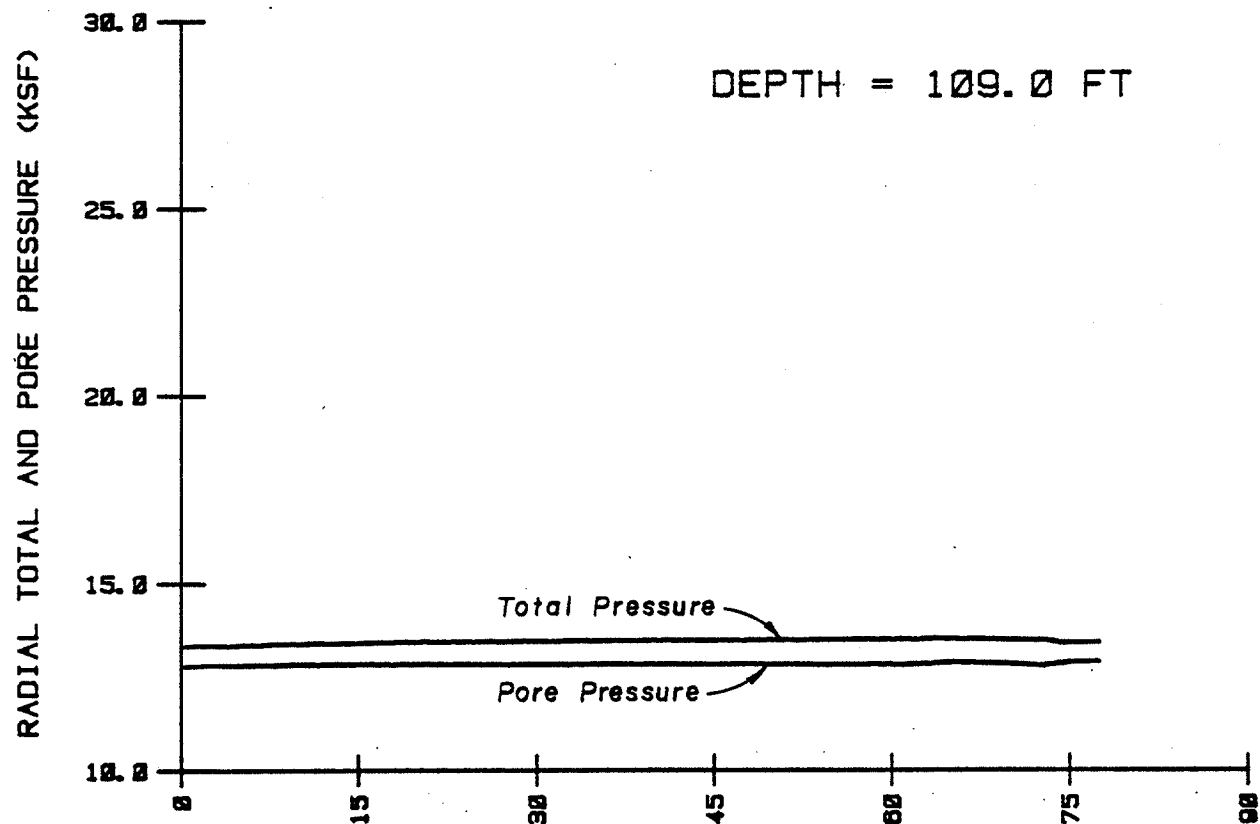
SOIL PRESSURE VARIATIONS AT THE 199-FOOT DEPTH DURING THE STATIC TENSION TEST
(1 inch = 25.4 mm, 1 ft = 0.305 m, 1 kip = 4.45 kN, 1 ksf = 47.9 kPa)



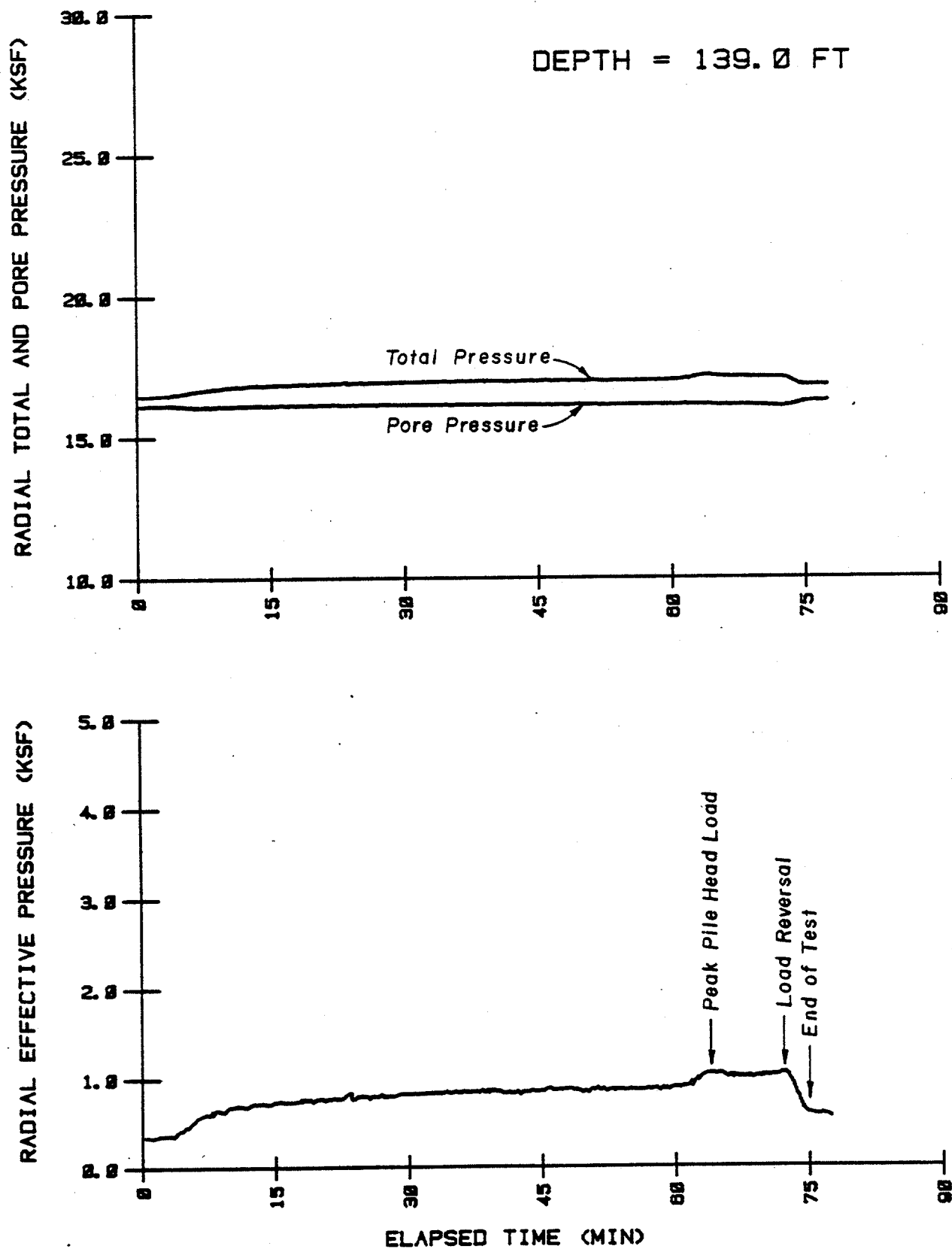
SOIL PRESSURE VARIATIONS AT THE 224-FOOT DEPTH DURING THE STATIC TENSION TEST
(1 inch = 25.4 mm, 1 ft = 0.305 m, 1 kip = 4.45 kN, 1 ksf = 47.9 kPa)



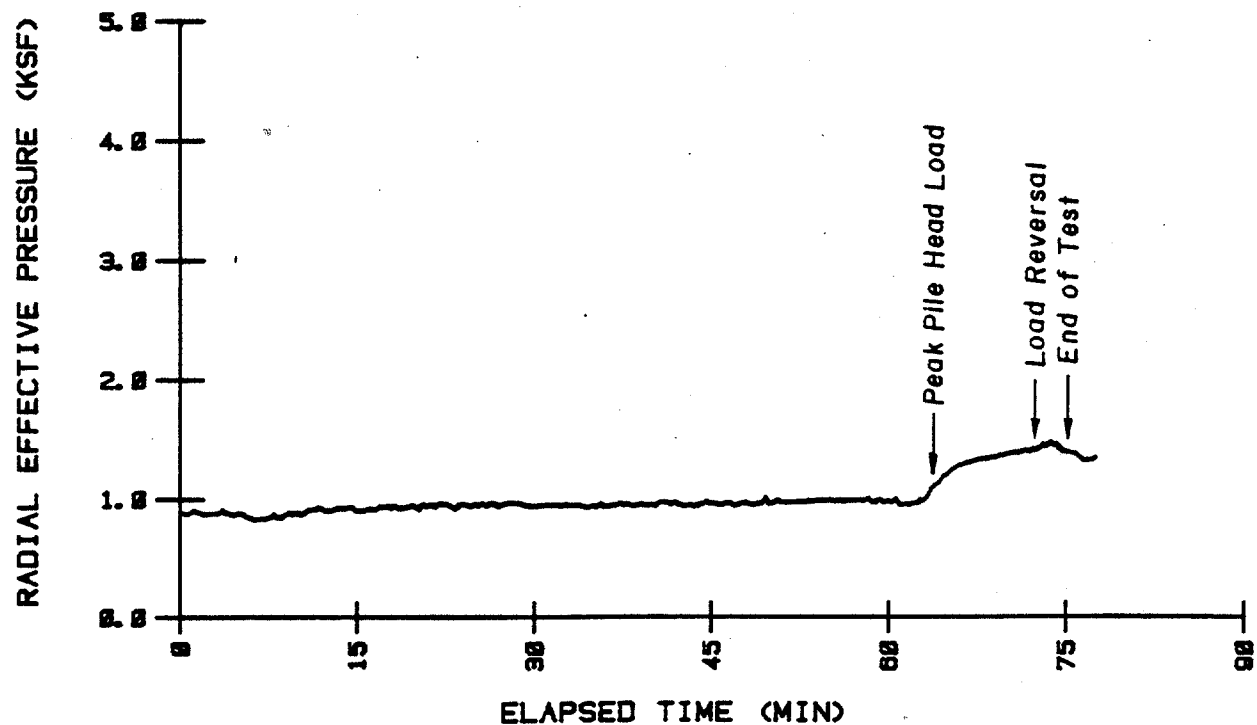
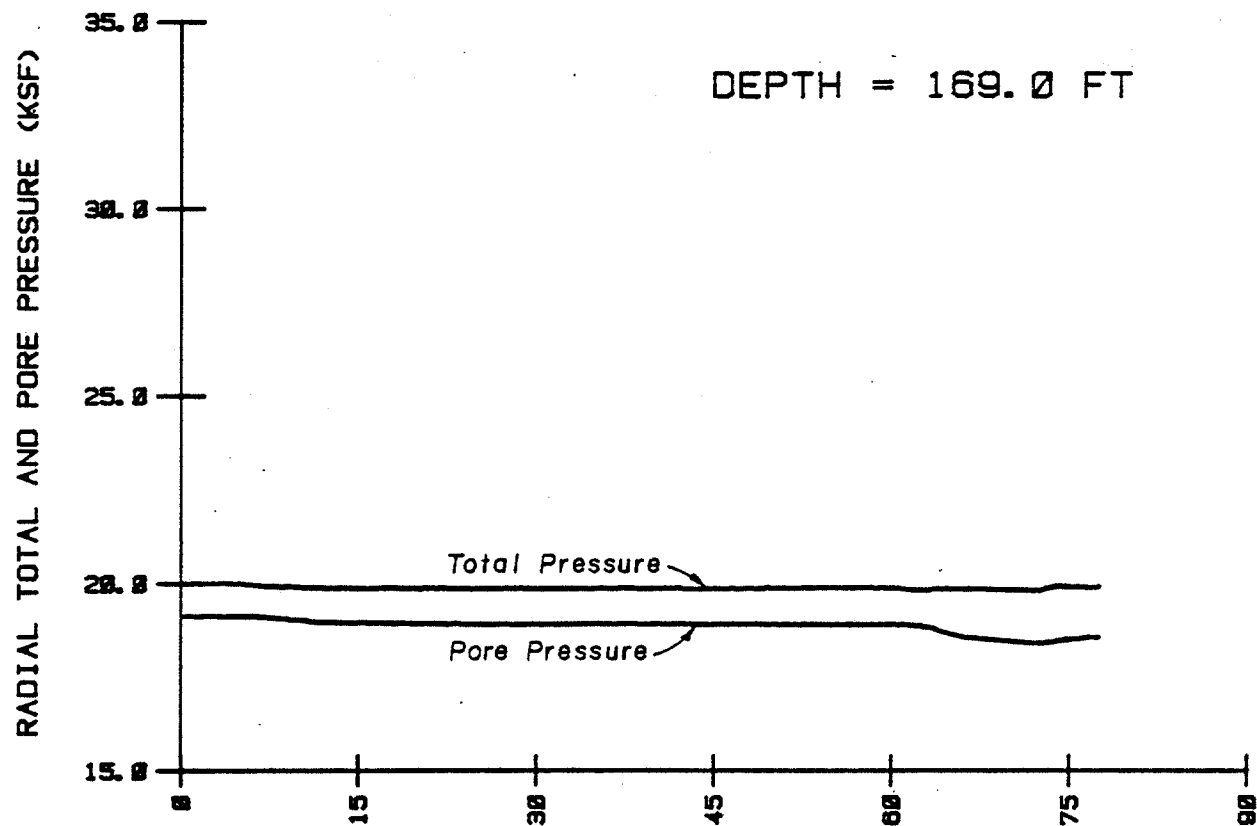
SOIL PRESSURE VARIATIONS AT THE 79-FOOT DEPTH DURING THE COMPRESSION TEST
(1 inch = 25.4 mm, 1 ft = 0.305 m, 1 kip = 4.45 kN, 1 ksf = 47.9 kPa)



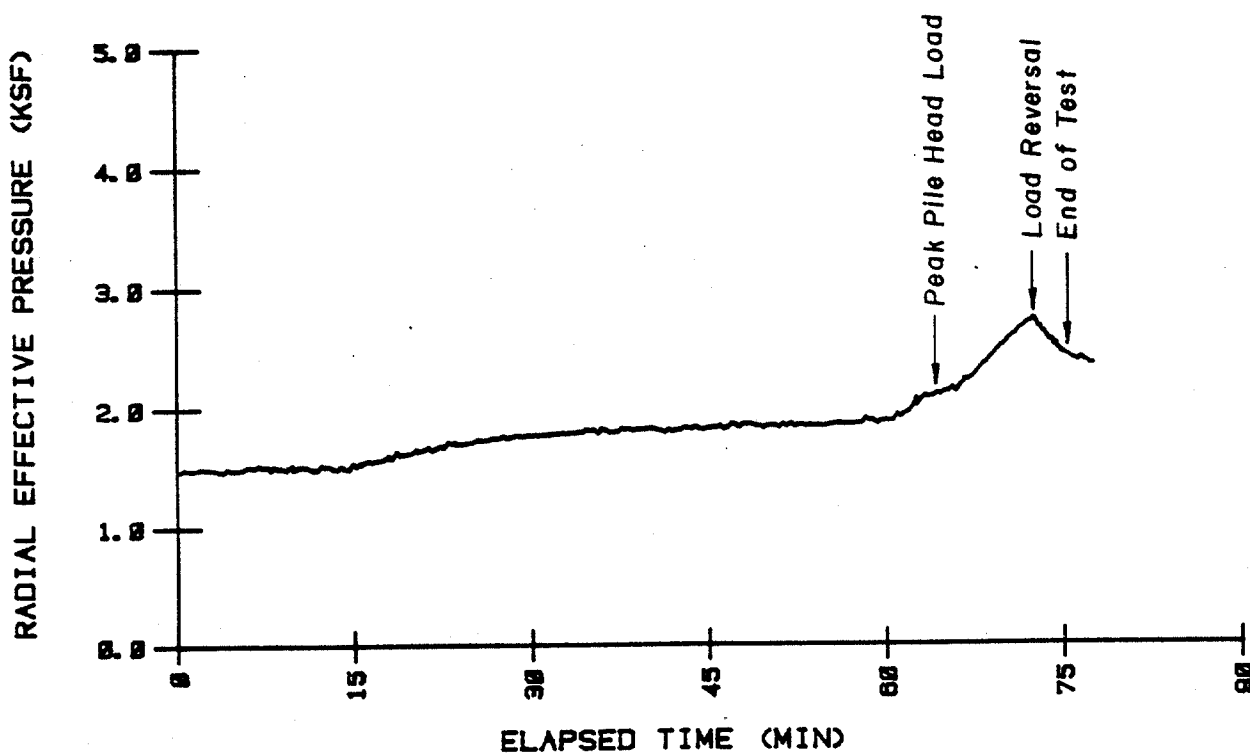
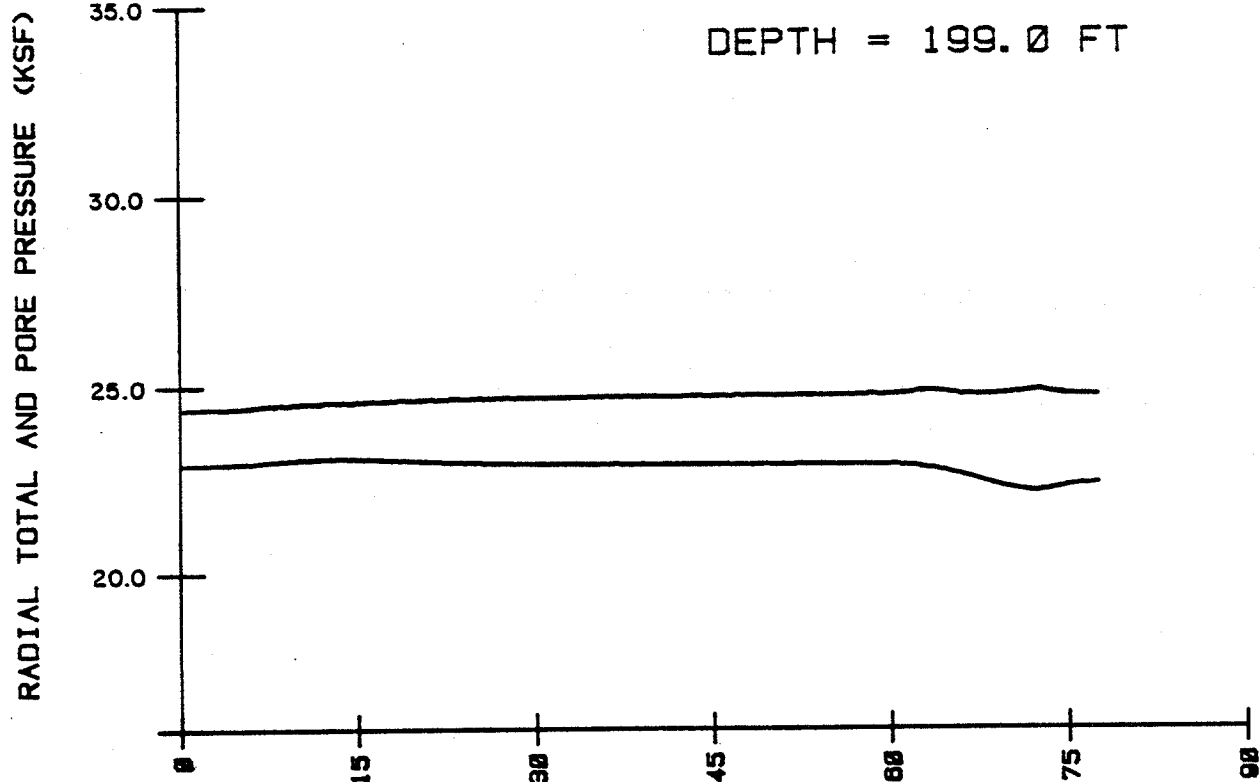
SOIL PRESSURE VARIATIONS AT THE 109-FOOT DEPTH DURING THE COMPRESSION TEST
(1 inch = 25.4 mm, 1 ft = 0.305 m, 1 kip = 4.45 kN, 1 ksf = 47.9 kPa)



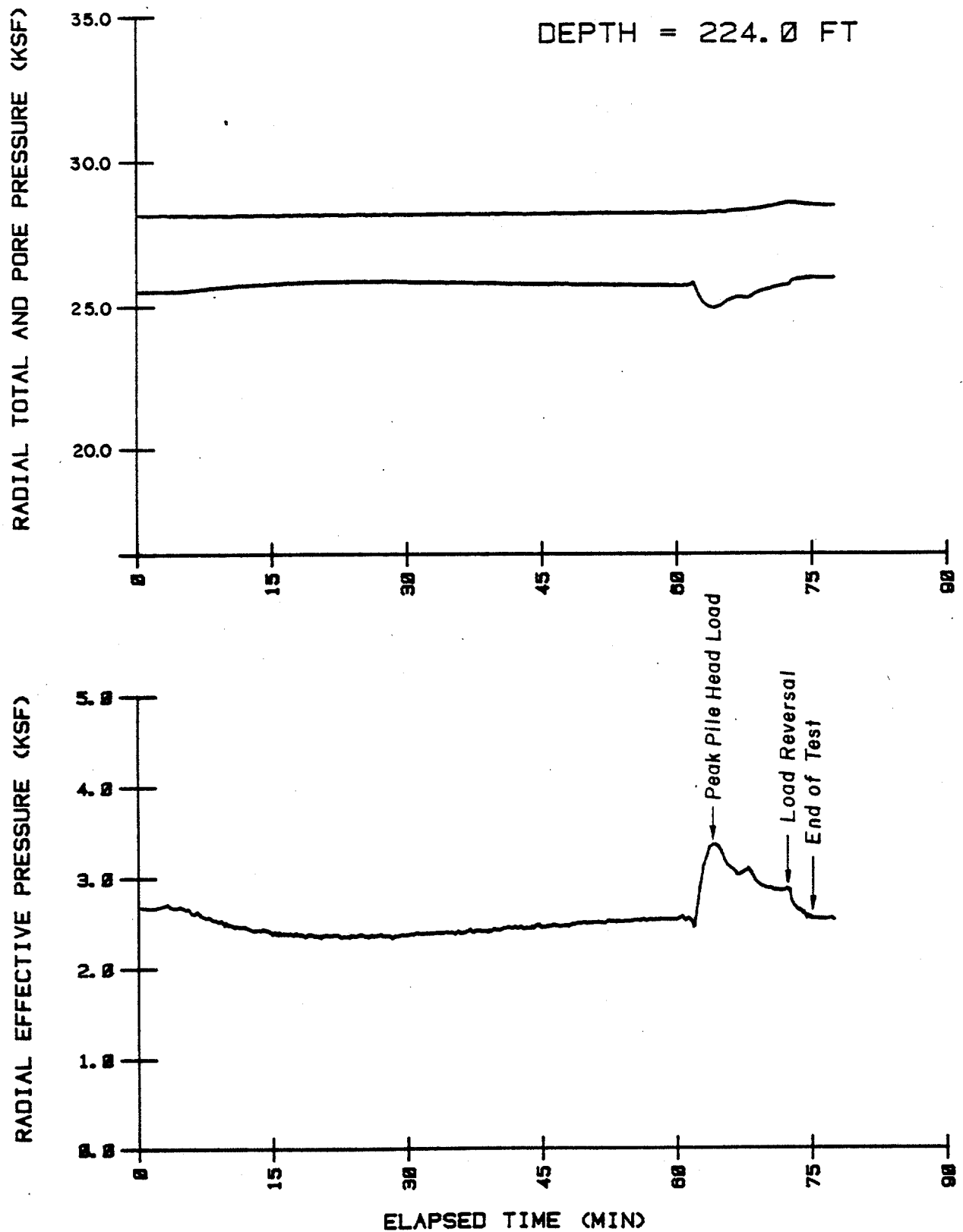
SOIL PRESSURE VARIATIONS AT THE 139-FOOT DEPTH DURING THE COMPRESSION TEST
(1 inch = 25.4 mm, 1 ft = 0.305 m, 1 kip = 4.45 kN, 1 ksf = 47.9 kPa)



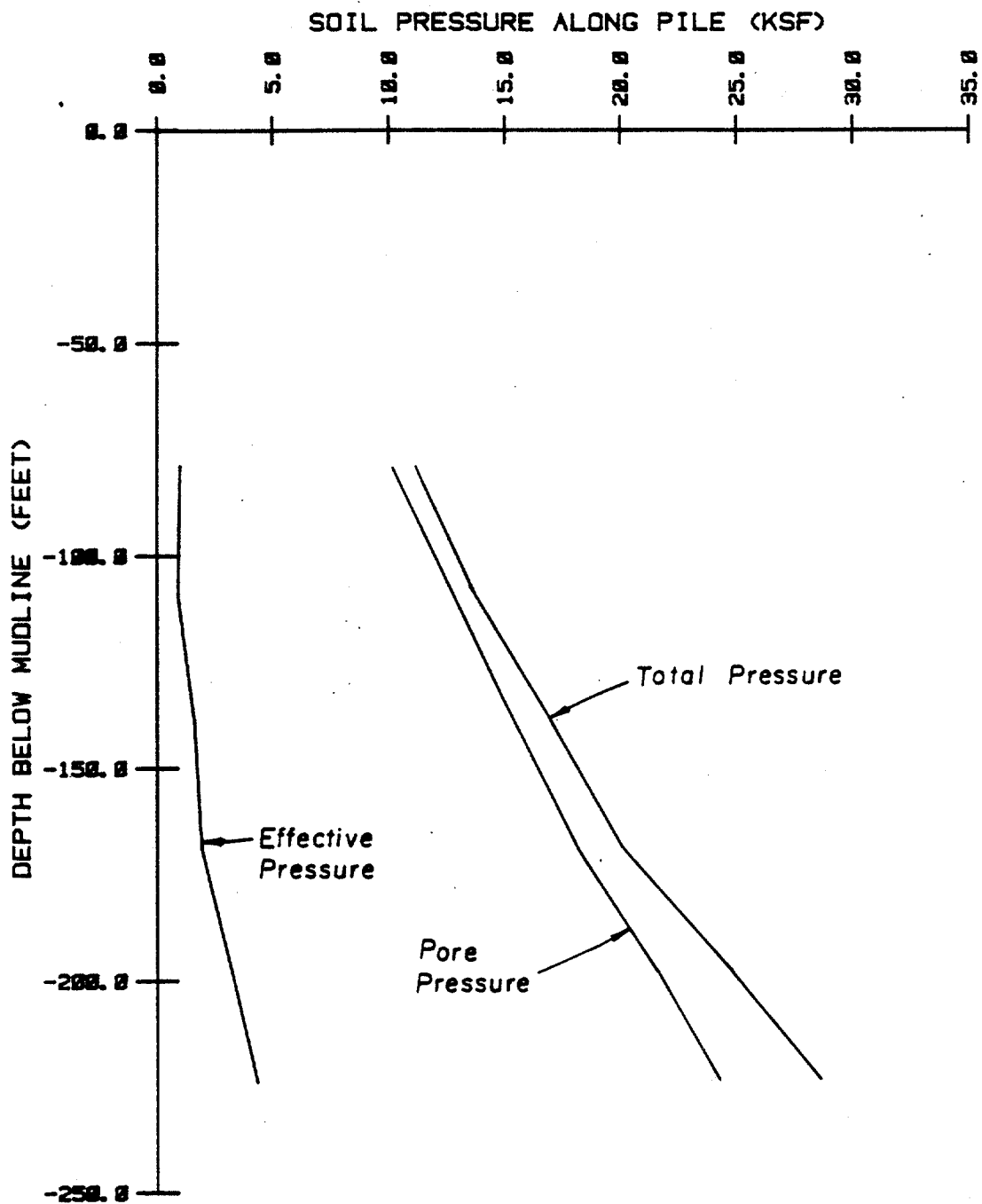
SOIL PRESSURE VARIATIONS AT THE 169-FOOT DEPTH DURING THE COMPRESSION TEST
(1 inch = 25.4 mm, 1 ft = 0.305 m, 1 kip = 4.45 kN, 1 ksf = 47.9 kPa)



SOIL PRESSURE VARIATIONS AT THE 199-FOOT DEPTH DURING THE COMPRESSION TEST
(1 inch = 25.4 mm, 1 ft = 0.305 m, 1 kip = 4.45 kN, 1 ksf = 47.9 kPa)

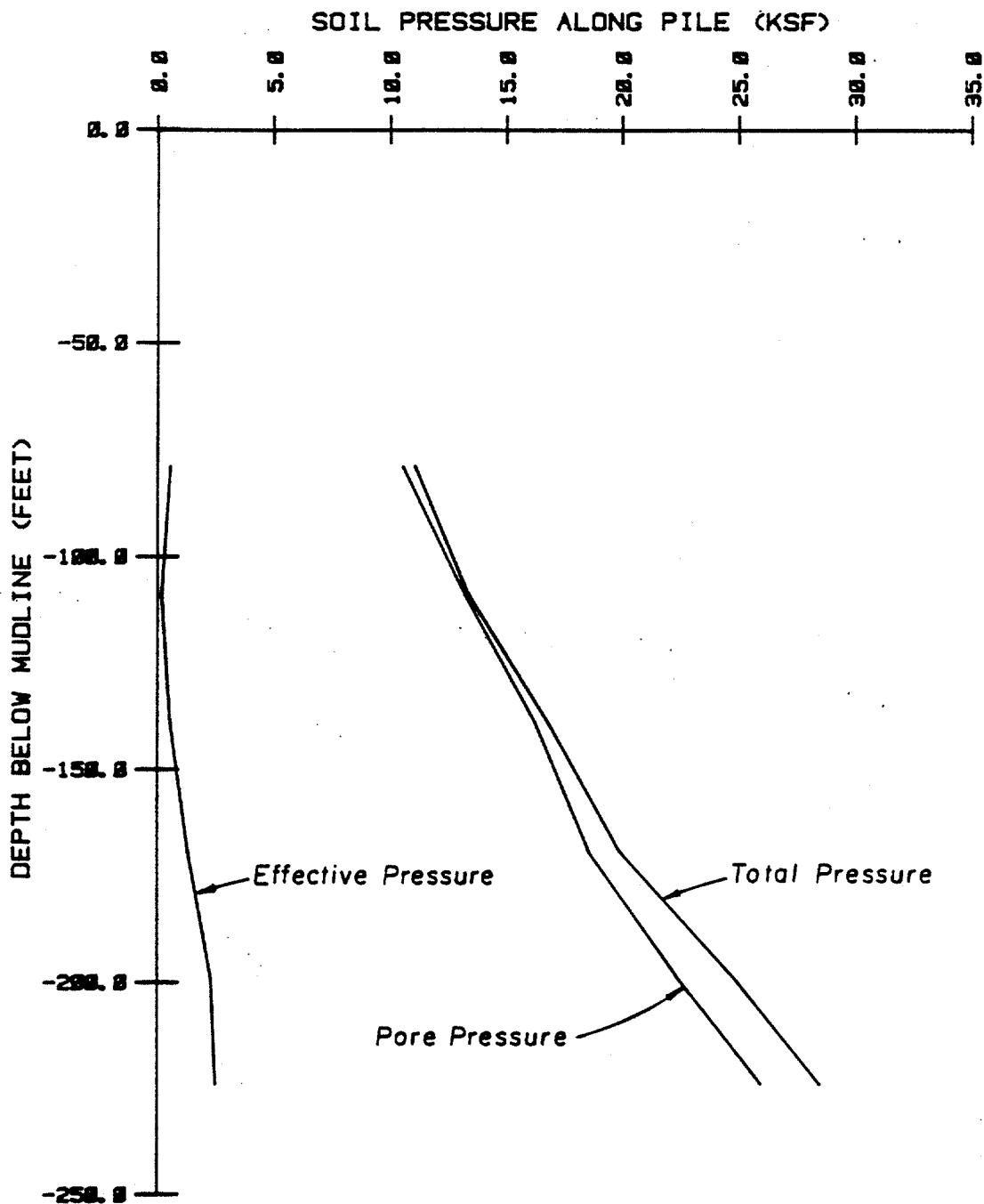


SOIL PRESSURE VARIATIONS AT THE 224-FOOT DEPTH DURING THE COMPRESSION TEST
(1 inch = 25.4 mm, 1 ft = 0.305 m, 1 kip = 4.45 kN, 1 ksf = 47.9 kPa)



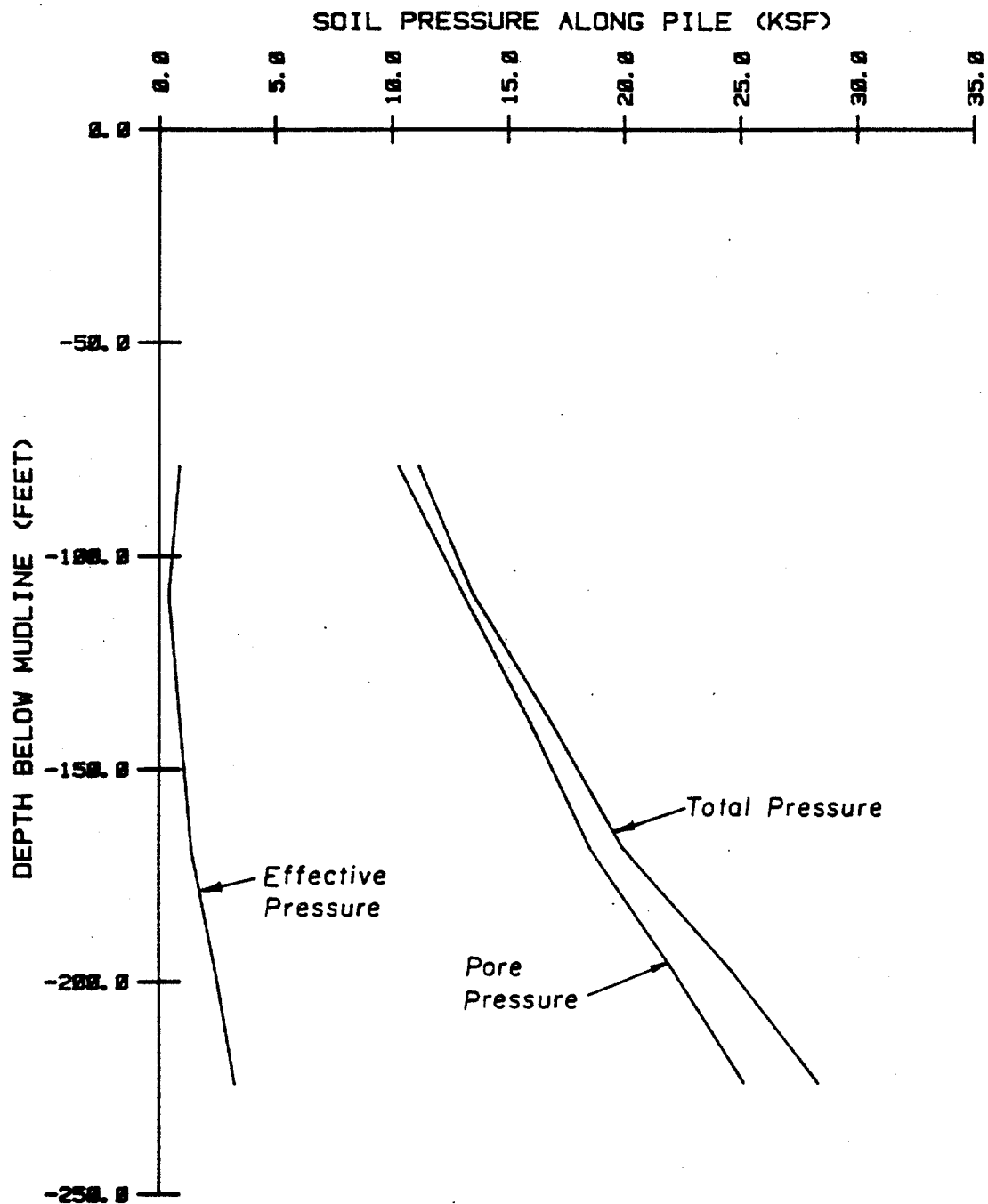
SOIL PRESSURE PROFILES PRIOR TO THE INITIAL LOAD TEST AFTER PARTIAL CONSOLIDATION

(1 inch = 25.4 mm, 1 ft = 0.305 m, 1 kip = 4.45 kN, 1 ksf = 47.9 kPa)



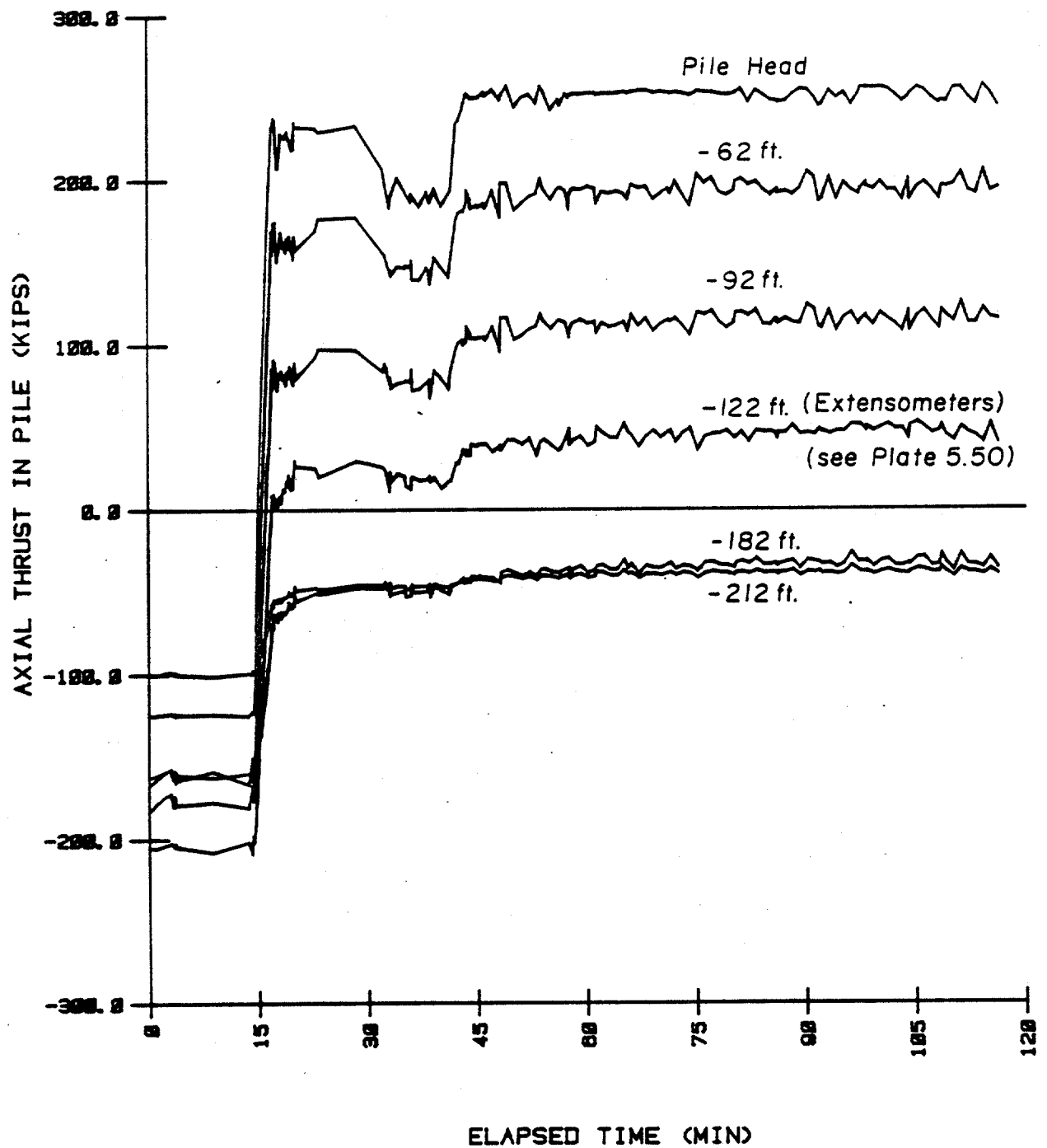
SOIL PRESSURE PROFILES AT THE END OF THE TENSION AND COMPRESSION TESTS

(1 inch = 25.4 mm, 1 ft = 0.305 m, 1 kip = 4.45 kN, 1 ksf = 47.9 kPa)



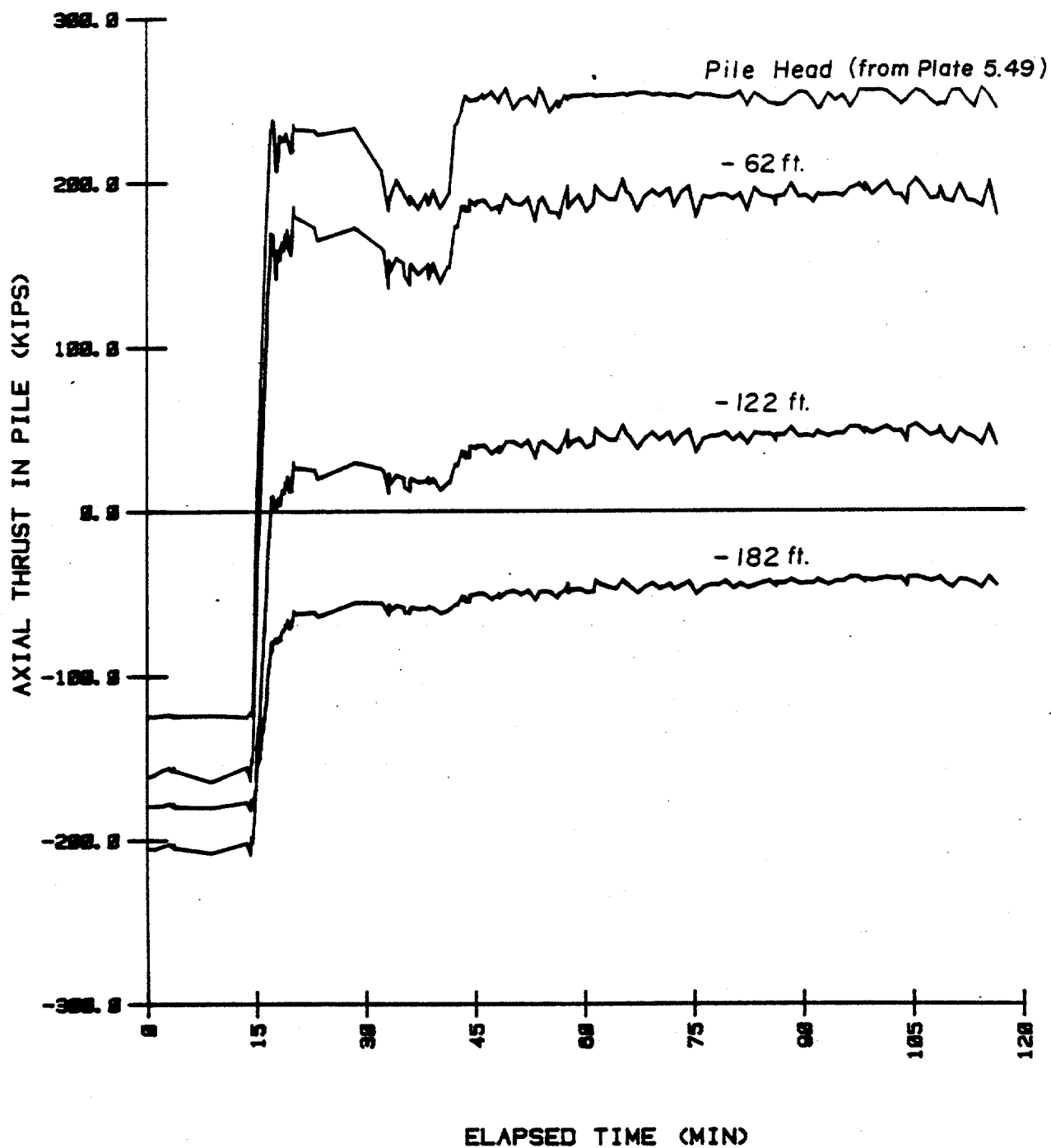
SOIL PRESSURE PROFILES AT END OF THE 18-HOUR EQUILIBRATION PERIOD

(1 inch = 25.4 mm, 1 ft = 0.305 m, 1 kip = 4.45 kN, 1 ksf = 47.9 kPa)



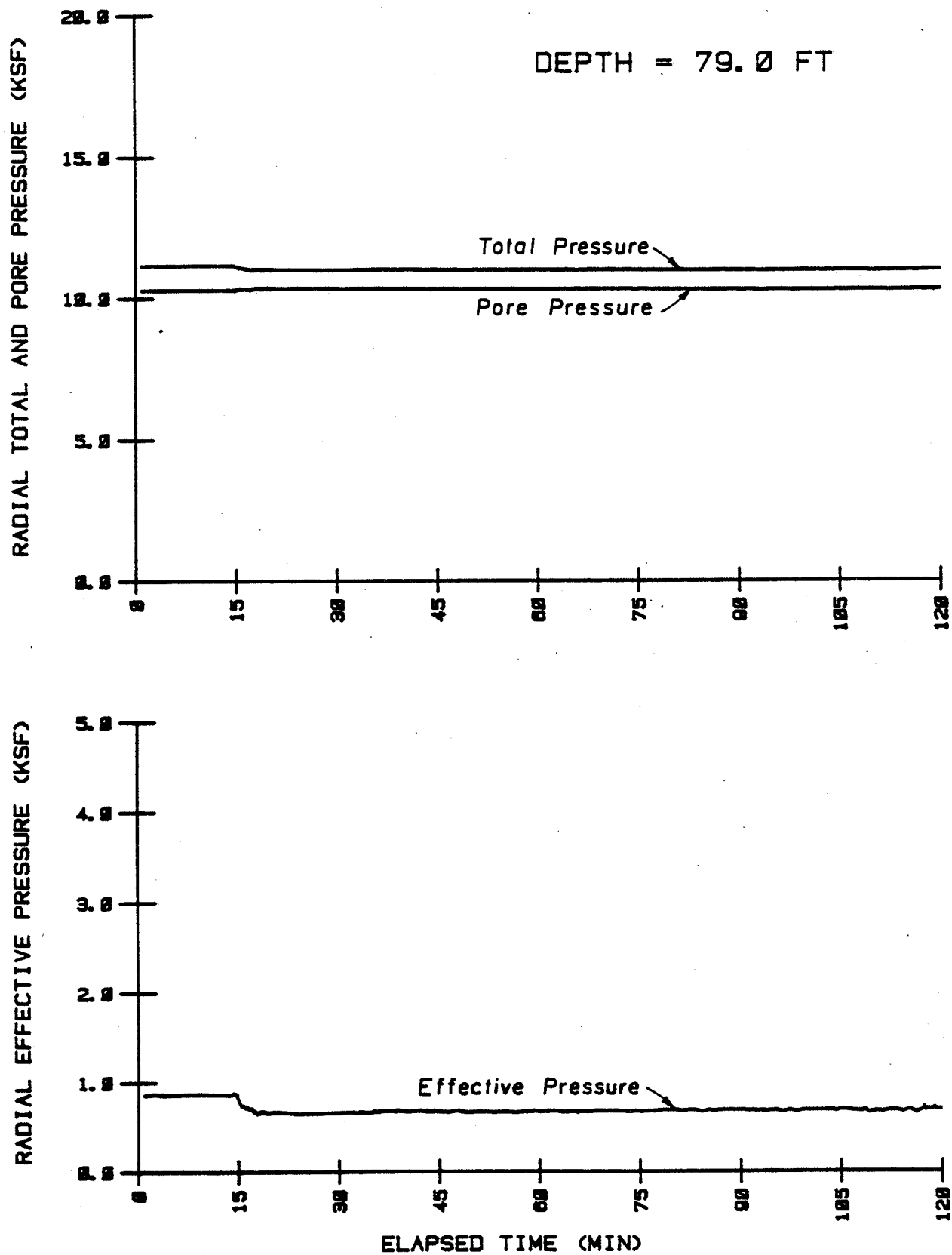
VARIATION IN AXIAL THRUST MEASURED BY THE STRAIN MODULES DURING THE CREEP TEST

(1 inch = 25.4 mm, 1 ft = 0.305 m, 1 kip = 4.45 kN, 1 ksf = 47.9 kPa)

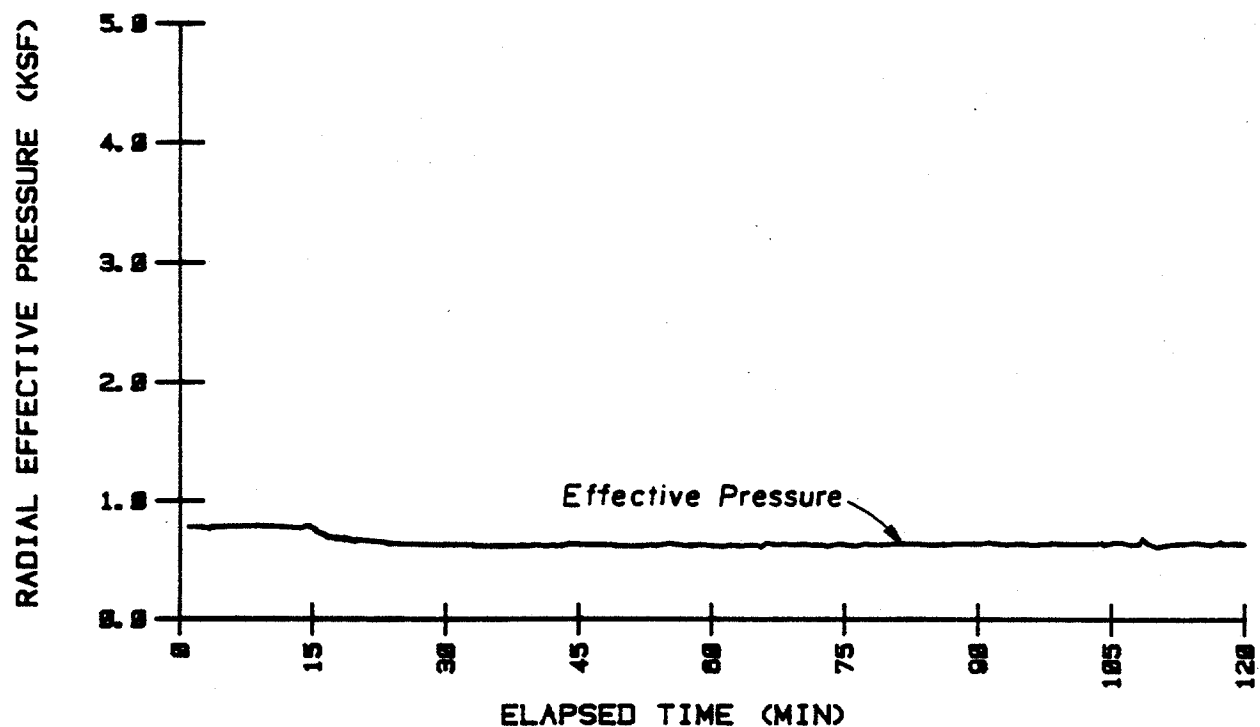
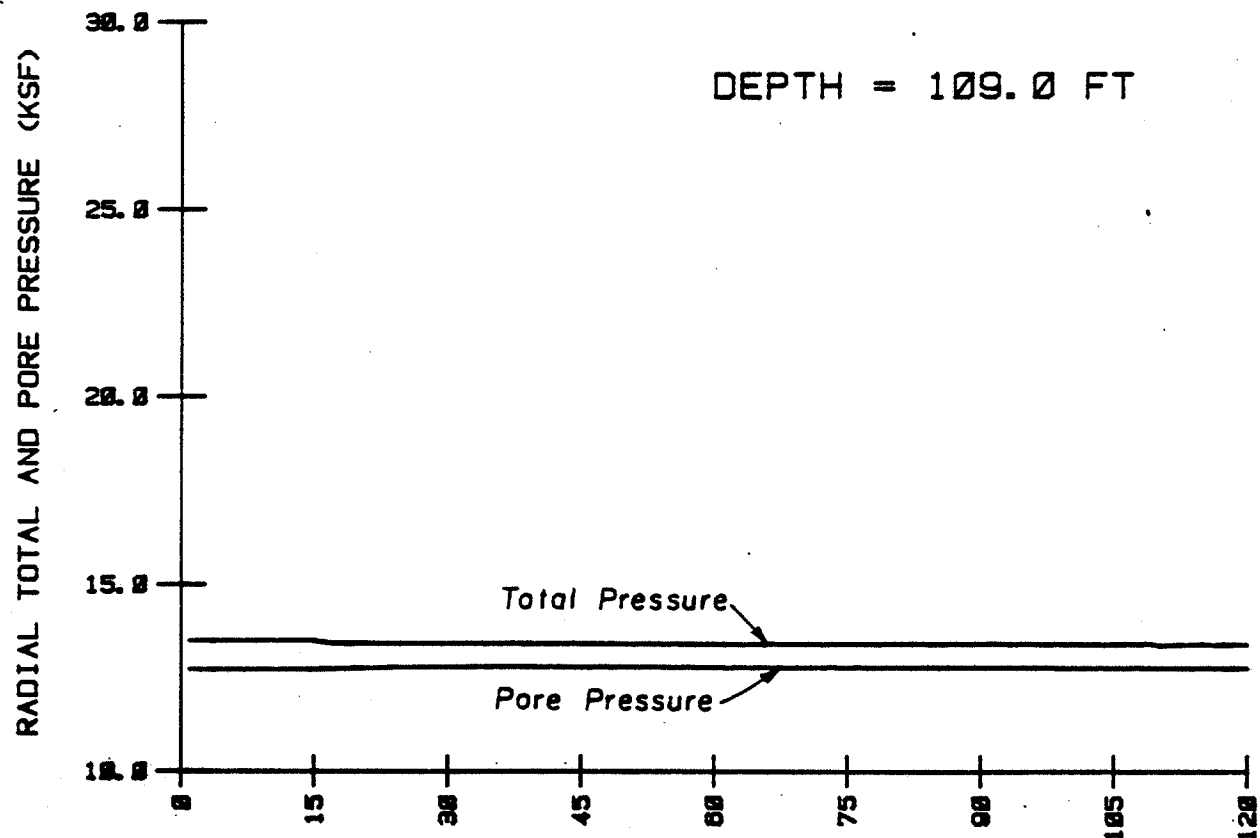


VARIATION IN AXIAL THRUST MEASURED BY THE EXTENSOMETERS DURING THE CREEP TEST

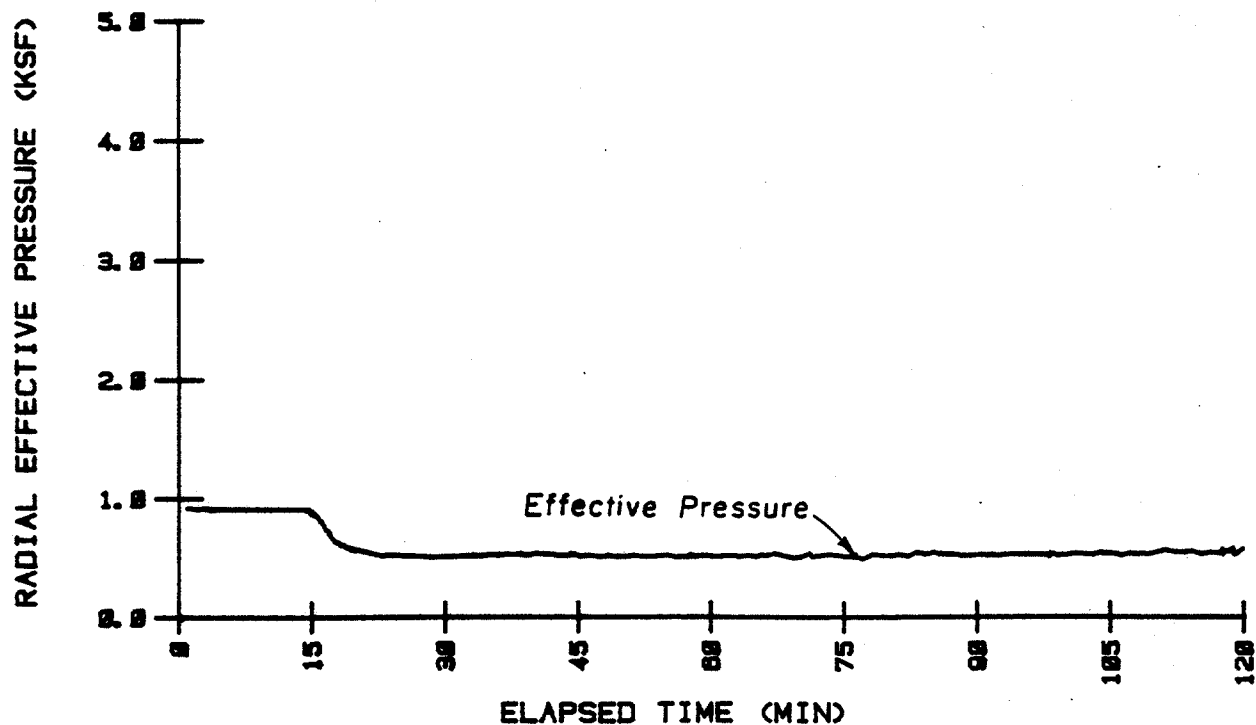
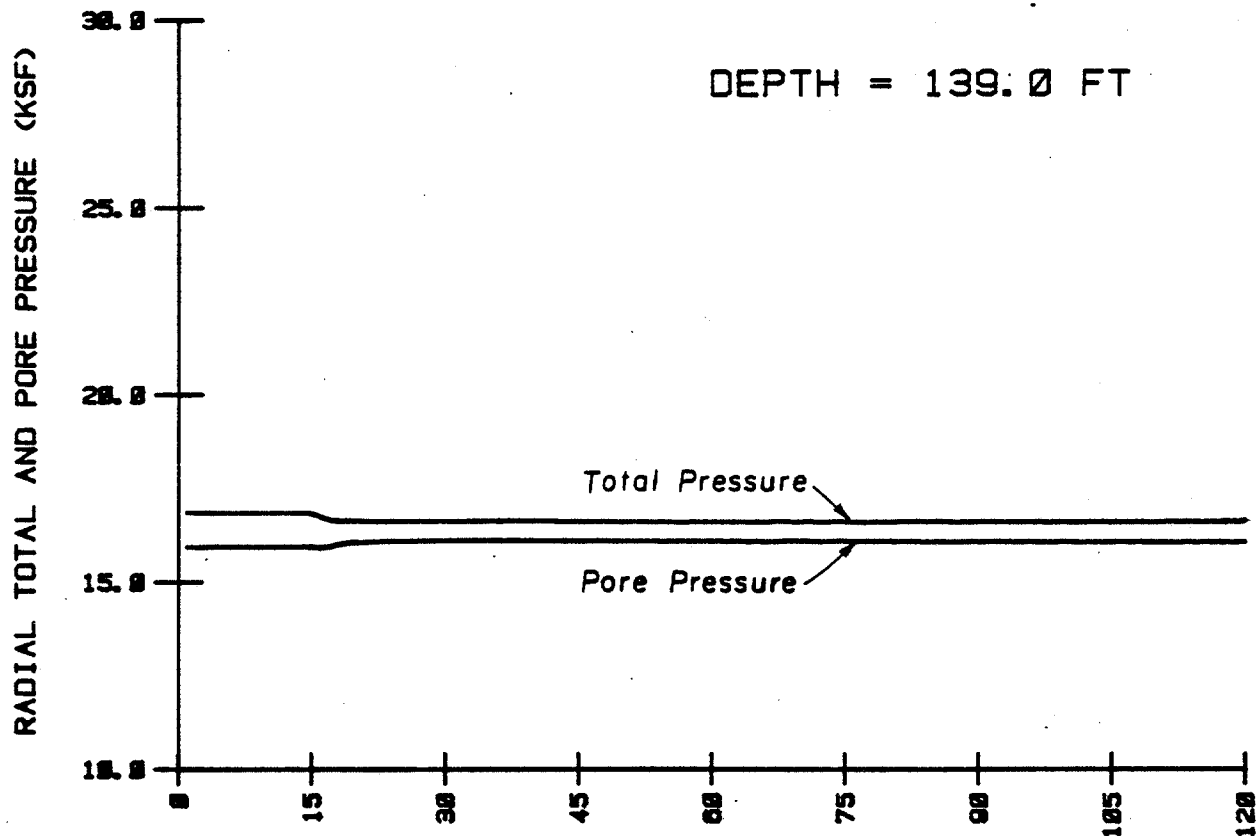
(1 inch = 25.4 mm, 1 ft = 0.305 m, 1 kip = 4.45 kN, 1 ksf = 47.9 kPa)



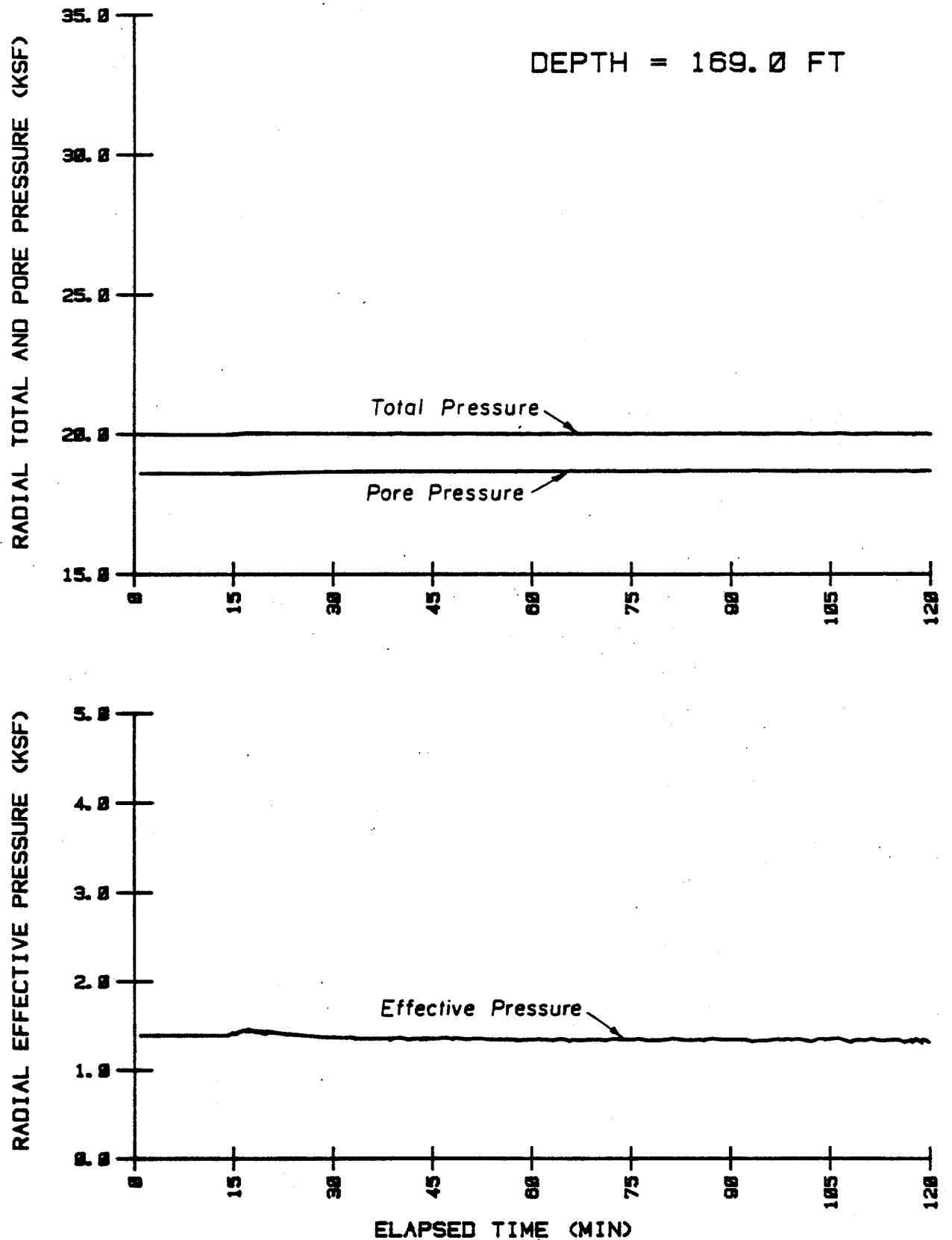
VARIATION IN SOIL PRESSURES AT THE 79-FOOT DEPTH DURING THE CREEP TEST
(1 inch = 25.4 mm, 1 ft = 0.305 m, 1 kip = 4.45 kN, 1 ksf = 47.9 kPa)



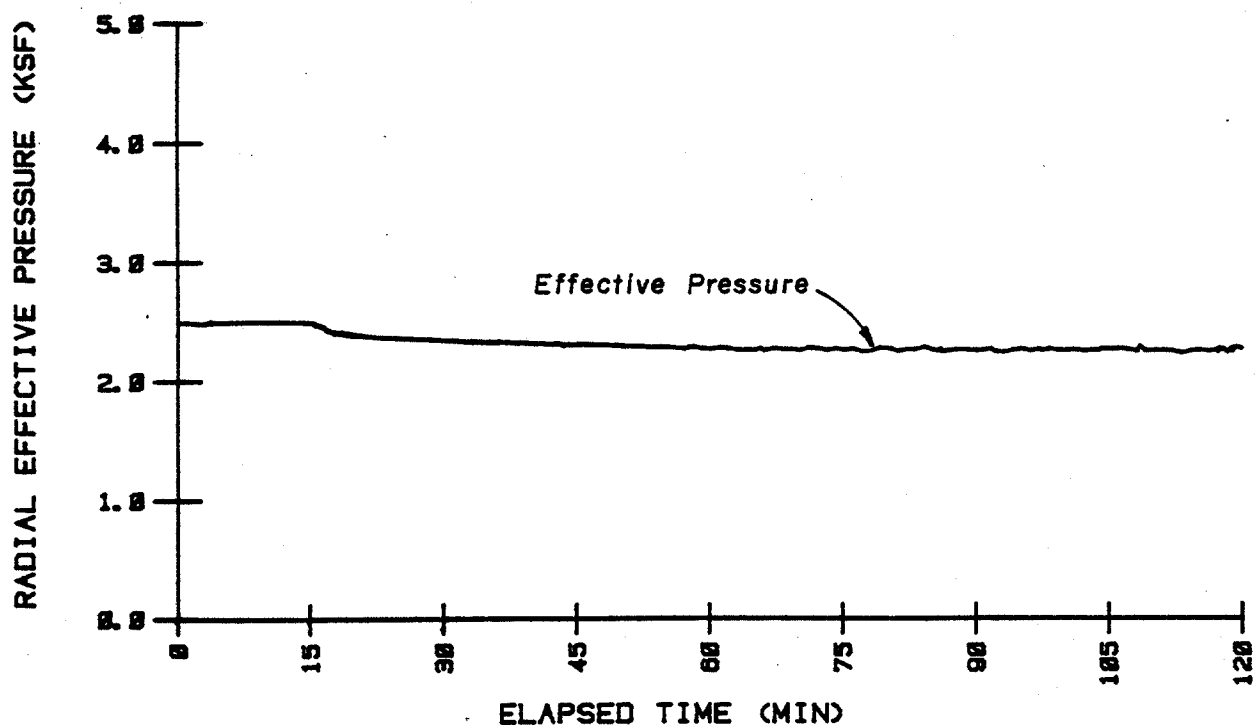
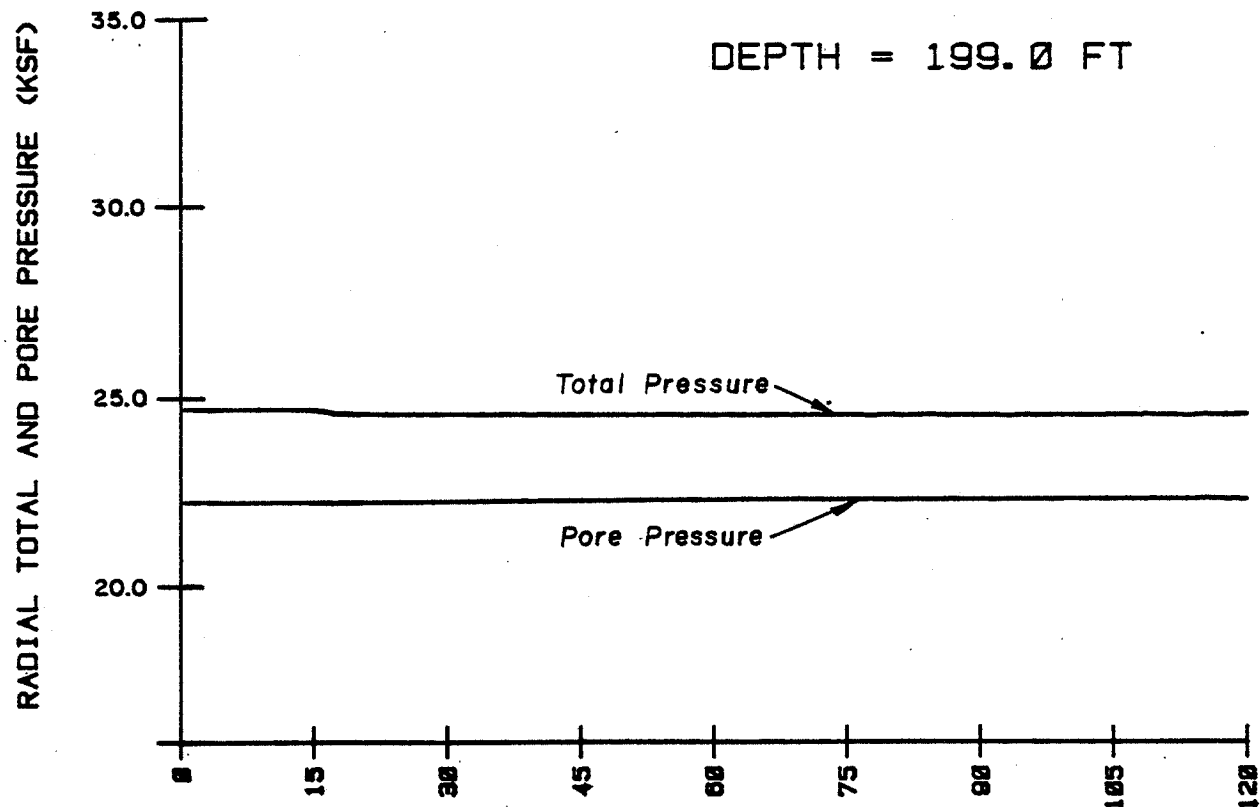
VARIATION IN SOIL PRESSURES AT THE 109-FOOT DEPTH DURING THE CREEP TEST
(1 inch = 25.4 mm, 1 ft = 0.305 m, 1 kip = 4.45 kN, 1 ksf = 47.9 kPa)



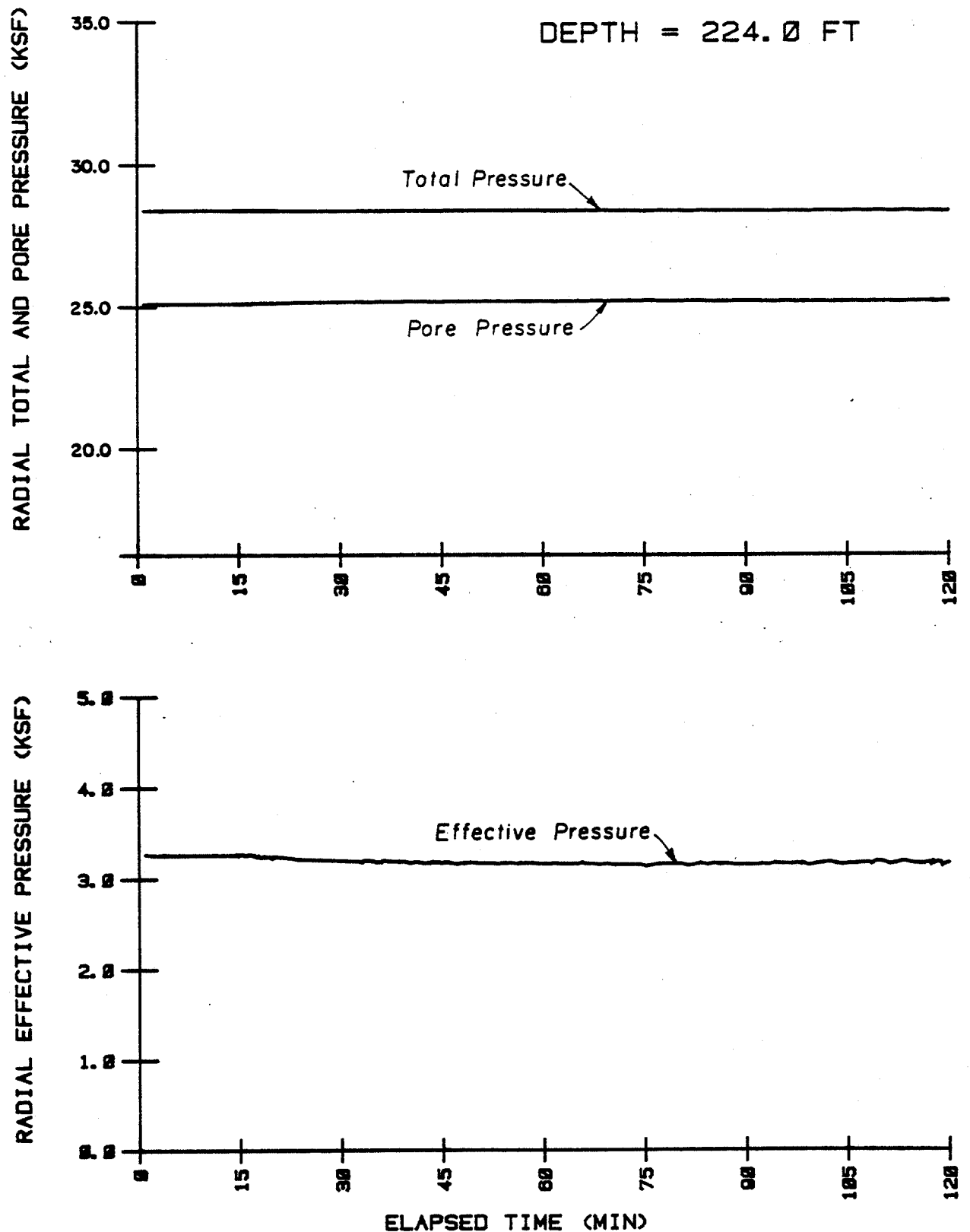
VARIATION IN SOIL PRESSURES AT THE 139-FOOT DEPTH DURING THE CREEP TEST
(1 inch = 25.4 mm, 1 ft = 0.305 m, 1 kip = 4.45 kN, 1 ksf = 47.9 kPa)



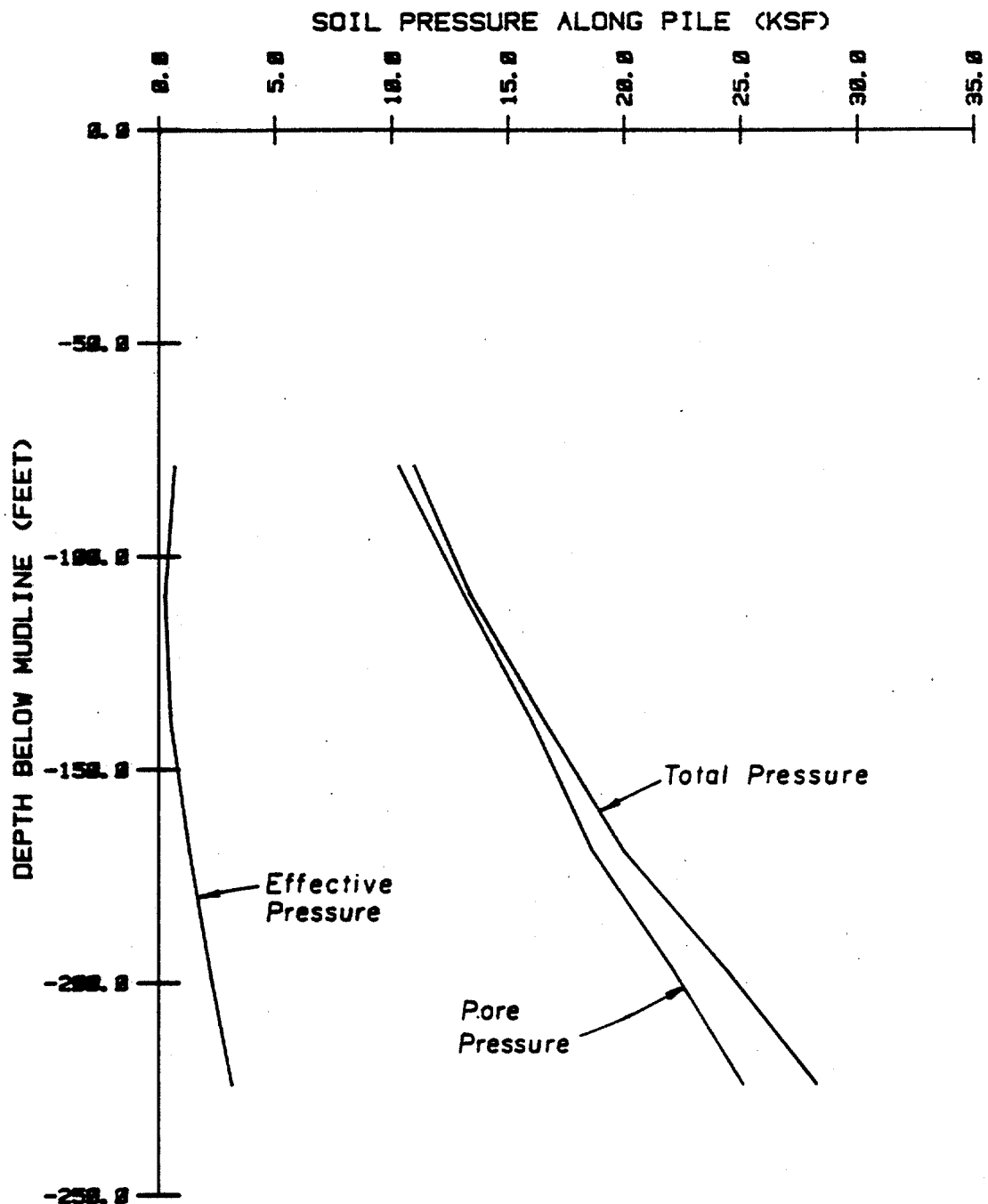
VARIATION IN SOIL PRESSURES AT THE 169-FOOT DEPTH DURING THE CREEP TEST
(1 inch = 25.4 mm, 1 ft = 0.305 m, 1 kip = 4.45 kN, 1 ksf = 47.9 kPa)



VARIATION IN SOIL PRESSURES AT THE 199-FOOT DEPTH DURING THE CREEP TEST
(1 inch = 25.4 mm, 1 ft = 0.305 m, 1 kip = 4.45 kN, 1 ksf = 47.9 kPa)

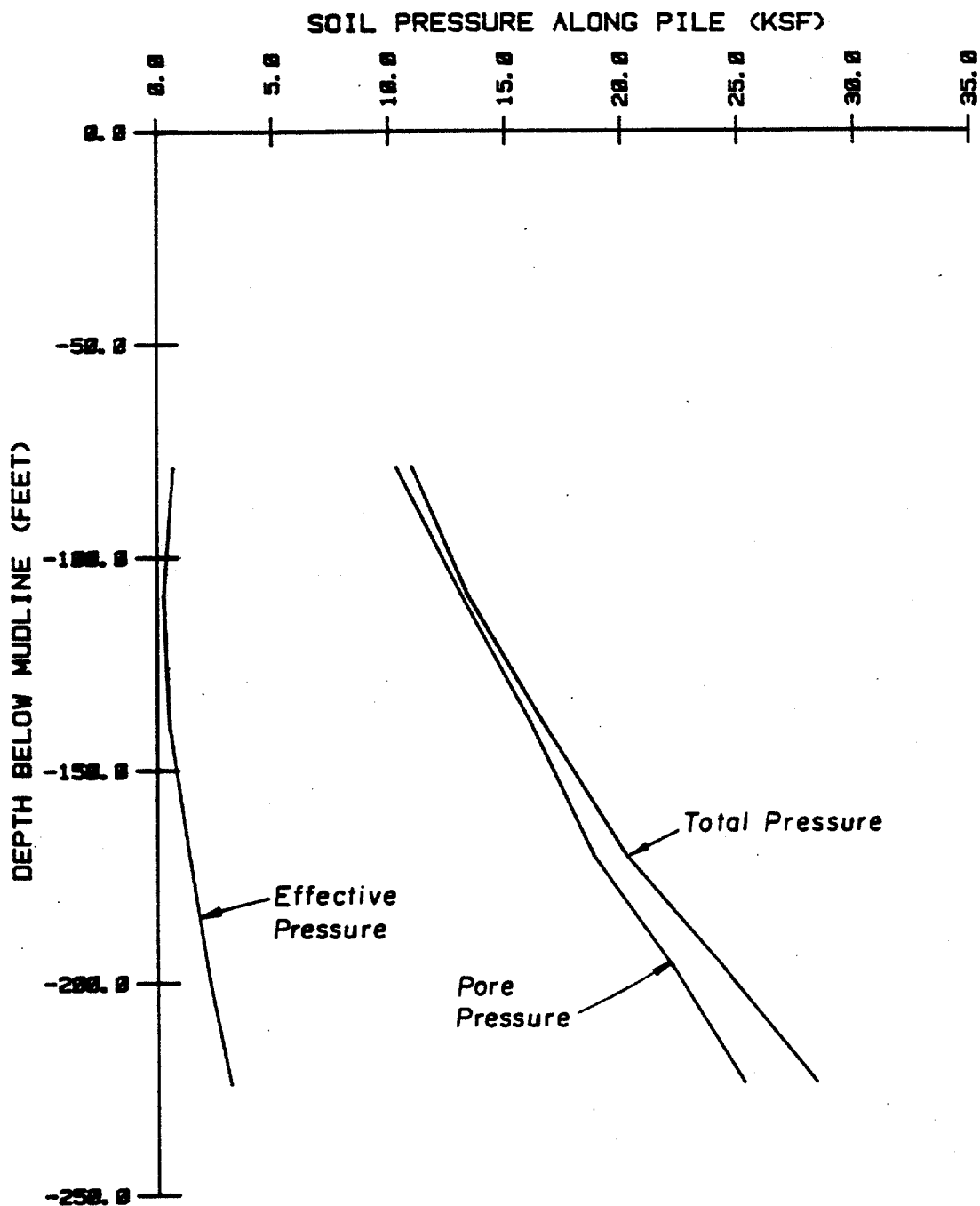


VARIATION IN SOIL PRESSURES AT THE 224-FOOT DEPTH DURING THE CREEP TEST
(1 inch = 25.4 mm, 1 ft = 0.305 m, 1 kip = 4.45 kN, 1 ksf = 47.9 kPa)



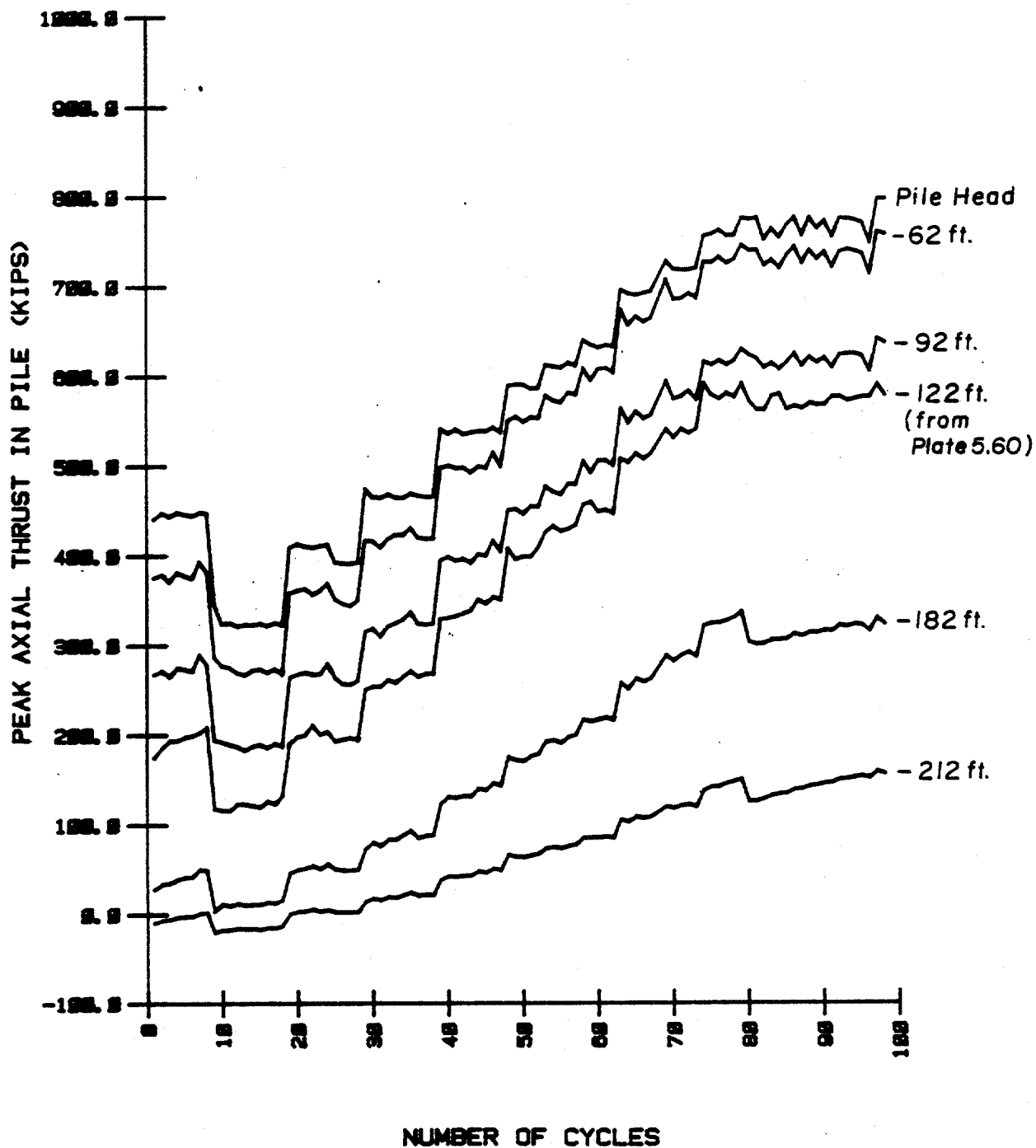
SOIL PRESSURE PROFILES AT THE BEGINNING OF THE CREEP TEST

(1 inch = 25.4 mm, 1 ft = 0.305 m, 1 kip = 4.45 kN, 1 ksf = 47.9 kPa)



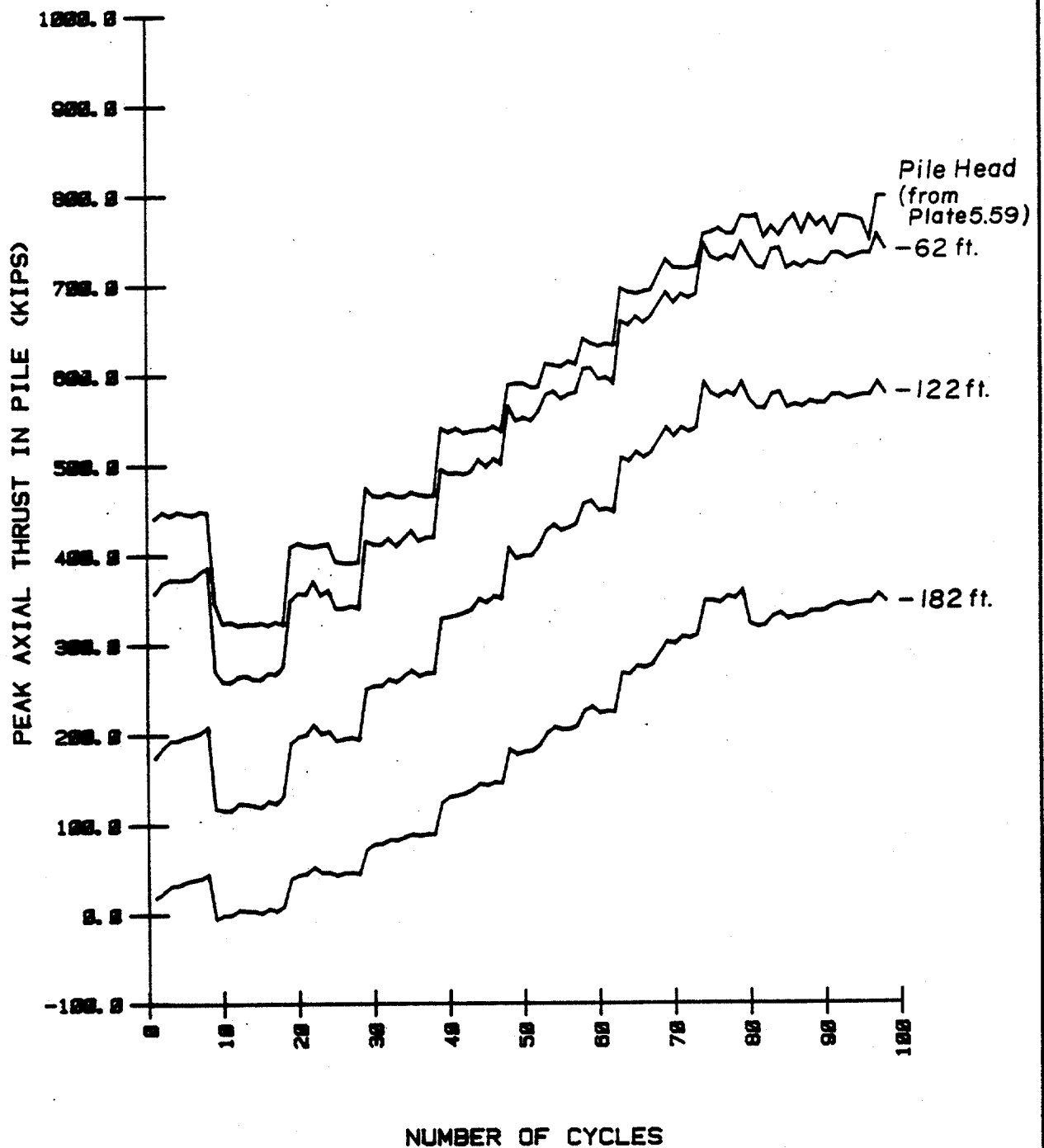
SOIL PRESSURE PROFILES AT THE END OF THE CREEP TEST

(1 inch = 25.4 mm, 1 ft = 0.305 m, 1 kip = 4.45 kN, 1 ksf = 47.9 kPa)



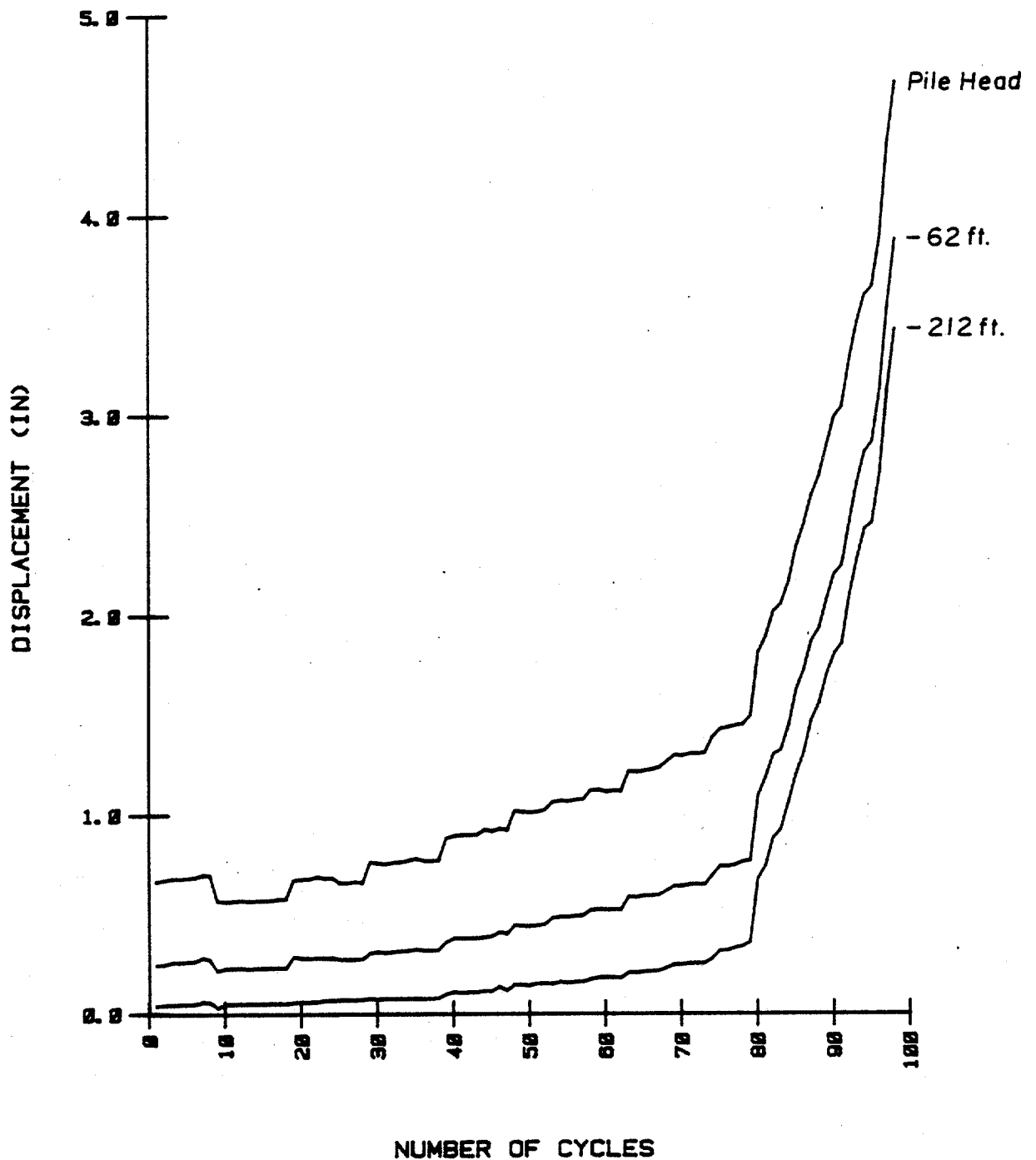
MAXIMUM AXIAL THRUST MEASURED BY THE STRAIN MODULES
DURING THE ONE-WAY CYCLIC TENSION TEST

(1 inch = 25.4 mm, 1 ft = 0.305 m, 1 kip = 4.45 kN, 1 ksf = 47.9 kPa)



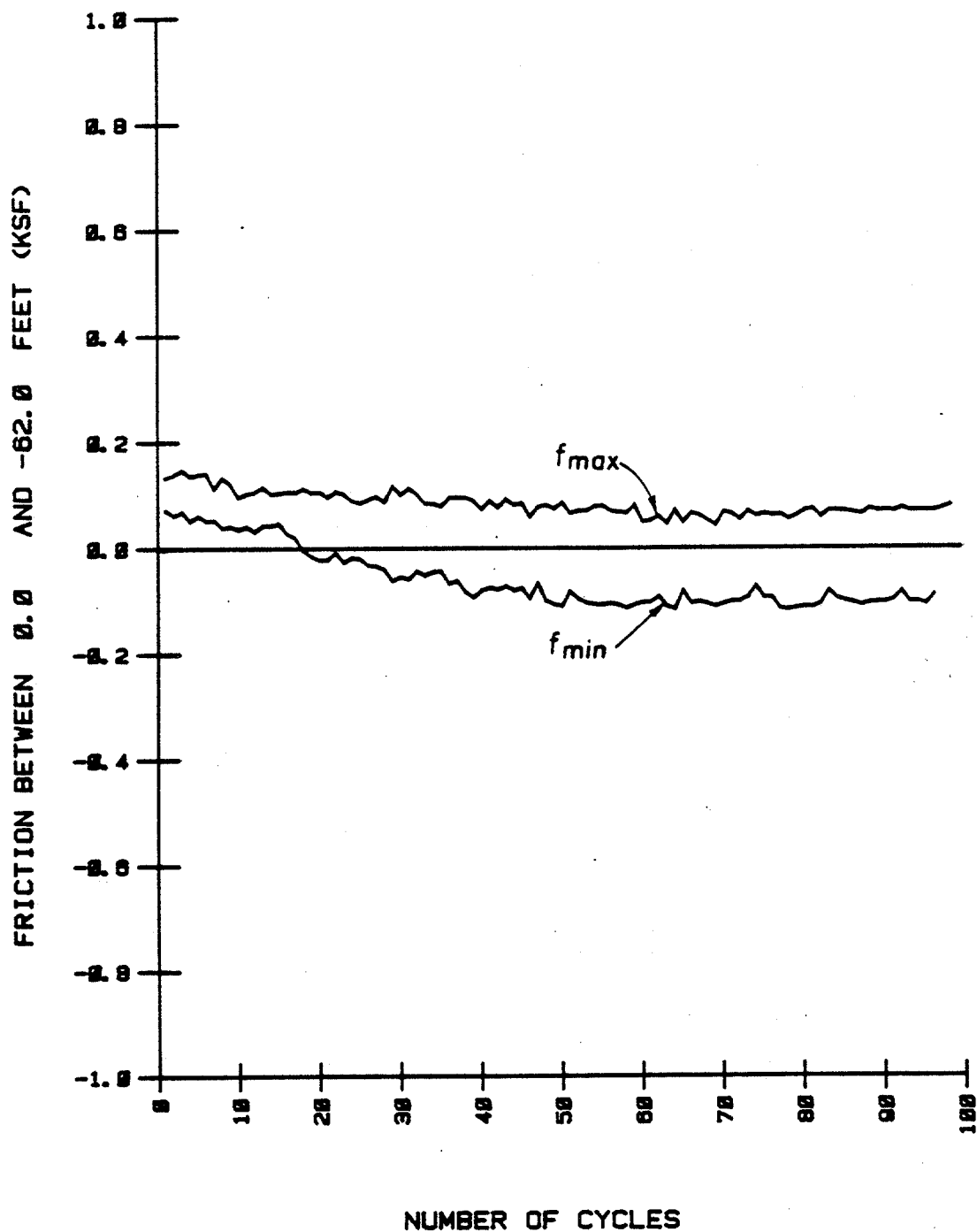
MAXIMUM AXIAL THRUST MEASURED BY THE EXTENSOMETERS
DURING THE ONE-WAY CYCLIC TENSION TESTS

(1 inch = 25.4 mm, 1 ft = 0.305 m, 1 kip = 4.45 kN, 1 ksf = 47.9 kPa)



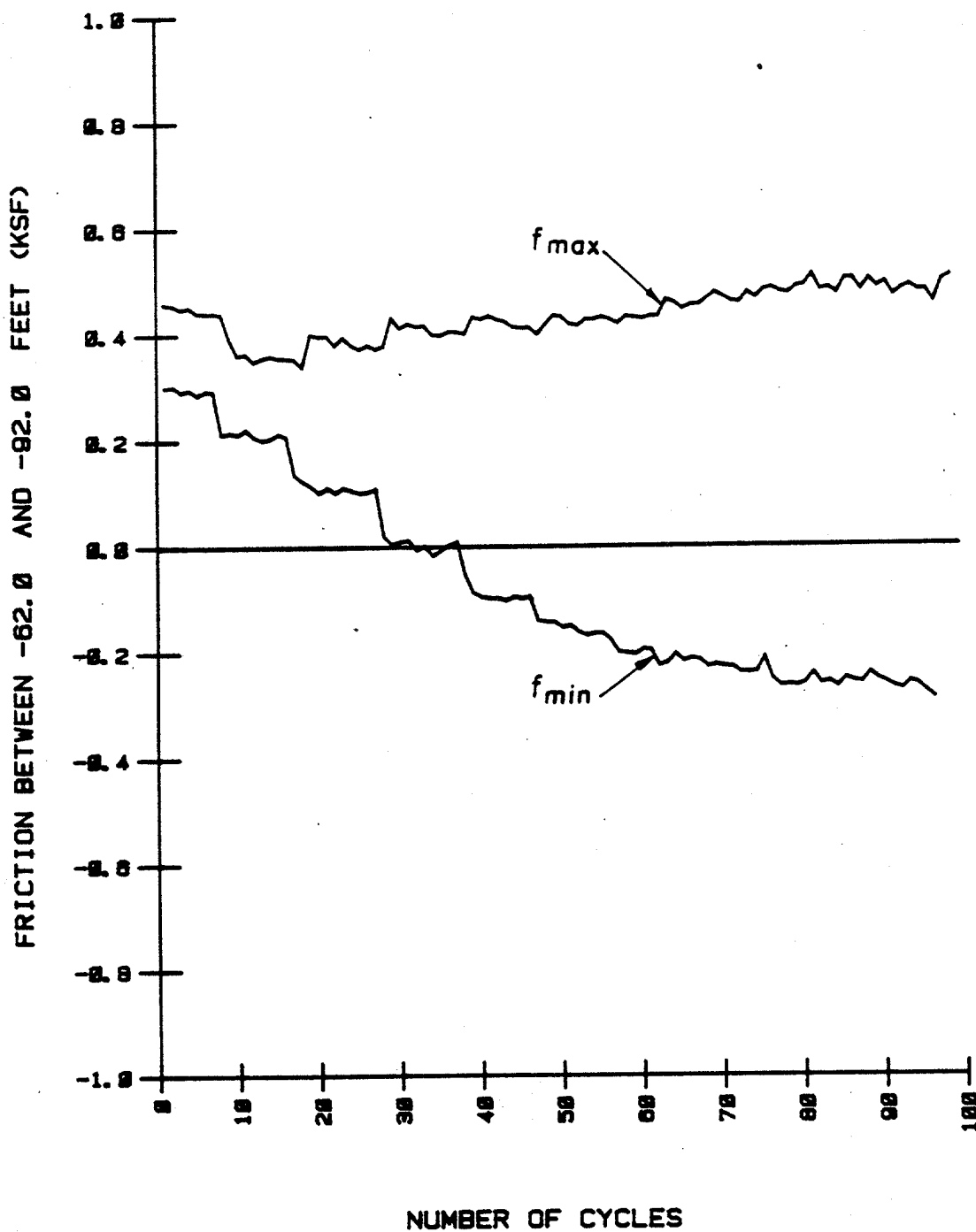
PILE DISPLACEMENTS MEASURED AT THE PEAK TENSION LOAD
DURING THE ONE-WAY CYCLIC TENSION TESTS

(1 inch = 25.4 mm, 1 ft = 0.305 m, 1 kip = 4.45 kN, 1 ksf = 47.9 kPa)



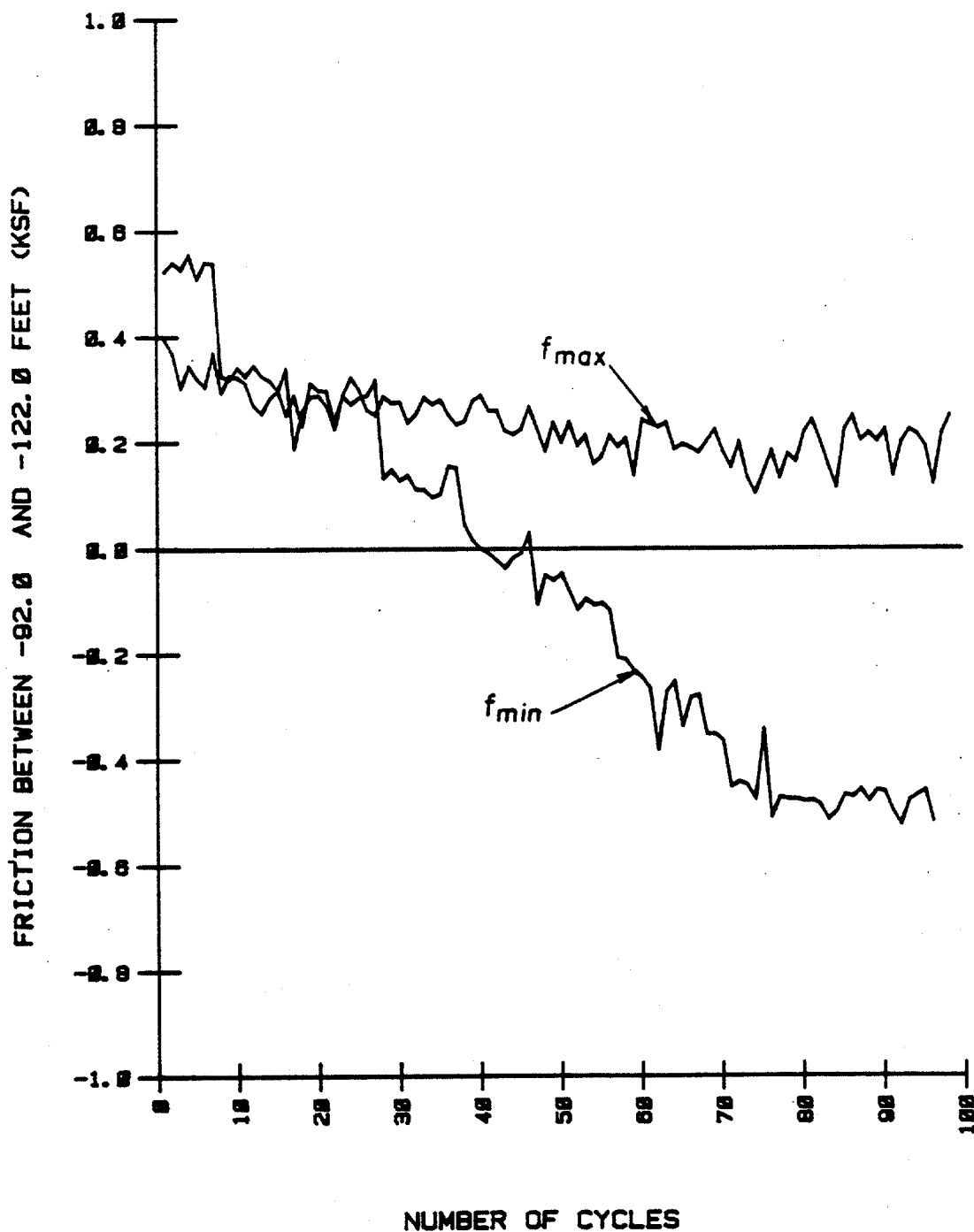
VARIATIONS IN THE MAXIMUM AND MINIMUM SHEAR TRANSFER BETWEEN THE DEPTHS OF 0 AND 62 FEET DURING THE ONE-WAY CYCLIC TENSION TESTS

(1 inch = 25.4 mm, 1 ft = 0.305 m, 1 kip = 4.45 kN, 1 ksf = 47.9 kPa)



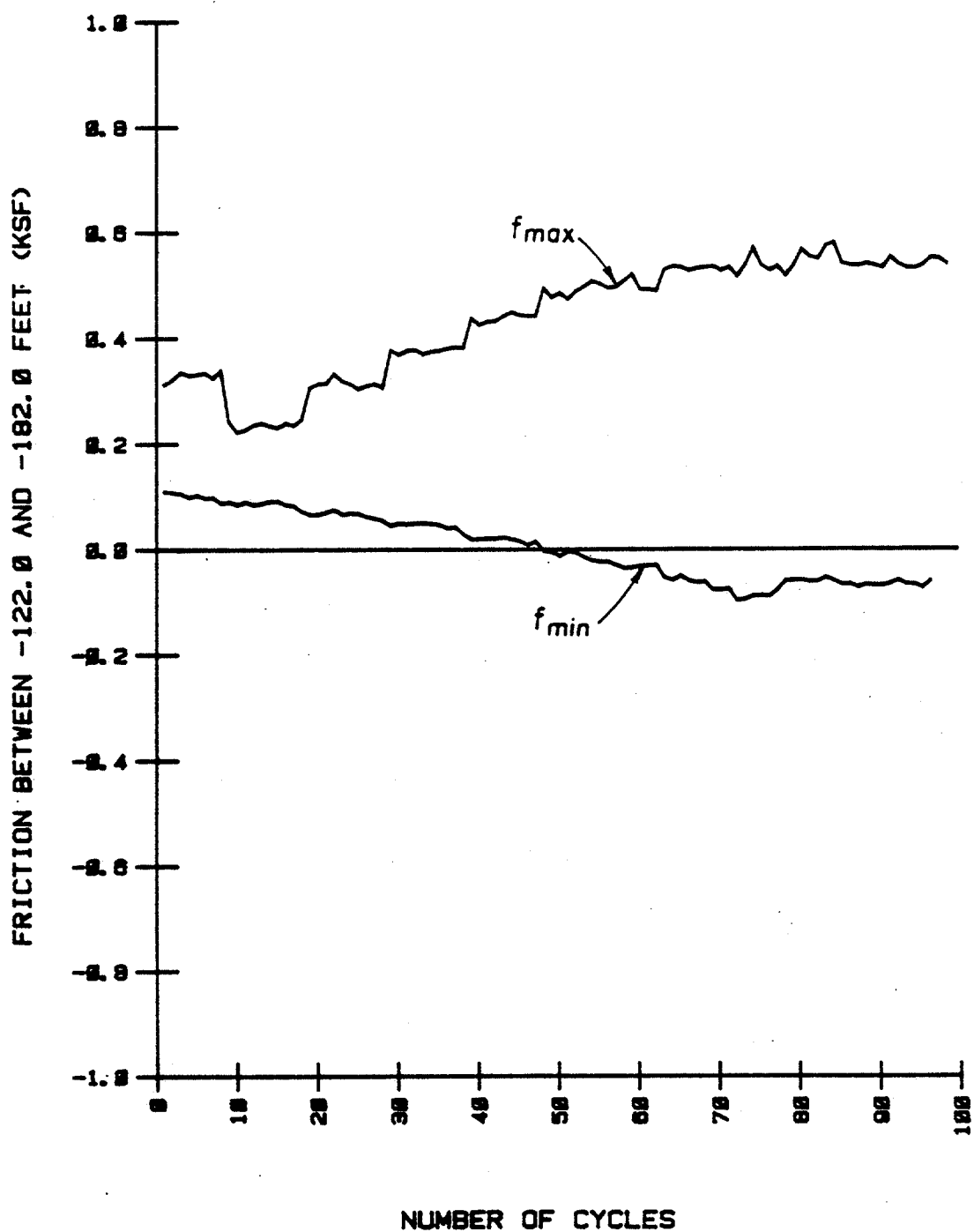
VARIATIONS IN THE MAXIMUM AND MINIMUM SHEAR TRANSFER BETWEEN THE DEPTHS OF 62 AND 92 FEET DURING THE ONE-WAY CYCLIC TENSION TESTS

(1 inch = 25.4 mm, 1 ft = 0.305 m, 1 kip = 4.45 kN, 1 ksf = 47.9 kPa)



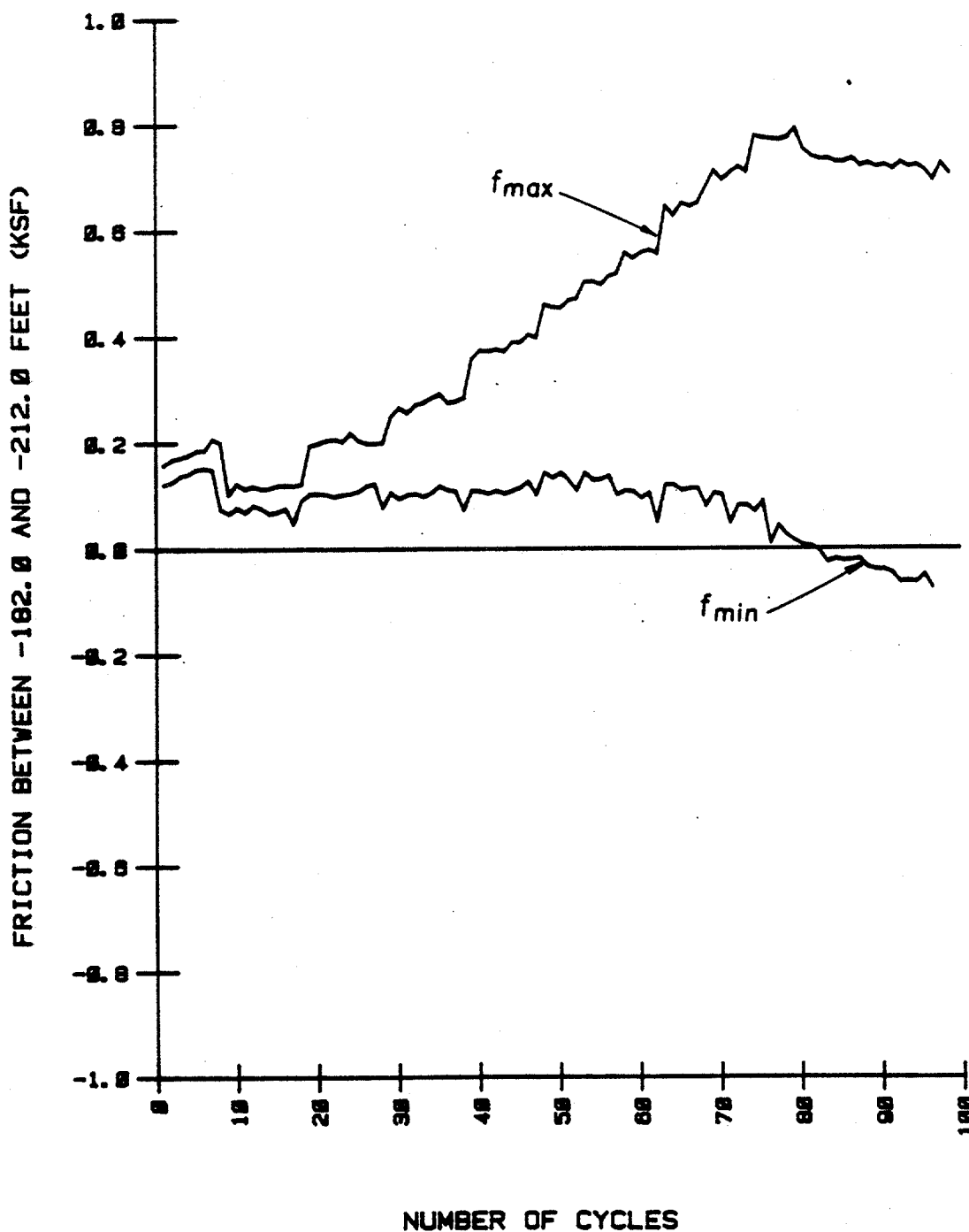
VARIATIONS IN THE MAXIMUM AND MINIMUM SHEAR TRANSFER BETWEEN THE DEPTHS OF 92 AND 122 FEET DURING THE ONE-WAY CYCLIC TENSION TESTS

(1 inch = 25.4 mm, 1 ft = 0.305 m, 1 kip = 4.45 kN, 1 ksf = 47.9 kPa)



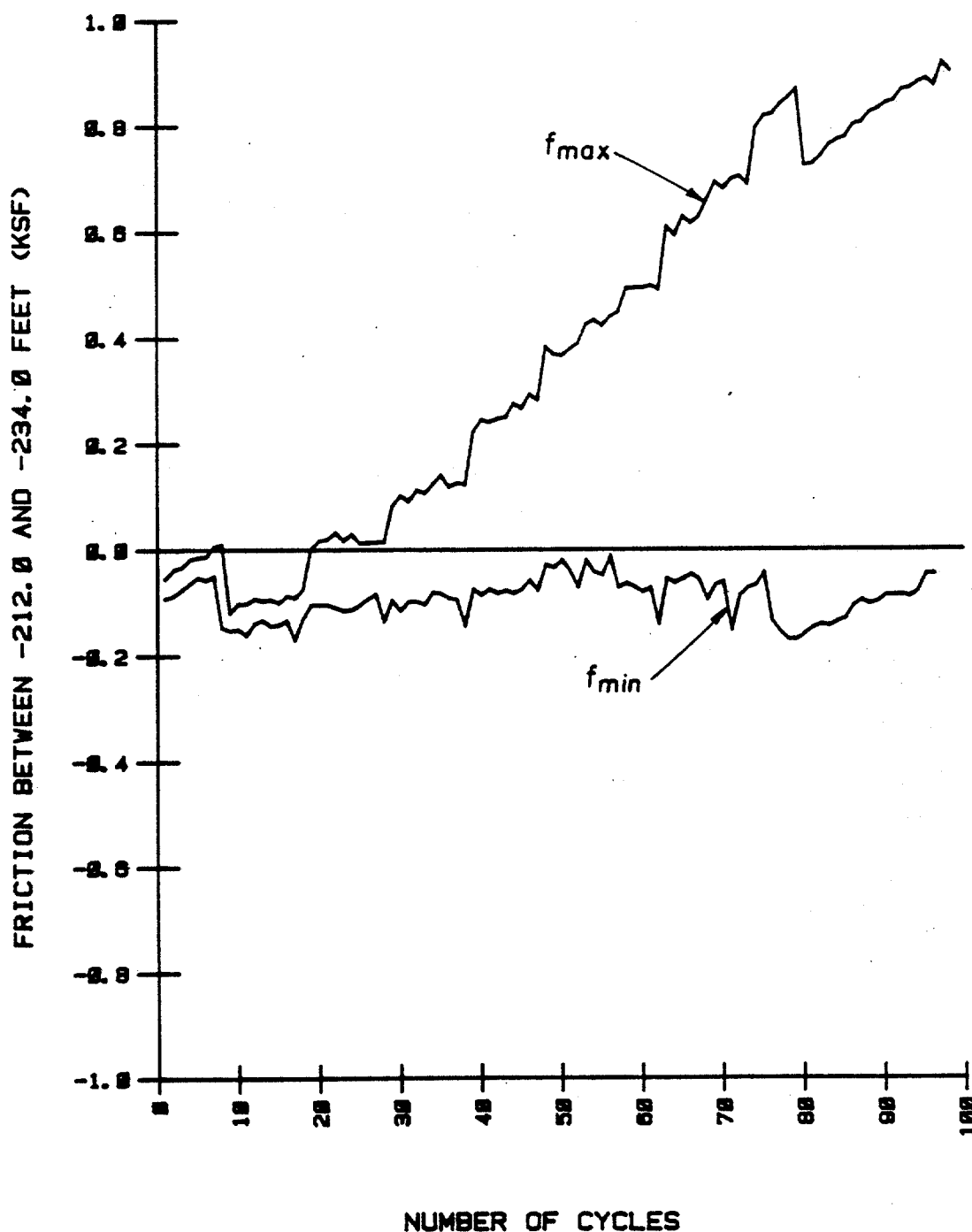
VARIATIONS IN THE MAXIMUM AND MINIMUM SHEAR TRANSFER BETWEEN THE DEPTHS OF 122 AND 182 FEET DURING THE ONE-WAY CYCLIC TENSION TESTS

(1 inch = 25.4 mm, 1 ft = 0.305 m, 1 kip = 4.45 kN, 1 ksf = 47.9 kPa)



VARIATIONS IN THE MAXIMUM AND MINIMUM SHEAR TRANSFER BETWEEN THE DEPTHS OF 182 AND 212 FEET DURING THE ONE-WAY CYCLIC TENSION TESTS

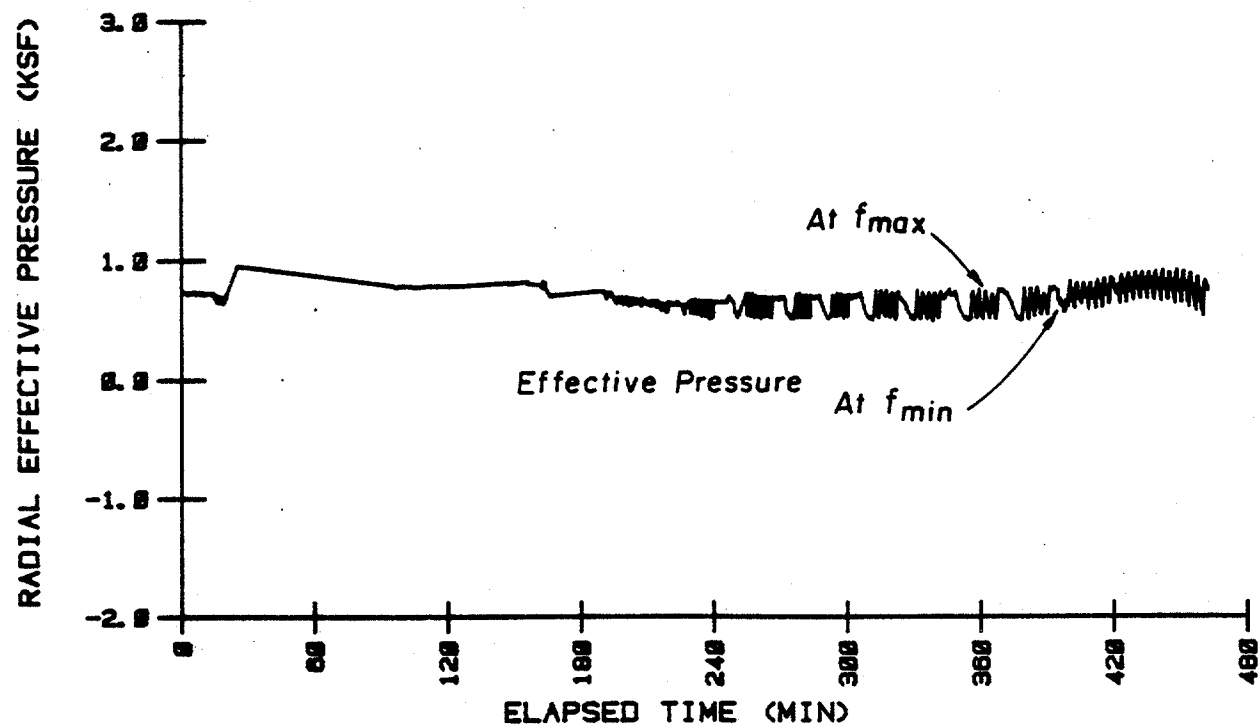
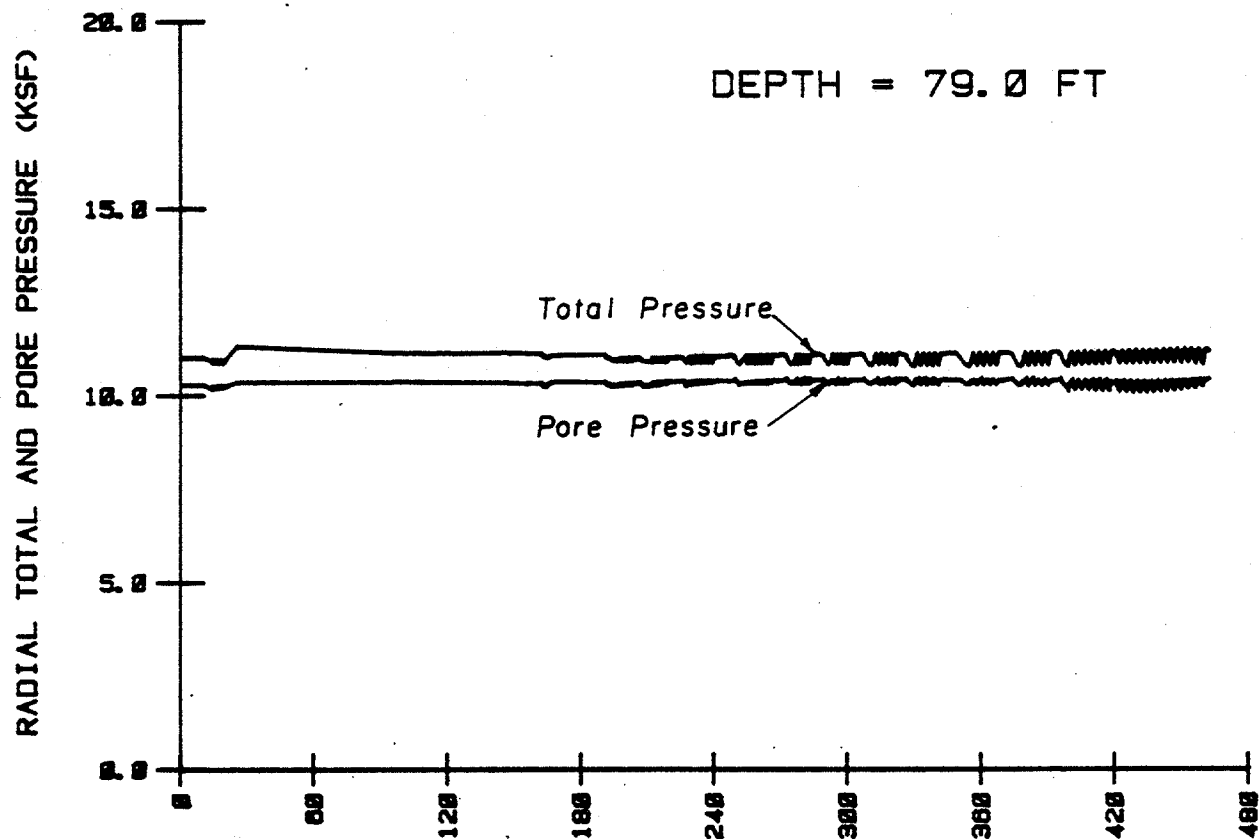
(1 inch = 25.4 mm, 1 ft = 0.305 m, 1 kip = 4.45 kN, 1 ksf = 47.9 kPa)



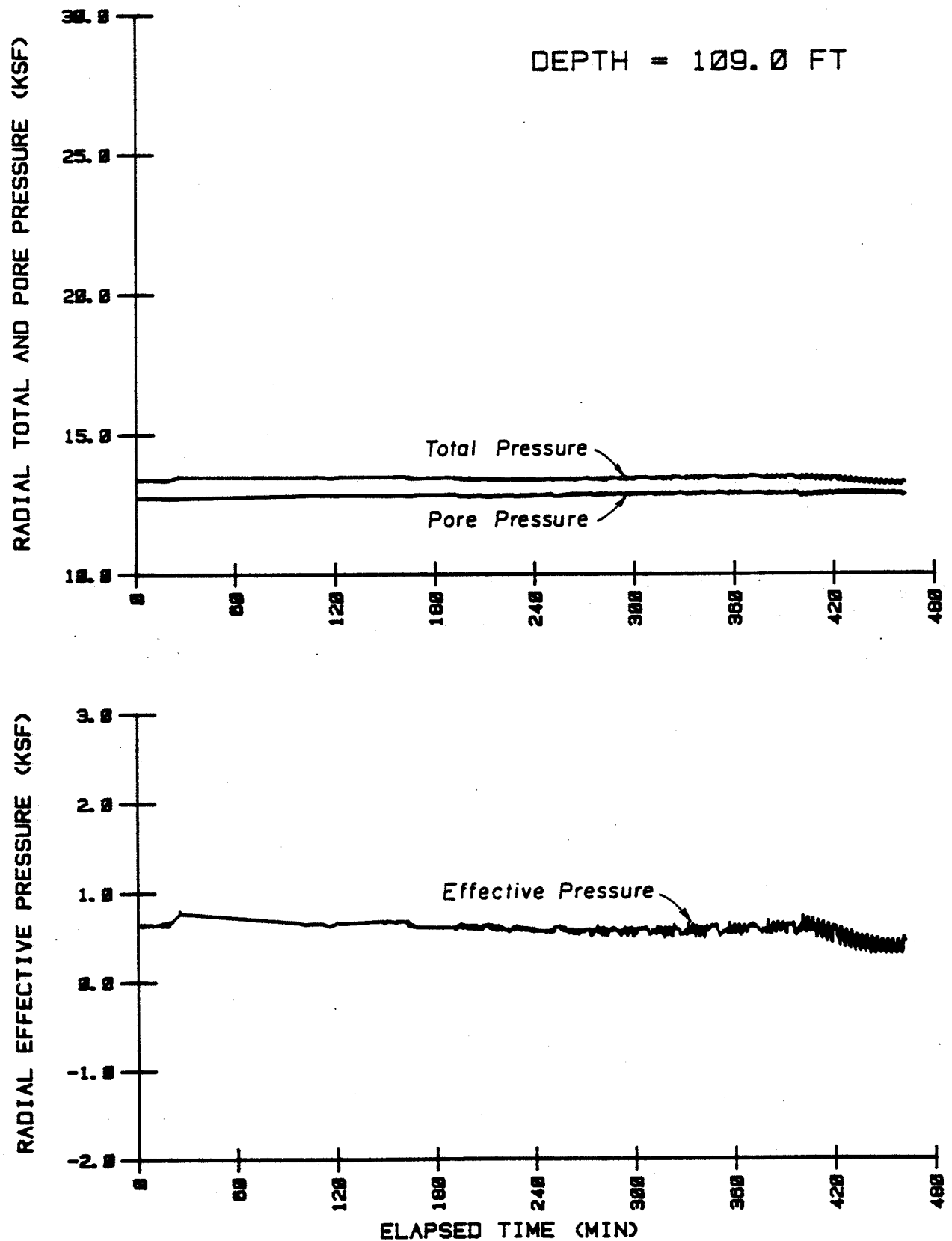
VARIATIONS IN THE MAXIMUM AND MINIMUM SHEAR TRANSFER BETWEEN THE DEPTHS OF 212 AND 234 FEET DURING THE ONE-WAY CYCLIC TENSION TESTS

(1 inch = 25.4 mm, 1 ft = 0.305 m, 1 kip = 4.45 kN, 1 ksf = 47.9 kPa)

(1 inch = 25.4 mm, 1 ft = 0.305 m, 1 kip = 4.45 kN, 1 ksf = 47.9 kPa)

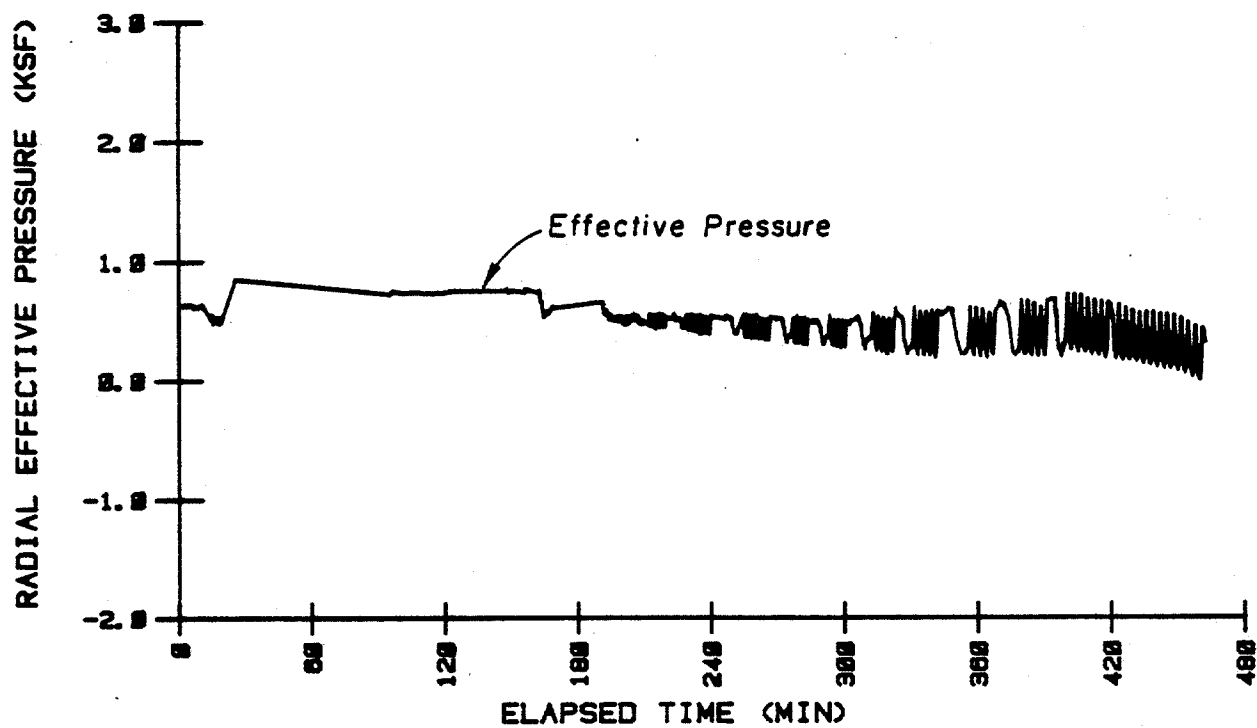
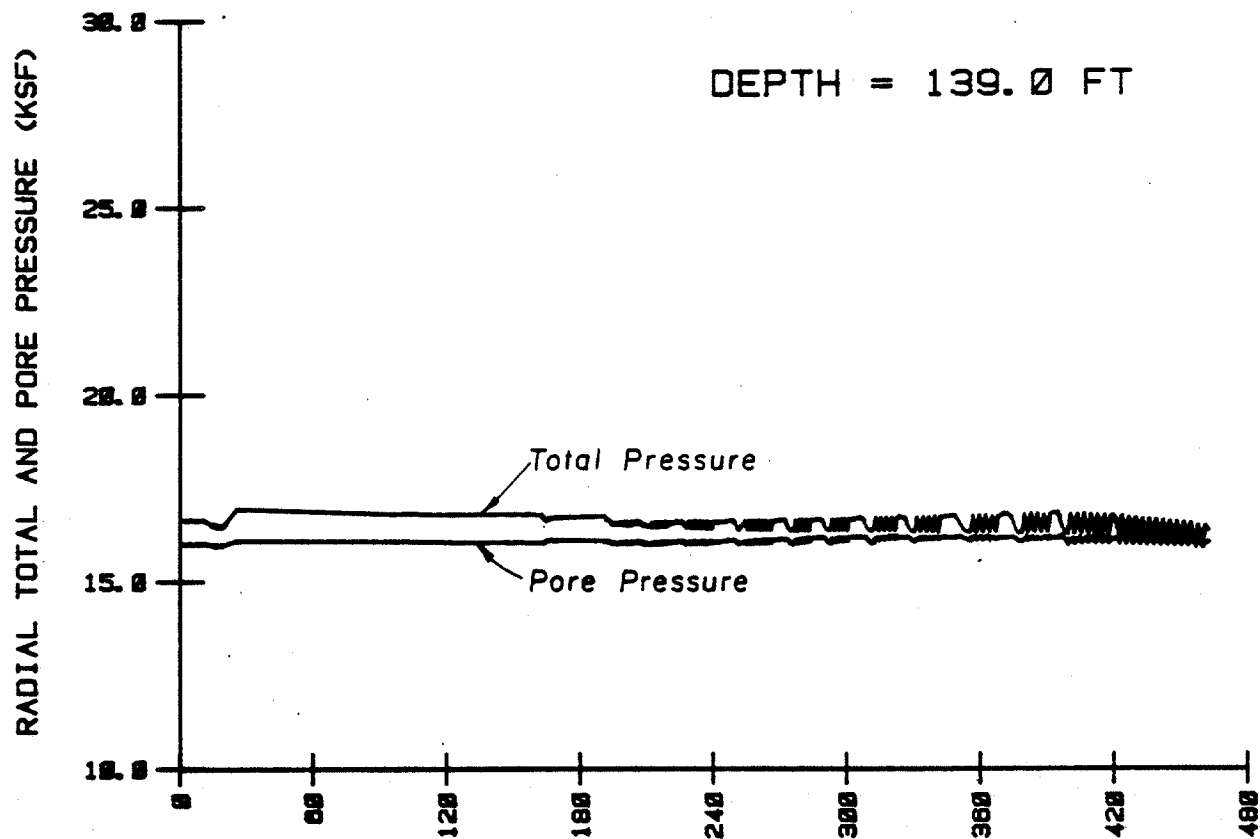


VARIATION IN SOIL PRESSURES AT THE 79-FOOT DEPTH
DURING THE ONE-WAY CYCLIC TENSION TESTS



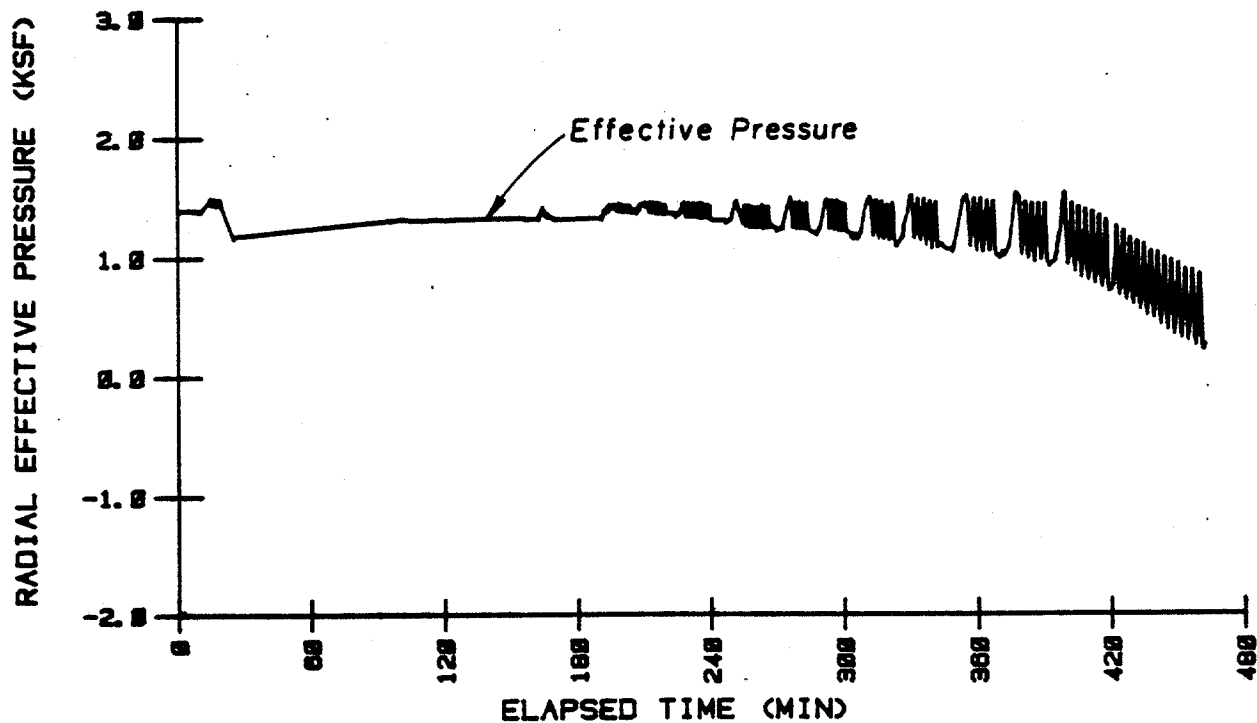
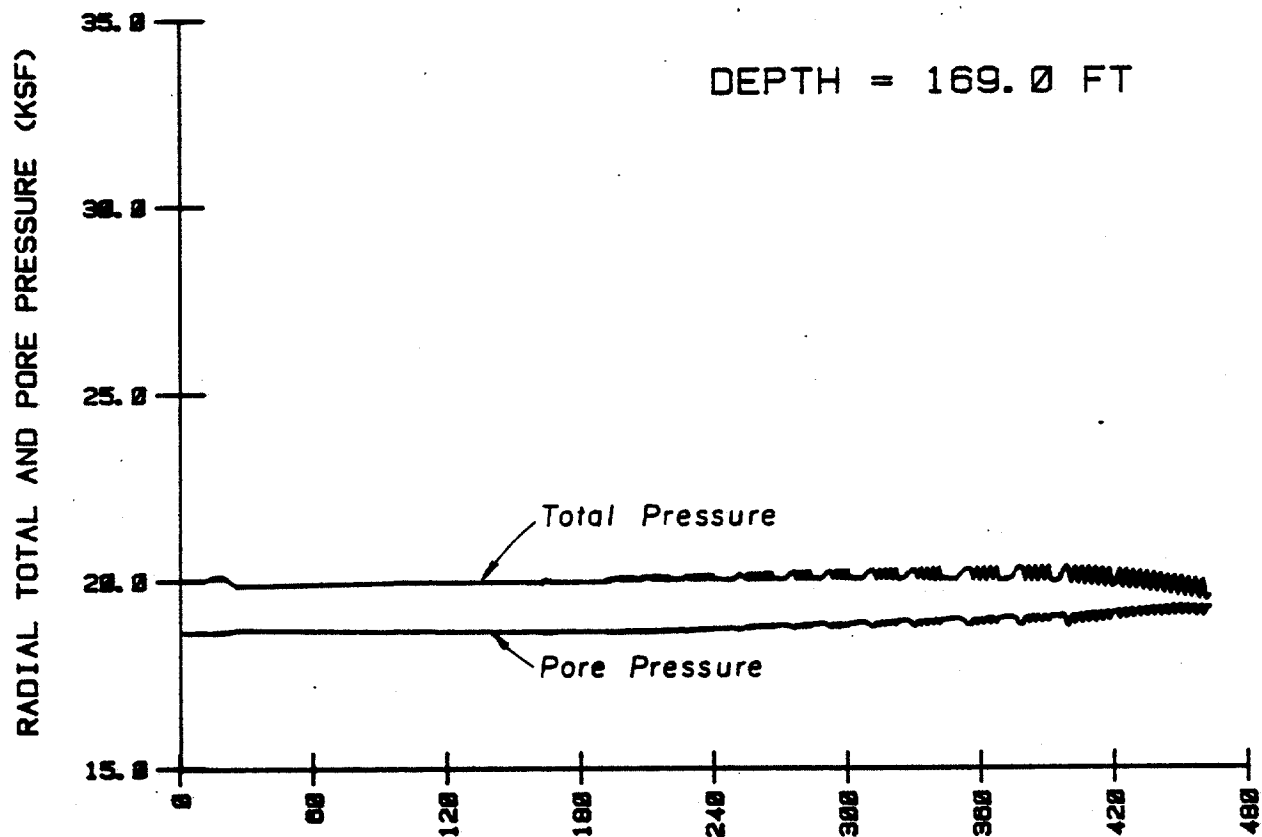
VARIAION IN SOIL PRESSURES AT THE 109-FOOT DEPTH
DURING THE ONE-WAY CYCLIC TENSION TESTS
(1 inch = 25.4 mm, 1 ft = 0.305 m, 1 kip = 4.45 kN, 1 ksf = 47.9 kPa)

(1 inch = 25.4 mm, 1 ft = 0.305 m, 1 kip = 4.45 kN, 1 ksf = 47.9 kPa)



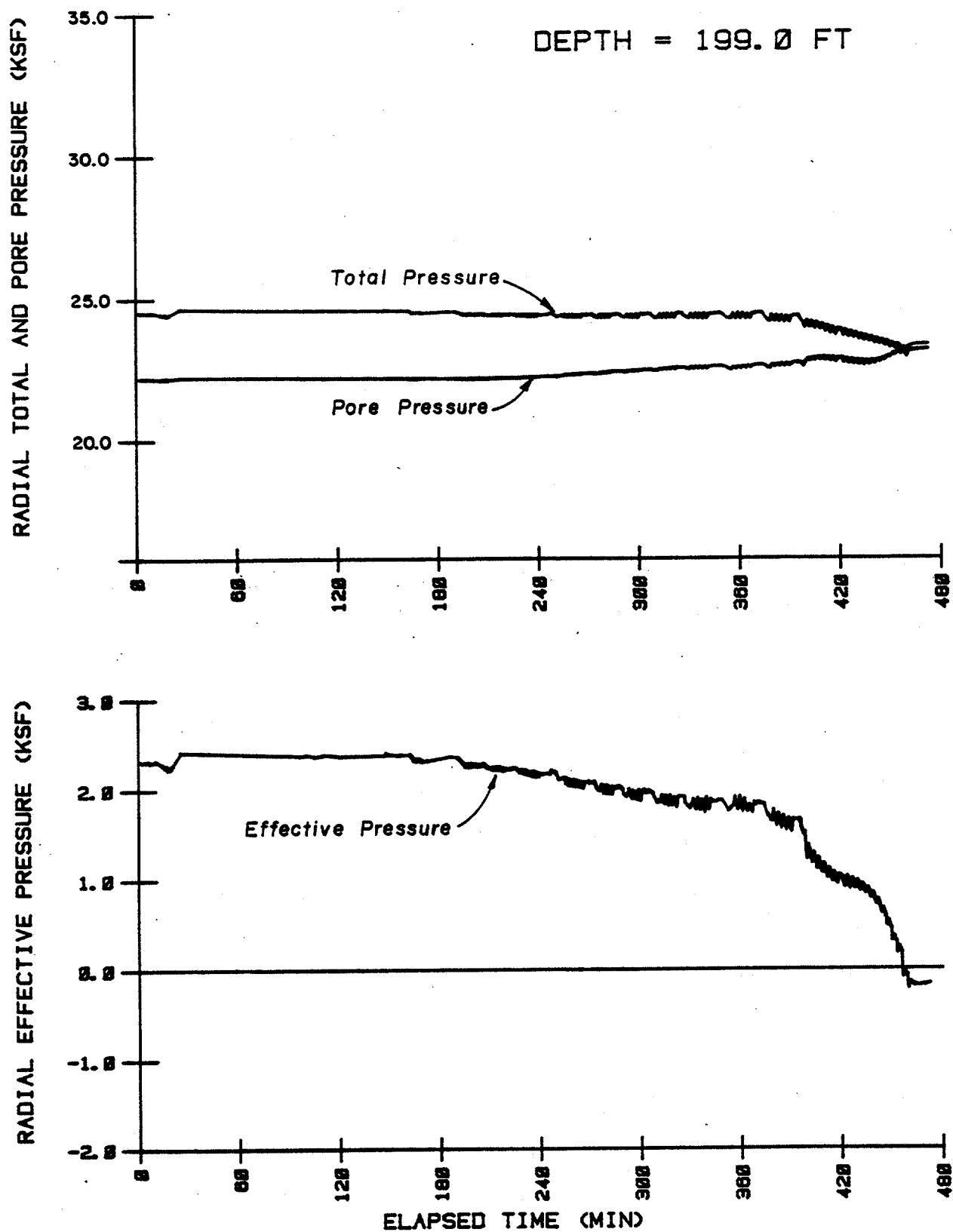
VARIATION IN SOIL PRESSURES AT THE 139-FOOT DEPTH
DURING THE ONE-WAY CYCLIC TENSION TESTS

(1 inch = 25.4 mm, 1 ft = 0.305 m, 1 kip = 4.45 kN, 1 ksf = 47.9 kPa)

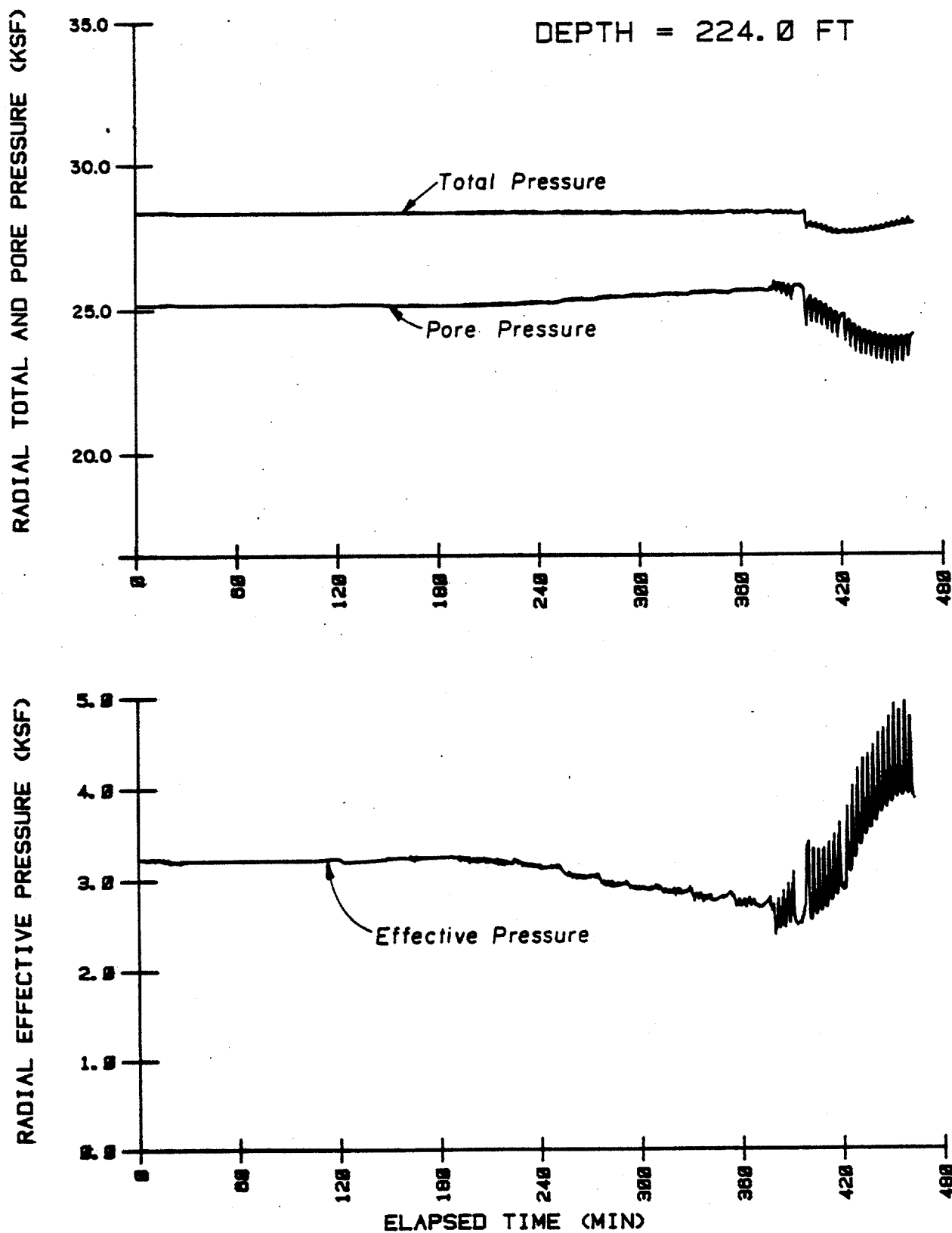


VARIATION IN SOIL PRESSURES AT THE 169-FOOT DEPTH
DURING THE ONE-WAY CYCLIC TENSION TESTS

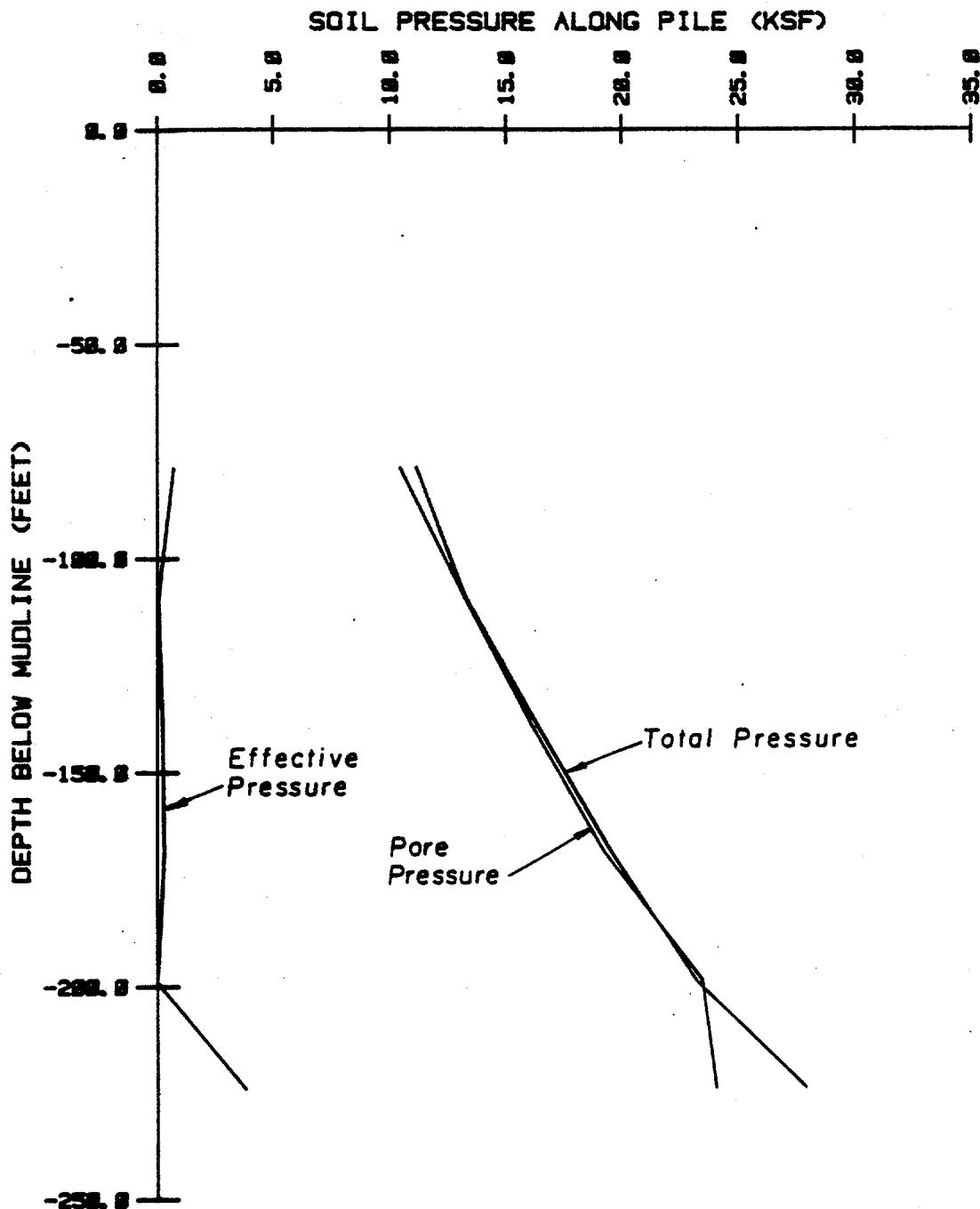
(1 inch = 25.4 mm, 1 ft = 0.305 m, 1 kip = 4.45 kN, 1 ksf = 47.9 kPa)



VARIATION IN SOIL PRESSURES AT THE 199-FOOT DEPTH
DURING THE ONE-WAY CYCLIC TENSION TESTS

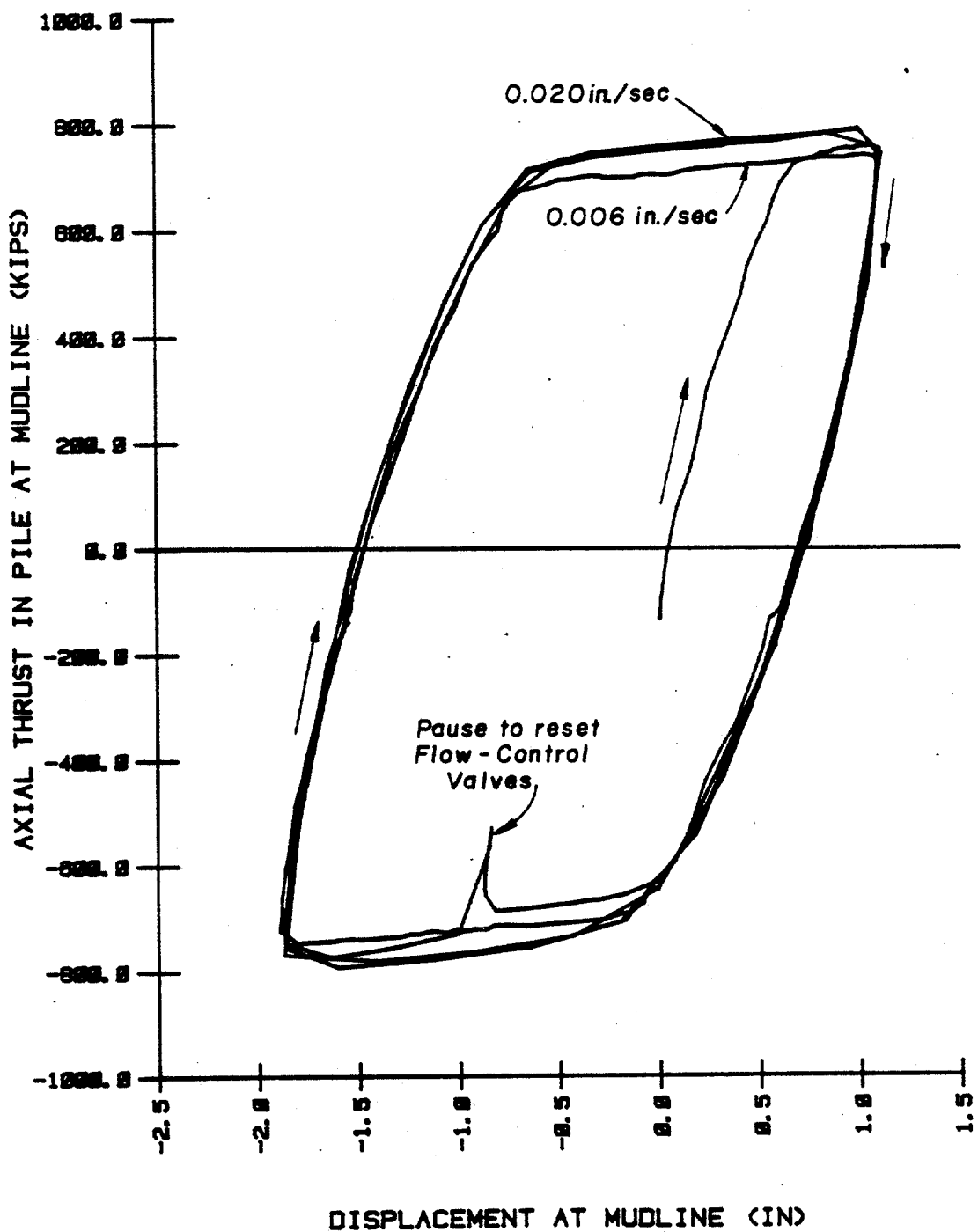


VARIATION IN SOIL PRESSURES AT THE 224-FOOT DEPTH
DURING THE ONE-WAY CYCLIC TENSION TESTS
(1 inch = 25.4 mm, 1 ft = 0.305 m, 1 kip = 4.45 kN, 1 ksf = 47.9 kPa)



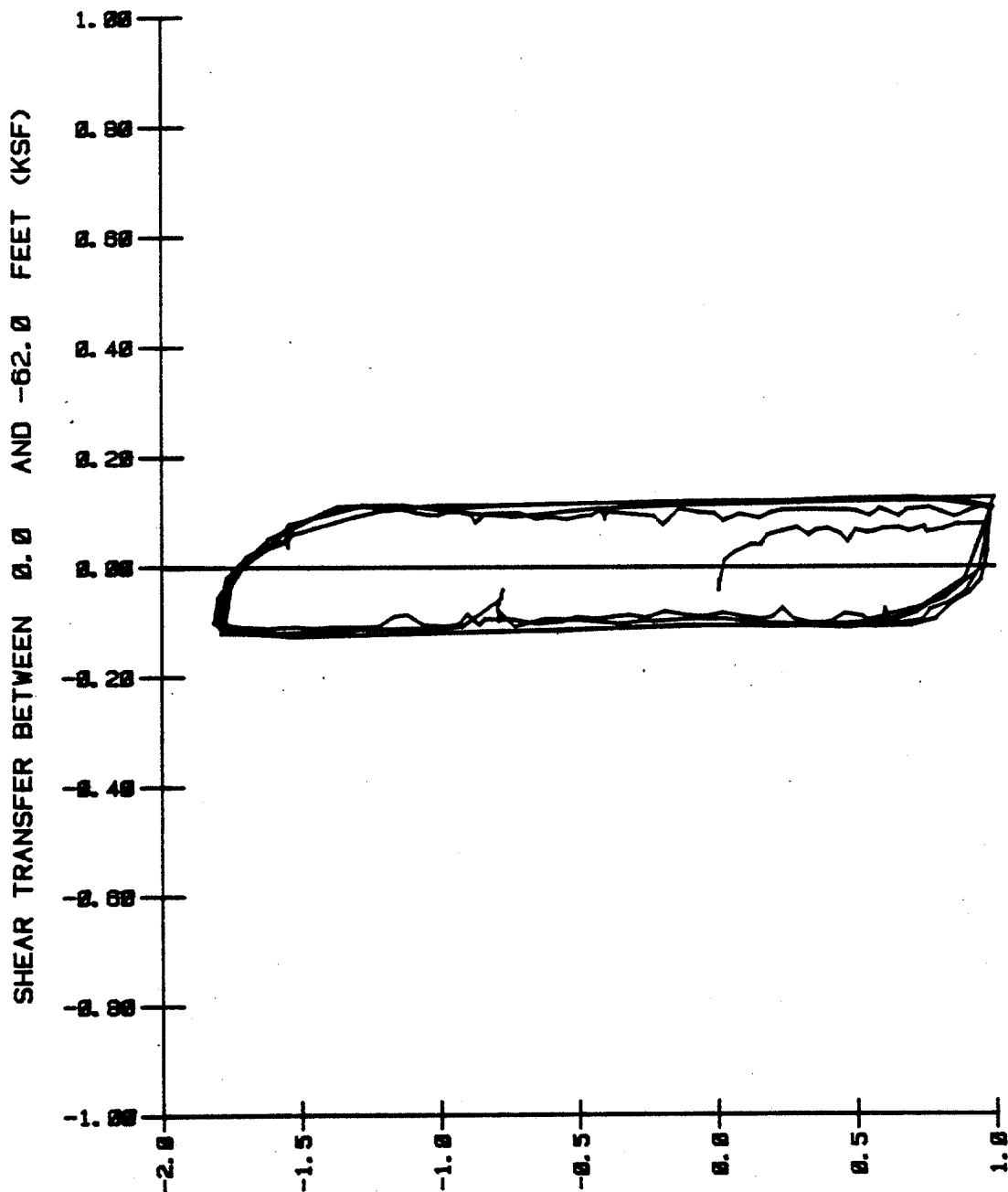
SOIL PRESSURE PROFILES AT THE END OF THE ONE-WAY CYCLIC TENSION TESTS

(1 inch = 25.4 mm, 1 ft = 0.305 m, 1 kip = 4.45 kN, 1 ksf = 47.9 kPa)



LOAD-DISPLACEMENT BEHAVIOR AT THE MUDLINE DURING THE TWO-WAY CYCLIC TESTS

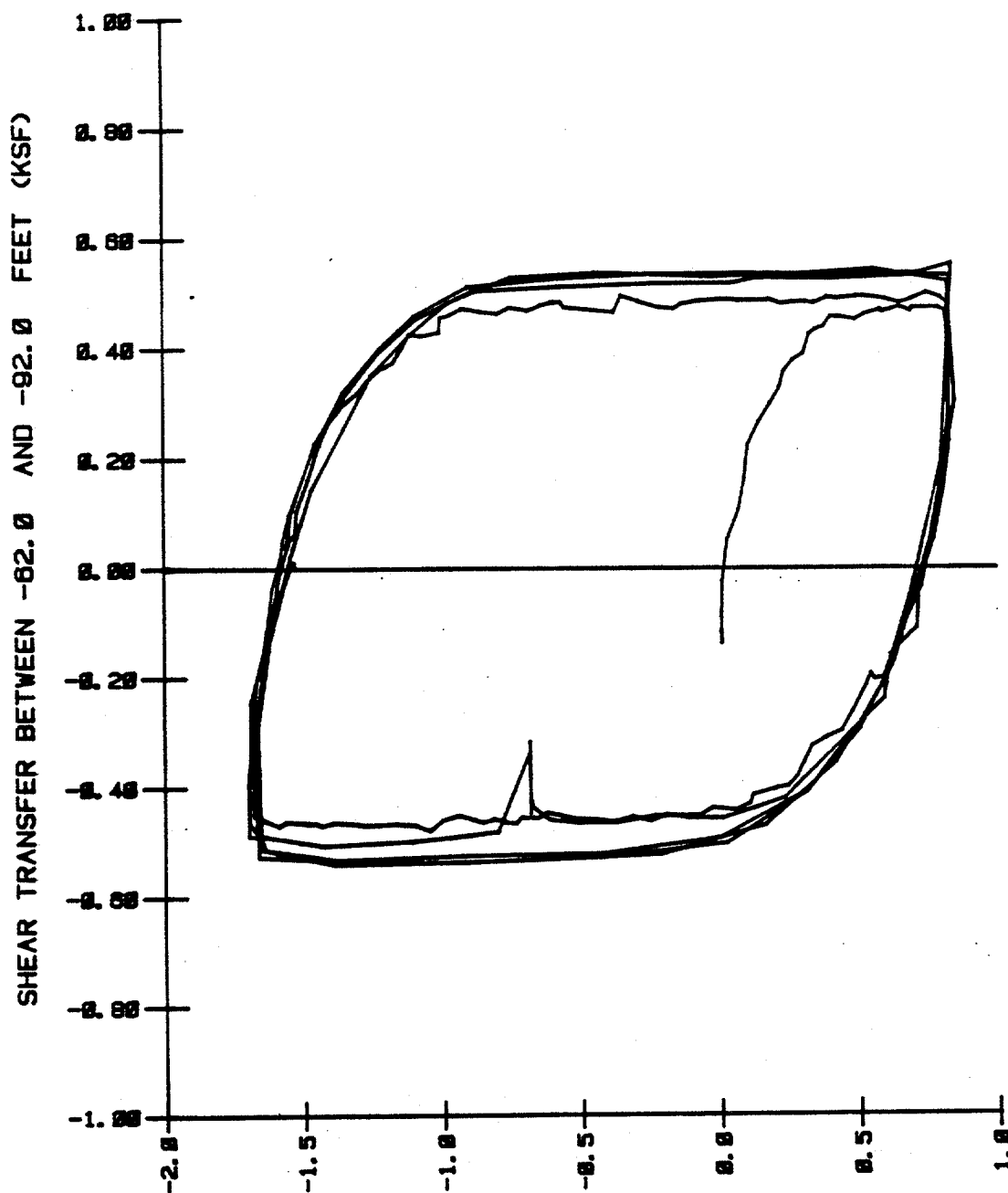
(1 inch = 25.4 mm, 1 ft = 0.305 m, 1 kip = 4.45 kN, 1 ksf = 47.9 kPa)



DISPLACEMENT AT -31.0 FEET (IN)

SHEAR TRANSFER VERSUS DISPLACEMENT BETWEEN THE DEPTHS OF 0 AND 62 FEET
DURING THE TWO-WAY CYCLIC TESTS - STRAIN MODULES

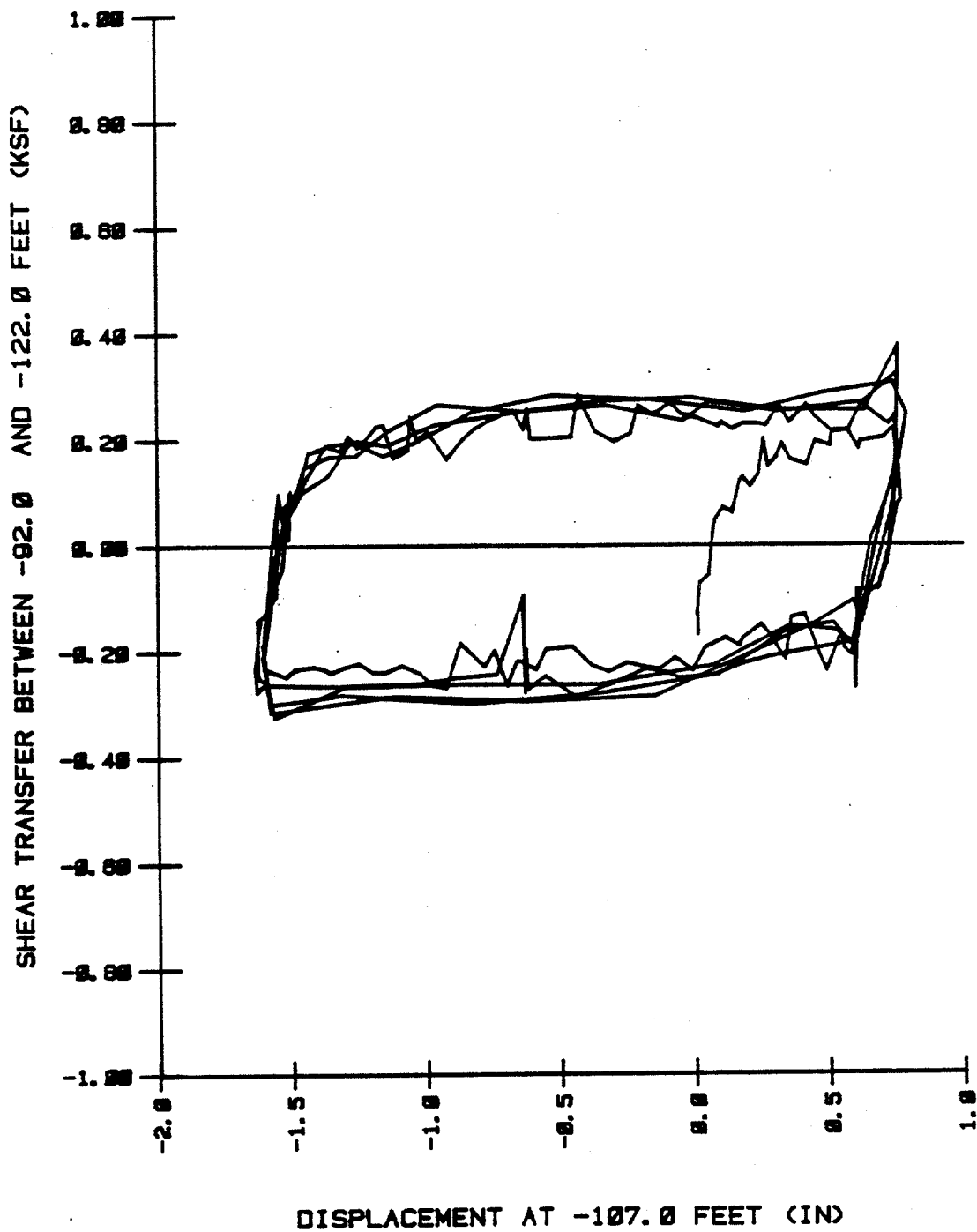
(1 inch = 25.4 mm, 1 ft = 0.305 m, 1 kip = 4.45 kN, 1 ksf = 47.9 kPa)



DISPLACEMENT AT -77.0 FEET (IN)

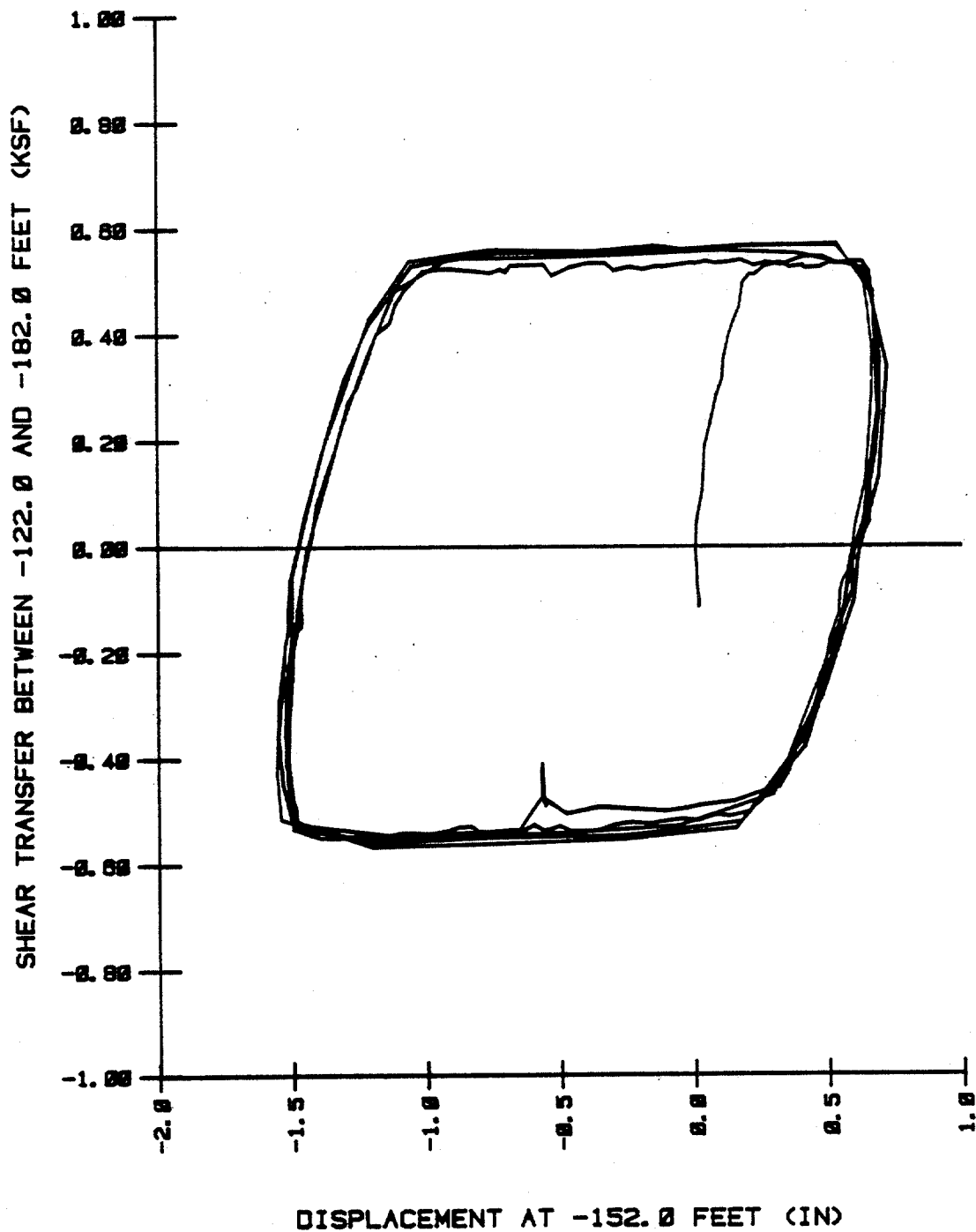
SHEAR TRANSFER VERSUS DISPLACEMENT BETWEEN THE DEPTHS OF 62 AND 92 FEET
DURING THE TWO-WAY CYCLIC TESTS - STRAIN MODULES

(1 inch = 25.4 mm, 1 ft = 0.305 m, 1 kip = 4.45 kN, 1 ksf = 47.9 kPa)



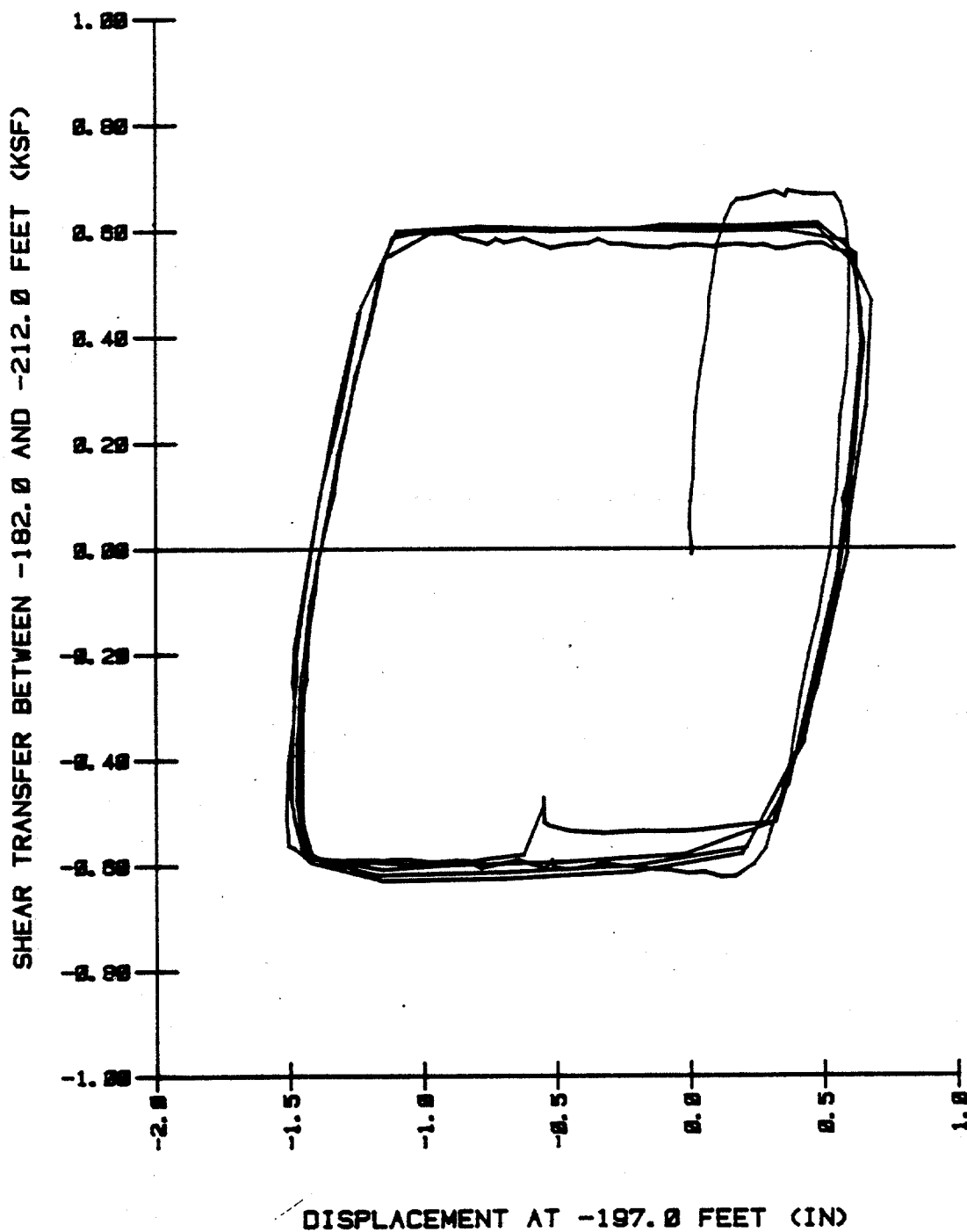
SHEAR TRANSFER VERSUS DISPLACEMENT BETWEEN THE DEPTHS OF 92 AND 122 FEET
DURING THE TWO-WAY CYCLIC TESTS - STRAIN MODULES

(1 inch = 25.4 mm, 1 ft = 0.305 m, 1 kip = 4.45 kN, 1 ksf = 47.9 kPa)



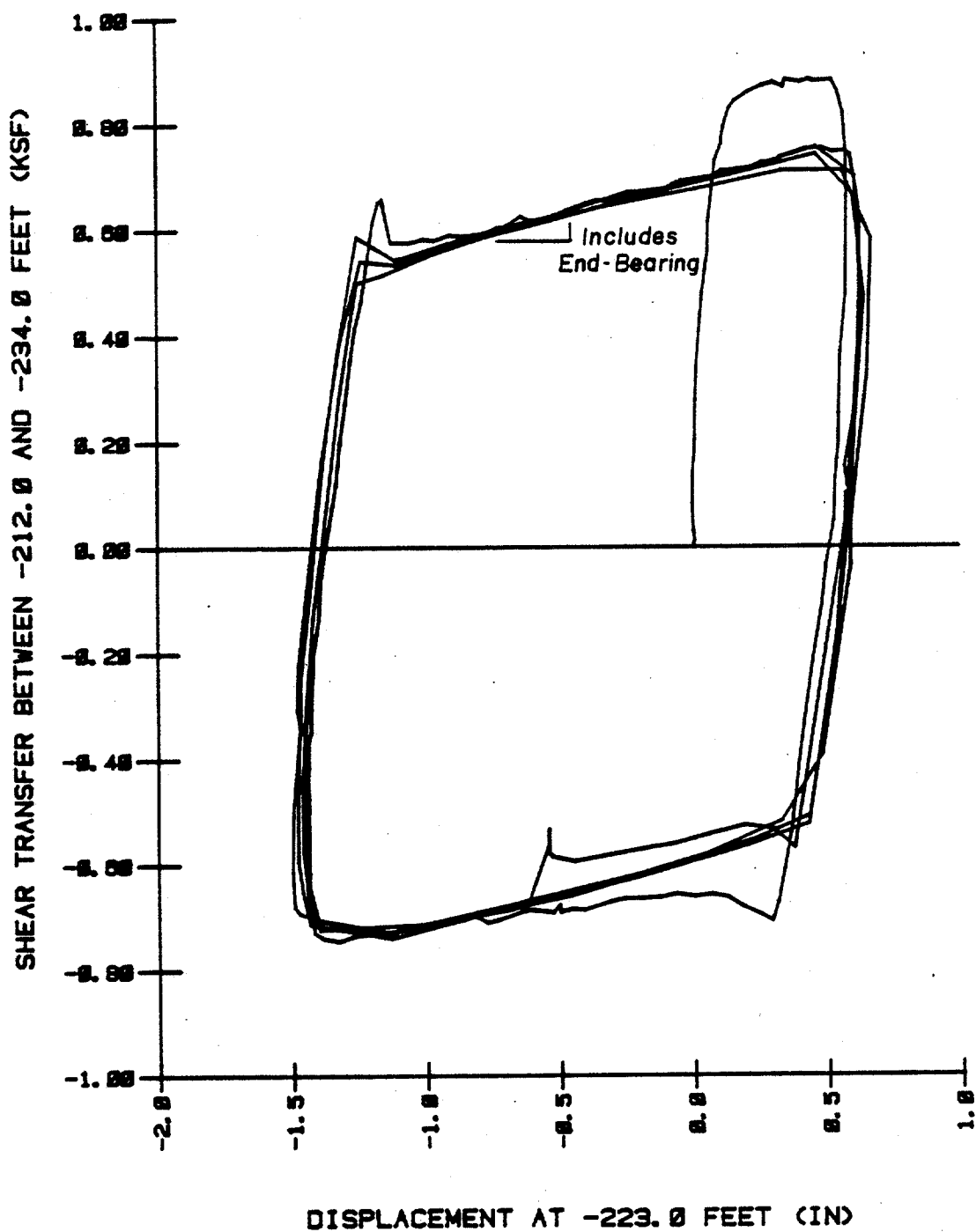
SHEAR TRANSFER VERSUS DISPLACEMENT BETWEEN THE DEPTHS OF 122 AND 182 FEET
DURING THE TWO-WAY CYCLIC TESTS - STRAIN MODULES

(1 inch = 25.4 mm, 1 ft = 0.305 m, 1 kip = 4.45 kN, 1 ksf = 47.9 kPa)



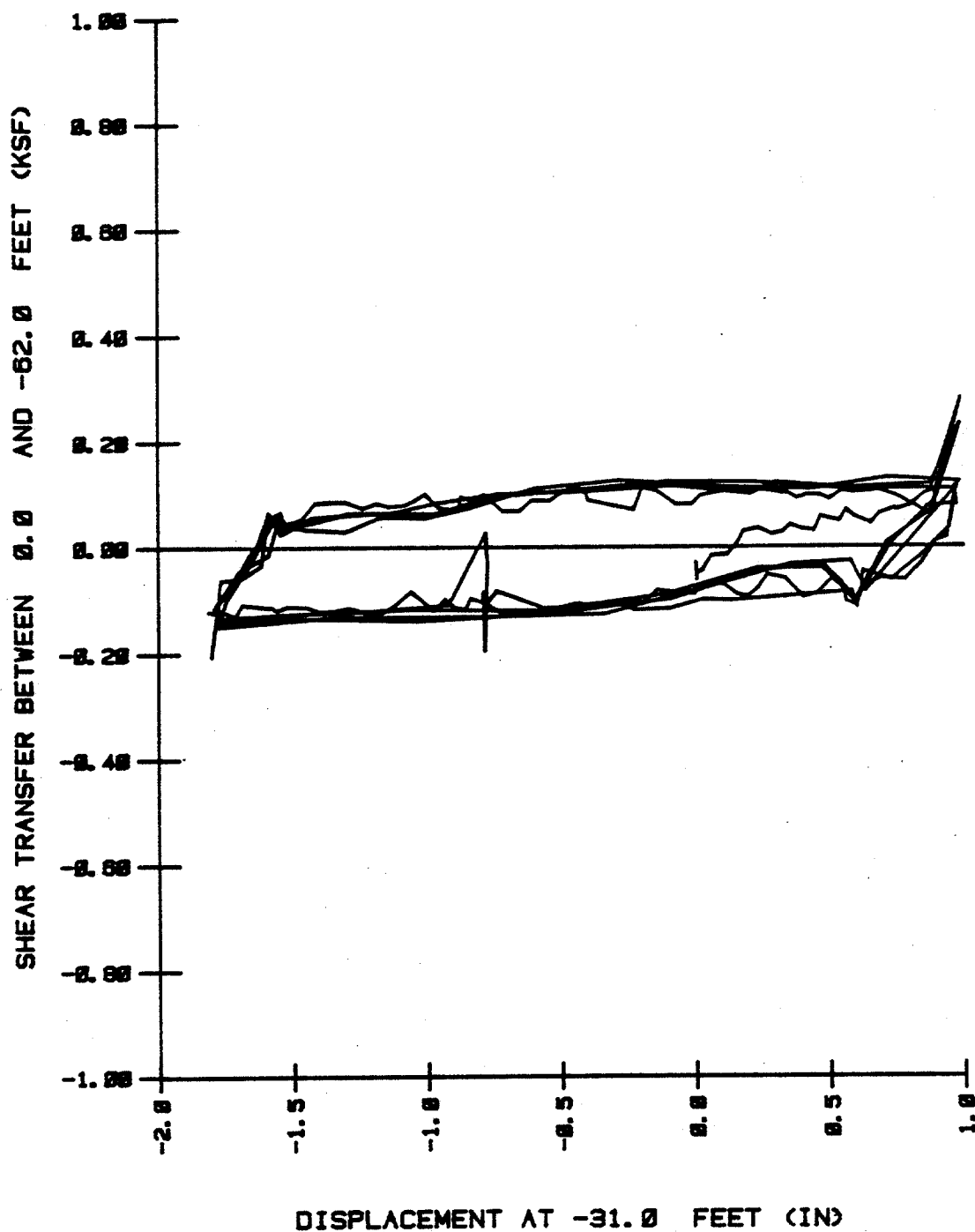
SHEAR TRANSFER VERSUS DISPLACEMENT BETWEEN THE DEPTHS OF 182 AND 212 FEET
DURING THE TWO-WAY CYCLIC TESTS - STRAIN MODULES

(1 inch = 25.4 mm, 1 ft = 0.305 m, 1 kip = 4.45 kN, 1 ksf = 47.9 kPa)



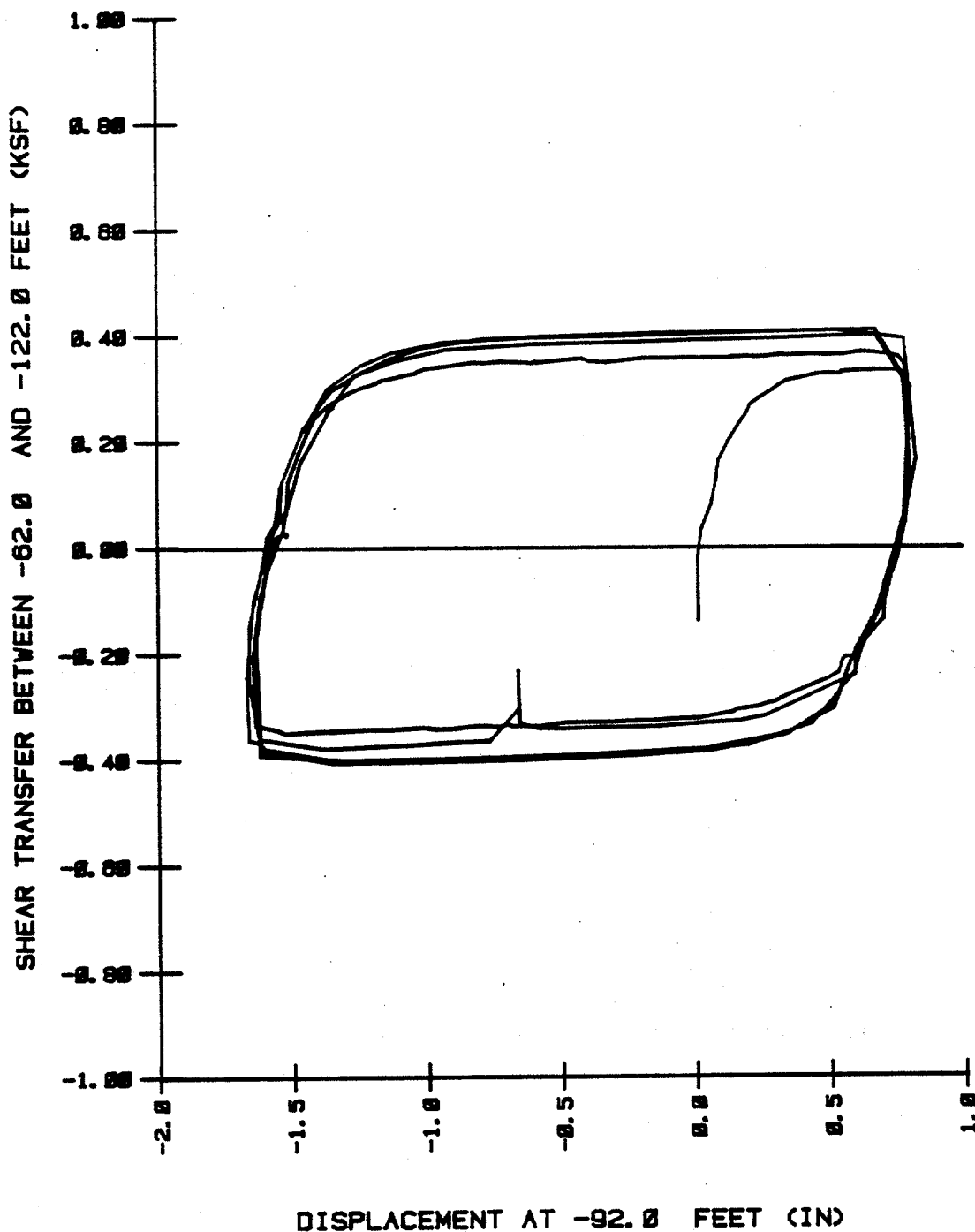
SHEAR TRANSFER VERSUS DISPLACEMENT BETWEEN THE DEPTHS OF 212 AND 234 FEET
DURING THE TWO-WAY CYCLIC TESTS - STRAIN MODULES

(1 inch = 25.4 mm, 1 ft = 0.305 m, 1 kip = 4.45 kN, 1 ksf = 47.9 kPa)



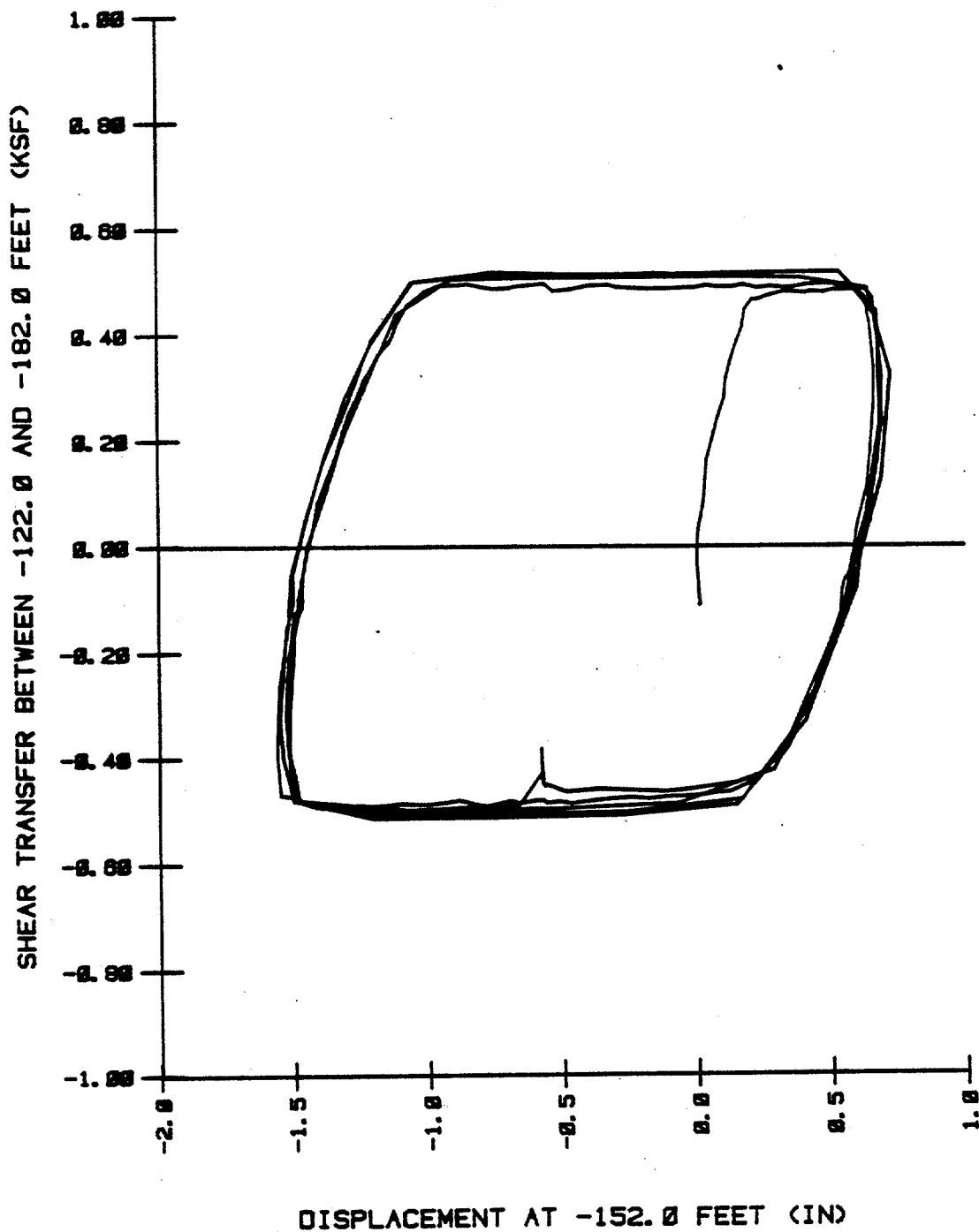
SHEAR TRANSFER VERSUS DISPLACEMENT BETWEEN THE DEPTHS OF 0 AND 62 FEET
DURING THE TWO-WAY CYCLIC TESTS - EXTENSOMETERS

(1 inch = 25.4 mm, 1 ft = 0.305 m, 1 kip = 4.45 kN, 1 ksf = 47.9 kPa)



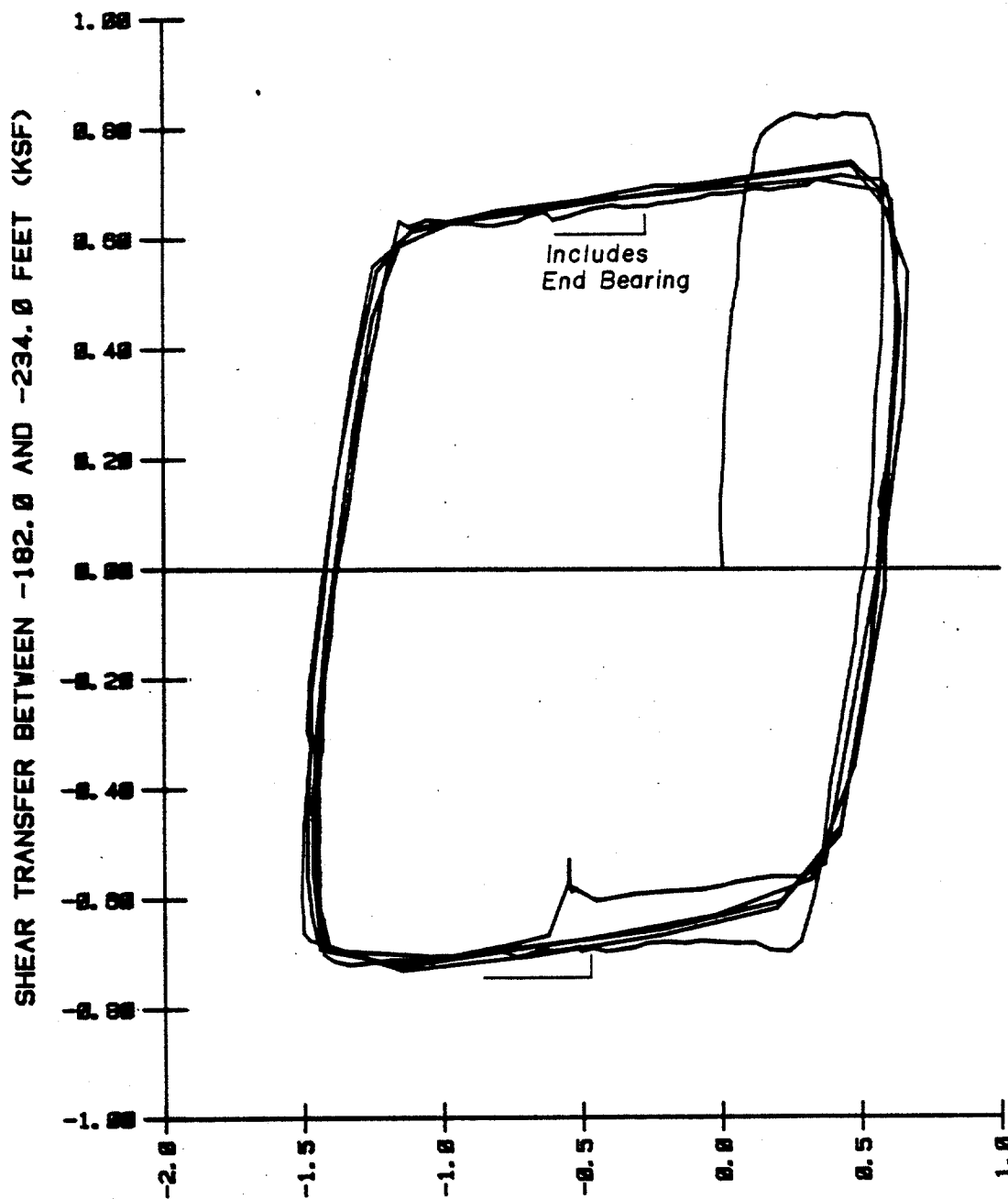
SHEAR TRANSFER VERSUS DISPLACEMENT BETWEEN THE DEPTHS OF 62 AND 122 FEET
DURING THE TWO-WAY CYCLIC TESTS - EXTENSOMETERS

(1 inch = 25.4 mm, 1 ft = 0.305 m, 1 kip = 4.45 kN, 1 ksf = 47.9 kPa)



SHEAR TRANSFER VERSUS DISPLACEMENT BETWEEN THE DEPTHS OF 122 AND 182 FEET
DURING THE TWO-WAY CYCLIC TESTS - EXTENSOMETERS

(1 inch = 25.4 mm, 1 ft = 0.305 m, 1 kip = 4.45 kN, 1 ksf = 47.9 kPa)

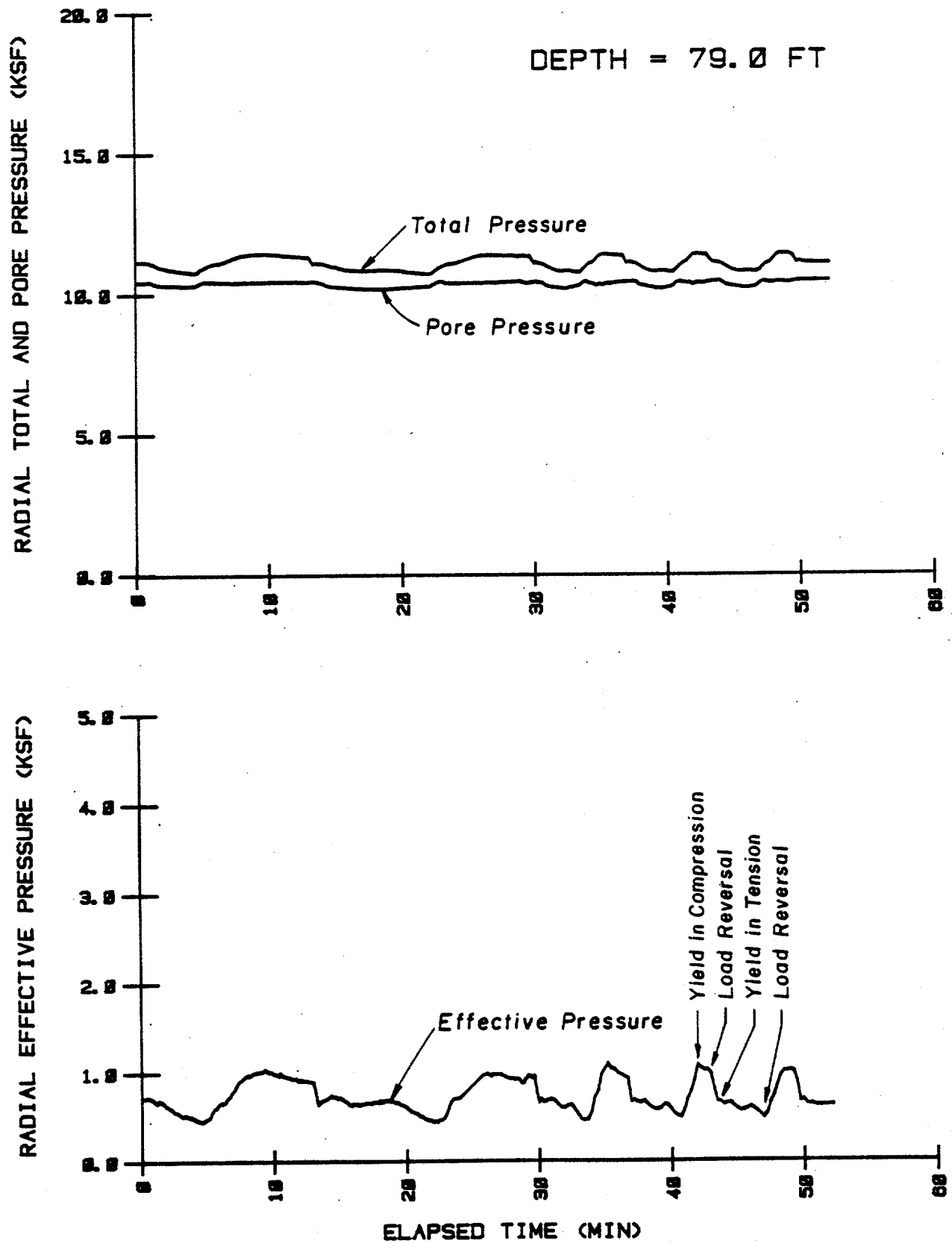


DISPLACEMENT AT -208.0 FEET (IN)

SHEAR TRANSFER VERSUS DISPLACEMENT BETWEEN THE DEPTHS OF 182 AND 234 FEET
DURING THE TWO-WAY CYCLIC TESTS - EXTENSOMETERS

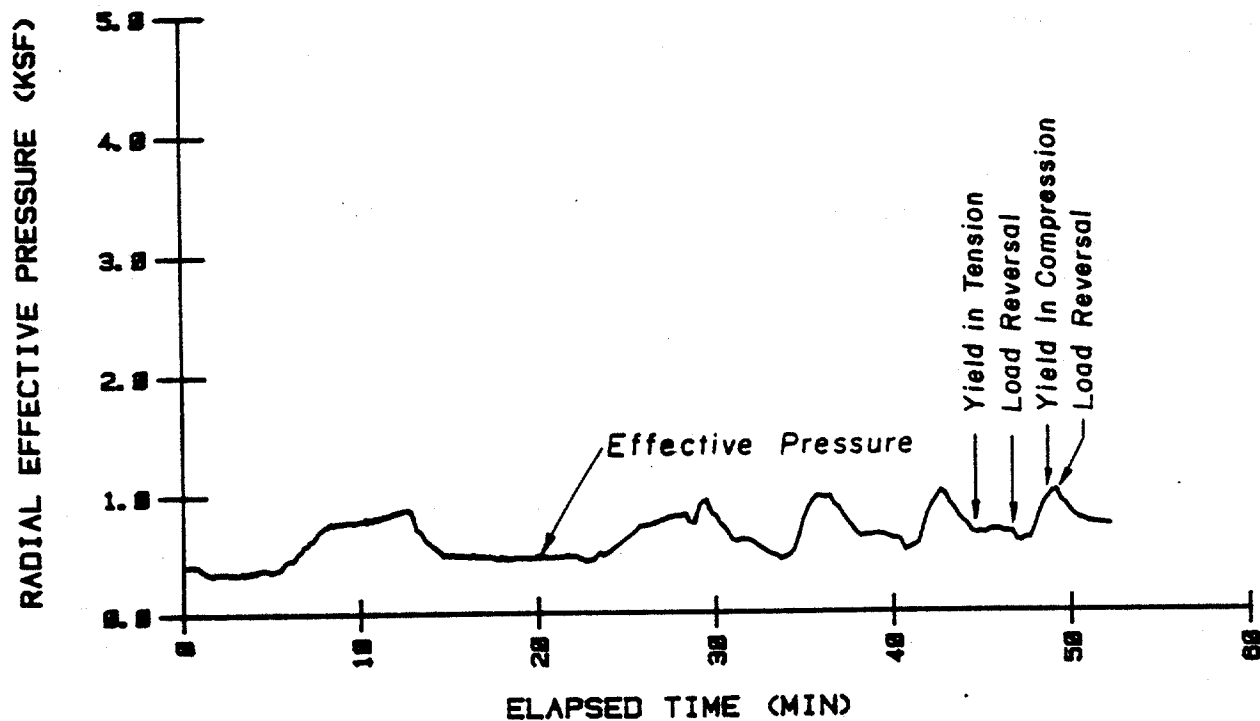
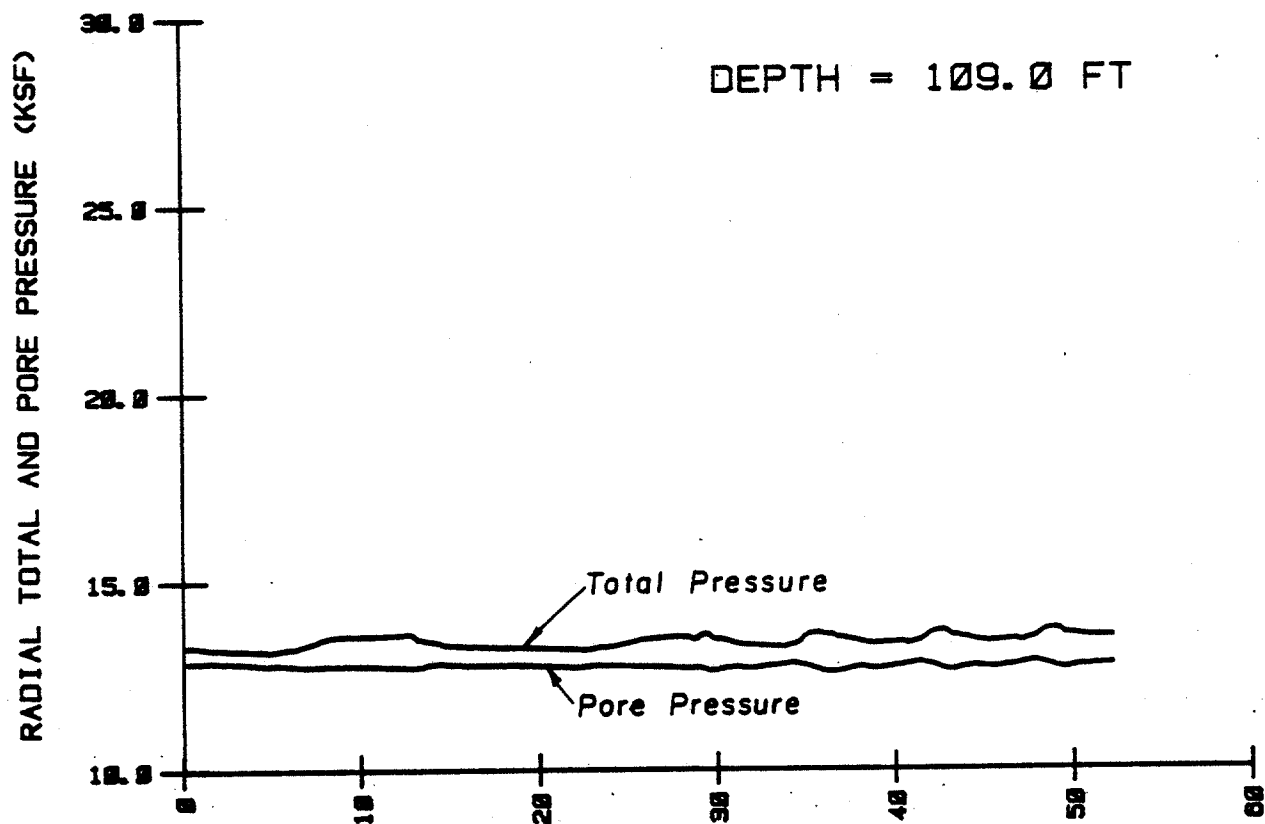
(1 inch = 25.4 mm, 1 ft = 0.305 m, 1 kip = 4.45 kN, 1 ksf = 47.9 kPa)

(1 inch = 25.4 mm, 1 ft = 0.305 m, 1 kip = 4.45 kN, 1 ksf = 47.9 kPa)



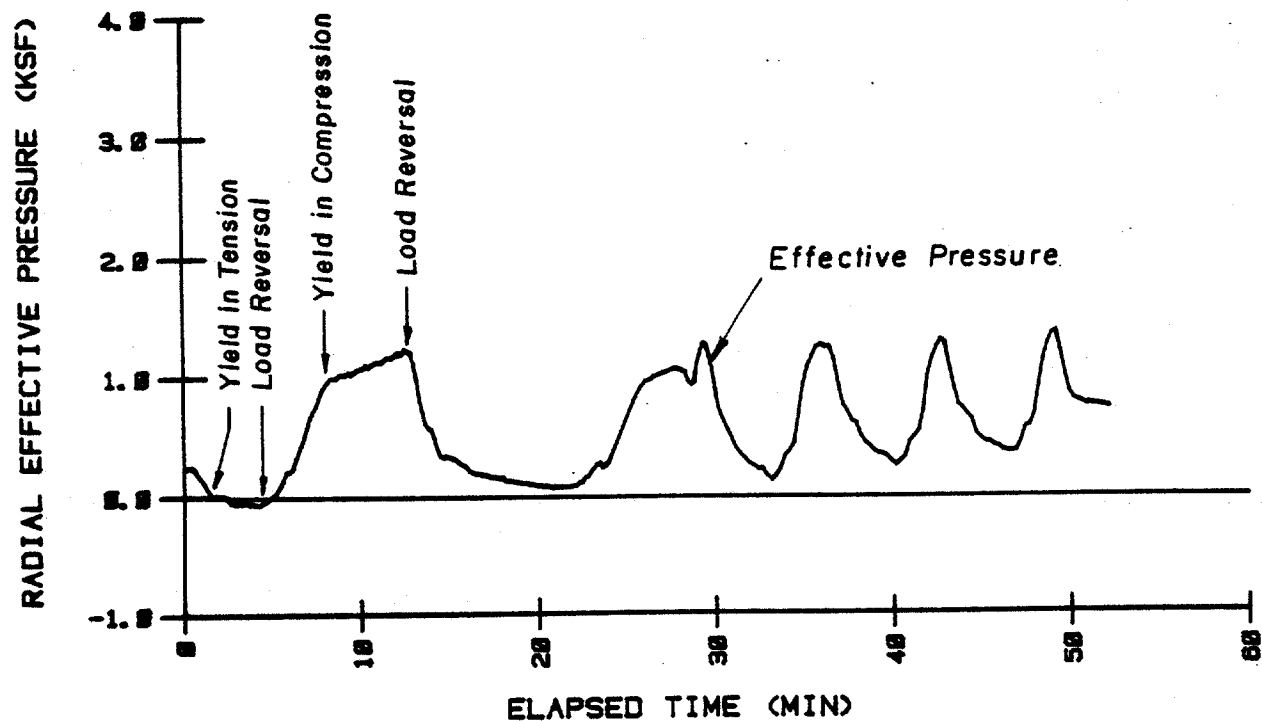
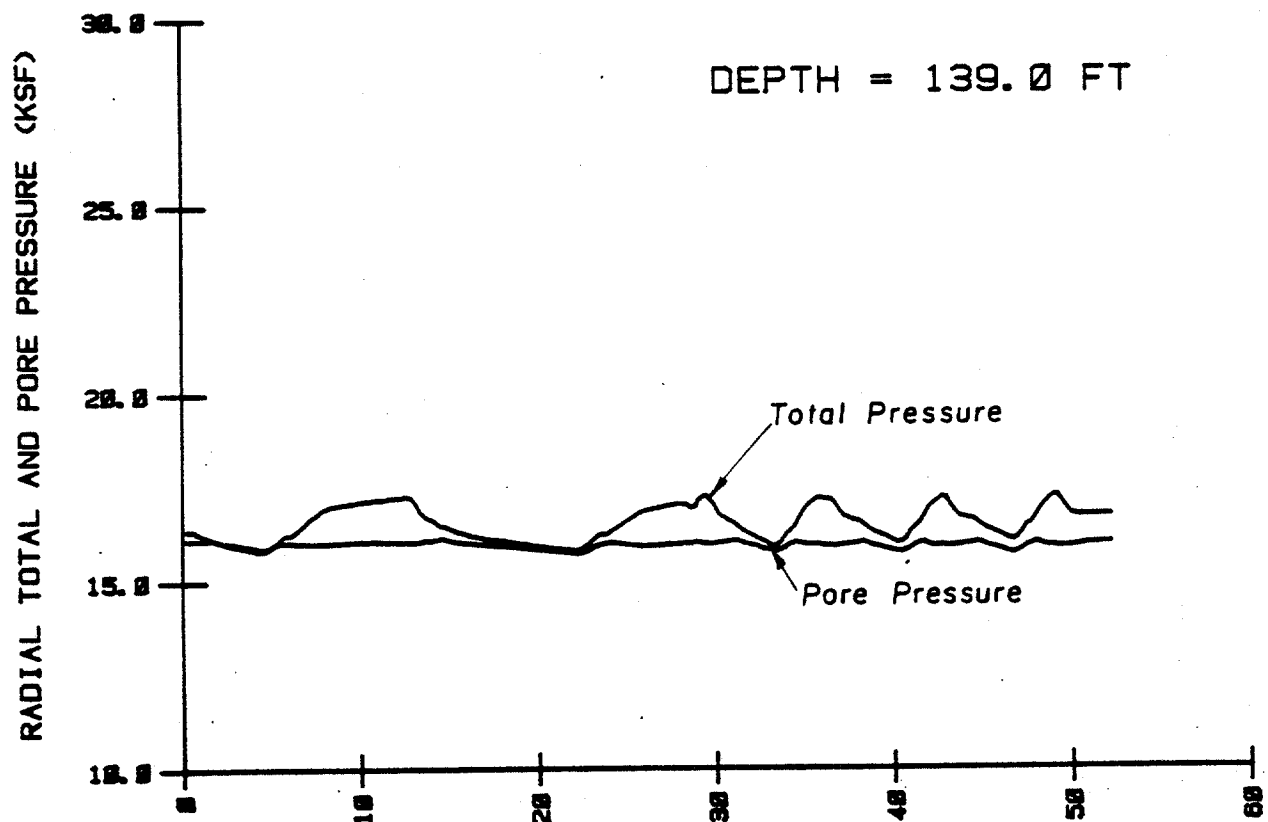
VARIATION IN SOIL PRESSURES AT THE 79-FOOT DEPTH
DURING THE TWO-WAY CYCLIC TESTS

(1 inch = 25.4 mm, 1 ft = 0.305 m, 1 kip = 4.45 kN, 1 ksf = 47.9 kPa)



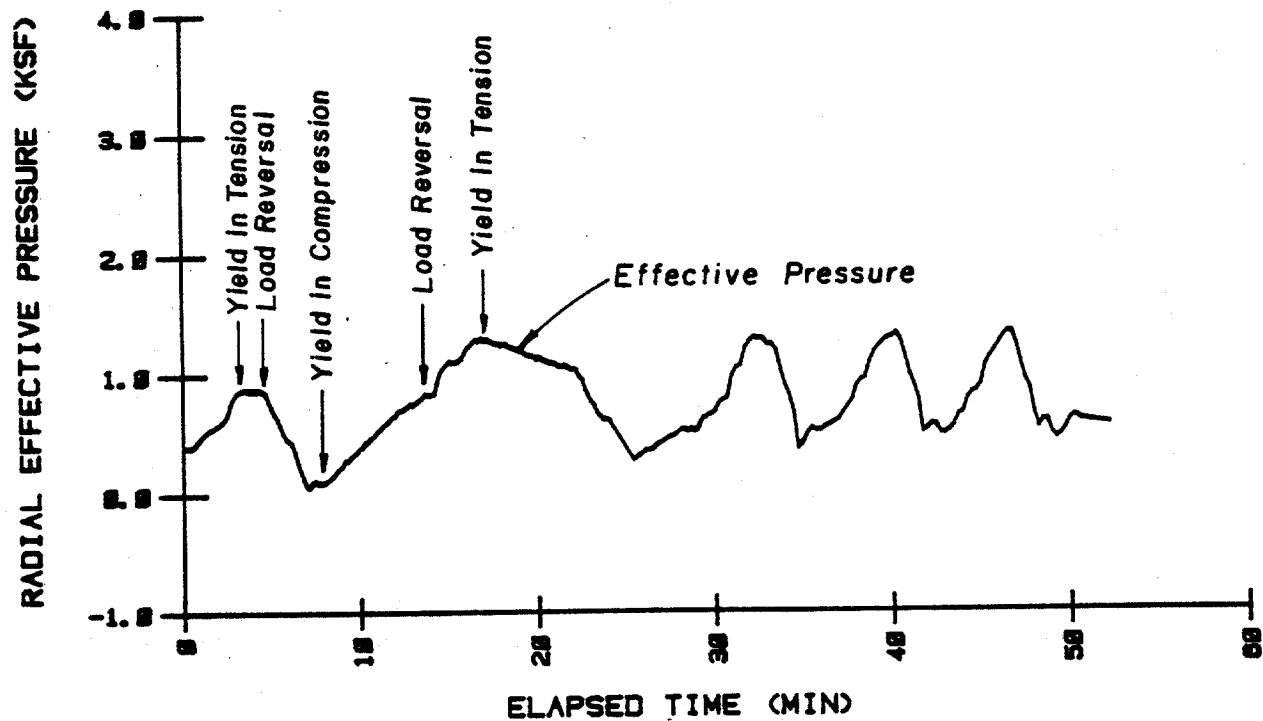
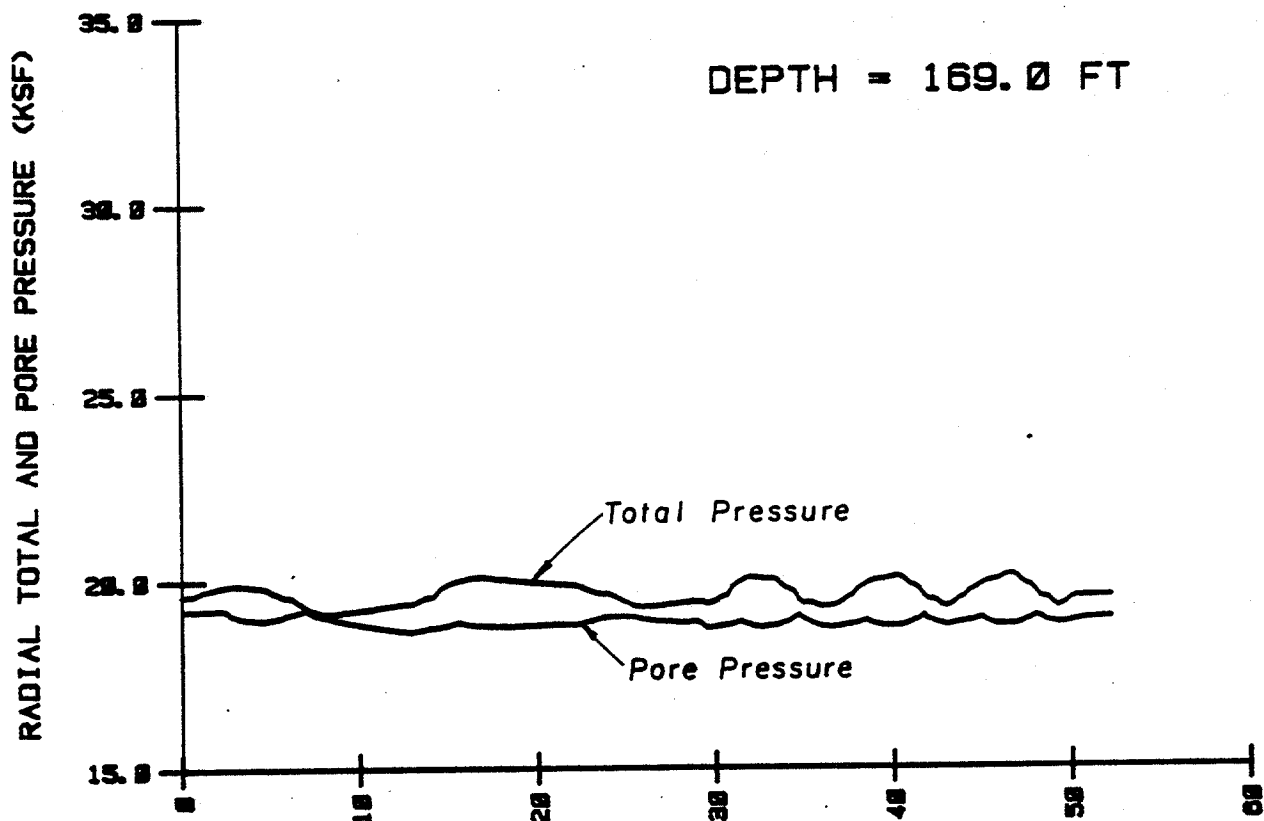
VARIATION IN SOIL PRESSURES AT THE 109-FOOT DEPTH
DURING THE TWO-WAY CYCLIC TESTS

(1 inch = 25.4 mm, 1 ft = 0.305 m, 1 kip = 4.45 kN, 1 ksf = 47.9 kPa)



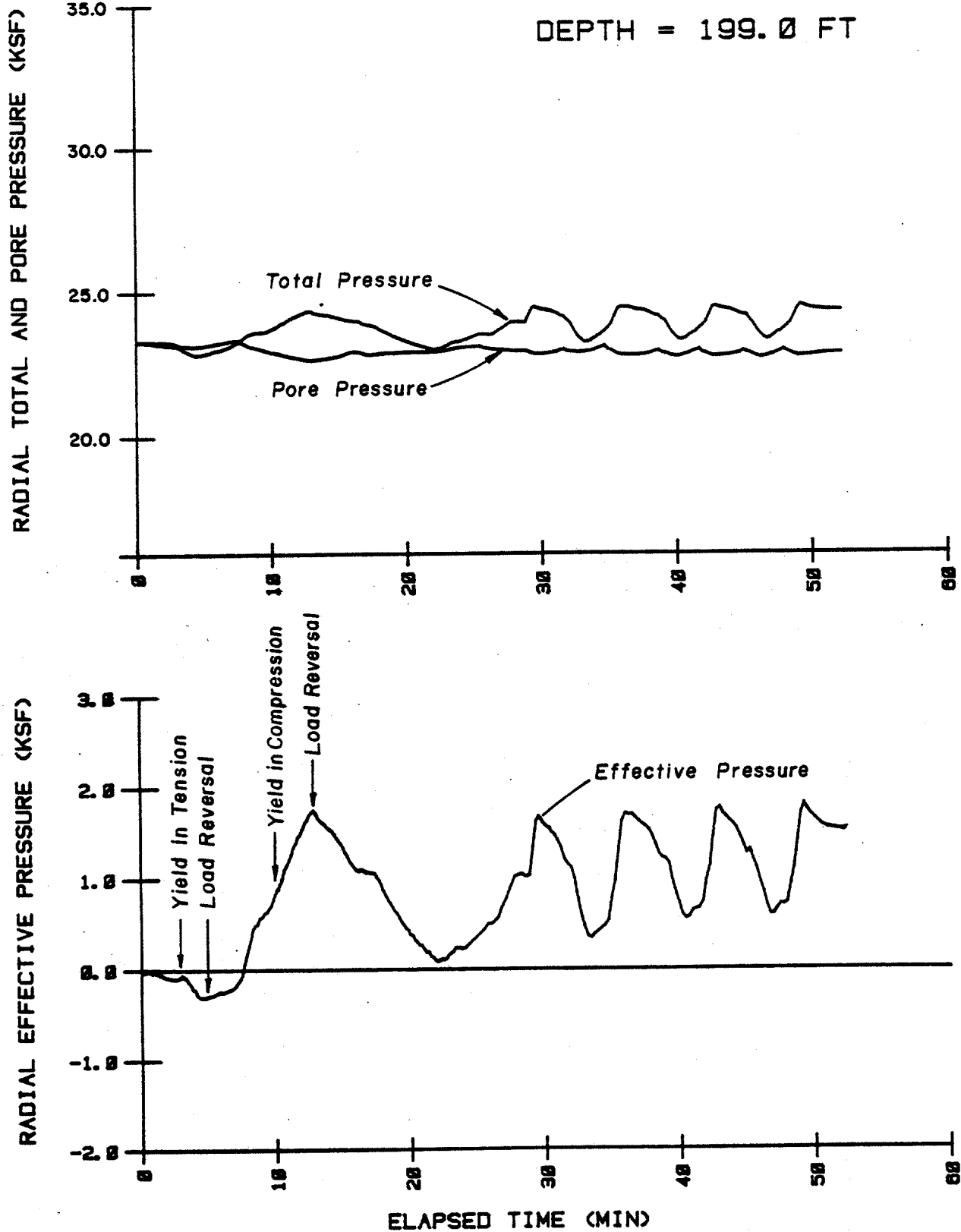
VARIATION IN SOIL PRESSURES AT THE 139-FOOT DEPTH
DURING THE TWO-WAY CYCLIC TESTS

(1 inch = 25.4 mm, 1 ft = 0.305 m, 1 kip = 4.45 kN, 1 ksf = 47.9 kPa)



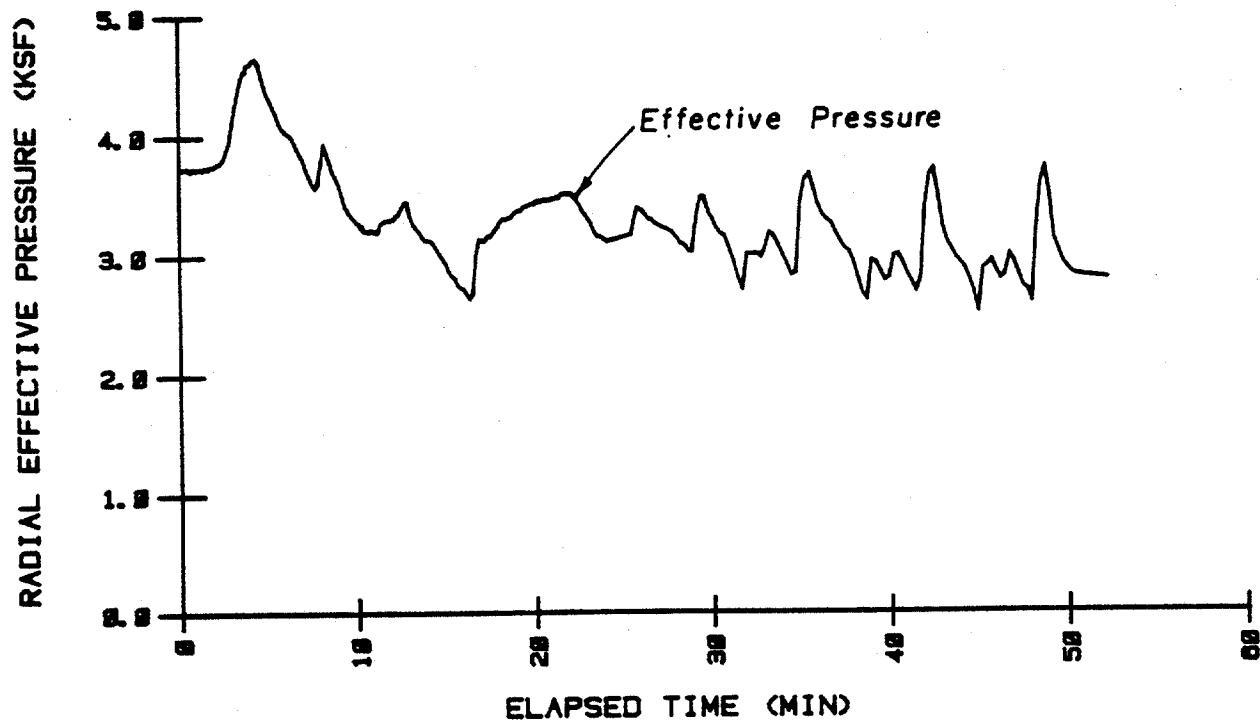
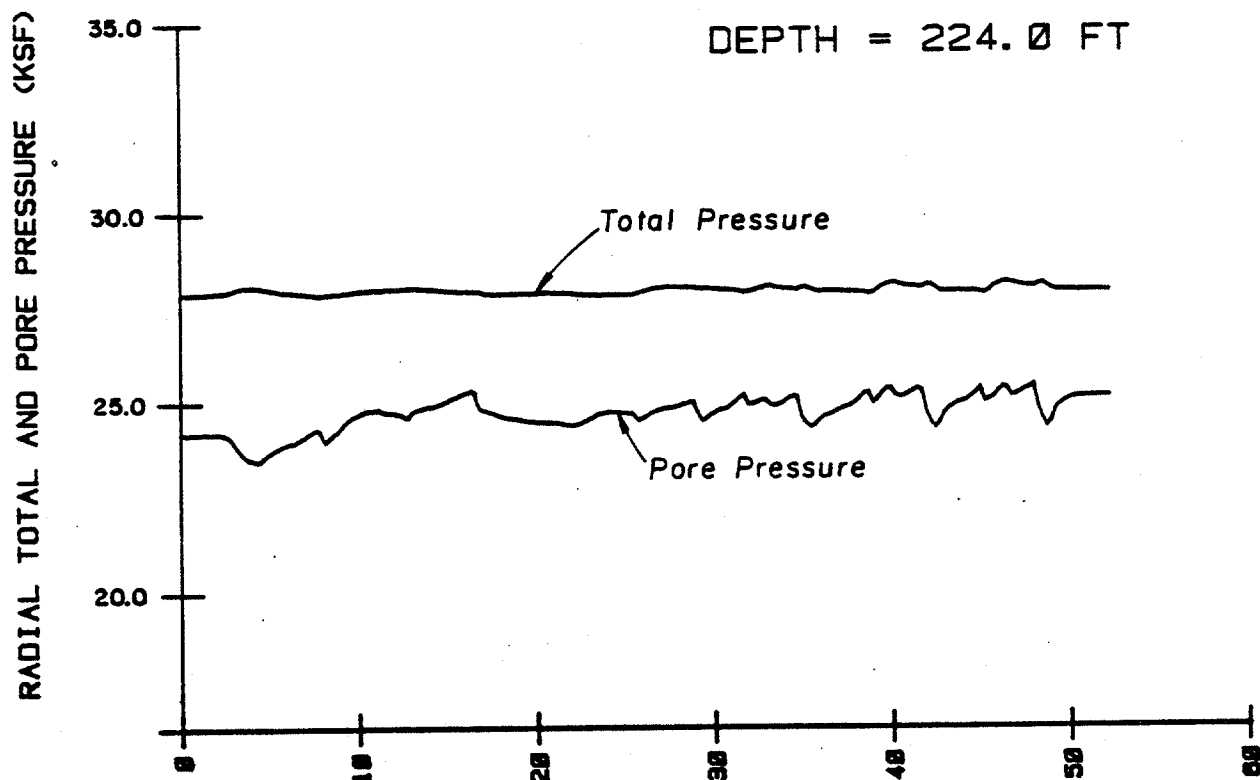
VARIATION IN SOIL PRESSURES AT THE 169-FOOT DEPTH
DURING THE TWO-WAY CYCLIC TESTS

(1 inch = 25.4 mm, 1 ft = 0.305 m, 1 kip = 4.45 kN, 1 ksf = 47.9 kPa)

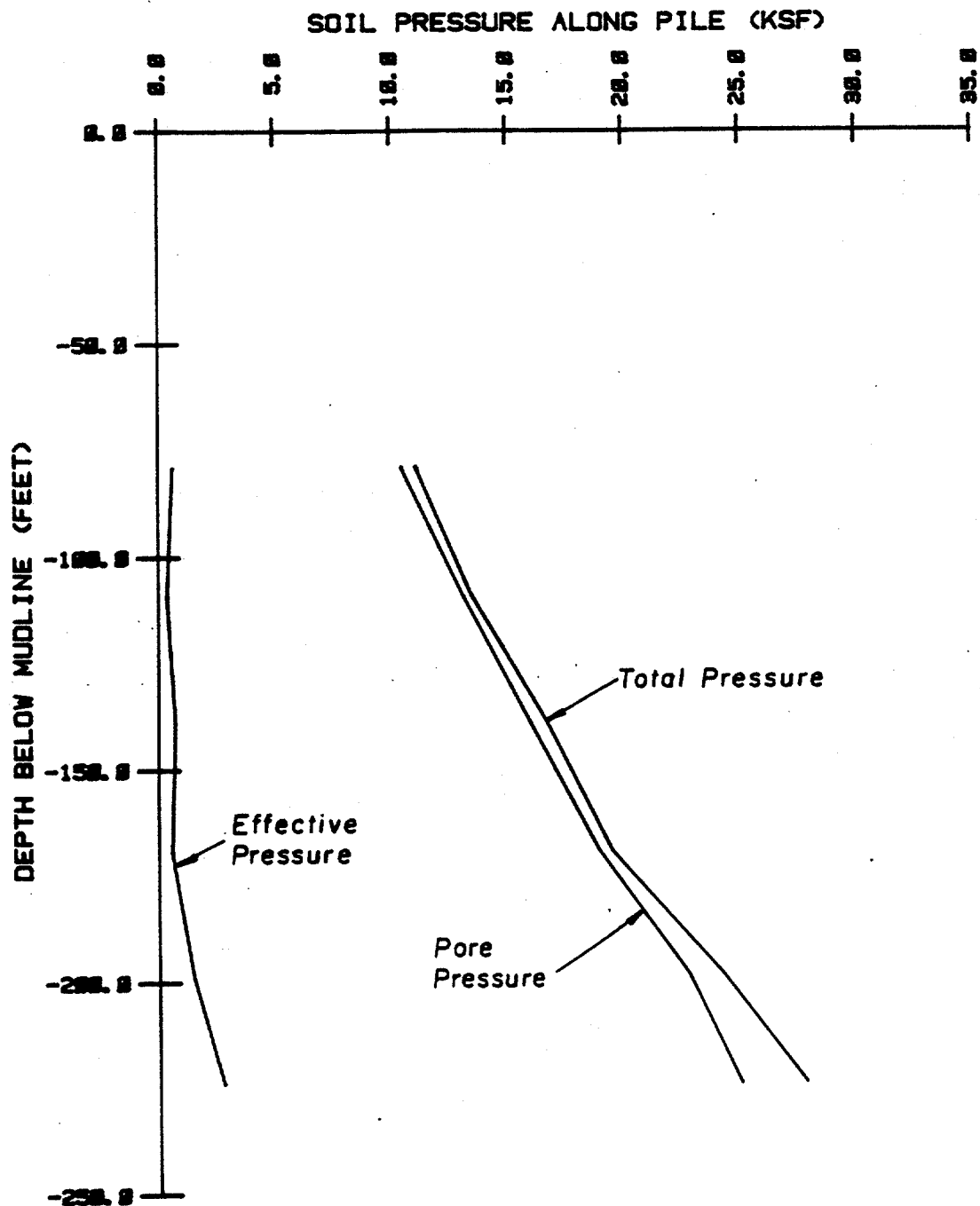


VARIATION IN SOIL PRESSURES AT THE 199-FOOT DEPTH
DURING THE TWO-WAY CYCLIC TESTS

(1 inch = 25.4 mm, 1 ft = 0.305 m, 1 kip = 4.45 kN, 1 ksf = 47.9 kPa)

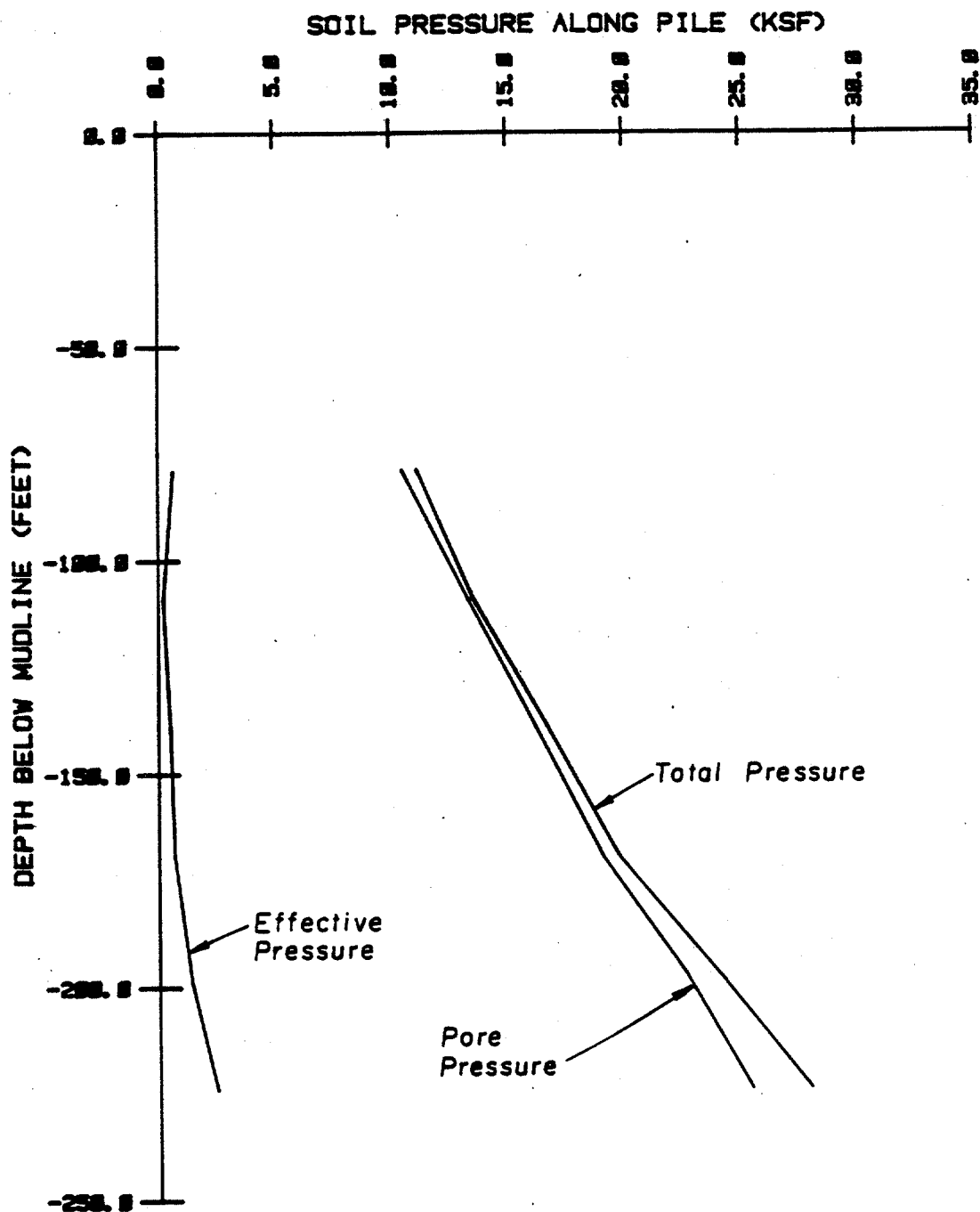


VARIATION IN SOIL PRESSURES AT THE 224-FOOT DEPTH
DURING THE TWO-WAY CYCLIC TESTS



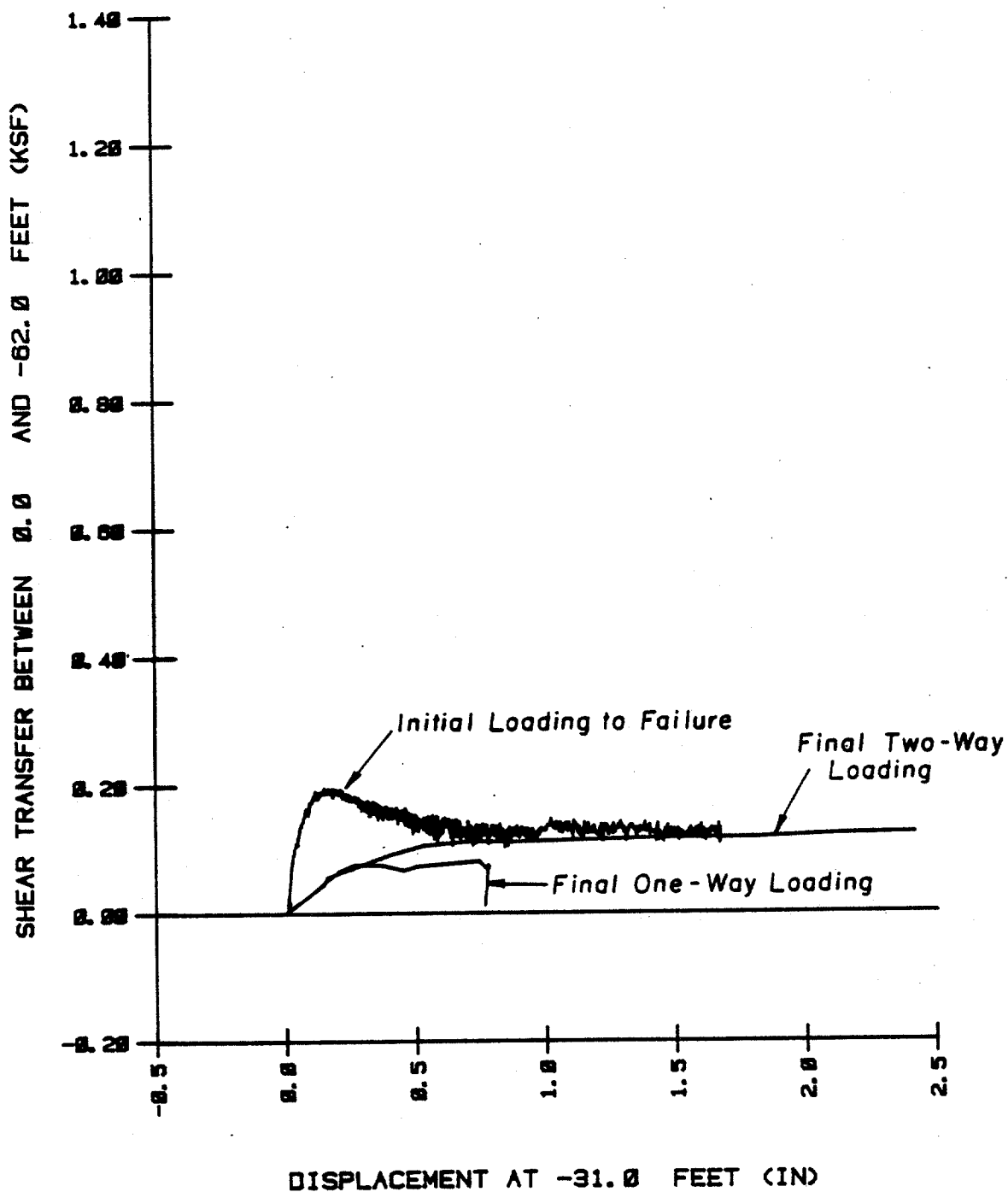
SOIL PRESSURE PROFILES AT THE END OF THE TWO-WAY CYCLIC TESTS

(1 inch = 25.4 mm, 1 ft = 0.305 m, 1 kip = 4.45 kN, 1 ksf = 47.9 kPa)



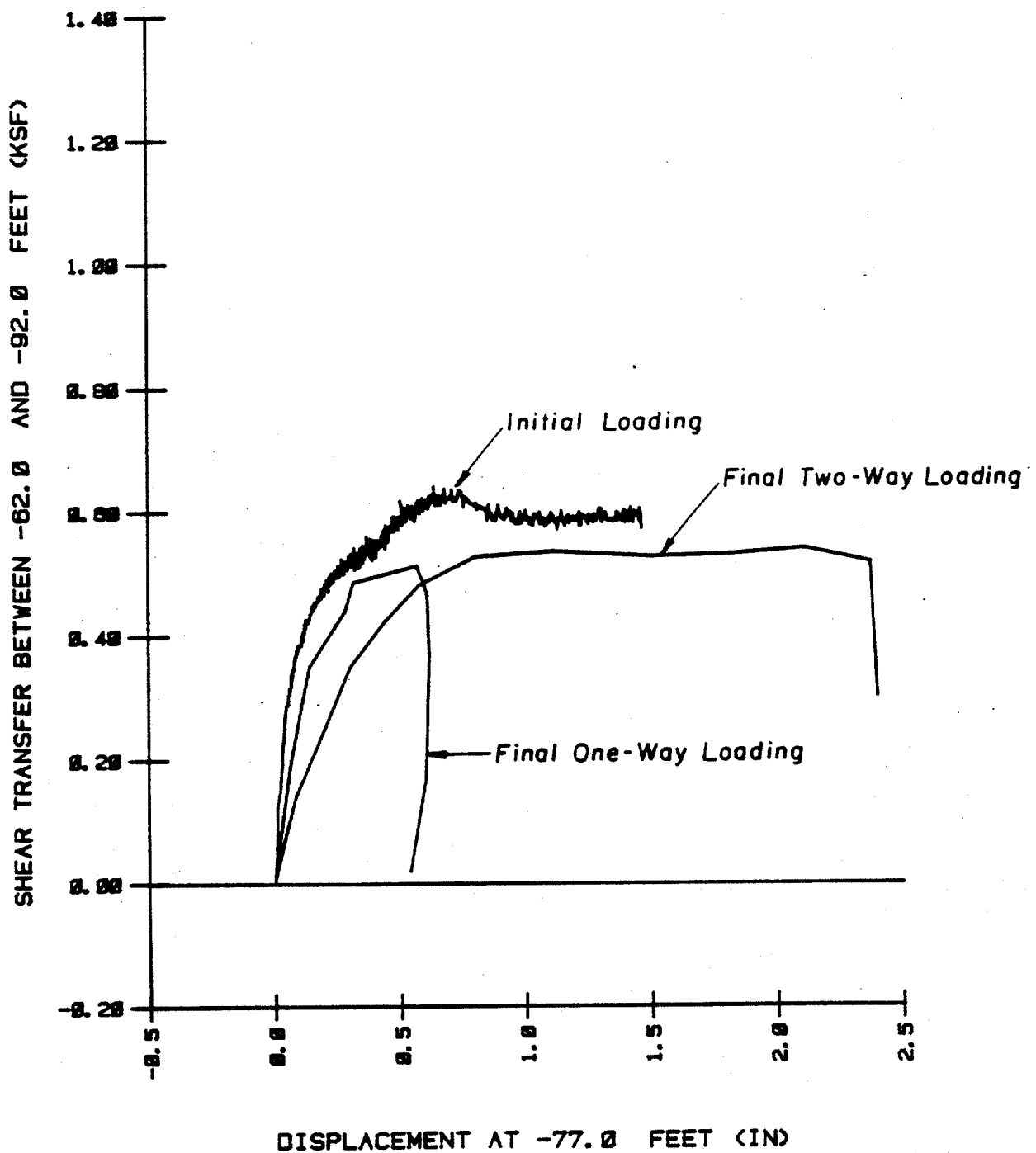
SOIL PRESSURE PROFILES AFTER A 28.5-HOUR EQUILIBRATION PERIOD

(1 inch = 25.4 mm, 1 ft = 0.305 m, 1 kip = 4.45 kN, 1 ksf = 47.9 kPa)



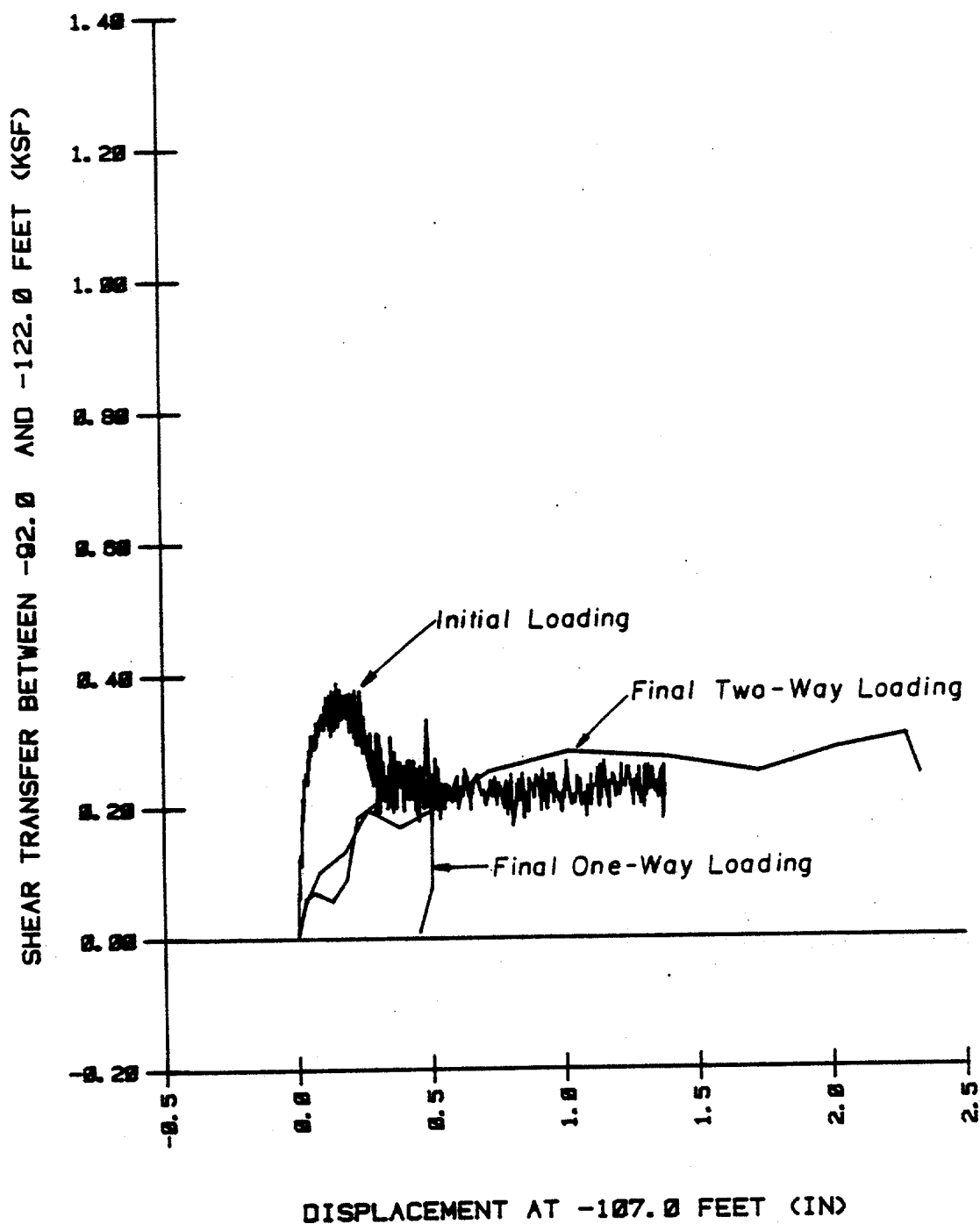
COMPARISON OF SHEAR TRANSFER VERSUS DISPLACEMENT BETWEEN
THE DEPTHS OF 0 AND 62 FEET - STRAIN MODULES

(1 inch = 25.4 mm, 1 ft = 0.305 m, 1 kip = 4.45 kN, 1 ksf = 47.9 kPa)



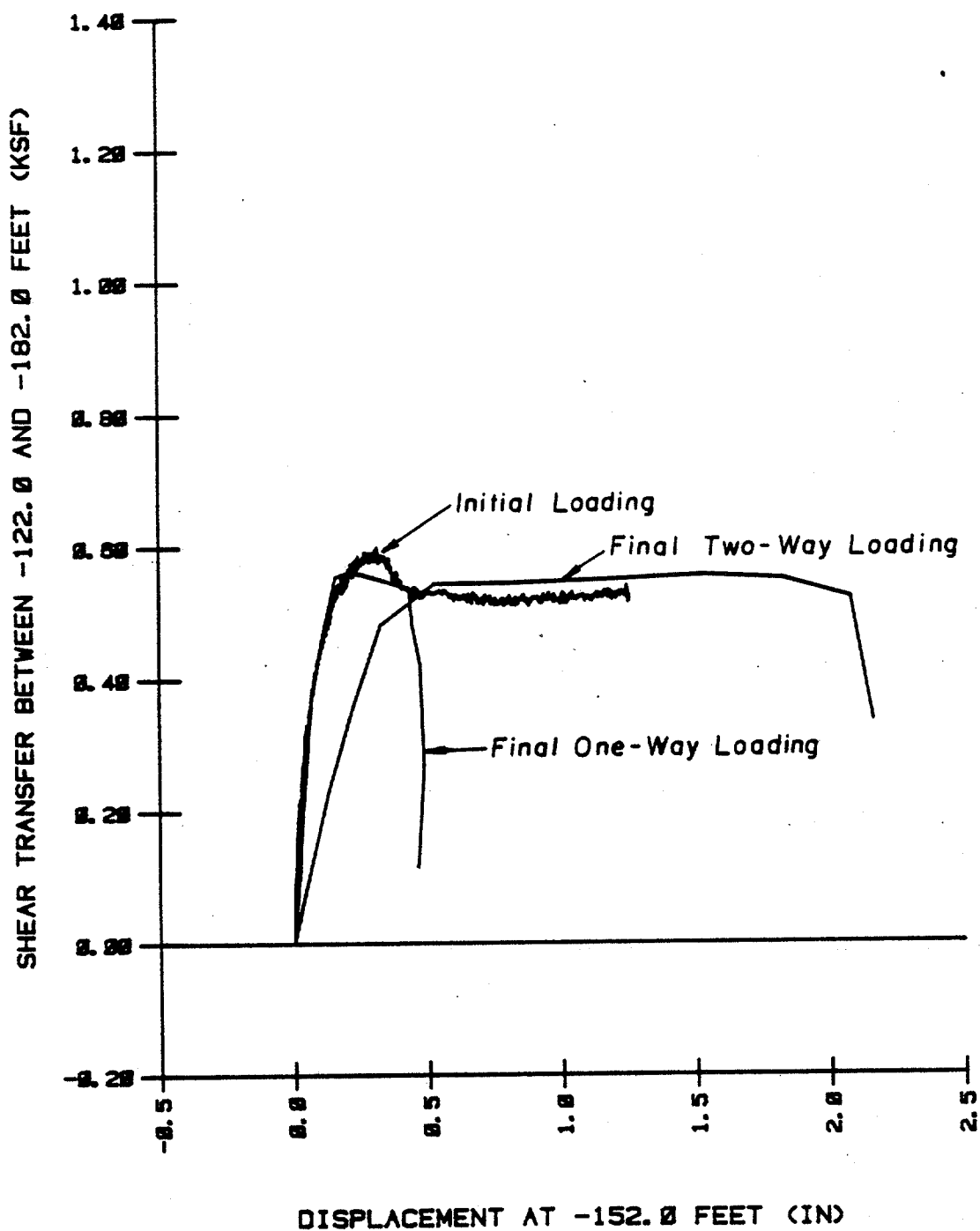
COMPARISON OF SHEAR TRANSFER VERSUS DISPLACEMENT BETWEEN
THE DEPTHS OF 62 AND 92 FEET - STRAIN MODULES

(1 inch = 25.4 mm, 1 ft = 0.305 m, 1 kip = 4.45 kN, 1 ksf = 47.9 kPa)



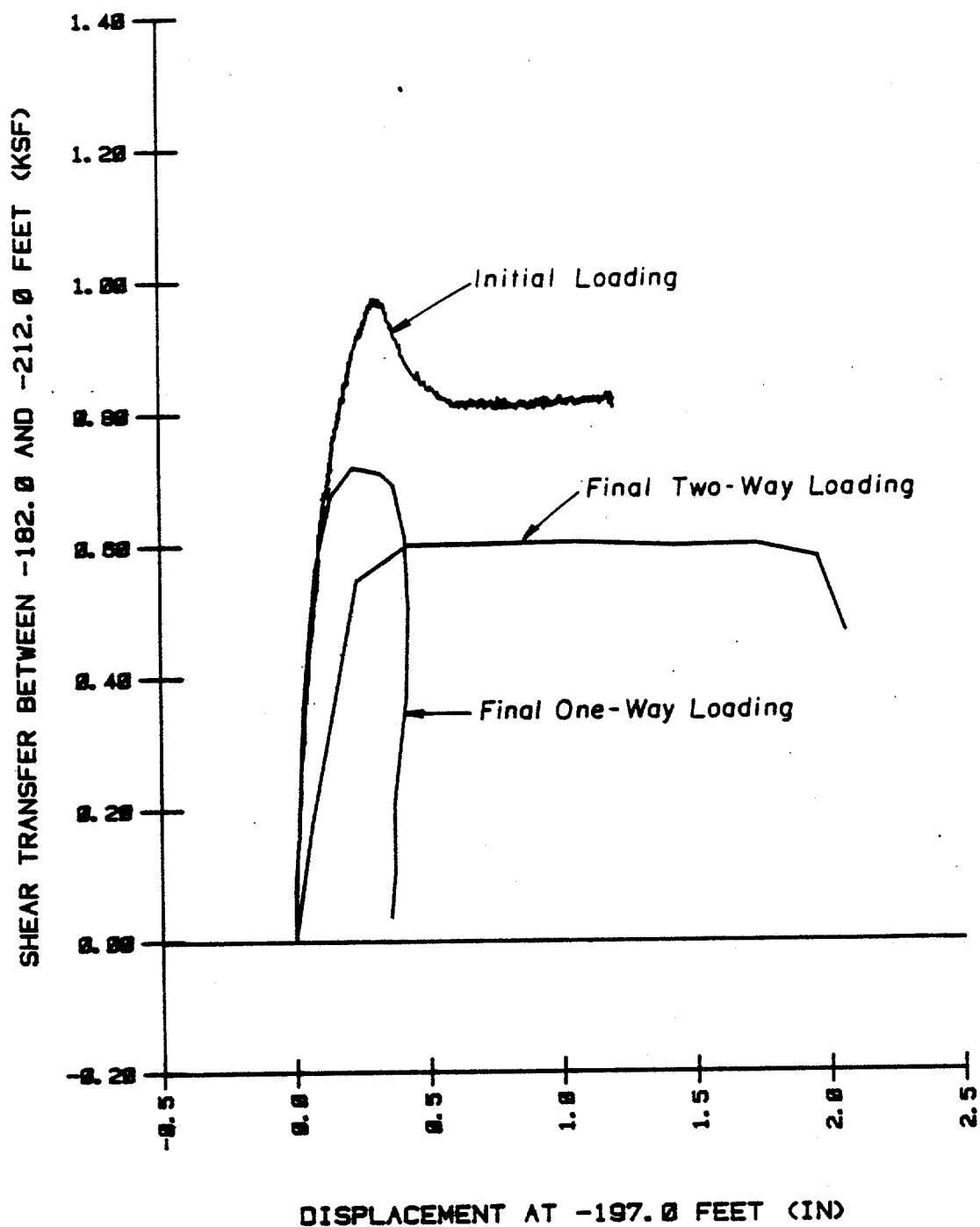
COMPARISON OF SHEAR TRANSFER VERSUS DISPLACEMENT BETWEEN
THE DEPTHS OF 92 AND 122 FEET - STRAIN MODULES

(1 inch = 25.4 mm, 1 ft = 0.305 m, 1 kip = 4.45 kN, 1 ksf = 47.9 kPa)



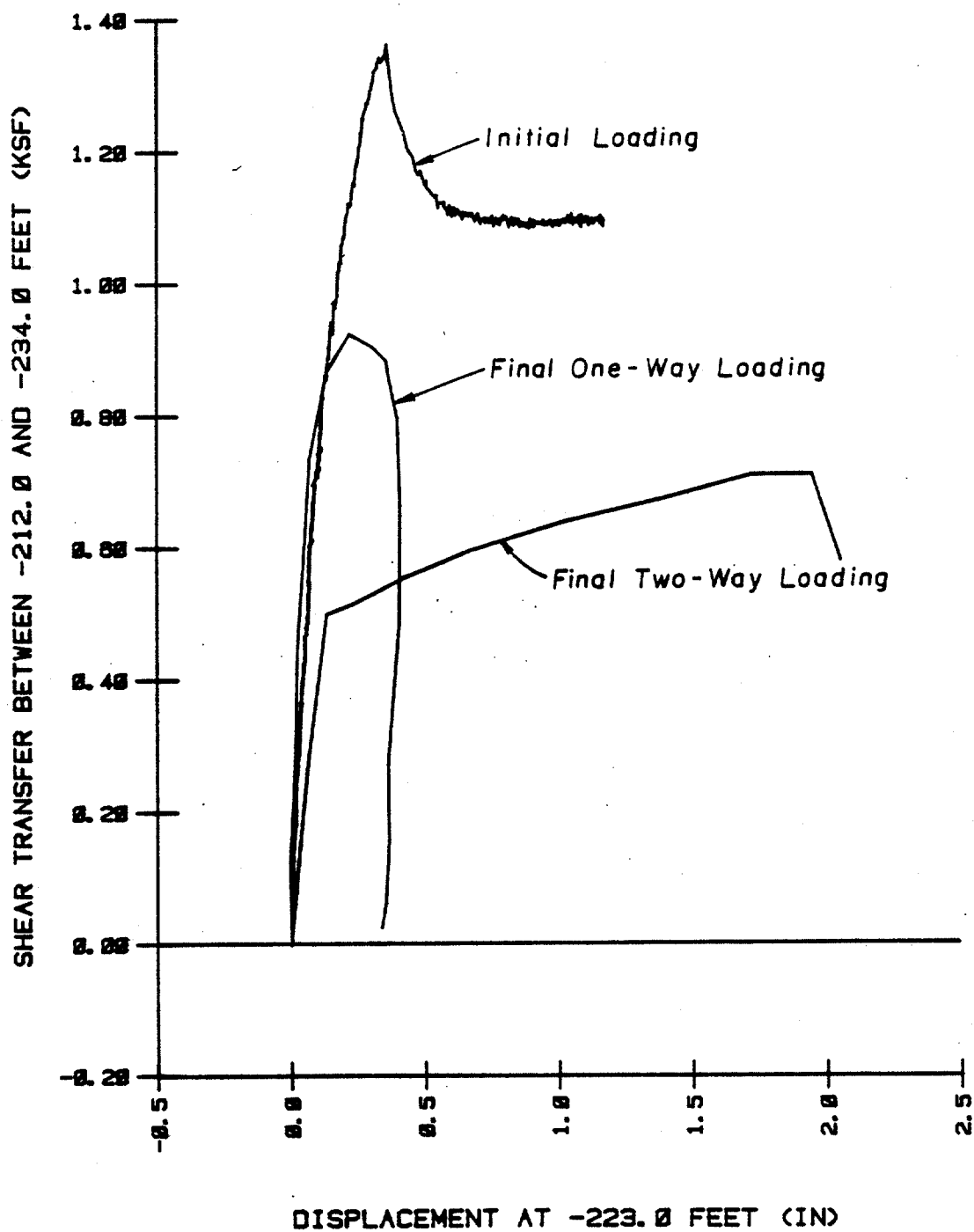
COMPARISON OF SHEAR TRANSFER VERSUS DISPLACEMENT BETWEEN
THE DEPTHS OF 122 AND 182 FEET - STRAIN MODULES

(1 inch = 25.4 mm, 1 ft = 0.305 m, 1 kip = 4.45 kN, 1 ksf = 47.9 kPa)



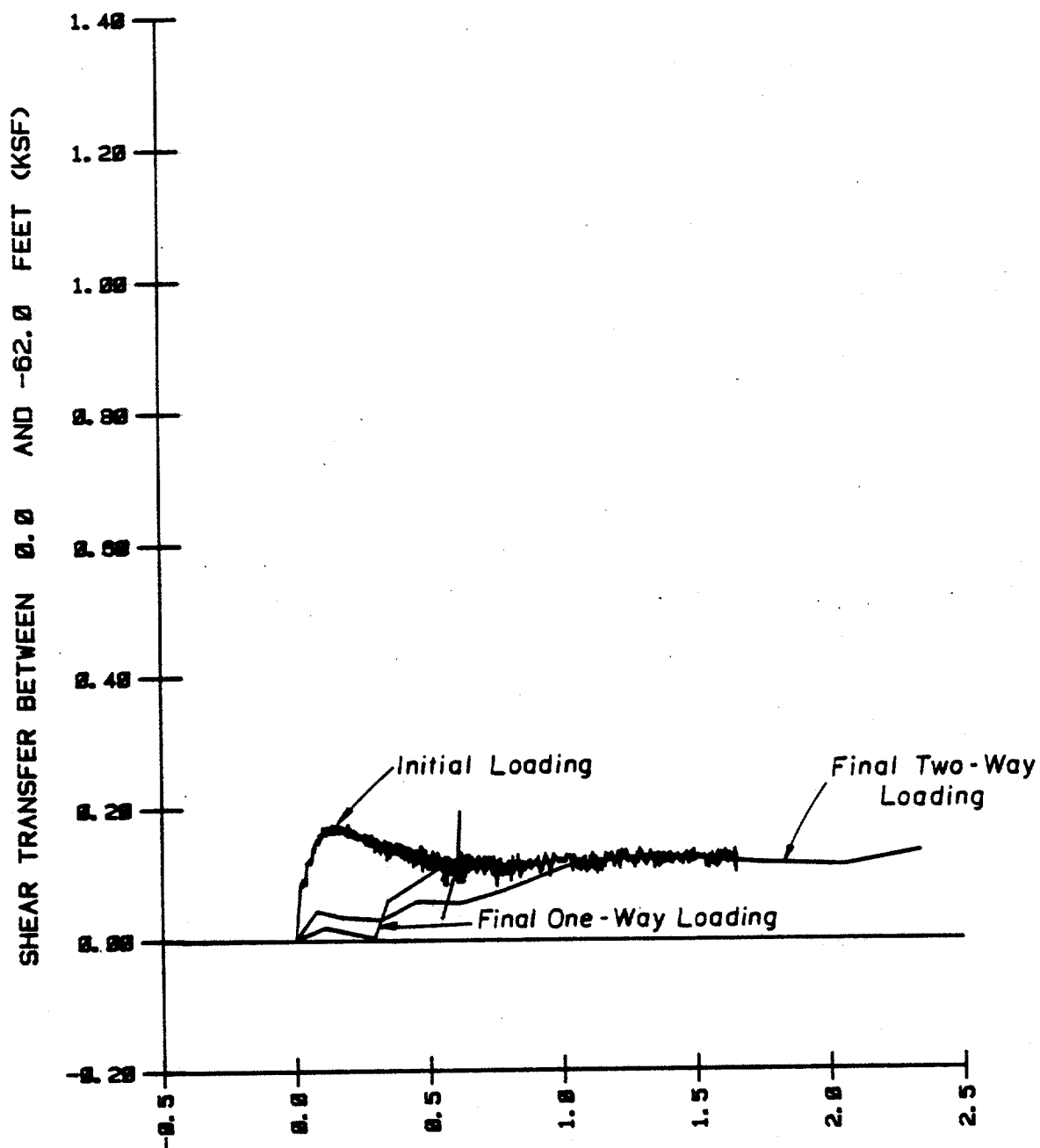
COMPARISON OF SHEAR TRANSFER VERSUS DISPLACEMENT BETWEEN
THE DEPTHS OF 182 AND 212 FEET - STRAIN MODULES

(1 inch = 25.4 mm, 1 ft = 0.305 m, 1 kip = 4.45 kN, 1 ksf = 47.9 kPa)



COMPARISON OF SHEAR TRANSFER VERSUS DISPLACEMENT BETWEEN
THE DEPTHS OF 212 AND 234 FEET - STRAIN MODULES

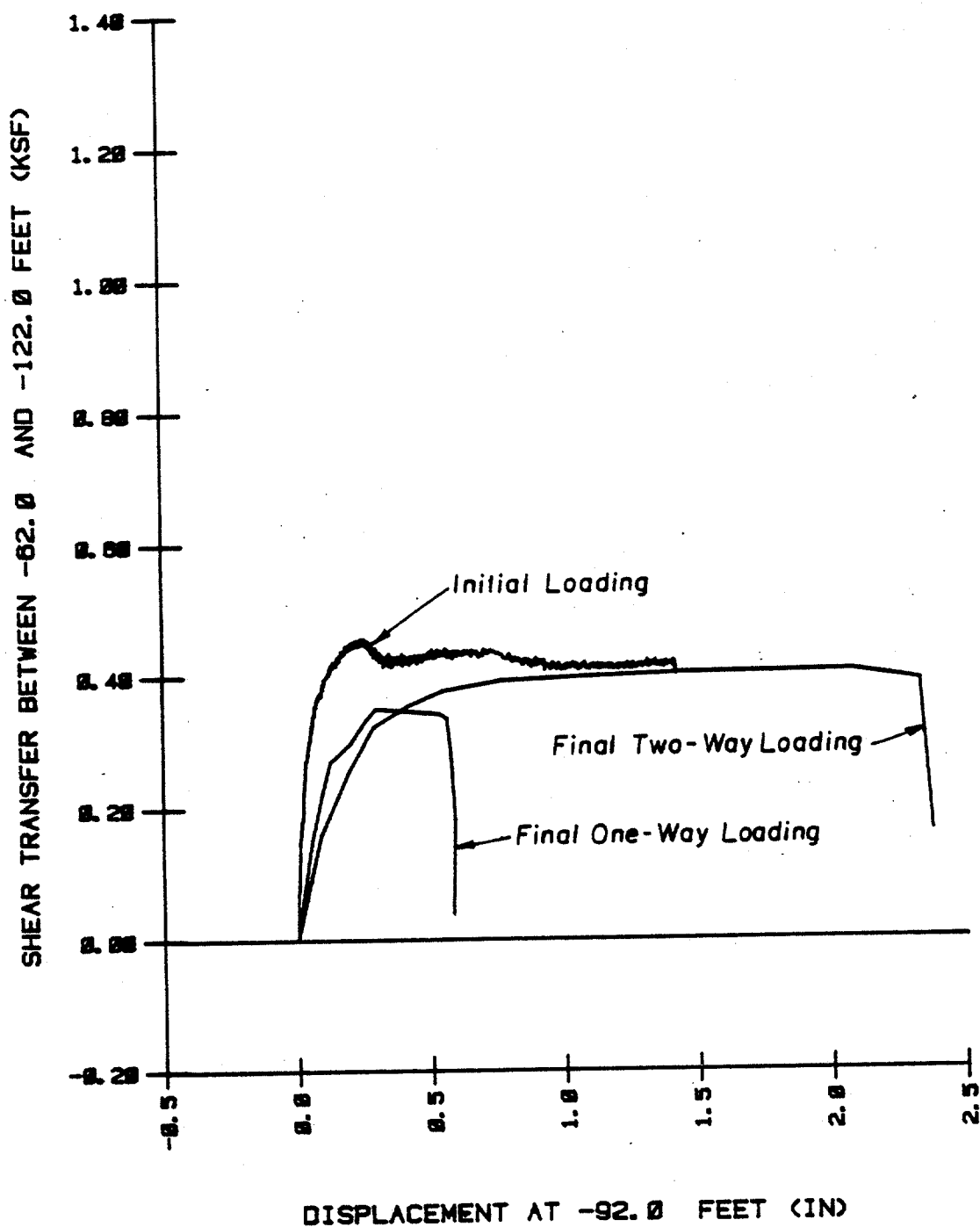
(1 inch = 25.4 mm, 1 ft = 0.305 m, 1 kip = 4.45 kN, 1 ksf = 47.9 kPa)



DISPLACEMENT AT -31.0 FEET (IN)

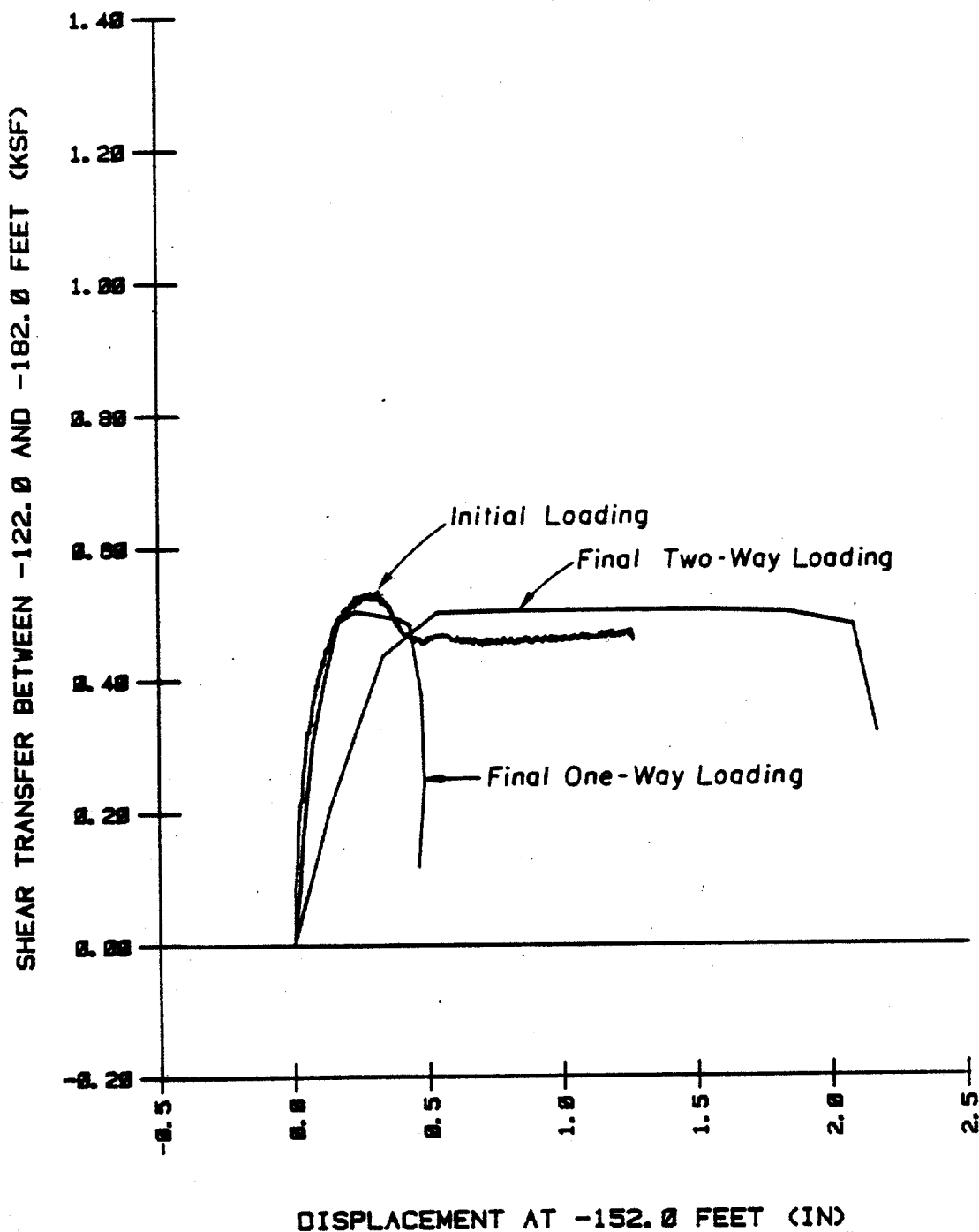
COMPARISON OF SHEAR TRANSFER VERSUS DISPLACEMENT BETWEEN
THE DEPTHS OF 0 AND 62 FEET - EXTENSOMETERS

(1 inch = 25.4 mm, 1 ft = 0.305 m, 1 kip = 4.45 kN, 1 ksf = 47.9 kPa)



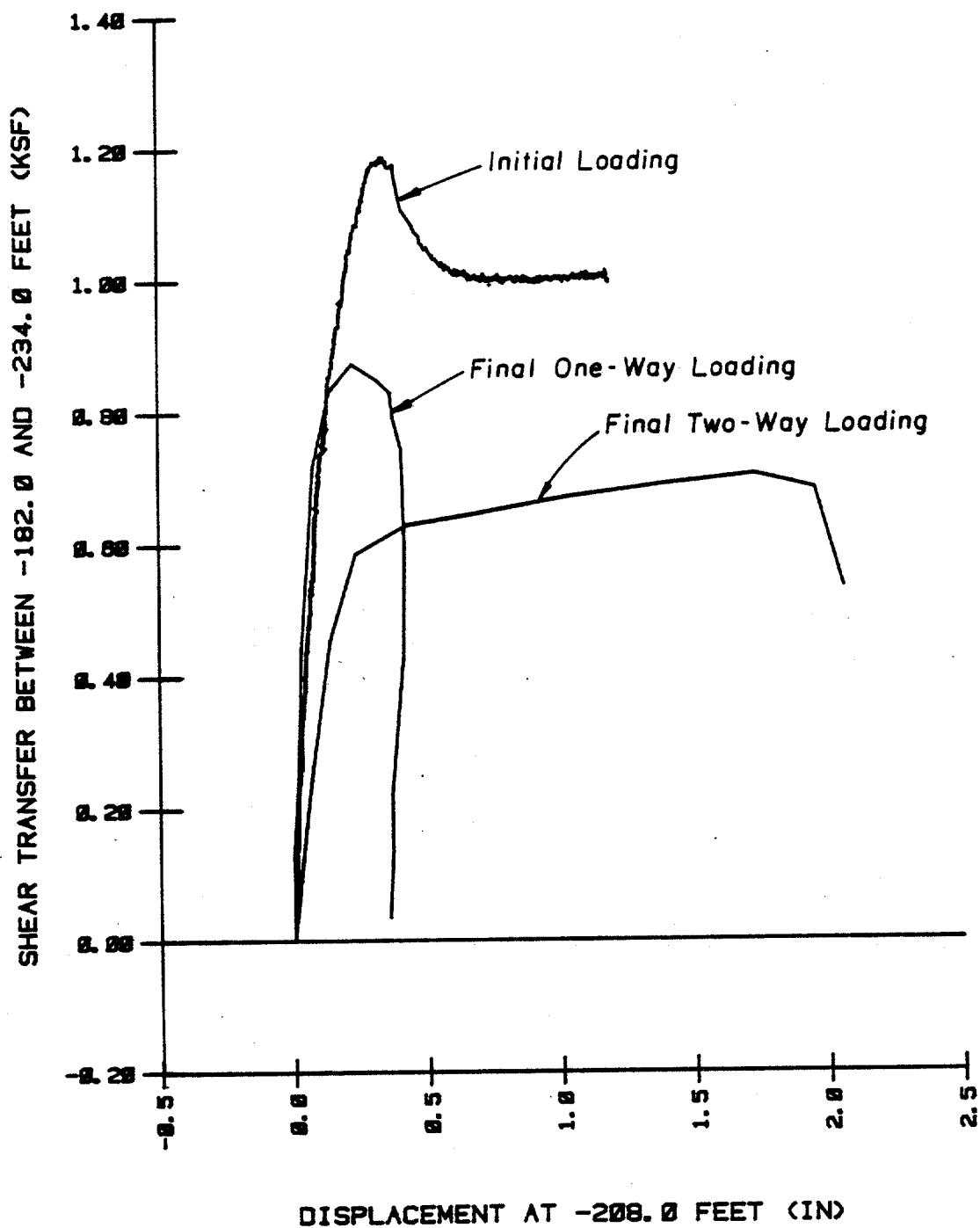
COMPARISON OF SHEAR TRANSFER VERSUS DISPLACEMENT BETWEEN
THE DEPTHS OF 62 AND 122 FEET - EXTENSOMETERS

(1 inch = 25.4 mm, 1 ft = 0.305 m, 1 kip = 4.45 kN, 1 ksf = 47.9 kPa)



COMPARISON OF SHEAR TRANSFER VERSUS DISPLACEMENT BETWEEN
THE DEPTHS OF 122 AND 182 FEET - EXTENSOMETERS

(1 inch = 25.4 mm, 1 ft = 0.305 m, 1 kip = 4.45 kN, 1 ksf = 47.9 kPa)

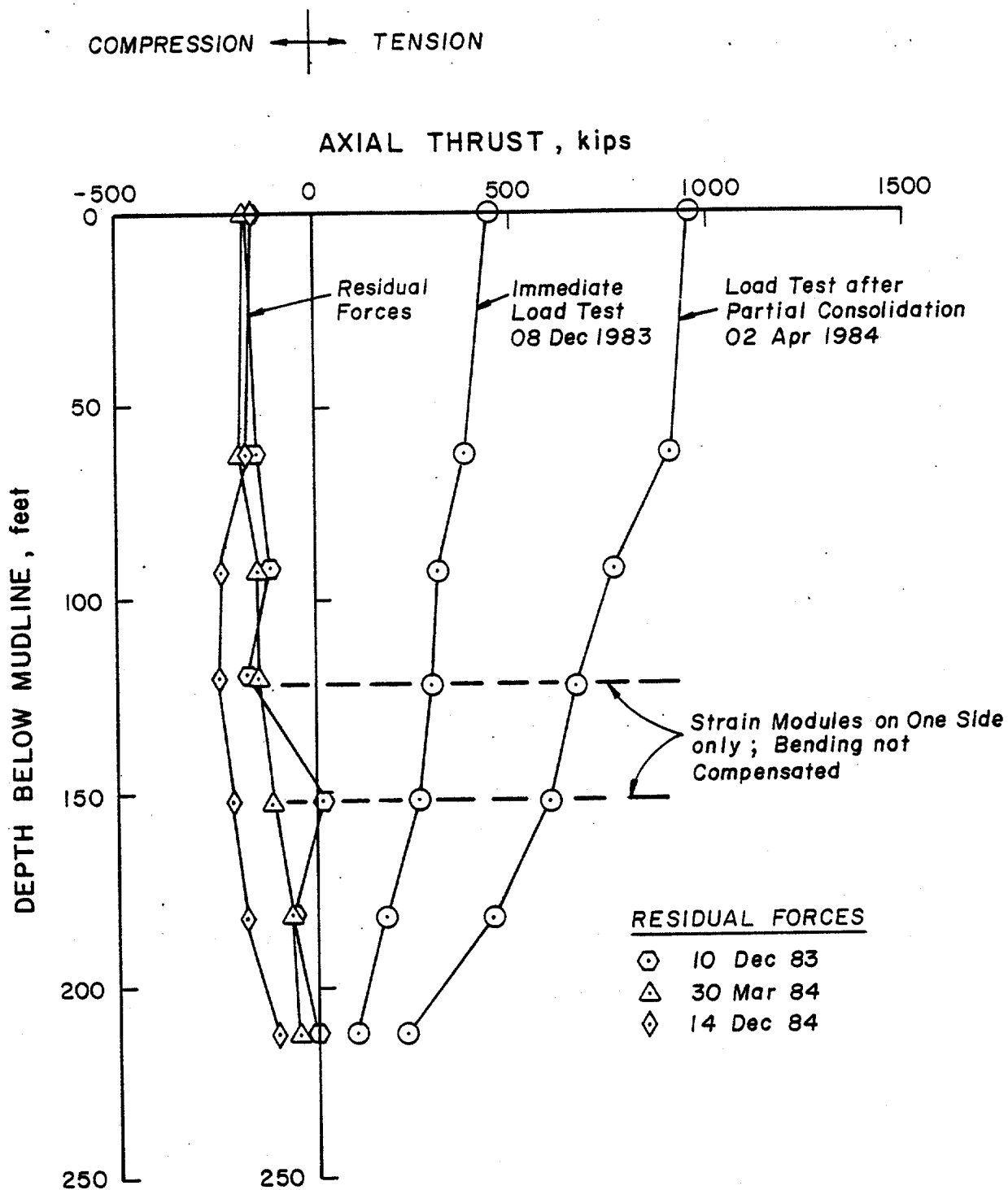


COMPARISON OF SHEAR TRANSFER VERSUS DISPLACEMENT BETWEEN
THE DEPTHS OF 182 AND 234 FEET - EXTENSOMETERS

(1 inch = 25.4 mm, 1 ft = 0.305 m, 1 kip = 4.45 kN, 1 ksf = 47.9 kPa)

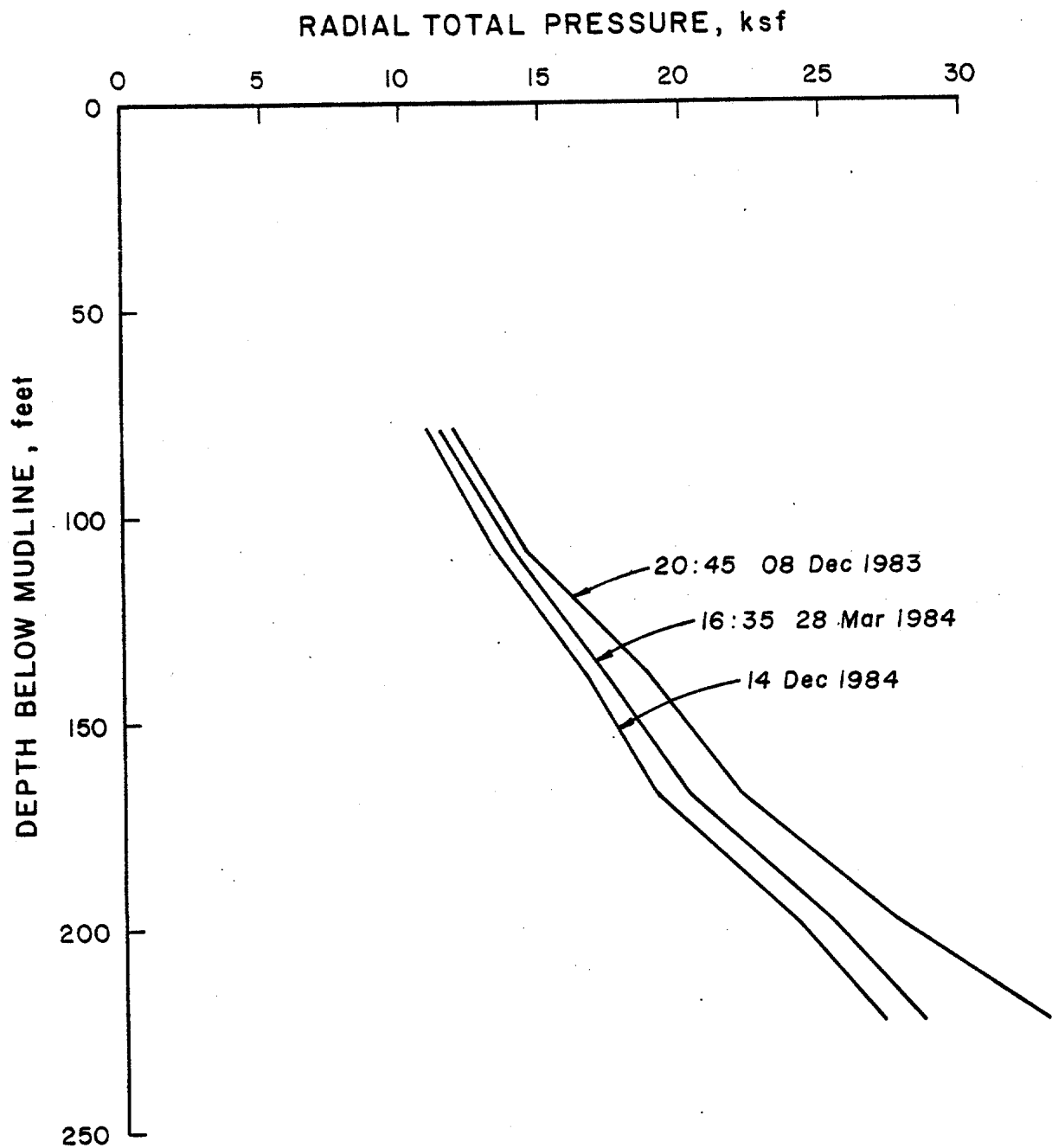
APPENDIX 6

ILLUSTRATIONS FOR CHAPTER 6



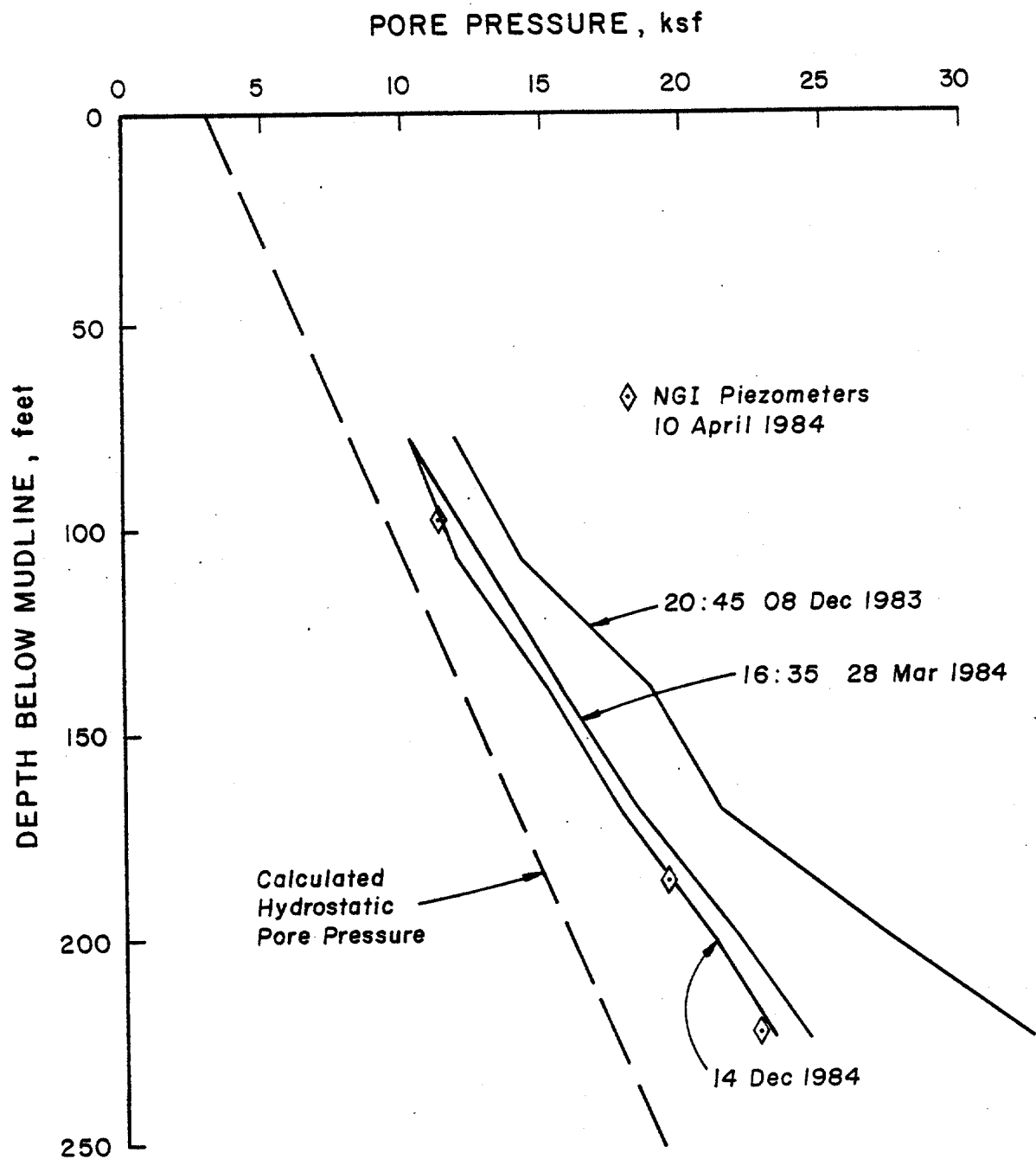
COMPARISON OF MEASURED LOAD DISTRIBUTIONS IN THE PILE - STRAIN MODULES

(1 inch = 25.4 mm, 1 ft = 0.305 m, 1 kip = 4.45 kN, 1 ksf = 47.9 kPa)



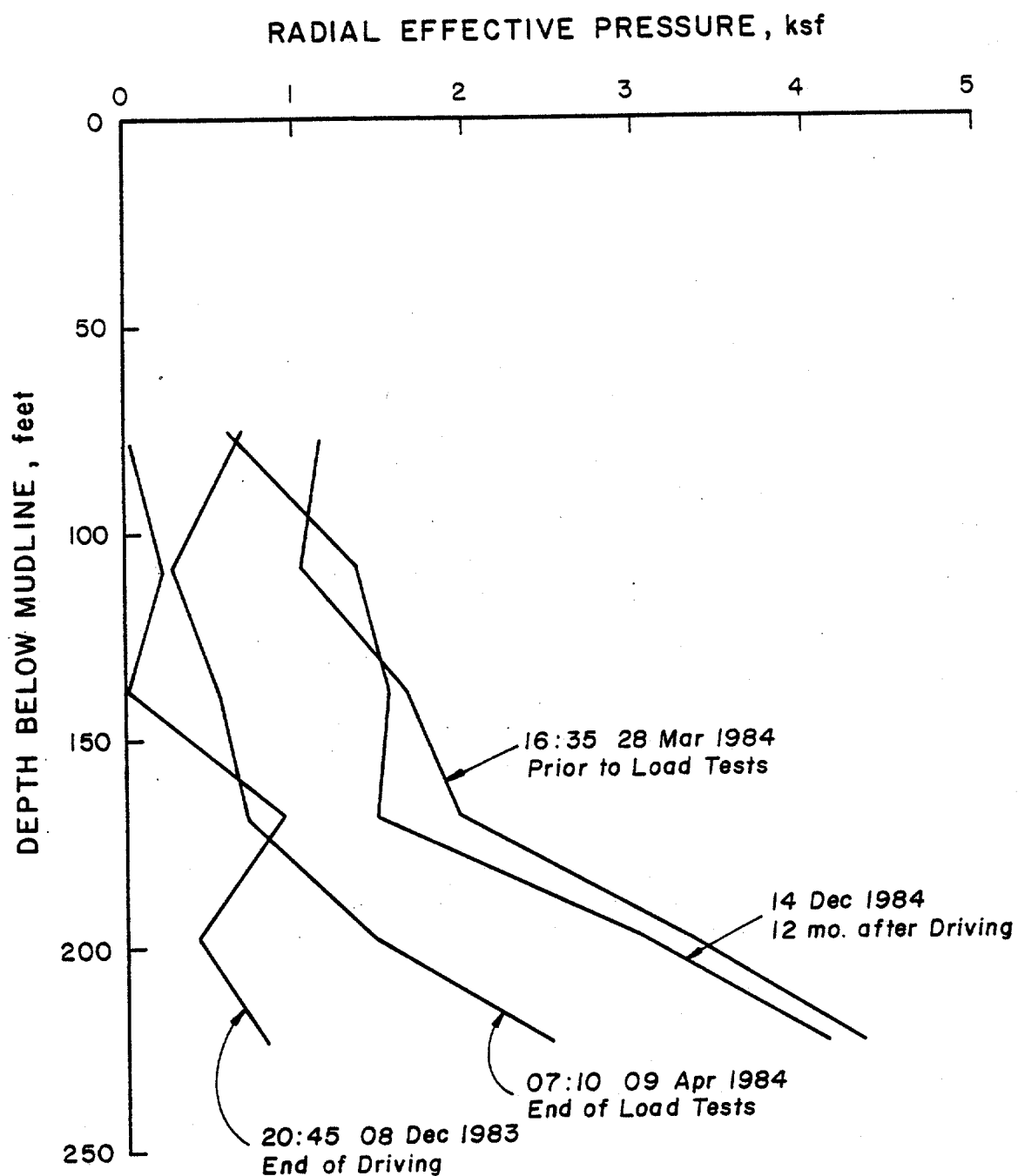
COMPARISON OF MEASURED TOTAL PRESSURE PROFILES

(1 inch = 25.4 mm, 1 ft = 0.305 m, 1 kip = 4.45 kN, 1 ksf = 47.9 kPa)



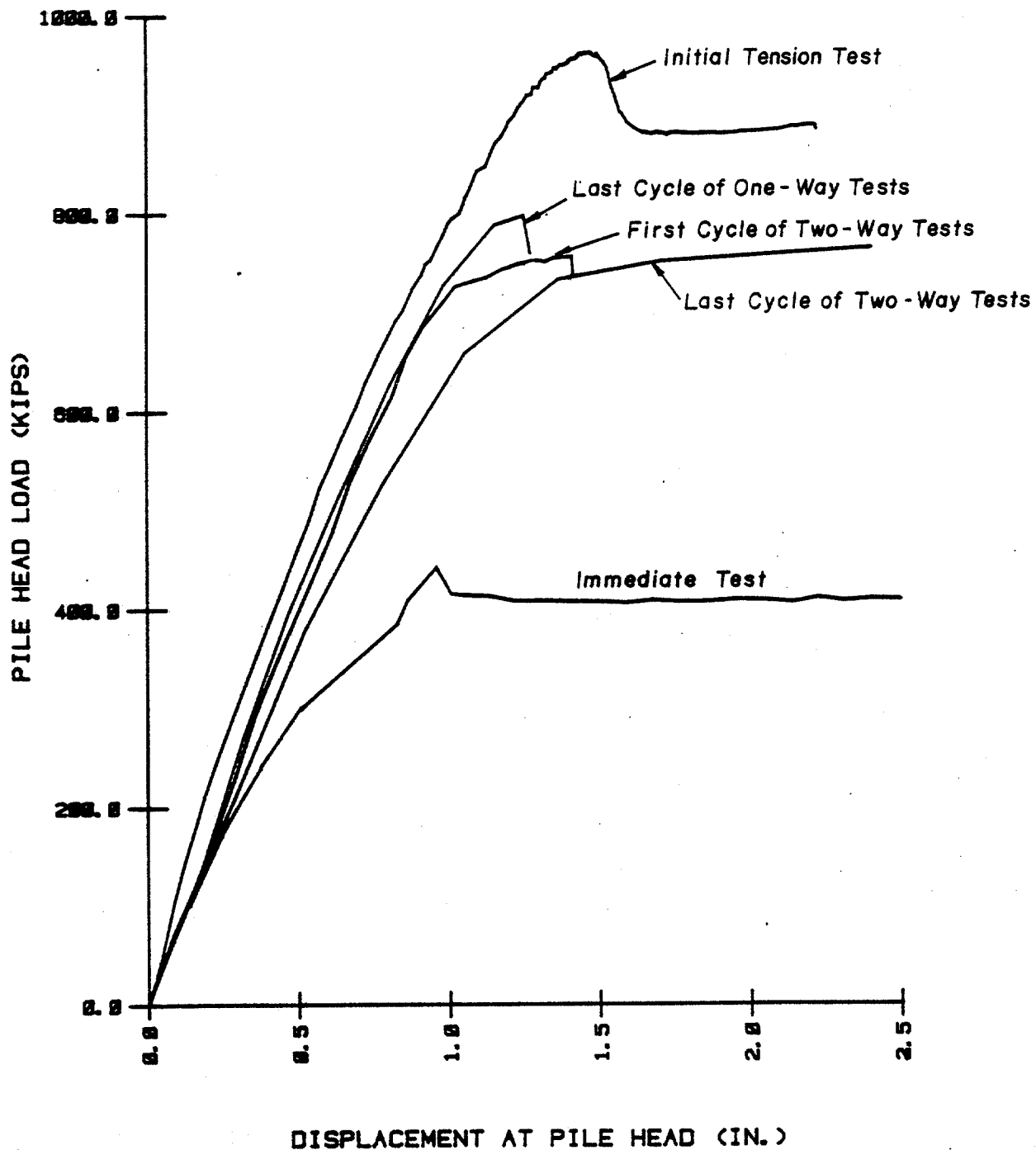
COMPARISON OF MEASURED PORE PRESSURE PROFILES

(1 inch = 25.4 mm, 1 ft = 0.305 m, 1 kip = 4.45 kN, 1 ksf = 47.9 kPa)



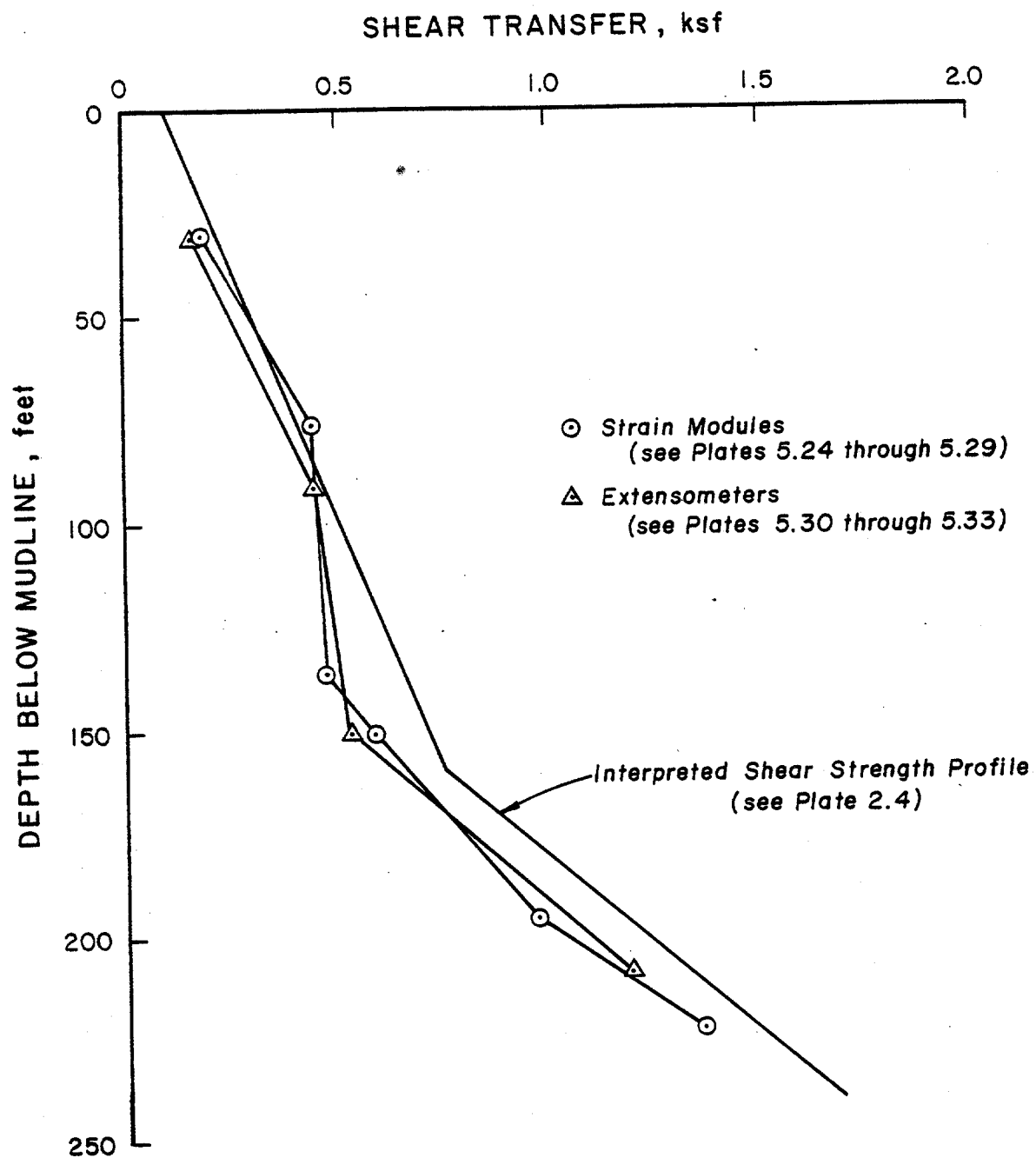
COMPARISON OF CALCULATED RADIAL EFFECTIVE PRESSURE PROFILES

(1 inch = 25.4 mm, 1 ft = 0.305 m, 1 kip = 4.45 kN, 1 ksf = 47.9 kPa)



COMPARISON OF PILE HEAD LOAD - DISPLACEMENT BEHAVIOR

(1 inch = 25.4 mm, 1 ft = 0.305 m, 1 kip = 4.45 kN, 1 ksf = 47.9 kPa)



PEAK SHEAR TRANSFER DEVELOPED ALONG PILE DURING THE STATIC TENSION TEST

(1 inch = 25.4 mm, 1 ft = 0.305 m, 1 kip = 4.45 kN, 1 ksf = 47.9 kPa)

APPENDIX 7

DYNAMIC PILE MEASUREMENTS

TESTING AND ANALYSIS

PILE DRIVING SYSTEMS • DYNAMICS • STRUCTURES

**Dynamic Pile Tests
Performed December 1983**

**WEST DELTA 58A PLATFORM
GULF OF MEXICO**

May 1984

GOBLE & ASSOCIATES, INC • PILE DYNAMICS, INC.

4423 EMERY INDUSTRIAL PARKWAY • WARRENSVILLE HEIGHTS, OHIO 44128

PHONE 216-831-6131 • TELEX 985-662

Dynamic Pile Tests

Performed
December 1983

at the

West Delta 58A Platform
Gulf of Mexico

Submitted to

The Earth Technology Corporation
Houston, Texas

by

Pile Dynamics, Inc.
4423 Emery Industrial Parkway
Warrensville Heights, Ohio 44128

May 1984

PILE DYNAMICS, INC.

TABLE OF CONTENTS

	<u>Page</u>
INTRODUCTION	1
TEST DETAILS	1
Hammer	1
Pile	1
Soil	2
TEST PROCEDURE	2
RESULTS	4
Hammer Performance	4
Stresses	6
Capacity	7
CONCLUSIONS	9
TABLE 1: DRIVING SUMMARY FOR TP2	10
TABLE 2: DRIVING SUMMARY FOR TP3	11
TABLE 3: CAPWAP SUMMARY	12
FIGURE 1: PLOTS OF BLOW COUNT, MAXIMUM ENERGY AND MAXIMUM FORCE VS DEPTH OBTAINED DURING DRIVING	13
FIGURE 2: PLOTS OF UNIT SKIN FRICTION VS DEPTH OBTAINED FROM CAPWAP/C	14
FIGURE 3: STATIC TEST SIMULATIONS	15
APPENDIX A: DESCRIPTION OF METHODS	
APPENDIX B: RESULTS FROM CAPWAP/C	
APPENDIX C: PLOTS OF FORCE AND VELOCITY	

INTRODUCTION

This report was written at the request of Mr. Wei Chou Ping of The Earth Technology Corporation, Houston, Texas. It covers the dynamic pile testing using the Pile Driving Analyzer system for the tension test pile driven at the West Delta 58A platform in December 1983.

TEST DETAILS

Hammer

The hammer used for these tests was a Delmag D30-13, an open end diesel hammer with a ram weight, $W = 6.6$ kips. This hammer is best rated on its developed potential energy Wh ; the stroke h can be calculated from the blows per minute (BPM) of the hammer from the equation

$$h[\text{ft}] = 4(60/\text{BPM})^2 - 0.3$$

The D30-13 hammer has a four step adjustable fuel pump; the stroke is dependent upon both this fuel setting and the pile size and soil resistance. In general, the first add-on, TP2, was driven with setting 2 while the last section, TP3, was driven using the highest setting (HS 4). The capblock consisted of a 22 inch diameter oak block with a thickness of 6 inches.

Pile

The pile was an open end 30 inch diameter pipe with a wall thickness of $3/4$ inch. The basic cross section area was 68.9 in^2 (impedance $EA/c = 123 \text{ k-s/ft}$; the elastic modulus, E , was 30000 ksi and the wave speed, c , was 16800 ft/s). The first section was 180 feet long and was instrumented by The Earth Technology Corporation with strain modules, pore and total pressure cells, and extensometers. Each of the next two sections was 90 feet

long; the top section had an extensive mass for static test application at a location 7 to 10 feet below the top.

The Earth Technology's instrumentation was protected by a series of angles and tubes which increased the cross sectional area. In the bottom section the protective angles were attached to the interior of the pile. At a location approximately 160 to 170 feet above the pile tip, the cables were passed from the inside to the outside, and extra channels were required. To facilitate the protection on the two add-on sections, the channels for cable protection were welded in place on the exterior of the pile after the splice was made and the cables positioned. The extensometer tubes continued to the top on the inside of the pile. Because of the extra tubes and channels which were not continuously welded, care must be taken when converting strain measurements to force. The impedance of the pile along the length (assumed for the tests reported in this report) can be found in Appendix B.

Soil

The soils at the test site consisted of soft clays. Although beyond the scope of this report, it may be mentioned that the clays in the lowest stratum were somewhat stiffer than those closer to the mudline. The mudline was 50 feet below the water surface and 110 feet below the depth reference point (floor of the load platform).

TEST PROCEDURE

Two strain transducers and two accelerometers were attached on opposite sides (to cancel bending effects) of the pile near the top. The transducers were reusable and attached by bolts. The transducers were connected into a single cable which was then input to a Pile Driving Analyzer (PDA).

The PDA, a model GB manufactured by Pile Dynamics, Inc., had separate

signal conditioning for each transducer. The PDA converts the conditioned and calibrated signals to digital form with an analog to digital converter (A/D) for use by its M68000 microprocessor. The PDA then computed the energy transferred to the pile (ENTHRU), maximum forces and velocities, and the driving resistance from the Case-Goble Method; a result was obtained and printed for each hammer blow in real time as the pile was driven. The analog force and velocity signals were stored on FM tape for further analysis. An oscilloscope was used for data quality inspection and pile damage detection.

The first add-on section TP2 was driven on December 6. Following a two day wait due to splicing, welding the protective channels for The Earth Technology's instrumentation, and a delay due to bad weather, the last add-on section TP3 was installed on December 8, finishing at 9:10 pm. After quick attachment of the hydraulic jacks, a tension test was begun at 11:23 pm and continued until 12:26 am on December 9; load increments of 100 psi were applied and instrumentation read before proceeding to the next load increment. After a plunging failure, the load was released in increments ending at 12:26 am. At 1:01 am, a compression test was started which followed the same procedure, ending at 1:31 am. Further description of the static test results is beyond the scope of this report. After removal of the static testing equipment, the pile was again tested dynamically by a restrike beginning at 3:05 am.

The tape recorded signals were returned to the laboratory where they were again input to the PDA. The digitized force and velocity records were then output from the PDA via a RS232 interface to a minicomputer for further analysis by the CAPWAP/C procedure. Four blows were selected; one each from the end of TP2, the beginning of TP3, the end of driving of TP3, and the restrike of TP3 after the load tests.

CAPWAP/C is a procedure which uses the measured velocity data, pile model (impedance vs length), and assumed soil parameters to compute the pile force (or force can be input to compute the velocity curve). By iteratively adjusting the assumed soil parameters and comparing the computed and measured force curves until a "best match" is obtained, a soil model is

obtained which includes static capacity and its distribution, damping parameters and soil quakes. Finally, a static analysis using the pile model and derived soil model results in a load displacement curve as obtained in a static load test.

RESULTS

A summary of the results obtained during driving is given for TP2 in Table 1, and for TP3 in Table 2. These summaries list average values of various quantities for approximately every five feet of driving since conditions were rather uniform. These quantities are: blows per foot, blows per minute for computation of stroke and potential energy Wh), maximum transferred energy, maximum force, and total soil resistance RT (sum of static and damping resistance). The static capacity can be obtained from the equation

$$RS = RT - J(2F - RT)$$

where F can be approximated by the maximum force and J is a dimensionless damping constant, often found by experience to be about 0.3 for soils in the Gulf of Mexico. Additional information on the methods employed during both field testing and laboratory analysis of this project may be found in Appendix A.

Results of the CAPWAP/C analysis were compiled in Appendix B. Summarized results for each blow were listed in Table 3. Plots of force and velocity (dashed) as obtained from digitizing are shown in Appendix C.

Hammer Performance

At the beginning of TP2 for hammer setting 1 (HS 1) and easy driving, the blow rate averaged 54 blows per minute. This rate corresponds to a stroke of 4.6 feet and a maximum available (Wh) energy of 30.6 kip feet. Since

the actual transferred energy was typically only 4.8 kip-ft, transfer ratios (ENTHRU/Wh) were a very poor 15%. For HS 2 and TP2, the typical blow rate was 44 blows per minute. This rate corresponds to a stroke of 7.1 feet and a Wh of 47.1 kip-ft; since the transferred energy was about 8 kip-feet, the transfer ratio was again low at 17 percent.

TP3 was driven with the hammer in the HS 4 position. The blow rate (41 BPM) was practically constant for the entire section. This blow rate corresponds to a stroke of 8.3 feet and a potential energy of 54.6 kip-ft. The transferred energy revealed interesting information. ENTHRU was at first approximately 13 kip-ft (24% of 55 kip-ft) and declined steadily to only 9 kip-ft (16%) at a depth of 287 feet, 1700 blows later. This suggests that the hammer began to preignite as it became warmer; the gasses combust earlier before impact causing extra energy to be used in compressing the now higher pressure gasses prior to impact. This energy is therefore not available to be transferred to the pile, resulting in still lower transfer energy as the problem becomes worse.

Preignition does not fully explain the poor hammer transfer. The soft oak cushion also absorbed a significant amount of energy compared with other capblock materials (for example, aluminum/micarta, conbest, Force 10, etc.). This soft capblock was beneficial in reducing potentially harmful (to The Earth Technology's instrumentation) accelerations. Typical accelerations for TP2 at HS 2 were 60 to 70 g's, while for HS 4 on TP3 they were 70 to 90 g's at the beginning and only 50 to 60 g's just prior to the 287 foot mark when preignition caused further softening of the impact.

After a short break at 287 feet to read The Earth Technology's instruments, driving continued. The initial, slightly decreased blow count is explained by an improvement in the energy transfer (cooler hammer). However, continuation of driving resulted in the burning of the oak capblock at the 300 foot mark. After this time, the capblock became stiffer and apparently absorbed less energy, resulting in a gradual increase in transferred energy. By comparison, accelerations at the end of TP3 and 5200 blows were 200 g's. After a second break at 317 feet, the performance again improved (16 kip-feet or 29 percent) due to hammer cooling during the break. After

the 6 hour break for static testing, the hammer performed at an average of 17 kip-feet or 31 percent transfer ratio, compared to 15 kip-feet and 27 percent at the end of driving. That preignition was a contributing factor to poor energy transfer may be observed in the slow build up of force prior to impact (see for instance the force plots in Appendix B). At the end of driving, this force was higher than at the beginning of TP3 or during restrike.

Thus, while preignition continued to caused a problem and gradual degradation of hammer performance, the change in capblock properties from soft to hard as the oak burned more than compensated for this preignition loss and actually resulted in a better energy transferred to the pile at the very end of driving.

Stresses

Pile forces were never larger than 1020 kips. With an assumed area of 78 in², this represents a stress of only 13 ksi. The low stress level is associated with a soft cushion, a large helmet (which further filters the peak forces due its inertia), and preignition. In fact, during TP3 it was observed that stress changes were similar to the energy transfer changes. At the beginning of driving, peak forces decrease as preignition increases, while later the forces gradually increase as the oak capblock burns and becomes stiffer. Figure 1 shows a summary of the pile installation observations.

The CAPWAP/C analysis tracks the force wave through the pile as a function of both time and length along the pile. The figures in Appendix B show the forces calculated for the top, middle and bottom of TP1 for each of the analyzed blows. The tables show the forces in selected segments for some blows.

Capacity

For long offshore piles, static capacity from dynamic tests is usually determined by CAPWAP or CAPWAP/C (CAPWAP/C is the program version preferred for long piles). This is even more the case when the pile is nonuniform, as in the present case due to varying protective channels and instrumentation tubes. However, the simplified Case-Goble Method as used in the PDA, are often "calibrated" by comparison with CAPWAP/C to obtain the correct damping factor. It may then be applied to many blows with little computational effort. Although not often available for offshore piles, the same back calculation of the Case damping constant could be made from comparison with the load test failure load (a common technique for land piles). The previous equation can be solved for J as

$$J = (RT - RS)/(2F - RT)$$

where RS is the ultimate load as defined by either CAPWAP/C or the load test. It often helps to allow a reasonable tolerance in the failure load (different failure definitions give different ultimate loads), leading to a range of acceptable J values. It should be emphasized that the resistance values given in Tables 1 and 2 are not the static capacity but rather the total driving resistance (static plus dynamic).

Results for each blow analyzed by CAPWAP/C are given in Appendix B and contain

- (a) the force and velocity records of the analyzed blow,
- (b) the force and velocity matches (using the respective complement quantity as input),
- (c) a graphic summary of resistance per element (each soil element is approximately 10 feet),
- (d) the sum of these values (force in the pile at ultimate load vs length below the pile top),

(e) a static load test simulation.

The reader is encouraged to review the entire contents of this appendix.

The summary in Table 3 shows that the static capacity for TP2 EOD (end of drive) was 144 kips. This resistance acted primarily on the skin and was almost uniformly distributed. The skin Smith damping parameter of 0.29 s/ft is high, but it must be recognized that the total damping (Case definition) is low; the Smith definition takes the total damping divided by the total static. The toe capacity and toe damping are both very small, even though the Smith damping constant for the toe is large; a drastic reduction in this value would cause only a small change in the force match due to the very low static resistance. The accuracy of the Smith parameters only becomes of importance when the element static resistance becomes large, generally at high blow counts. The soil quakes were found to be 0.05 and 0.07 inches for the skin and toe, respectively, although the value for the toe is not very sensitive due to the resistance and the same arguments as for the toe damping factors.

For TP3 BOD (beginning of drive) after the two day wait, the total capacity increased to 195 kips and was distributed again relatively uniformly over the skin. Skin damping was 0.27 s/ft (Smith value) and skin quake was 0.06 inches. As for TP2 EOD, the toe resistance values are not at all critical in the CAPWAP matching due to the low toe static resistance.

The CAPWAP/C analysis indicated the following for the end of drive of TP3. The total capacity had increased to 579 kips. The resistance was about 1.2 kips/foot (12 kips/element) for the upper approximately 90 feet of penetration and then increased rather uniformly in the lower half of penetration to a peak of 4.1 kips/foot (0.5 ksf) unit friction resistance based on the 30 inch diameter) at 40 feet above the tip. The Smith damping factors were 0.18 and 0.12 s/ft for the skin and toe, respectively. The soil quakes were 0.06 inches at the skin and 0.15 at the toe. The toe static resistance was about 50 kips.

The tension load test was begun about two hours later and may have included

some minor effects due to soil setup during that time. The compression test which immediately followed the tension load, failed at a lower ultimate resistance than the tension test load. This was possibly due to soil remolding by the pull out test.

The restrike which followed 1.5 hours later showed a CAPWAP capacity of 600 kips with 550 kips on the skin. Again, the distribution was 1.1 kips/foot (0.15 ksf) in the upper soil layers and increased to at most 5.2 kips/foot near the tip. Damping constants and quakes were similar to those obtained at the end of driving.

CONCLUSIONS

Figure 1 contains a summary of the driving parameters from the PDA and blow count records. The resistance distribution information is plotted in Figure 2 as skin friction per unit pile length for all blows analyzed. The static test simulations are summarized in Figure 3. The results indicate that the hammer performance was not very good due to both a soft cushion and also preignition. Pile stresses were low. The ultimate static capacity, as determined by the dynamic tests presented here, was approximately 600 kips; this result is representative of the time of testing and does not include significant setup effects, which over a long period of time could result in a higher capacity. Restrike testing after a long period would allow these methods to apply to the service conditions.

Table 1: Driving Summary for TP2

Depth	Bl/Ft	Bl/Min	EMX	FMX	RT(J=0)	Remarks
165	--	56	4.0	600	---	HS 1
175	--	54	3.8	600	---	----
185	9	55	4.0	600	180	----
190	12	54	4.2	610	220	----
195	16	55	4.6	640	220	----
200	17	54	4.8	640	240	----
205	22	53	4.8	650	260	----
210	15	46	8.4	820	300	HS 2
215	18	46	8.0	740	300	----
220	19	44	8.0	680	300	----
225	21	45	7.8	620	280	----
229	39	51	4.0	500	290	HS 1
230	24	44	7.9	650	310	HS 2
235	29	44	7.0	540	260	----
240	29	44	8.0	600	320	----
245	31	43.7	8.6	670	360	----
248	34	44	8.0	700	420	----
250	36	44	8.4	750	480	----

1430 blows

Table 2: Driving Summary for TP3

Depth	Bl/Ft	Bl/Min	EMX	FMX	RT (J=0)	Remarks
---	--	48	7.6	600	600	First 2 Blows
250	--	53	5.0	480	460	HS 1
---	--	43.5	11.0	720	460	HS 2
---	--	41	12.5	800	500	HS 3
---	--	41	13.0	800	510	HS 4
255	32	NA	13.2	810	540	-----
260	38	41	12.0	780	490	BN 370
265	42	41	12.0	770	500	BN 566
270	45	41.5	11.0	720	470	BN 781
275	50	42	10.6	700	480	BN 1024
280	53	41.5	10.5	680	480	BN 1282
285	61	41.5	9.0	600	480	BN 1575
---	--	----	----	---	---	Break at 287
290	59	42	10.4	700	560	BN 1874
295	60	41.5	10.6	720	580	BN 2169
300	61	NA	11.0	760	640	BN 2468
305	70	41.5	10.6	770	650	BN 2793
310	63	41.5	12.0	880	760	BN 3124
315	62	41	13.2	940	800	BN 3438
---	--	----	----	---	---	Break at 317
320	57	40.5	16.0	1020	880	BN 3726
325	61	41	15.7	1000	870	BN 4021
330	70	NA	14.8	950	900	BN 4352
335	70	40.5	15.0	930	870	BN 4697
340	72	40	15.0	970	880	BN 5051
342	69	NA	15.0	950	890	BN 5204
BOR	84	NA	17.0	1020	1000	

Table 3: CAPWAP Summary

Data	Ultimate Capacity-kips		Case		Damping		Quakes	
	Skin	Toe Total	Skin	Toe	Smith	(s/ft)	Skin	Toe
TP2 EOD	131.6	12.5	.25	.025	.29	.32	.05	.07
TP3 BOD	190.3	4.2	.33	.01	.27	.40	.06	.10
TP3 EOD	527.5	51.4	.62	.04	.18	.12	.06	.15
TP3 Restrike	550.1	49.9	.65	.02	.18	.06	.06	.11

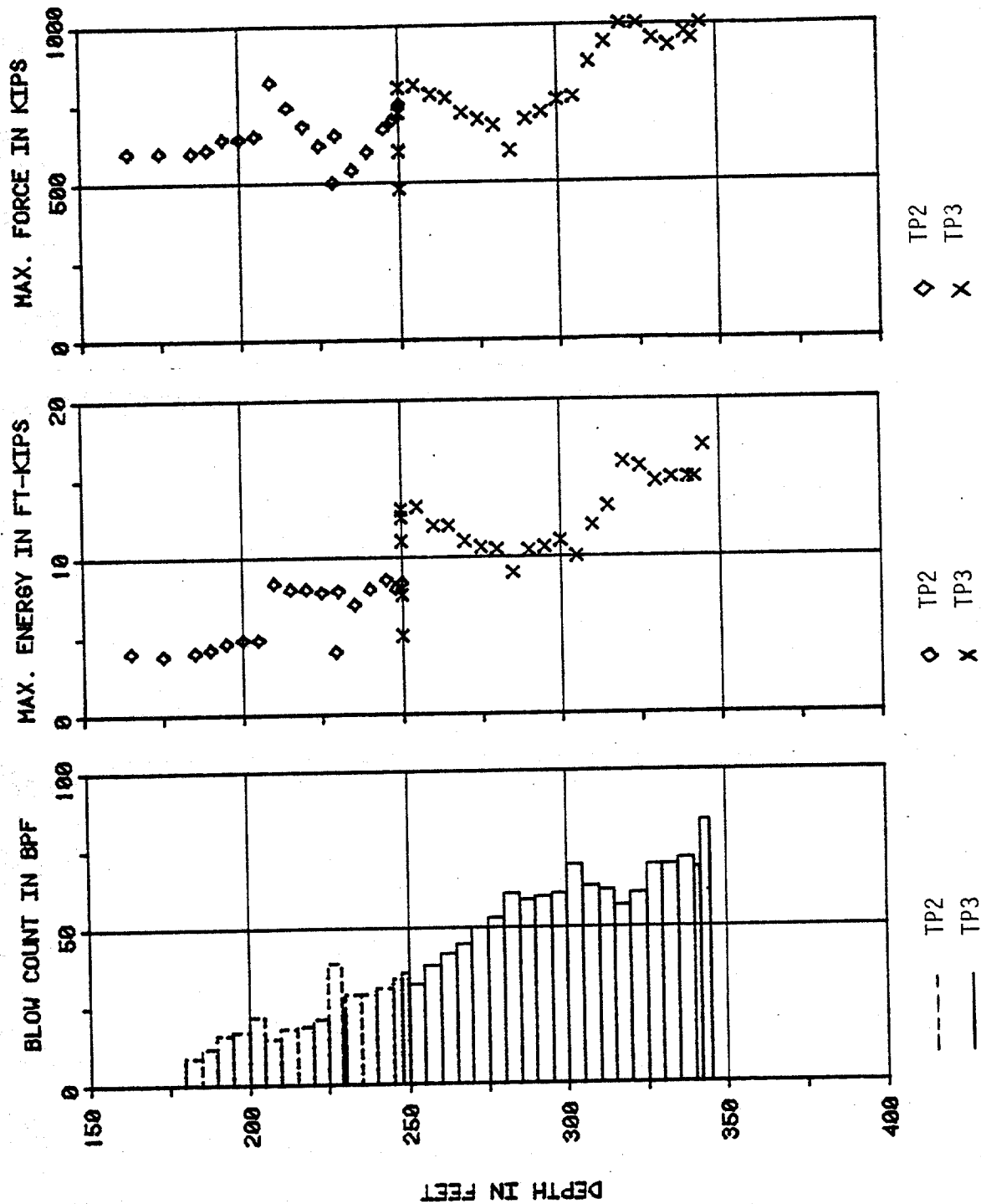


Figure 1: Plots of Blow Count, Maximum Energy and Maximum Force vs Depth Obtained During Driving

PILE DYNAMICS, INC.

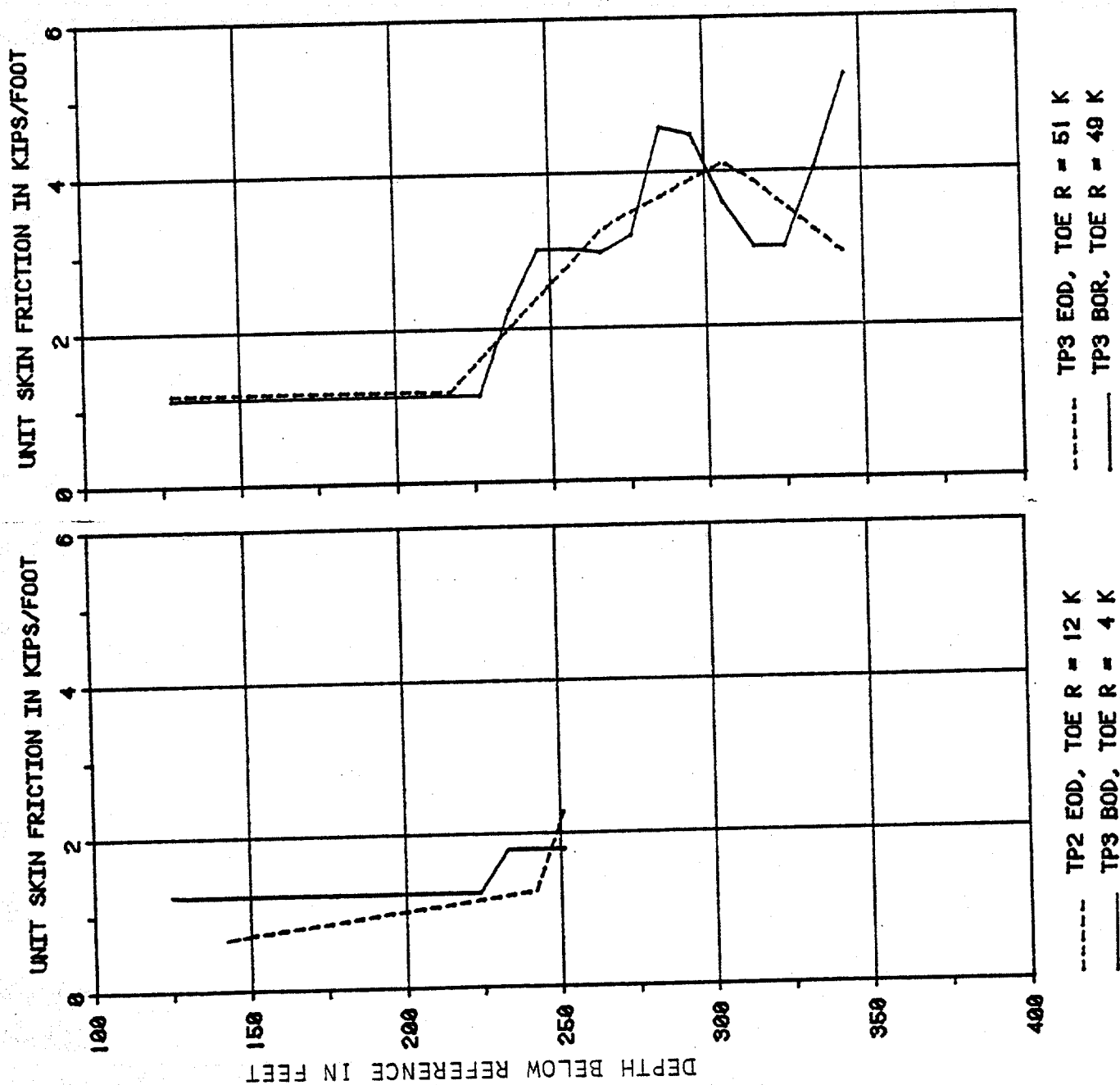


Figure 2: Plots of Unit Skin Friction vs Depth
obtained from CAPWAP/C

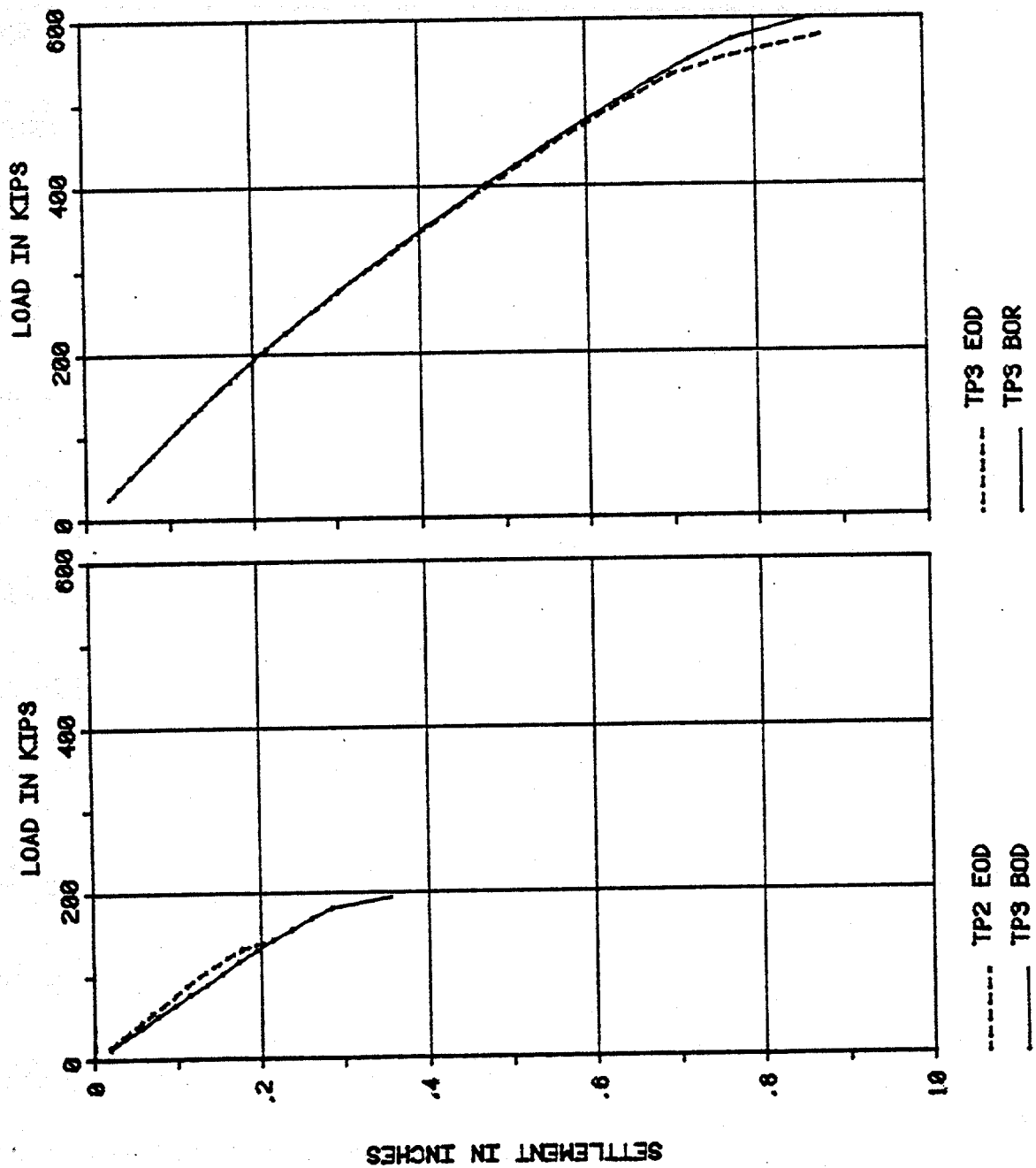


Figure 3: Static Test Simulations

APPENDIX B

RESULTS FROM CAPWAP/C

G & A
WD 58A, TP2, EDD

PROGRAMS: CAPWAP/C RESULTS

BLOW NO. 4 30-APR-84

IS	DEPTH FT	QUAKE IN	RES KIPS	SUM RES KIPS	VISC. J KIPS/F/S	IMPDNCE KIPS/F/S	T-SLACK IN	C-SLACK IN	IP
0	0.0	0.000	0.0	144.0					1
0	3.3	0.000	0.0	144.0	0.0	140.1	0.0000	0.0000	2
0	6.6	0.000	0.0	144.0	0.0	150.2	0.0000	0.0000	3
0	9.9	0.000	0.0	144.0	0.0	161.0	0.0000	0.0000	6
0	19.8	0.000	0.0	144.0	0.0	161.0	0.0000	0.0000	7
0	23.1	0.000	0.0	144.0	0.0	161.0	0.0000	0.0000	12
0	39.5	0.000	0.0	144.0	0.0	161.0	0.0000	0.0000	16
0	52.7	0.000	0.0	144.0	0.0	161.0	0.0000	0.0000	21
0	69.2	0.000	0.0	144.0	0.0	161.0	0.0000	0.0000	22
0	72.5	0.000	0.0	144.0	0.0	161.0	0.0000	0.0000	27
0	88.9	0.000	0.0	144.0	0.0	165.0	0.0000	0.0000	28
0	92.2	0.000	0.0	144.0	0.0	175.2	0.0000	0.0000	30
0	98.8	0.000	0.0	144.0	0.0	169.7	0.0000	0.0000	31
0	102.1	0.000	0.0	144.0	0.0	152.7	0.0000	0.0000	42
0	138.3	0.000	0.0	144.0	0.0	152.7	0.0000	0.0000	47
1	154.8	0.050	7.3	136.8	2.1	150.6	0.0000	0.0000	48
0	158.1	0.000	0.0	136.8	0.0	149.0	0.0000	0.0000	50
2	164.7	0.050	7.8	128.9	2.3	149.0	0.0000	0.0000	53
3	174.6	0.050	8.3	120.6	2.4	149.0	0.0000	0.0000	56
4	184.5	0.050	8.8	111.8	2.6	149.0	0.0000	0.0000	59
5	194.3	0.050	9.4	102.4	2.7	149.0	0.0000	0.0000	62
6	204.2	0.050	9.9	92.5	2.9	149.0	0.0000	0.0000	65
7	214.1	0.050	10.4	82.1	3.0	146.4	0.0000	0.0000	66
0	217.4	0.000	0.0	82.1	0.0	141.3	0.0000	0.0000	68
8	224.0	0.050	10.9	71.2	3.2	141.3	0.0000	0.0000	71
9	233.9	0.050	11.5	59.7	3.3	141.3	0.0000	0.0000	74
10	243.7	0.050	12.0	47.7	3.5	141.3	0.0000	0.0000	77
11	253.6	0.050	12.5	35.3	3.6	137.7	0.0000	0.0000	78
0	256.9	0.000	0.0	35.3	0.0	122.2	0.0000	0.0000	80
12	263.5	0.050	22.8	12.5	6.6	122.2	0.0000	0.0000	
PILE TOE		0.070	12.5		3.80				

RESISTANCE			CASE DAMPING		SMITH DAMPING		QUAKES	
SKIN	TOE	TOTAL	SKIN	TOE	SKIN	TOE	SKIN	TOE
KIPS	KIPS	KIPS			1/FT/S	1/FT/S	IN	IN
131.6	12.5	144.0	0.250	0.025	0.289	0.322	0.050	0.070
UNLOADING QUAKES IN PERCENT:							30	50

UNLOADING TO - 0.30 OF SU, ALPHA = 1.00

ENERGY		FORCES				DISPLACEMENTS	
MAX	FIN	MAX	I TMAX	MIN	I TMIN	TOP	TOE
FT-KIPS	FT-KIPS	KIPS	MS	KIPS	MS	IN	IN
9.1	8.8	790	23 25.	-407	10 51.	0.404	0.314

TIME INCR (MS) = 0.194

INT. PILE DAMPING (%) = 2.7

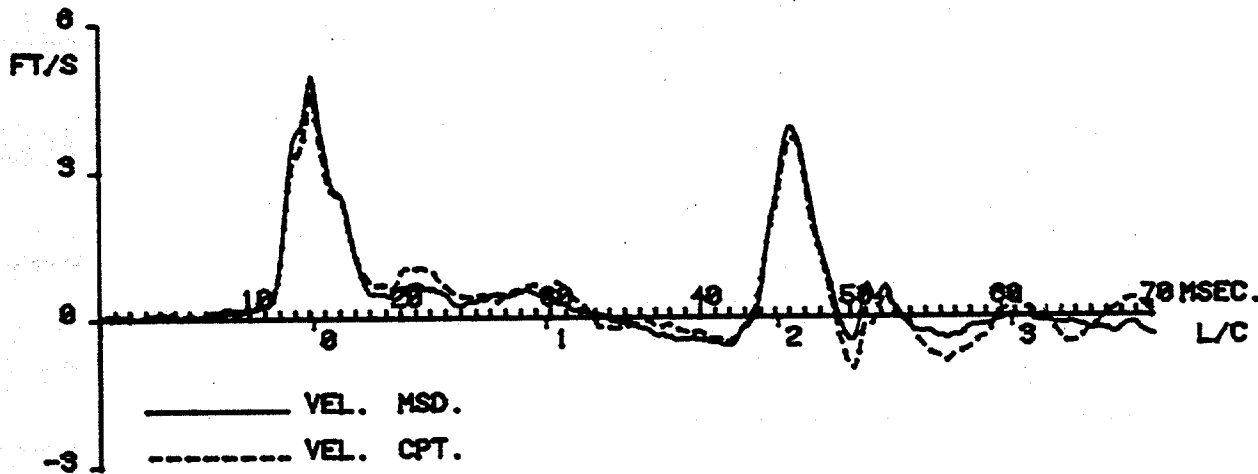
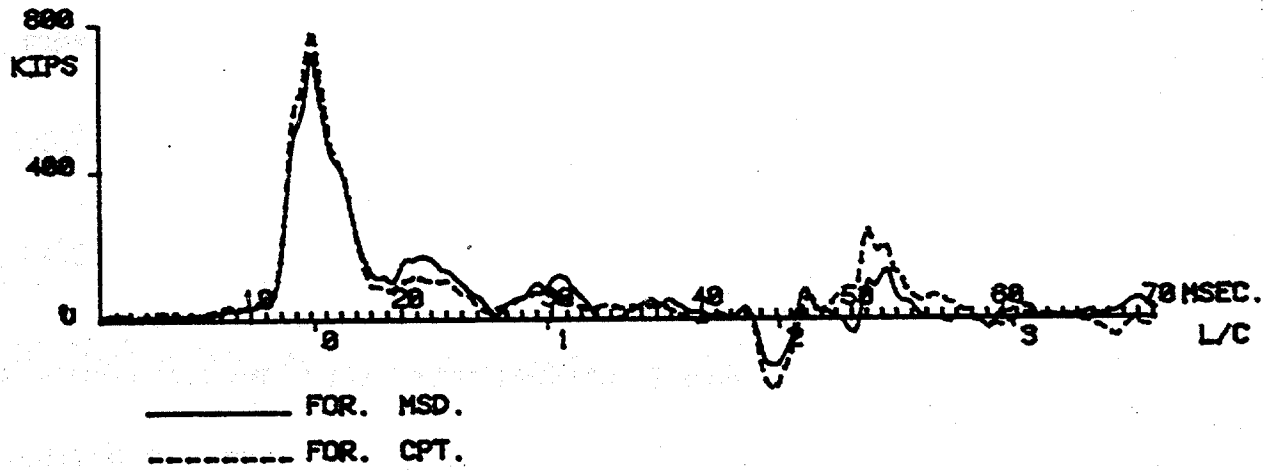
WD 58A, TP2, EDD
BLOW NO. 4

STATIC ANALYSIS

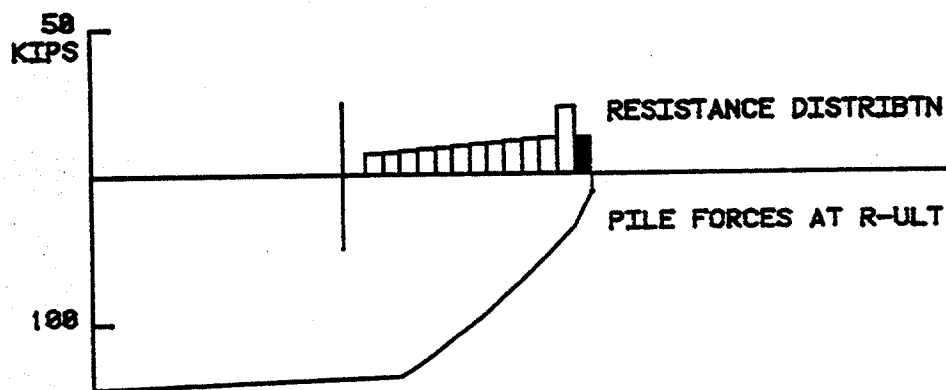
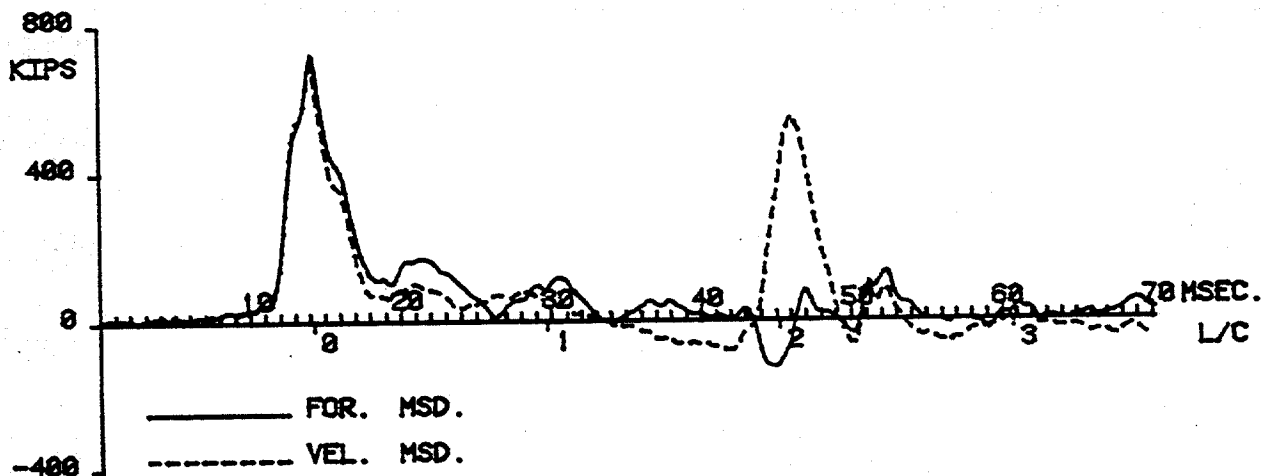
QAD(IN)= 0.000, EFAC= 1.000, CUT(FT)= 0.0

	LOAD	SET	BOT.	LOAD
	KIPS	IN		KIPS
1	0.0	0.000		0.0
2	11.4	0.014		0.6
3	22.8	0.028		1.1
4	34.1	0.043		1.7
5	45.5	0.057		2.2
6	55.5	0.069		2.7
7	66.9	0.084		3.3
8	78.2	0.098		3.8
9	89.6	0.112		4.4
10	99.8	0.125		4.9
11	110.9	0.141		5.6
12	122.6	0.159		6.3
13	133.3	0.177		7.6
14	144.0	0.217		12.5

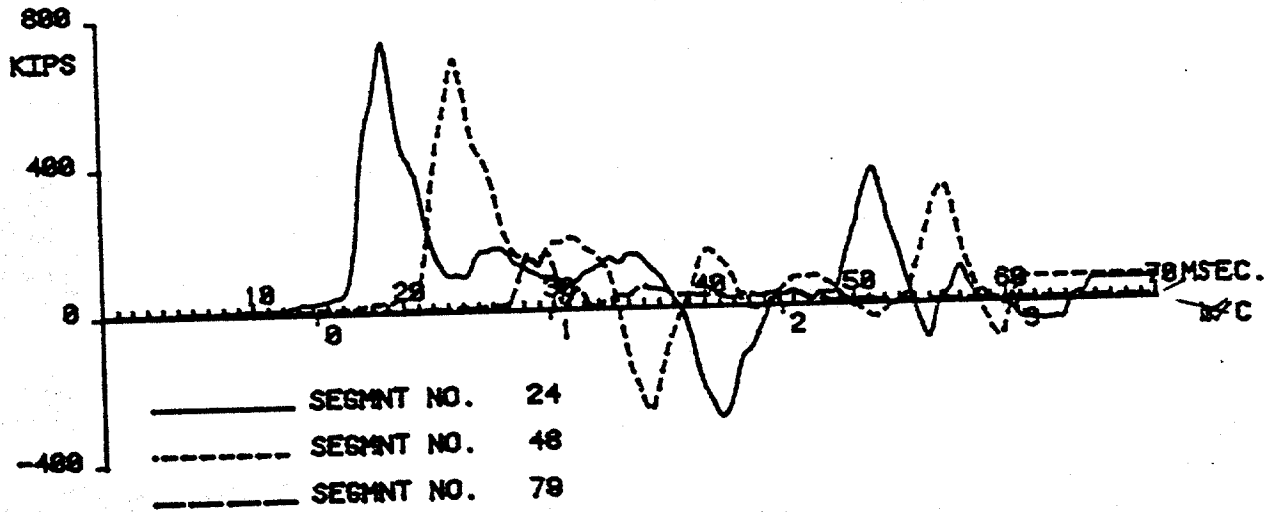
G & A PROGRAMS: CAPWAP/C RESULTS
 WD 58A, TP2, EOD
 BLOW NO. 4 30-APR-84



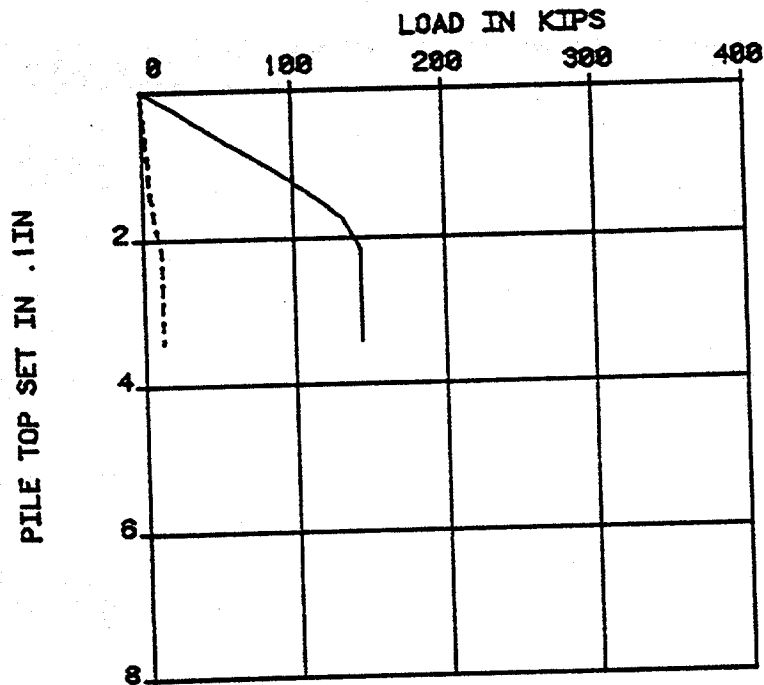
G & A PROGRAMS: CAPWAP/C RESULTS
 WD 58A, TP2, EOD
 BLOW NO. 4 30-APR-84



G & A PROGRAMS: CAPWAP/C RESULTS
WD 58A, TP2, EOD
BLOW NO. 4 30-APR-84



STATIC CAPWAP/C RESULTS
WD 58A, TP2, EOD
BLOW NO. 4
TOP LOAD BOTTOM LOAD



BLOW NO. 4 12-APR-84

RESISTANCE			CASE DAMPING	SMITH DAMPING		QUAKES	
SKIN	TOE	TOTAL	SKIN	TOE	SKIN	TOE	
KIPS	KIPS	KIPS			1/FT/S	1/FT/S	IN IN
190.3	4.2	194.5	0.330	0.010	0.267	0.404	0.060 0.100
UNLOADING QUAKES IN PERCENT:							25 100

ENERGY		FORCES					DISPLACEMENTS		
MAX	FIN	MAX	I	TMAX	MIN	I	TMIN	TOP	TOE
FT-KIPS	FT-KIPS	KIPS		MS	KIPS		MS	IN	IN
10.9	10.6	703	49	31.	-447	1	63.	0.294	0.369

INT. PILE DAMPING (%) = 2.0

WD 58A, TP3, BOD WITH 2 DAY WAIT								BLOW NO. 4				
TIME	FM	F/VC	VTP	DTP	FMD	VMD	DMD	FB	VB	DB	RS	RD
MS	KIPS		FT/S	IN	KIPS	FT/S		KIPS	FT/S	IN	KIPS	KIPS
13.4	9.5	0.0	0.00	0.00	9.5	0.00	0.00	9.5	0.00	0.00	0.0	0.0
14.3	11.2	0.0	-0.03	-0.00	9.5	0.00	0.00	9.5	0.00	0.00	0.0	0.0
15.3	6.7	-0.0	0.02	-0.00	9.5	0.00	0.00	9.5	0.00	0.00	0.0	0.0
16.3	13.4	0.0	0.00	-0.00	9.5	0.00	0.00	9.5	0.00	0.00	0.0	0.0
17.3	26.3	0.1	0.01	-0.00	9.5	0.00	0.00	9.5	0.00	0.00	0.0	0.0
18.3	25.2	0.1	0.08	0.00	9.5	0.00	0.00	9.5	0.00	0.00	0.0	0.0
19.3	150.7	1.0	0.62	0.00	9.5	0.00	0.00	9.5	0.00	0.00	0.0	0.0
20.2	455.0	3.1	2.61	0.02	9.5	0.00	0.00	9.5	0.00	0.00	0.0	0.0
21.2	687.5	4.5	4.39	0.06	9.5	0.00	0.00	9.5	0.00	0.00	0.0	0.0
22.2	683.0	4.2	4.18	0.11	9.5	0.00	0.00	9.5	0.00	0.00	0.0	0.0
23.2	578.8	3.4	3.28	0.16	9.5	0.00	0.00	9.5	0.00	0.00	0.0	0.0
24.2	442.1	2.5	2.26	0.19	9.2	-0.00	0.00	9.5	0.00	0.00	0.0	0.0
25.1	283.5	1.5	1.36	0.21	10.1	0.00	0.00	9.5	0.00	0.00	0.0	0.0
26.1	211.2	1.1	0.85	0.22	9.5	0.00	-0.00	9.5	0.00	0.00	0.0	0.0
27.1	217.4	1.3	0.89	0.23	16.1	0.04	0.00	9.5	0.00	0.00	-0.0	0.0
28.1	234.8	1.4	1.23	0.24	26.2	0.10	0.00	9.5	0.00	0.00	0.0	0.0
29.1	166.4	0.9	0.86	0.26	49.7	0.24	0.00	9.5	0.00	0.00	-0.0	0.0
30.1	119.9	0.6	0.64	0.26	295.4	1.66	0.01	9.5	0.00	0.00	0.0	0.2
31.0	89.6	0.5	0.22	0.27	599.7	3.56	0.04	9.5	0.00	0.00	0.4	0.8
32.0	90.2	0.5	0.36	0.27	685.4	4.30	0.09	9.5	0.00	0.00	1.3	2.2
33.0	95.2	0.5	0.46	0.28	628.5	4.09	0.14	9.5	0.00	0.00	5.3	11.0
34.0	90.2	0.5	0.35	0.28	492.8	3.29	0.19	9.5	0.00	0.00	19.1	29.6
35.0	100.3	0.6	0.33	0.29	343.5	2.32	0.22	9.5	0.00	0.00	38.1	51.6
36.0	55.5	0.3	0.08	0.29	186.3	1.24	0.24	9.5	-0.01	0.00	57.2	71.1
36.9	35.3	0.1	0.00	0.29	193.6	1.04	0.25	9.7	0.02	-0.00	75.7	85.4
37.9	63.9	0.4	0.10	0.29	282.1	1.43	0.27	10.4	0.11	0.00	95.6	94.3
38.9	49.9	0.2	0.07	0.29	246.2	1.19	0.28	11.1	0.14	0.00	115.0	98.1
39.9	40.3	0.1	0.01	0.29	158.2	0.59	0.29	15.9	0.72	0.01	136.9	106.1
40.9	72.8	0.3	0.01	0.29	132.9	0.28	0.30	40.2	3.57	0.03	166.6	127.7
41.8	57.7	0.2	-0.17	0.29	155.0	0.29	0.30	68.6	6.07	0.09	184.5	144.0
42.8	10.1	0.1	-0.16	0.29	151.3	0.19	0.30	69.9	6.20	0.16	185.0	141.7
43.8	-38.1	-0.1	-0.16	0.29	140.2	0.03	0.31	64.5	5.38	0.23	185.0	129.0
44.8	-39.8	-0.0	-0.23	0.29	153.8	0.06	0.31	54.6	3.84	0.29	185.0	111.0
45.8	-22.4	0.0	-0.08	0.28	156.6	0.11	0.31	43.7	2.12	0.32	185.0	92.2
46.8	3.4	0.0	-0.14	0.28	103.9	-0.21	0.31	34.0	0.55	0.33	184.9	76.4
47.7	40.3	0.0	-0.12	0.28	115.2	-0.21	0.30	34.1	0.54	0.34	185.0	70.9
48.7	33.6	-0.1	-0.23	0.28	132.8	-0.14	0.30	39.1	1.33	0.35	185.0	67.4
49.7	16.8	-0.3	-0.21	0.28	111.7	-0.26	0.30	35.2	0.75	0.37	185.0	50.3
50.7	12.3	-0.4	-0.20	0.27	71.4	0.21	0.30	29.8	-0.12	0.37	184.8	28.0
51.7	-9.0	-0.7	-0.36	0.27	-85.9	1.31	0.31	25.2	-0.39	0.37	177.8	10.8
52.7	21.9	-0.6	-0.43	0.27	-233.3	1.89	0.33	22.6	-0.12	0.36	162.4	-0.5
53.6	43.1	-0.5	-0.49	0.26	-265.3	1.65	0.35	20.3	-0.14	0.36	143.2	-8.3
54.6	54.3	-0.5	-0.48	0.26	-223.6	1.12	0.36	16.4	-0.30	0.36	115.9	-11.6
55.6	81.2	-0.4	-0.50	0.25	-111.1	0.62	0.37	14.6	-0.09	0.36	86.7	-11.0
56.6	68.9	-0.4	-0.43	0.24	-6.2	0.02	0.38	13.7	-0.14	0.36	57.6	-12.4
57.6	72.8	-0.4	-0.40	0.24	64.1	-0.34	0.38	9.9	-0.46	0.35	33.2	-15.0
58.5	103.1	-0.3	-0.43	0.23	66.6	-0.15	0.37	12.4	-0.07	0.35	8.8	-11.6
59.5	112.6	-0.2	-0.53	0.23	11.1	-0.11	0.37	13.1	0.05	0.35	3.5	-8.0
60.5	86.3	-0.3	-0.61	0.22	41.6	-0.43	0.37	11.4	-0.19	0.35	3.2	-6.5
61.5	-54.9	0.2	-0.34	0.22	46.2	-0.72	0.36	13.4	0.11	0.35	3.9	-3.3
62.5	-317.7	0.5	0.18	0.21	12.0	-0.77	0.35	14.7	0.23	0.35	4.6	-2.0
63.5	-432.0	0.6	0.45	0.22	12.8	-0.43	0.35	13.7	-0.01	0.35	4.9	-3.6
64.4	-300.3	1.3	0.89	0.23	8.8	-0.32	0.34	10.6	-0.32	0.35	3.4	-6.7
65.4	-91.3	1.6	1.09	0.24	16.2	-0.23	0.34	10.5	-0.33	0.34	3.5	-8.1
66.4	94.7	1.5	1.18	0.25	28.4	0.04	0.34	12.1	-0.05	0.34	4.0	-6.9
67.4	190.5	0.8	0.98	0.26	11.9	-0.17	0.34	12.4	-0.02	0.34	2.8	-7.0
68.4	164.2	0.2	0.69	0.27	39.4	-0.12	0.33	12.4	-0.01	0.34	0.1	-7.1
69.4	58.8	-0.0	0.44	0.28	42.0	0.18	0.33	12.4	-0.01	0.34	0.0	-6.7
70.3	42.6	-0.1	0.35	0.28	37.5	0.18	0.34	12.4	-0.01	0.34	0.4	-5.8
71.3	81.2	-0.4	0.39	0.29	30.9	0.04	0.34	12.4	-0.01	0.34	0.2	-2.7
72.3	85.2	-0.4	0.28	0.29	-44.9	-0.20	0.34	12.4	-0.01	0.34	0.4	-0.3
73.3	61.6	-0.3	0.02	0.29	-156.7	-0.86	0.33	12.4	-0.01	0.34	0.9	1.4
74.3	40.9	-0.2	-0.06	0.29	-116.5	-0.89	0.32	12.4	-0.01	0.34	1.8	1.1
75.2	2.2	-0.4	-0.31	0.29	28.4	-0.26	0.31	12.4	-0.01	0.34	-0.0	-1.3
76.2	-24.7	-0.4	-0.35	0.29	157.7	0.62	0.32	12.4	-0.01	0.34	0.0	0.0
77.2	-43.1	-0.4	-0.38	0.28	181.1	1.01	0.33	12.4	-0.01	0.34	0.0	0.0
78.2	-26.9	-0.5	-0.47	0.28	143.2	0.88	0.34	12.4	-0.01	0.34	0.0	0.0
79.2	-14.6	-0.4	-0.40	0.27	131.6	0.82	0.34	12.4	-0.01	0.34	0.0	0.0
80.2	-29.7	-0.2	-0.42	0.27	131.6	0.82	0.34	12.4	-0.01	0.34	0.0	0.0
81.1	-16.8	-0.2	-0.35	0.27	131.6	0.82	0.34	12.4	-0.01	0.34	0.0	0.0
82.1	-18.5	-0.2	-0.46	0.26	131.6	0.82	0.34	12.4	-0.01	0.34	0.0	0.0
83.1	-34.7	-0.1	-0.49	0.26	131.6	0.82	0.34	12.4	-0.01	0.34	0.0	0.0
84.1	-30.8	-0.2	-0.53	0.25	131.6	0.82	0.34	12.4	-0.01	0.34	0.0	0.0
85.1	-10.6	-0.4	-0.57	0.24	131.6	0.82	0.34	12.4	-0.01	0.34	0.0	0.0
86.1	9.0	-0.4	-0.53	0.24	131.6	0.82	0.34	12.4	-0.01	0.34	0.0	0.0
87.0	-16.8	-0.4	-0.58	0.23	131.6	0.82	0.34	12.4	-0.01	0.34	0.0	0.0
88.0	-41.5	-0.3	-0.57	0.22	131.6	0.82	0.34	12.4	-0.01	0.34	0.0	0.0
MIN-433.1		-0.7	-0.65	-0.00	-268.8	-1.04	-0.00	9.4	-0.46	-0.00	-0.1	-13.0
MAX 687.5		4.5	4.39	0.29	699.2	4.32	0.38	70.9	6.34	0.37	185.0	145.0

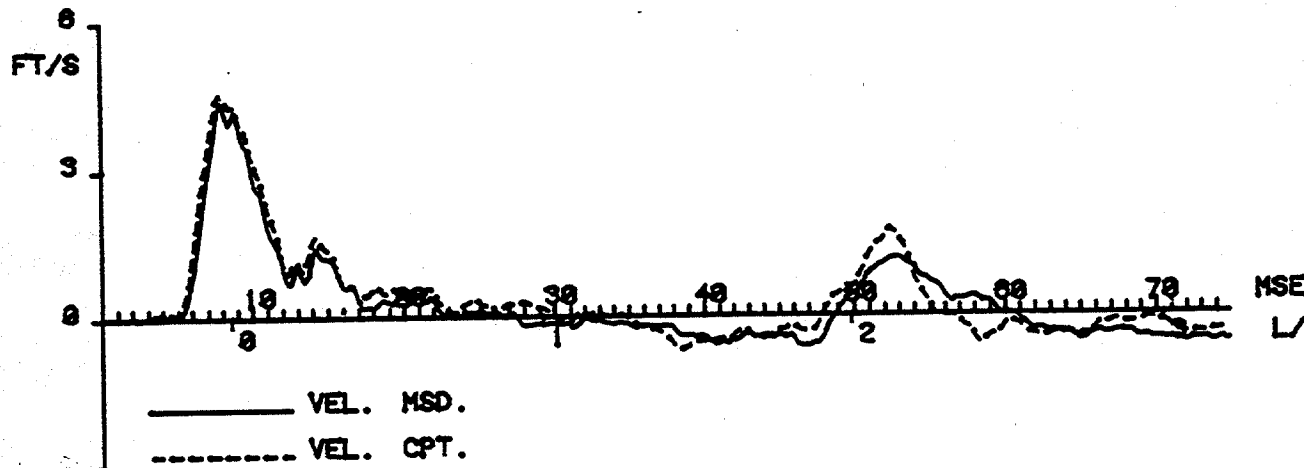
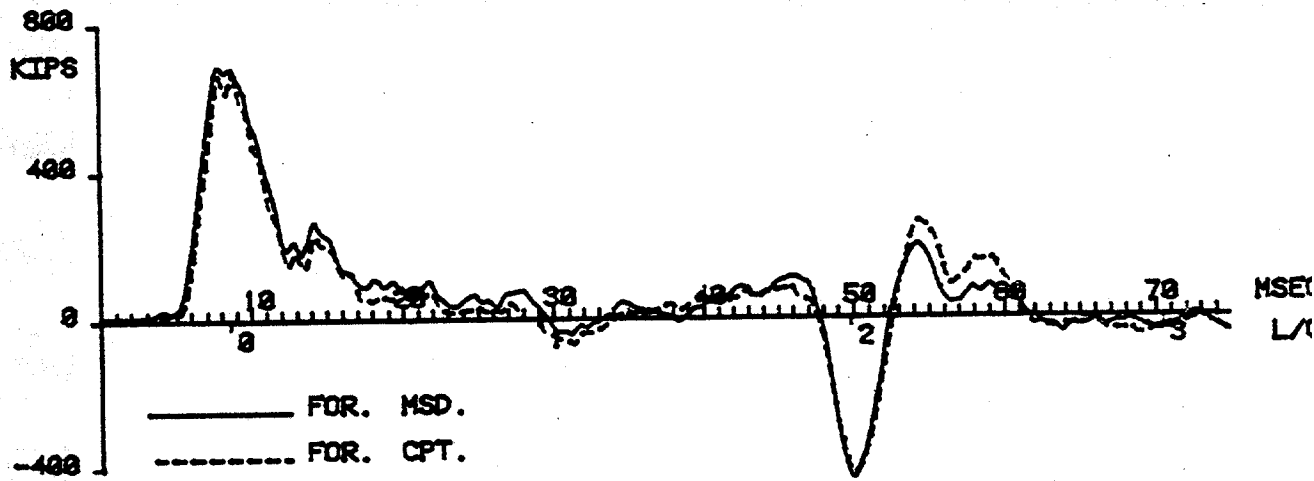
WD 58A, TP3, BOD WITH 2 DAY WAIT
BLOW NO. 4

STATIC ANALYSIS

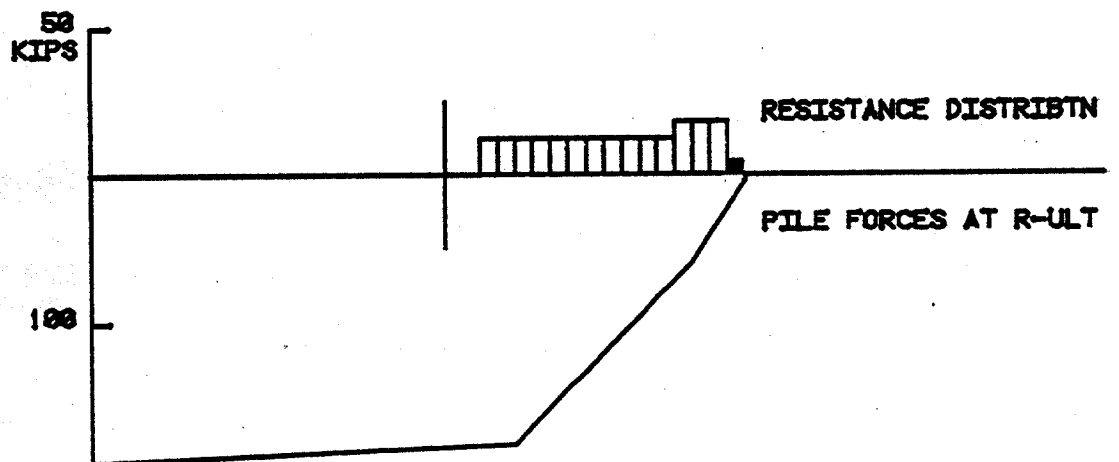
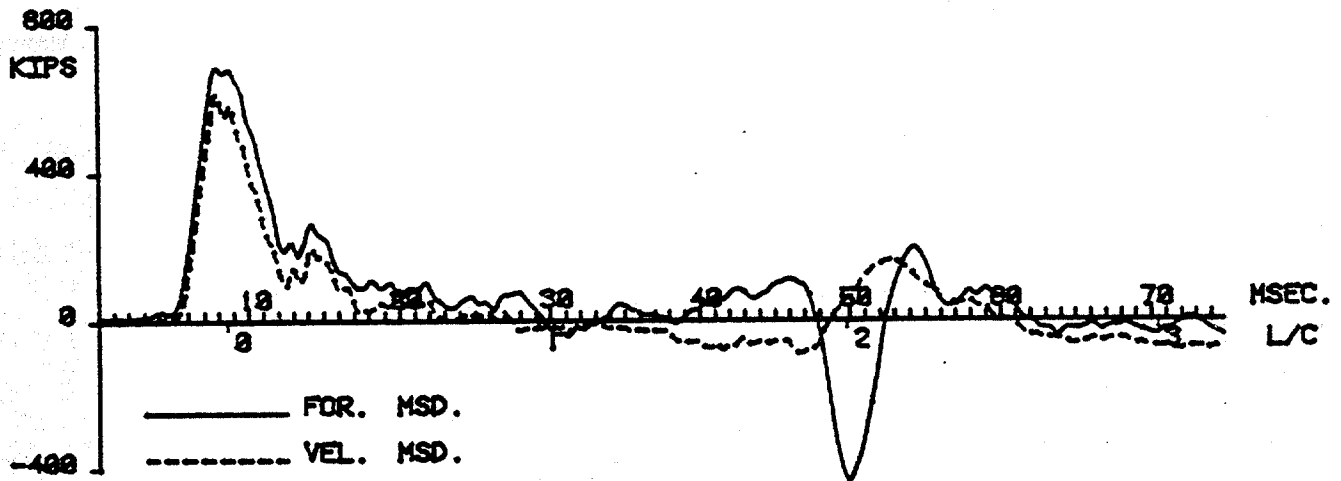
QAD(IN)= 0.000, EFAC= 1.000, CUT(FT)= 0.0

I	LOAD KIPS	SET IN	BOT. LOAD KIPS
1	0.0	0.000	0.0
2	13.0	0.019	0.1
3	26.1	0.039	0.2
4	39.1	0.058	0.4
5	52.2	0.077	0.5
6	65.2	0.097	0.6
7	78.2	0.116	0.7
8	91.3	0.135	0.8
9	104.3	0.154	1.0
10	117.4	0.174	1.1
11	131.1	0.195	1.2
12	142.8	0.214	1.4
13	155.7	0.236	1.5
14	169.5	0.261	1.8
15	181.7	0.286	2.1
16	194.5	0.357	4.2

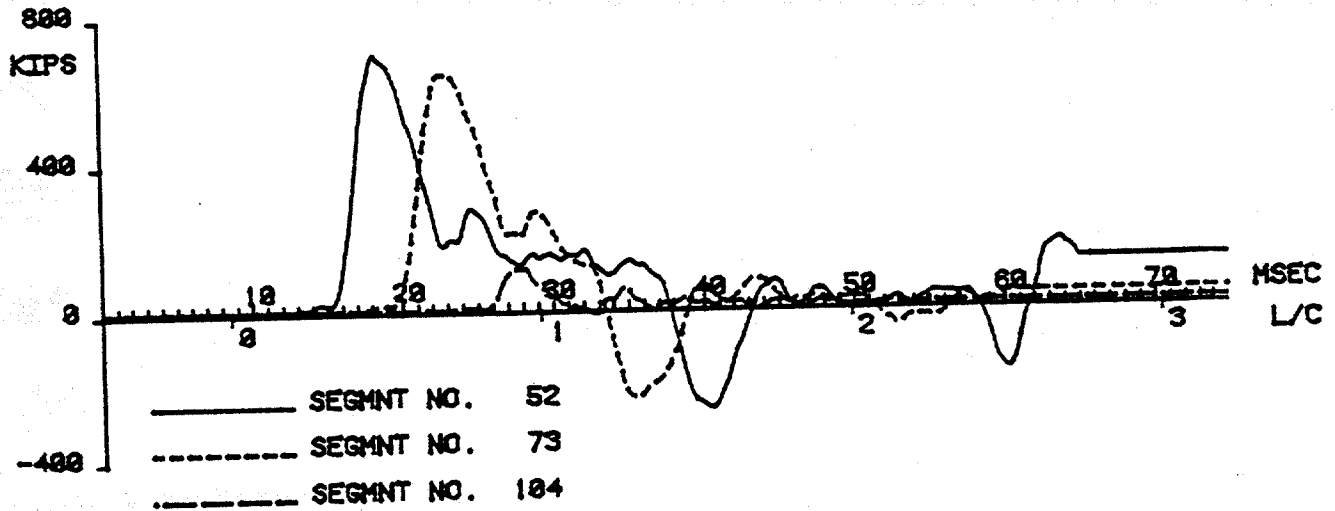
G & A PROGRAMS: CAPWAP/C RESULTS
 WD 58A, TP3, BOD WITH 2 DAY WAIT
 BLOW NO. 4 12-APR-84



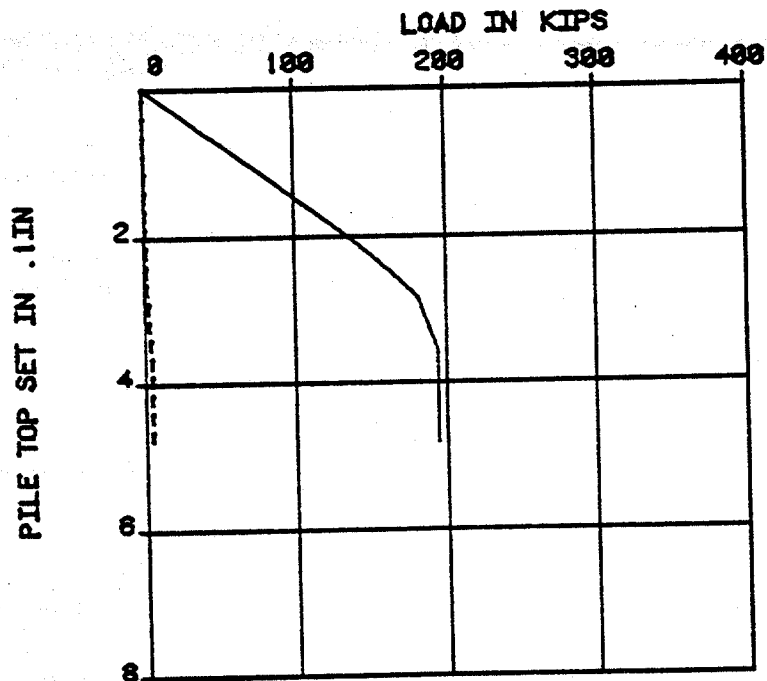
G & A PROGRAMS: CAPWAP/C RESULTS
 WD 58A, TP3, BOD WITH 2 DAY WAIT
 BLOW NO. 4 12-APR-84



G & A PROGRAMS: CAPWAP/C RESULTS
 WD 58A, TP3, BOD WITH 2 DAY WAIT
 BLOW NO. 4 12-APR-84



STATIC CAPWAP/C RESULTS
 WD 58A, TP3, BOD WITH 2 DAY WAIT
 BLOW NO. 4
 _____ TOP LOAD ----- BOTTOM LOAD



WD 58A. TP3, EOD

IS	DEPTH FT	QUAKE IN	RES KIPS	SUM RES KIPS	VISC. J KIPS/F/S	IMPDNCE KIPS/F/S	T-SLACK IN	C-SLACK IN	IP
0	0.0	0.000	0.0	578.9					1
0	3.3	0.000	0.0	578.9	2.0	139.9	0.0000	0.0000	3
0	9.9	0.000	0.0	578.9	0.0	139.9	0.0000	0.0000	4
0	13.1	0.000	0.0	578.9	0.0	147.2	0.0000	0.0000	5
0	16.4	0.000	0.0	578.9	0.0	160.8	0.0000	0.0000	6
0	19.7	0.000	0.0	578.9	0.0	160.8	0.0000	0.0000	10
0	32.9	0.000	0.0	578.9	0.0	160.8	0.0000	0.0000	21
0	69.0	0.000	0.0	578.9	0.0	160.8	0.0000	0.0000	39
1	128.1	0.060	11.9	567.0	2.2	160.8	0.0000	0.0000	42
2	138.0	0.060	11.9	555.0	2.2	160.8	0.0000	0.0000	45
3	147.9	0.060	11.9	543.1	2.2	160.8	0.0000	0.0000	48
4	157.7	0.060	11.9	531.2	2.2	160.8	0.0000	0.0000	51
5	167.6	0.060	11.9	519.2	2.2	160.8	0.0000	0.0000	52
0	170.9	0.000	0.0	519.2	0.0	164.5	0.0000	0.0000	53
0	174.1	0.000	0.0	519.2	0.0	175.0	0.0000	0.0000	54
6	177.4	0.060	11.9	507.3	2.2	175.0	0.0000	0.0000	55
0	180.7	0.000	0.0	507.3	0.0	170.1	0.0000	0.0000	56
0	184.0	0.000	0.0	507.3	0.0	152.5	0.0000	0.0000	57
7	187.3	0.060	11.9	495.4	2.2	152.5	0.0000	0.0000	60
8	197.1	0.060	11.9	483.5	2.2	152.5	0.0000	0.0000	63
9	207.0	0.060	11.9	471.5	2.2	152.5	0.0000	0.0000	66
10	216.9	0.060	11.8	459.7	2.1	152.5	0.0000	0.0000	69
11	226.7	0.060	15.9	443.8	2.9	152.5	0.0000	0.0000	72
12	236.6	0.060	20.1	423.7	3.6	150.7	0.0000	0.0000	73
0	239.9	0.000	0.0	423.7	0.0	148.8	0.0000	0.0000	75
13	246.4	0.060	24.2	399.5	4.4	148.8	0.0000	0.0000	78
14	256.3	0.060	28.3	371.2	5.1	148.8	0.0000	0.0000	81
15	266.1	0.060	32.5	338.7	5.9	148.8	0.0000	0.0000	84
16	276.0	0.060	34.9	303.8	6.3	148.8	0.0000	0.0000	87
17	285.9	0.060	36.9	266.8	6.7	148.8	0.0000	0.0000	90
18	295.7	0.060	39.0	227.8	7.0	147.1	0.0000	0.0000	91
0	299.0	0.000	0.0	227.8	0.0	141.2	0.0000	0.0000	93
19	305.6	0.060	41.1	186.8	7.4	141.2	0.0000	0.0000	96
20	315.4	0.060	38.7	148.1	7.0	141.2	0.0000	0.0000	99
21	325.3	0.060	35.5	112.6	6.4	141.2	0.0000	0.0000	102
22	335.1	0.060	32.2	80.4	5.8	140.3	0.0000	0.0000	103
0	338.4	0.000	0.0	80.4	0.0	122.0	0.0000	0.0000	105
23	345.0	0.060	29.0	51.4	5.2	122.0	0.0000	0.0000	
PILE TOE		0.150	51.4		6.15				

RESISTANCE			CASE DAMPING		SMITH DAMPING		QUAKES	
SKIN	TOE	TOTAL	SKIN	TOE	SKIN	TOE	SKIN	TOE
KIPS	KIPS	KIPS			1/FT/S	1/FT/S	IN	IN
527.5	51.4	578.9	0.620	0.040	0.181	0.119	0.060	0.150
UNLOADING QUAKES IN PERCENT:							40	100

UNLOADING TO - 0.00 OF SU, ALPHA = 1.00

ENERGY			FORCES			DISPLACEMENTS		
MAX	FIN	MAX	I TMAX	MIN	I TMIN	TOP	TOE	
FT-KIPS	FT-KIPS	KIPS	MS	KIPS	MS	IN	IN	
15.0	14.7	905	39 29.	-258	1 64.	0.335	0.175	

TIME INCR (MS) = 0.137

INT. PILE DAMPING (%) = 1.5
PILE DYNAMICS, INC.

WD 58A, TP3, EDD

BLOW NO. 4

			FORCES IN PILE									
TIME	FM	F/V/C,	10	21	31	42	52	63	73	84	94	104
MS	KIPS		KIPS	KIPS	KIPS	KIPS	KIPS	KIPS	KIPS	KIPS	KIPS	KIPS
12.2	-1.1	-7.2	-1.1	-1.1	-1.1	-1.1	-1.1	-1.1	-1.1	-1.1	-1.1	-1.1
13.2	7.8	-5.6	-1.1	-1.1	-1.1	-1.1	-1.1	-1.1	-1.1	-1.1	-1.1	-1.1
14.2	6.2	4.0	-6.8	-1.1	-1.1	-1.1	-1.1	-1.1	-1.1	-1.1	-1.1	-1.1
15.2	37.0	16.9	-6.1	-1.1	-1.1	-1.1	-1.1	-1.1	-1.1	-1.1	-1.1	-1.1
16.2	42.6	25.6	5.3	-1.1	-1.1	-1.1	-1.1	-1.1	-1.1	-1.1	-1.1	-1.1
17.2	62.8	34.1	18.5	-7.7	-1.1	-1.1	-1.1	-1.1	-1.1	-1.1	-1.1	-1.1
18.2	80.7	43.2	26.1	5.7	-1.1	-1.1	-1.1	-1.1	-1.1	-1.1	-1.1	-1.1
19.2	178.2	86.4	34.2	21.0	-8.0	-1.1	-1.1	-1.1	-1.1	-1.1	-1.1	-1.1
20.1	688.1	599.0	43.9	26.3	4.7	-1.1	-1.1	-1.1	-1.1	-1.1	-1.1	-1.1
21.1	915.0	825.5	86.3	31.3	20.9	-10.2	-1.1	-1.1	-1.1	-1.1	-1.1	-1.1
22.1	702.7	637.4	627.4	41.5	26.6	-2.3	-1.1	-1.1	-1.1	-1.1	-1.1	-1.1
23.1	553.6	483.5	851.2	61.1	30.8	18.7	-10.4	-1.1	-1.1	-1.1	-1.1	-1.1
24.1	381.6	323.3	641.0	530.7	41.3	28.5	-2.2	-1.1	-1.1	-1.1	-1.1	-1.1
25.1	395.0	341.9	468.3	797.5	60.8	28.3	17.9	-10.4	-1.1	-1.1	-1.1	-1.1
26.1	259.4	216.0	311.4	737.2	509.9	40.4	26.7	-6.2	-1.1	-1.1	-1.1	-1.1
27.1	220.2	207.4	336.2	541.8	790.5	57.8	25.2	9.2	-9.6	-1.1	-1.1	-1.1
28.0	211.3	160.8	210.2	372.0	754.1	346.1	35.2	22.3	-6.0	-1.1	-1.1	-1.1
29.0	89.1	66.1	205.7	333.4	556.7	730.2	50.4	22.9	7.9	-6.2	-1.1	-1.1
30.0	153.0	97.3	155.2	229.8	394.7	858.1	318.5	29.9	19.9	-6.1	-1.1	-1.1
31.0	110.9	61.4	63.2	226.5	353.4	627.0	691.2	43.4	20.3	4.1	-5.1	-1.1
32.0	100.3	80.2	97.6	153.3	262.5	478.8	800.0	164.3	26.3	15.9	-5.6	-1.1
33.0	107.6	57.0	66.8	100.5	258.9	367.8	552.6	592.6	38.2	18.6	3.1	-4.2
34.0	52.7	36.4	92.5	119.1	188.9	298.0	408.2	784.8	142.7	22.2	12.6	-1.7
35.0	68.4	27.3	74.6	120.3	149.1	242.7	301.3	567.4	542.6	30.0	13.9	6.3
35.9	88.5	27.1	62.9	146.7	137.0	172.8	272.4	420.5	720.4	71.5	18.2	6.9
36.9	60.5	49.2	57.0	116.7	117.8	159.0	233.2	290.9	531.0	470.9	22.6	0.7
37.9	48.9	44.5	59.5	88.8	138.6	142.3	162.5	302.0	403.4	643.7	46.3	2.7
38.9	49.3	63.8	93.6	58.7	102.7	172.9	147.2	238.8	289.9	515.9	367.0	6.7
39.9	78.4	44.4	67.5	67.3	107.3	154.8	127.7	212.7	303.8	374.3	477.6	27.3
40.9	118.2	64.4	63.2	75.2	97.3	121.3	175.4	202.8	236.7	256.5	383.0	266.9
41.9	65.6	44.3	36.2	70.0	105.7	129.4	162.1	154.6	204.1	279.6	247.2	144.9
42.8	-18.5	14.2	48.5	96.3	106.1	133.6	139.6	202.1	188.3	206.0	108.3	-4.4
43.8	-38.1	17.2	56.6	87.2	96.9	143.3	152.1	166.1	151.4	184.1	-76.0	-13.6
44.8	9.5	26.3	44.8	88.5	137.2	133.8	153.3	159.9	203.2	122.3	-190.4	-5.5
45.8	42.0	34.6	58.5	98.6	123.3	131.0	159.1	170.6	164.2	-91.1	-93.7	73.4
46.8	31.4	41.1	59.9	87.4	124.5	159.7	144.5	160.8	139.7	-76.9	-22.9	17.1
47.8	23.5	30.6	83.7	94.4	130.6	148.2	144.8	151.0	-14.7	10.3	20.4	47.1
48.8	46.5	54.6	79.3	95.6	111.0	131.9	169.5	120.2	-73.7	114.8	56.8	33.1
49.8	29.1	66.1	61.8	114.8	110.4	138.8	153.4	-17.4	-0.5	150.7	76.3	15.8
50.7	57.2	75.8	91.6	117.7	100.3	113.3	117.1	-57.7	94.5	102.8	90.3	67.1
51.7	78.4	71.2	99.9	84.0	116.8	102.5	4.7	11.6	150.7	103.4	80.6	29.7
52.7	53.8	59.1	103.7	94.0	119.6	80.7	-103.8	82.6	125.3	95.0	84.6	41.3
53.7	93.0	89.1	88.8	105.6	87.9	-19.6	-70.5	119.2	117.4	101.1	51.0	31.7
54.7	123.8	129.8	63.9	115.4	77.1	-93.5	40.9	80.8	72.2	94.5	51.8	32.3
55.7	114.9	122.8	92.9	100.3	20.2	-83.4	93.8	69.6	72.3	66.2	52.5	36.1
56.7	130.0	107.9	133.3	56.7	-94.1	15.6	98.9	52.8	58.7	21.2	49.5	38.3
57.7	91.9	86.2	131.6	13.1	-102.8	85.5	51.5	53.3	27.7	21.2	49.5	38.3
58.6	79.0	64.4	95.1	-96.7	-12.5	92.5	28.1	58.5	12.3	17.7	20.8	29.1
59.6	29.7	52.2	36.1	-70.8	65.7	46.8	54.8	14.3	0.6	7.8	15.0	38.7
60.6	-23.0	-0.4	-134.4	18.7	94.6	18.1	52.4	-19.0	11.8	3.4	10.2	16.7
61.6	-108.1	-28.3	-164.6	67.1	83.3	27.3	15.1	-8.6	-7.6	-1.0	6.4	26.7
62.6	-223.0	-226.2	-93.9	46.5	53.1	30.7	-25.6	2.5	-28.3	3.4	5.3	29.6
63.6	-246.0	-272.0	-6.4	0.0	40.4	59.8	-29.7	-18.1	-14.9	-5.2	15.3	24.3
64.6	-65.6	-85.5	-47.4	-24.6	-9.7	4.2	-10.9	-31.9	-8.8	-27.9	23.4	29.1
65.6	21.3	105.1	-117.4	-27.7	-27.2	-10.0	29.9	-47.4	-18.9	-0.4	14.6	23.9
66.5	29.7	179.2	-25.5	-85.7	-74.4	-42.6	-5.3	-26.9	-33.2	9.1	0.3	30.2
67.5	70.0	121.9	93.7	-138.1	-82.2	-65.8	-20.3	23.3	-35.0	2.0	10.5	17.8
68.5	54.9	104.8	129.2	-118.5	-127.2	-79.3	-53.7	-3.2	-9.7	-5.6	18.2	13.8
69.5	44.3	73.1	97.7	29.5	-177.0	-100.2	-68.7	-6.2	29.9	-23.7	9.2	13.8
70.5	38.1	41.2	54.0	79.5	-135.7	-127.4	-78.3	-25.2	15.6	-2.4	3.9	13.8
71.5	36.4	17.1	24.2	61.8	9.1	-177.8	-88.7	-53.6	2.7	21.9	3.9	13.8
72.5	1.1	-46.4	-7.9	40.1	62.0	-171.5	-105.2	-58.1	-18.9	32.0	3.9	13.8
73.5	-38.7	-74.6	-26.2	15.2	50.8	-16.9	-163.3	-77.4	-46.1	32.0	3.9	13.8
74.4	-4.5	-85.4	-65.2	-15.3	34.4	62.5	-149.2	-85.9	-51.6	32.0	3.9	13.8
75.4	-12.3	-84.9	-93.8	-29.9	18.4	75.1	-0.1	-147.7	-51.6	32.0	3.9	13.8
76.4	-12.9	-81.4	-99.0	-62.6	-0.6	57.4	65.7	-158.0	-51.6	32.0	3.9	13.8
77.4	-20.7	-104.9	-100.9	-92.8	-16.9	47.5	77.4	-158.0	-51.6	32.0	3.9	13.8
78.4	-42.0	-88.7	-87.4	-79.3	-43.3	14.4	47.6	-158.0	-51.6	32.0	3.9	13.8
79.4	-79.6	-96.5	-107.1	-86.4	-67.9	-5.9	47.6	-158.0	-51.6	32.0	3.9	13.8
80.4	-62.2	-88.4	-77.0	-69.9	-70.7	-30.5	47.6	-158.0	-51.6	32.0	3.9	13.8
81.4	-34.7	-79.1	-80.0	-79.2	-81.8	-30.5	47.6	-158.0	-51.6	32.0	3.9	13.8
82.3	-38.7	-57.1	-75.9	-73.6	-80.8	-30.5	47.6	-158.0	-51.6	32.0	3.9	13.8
83.3	-43.7	-38.2	-53.1	-68.0	-80.8	-30.5	47.6	-158.0	-51.6	32.0	3.9	13.8
84.3	-30.8	-32.7	-43.7	-88.3	-80.8	-30.5	47.6	-158.0	-51.6	32.0	3.9	13.8
85.3	-34.7	-24.1	-32.7	-88.3	-80.8	-30.5	47.6	-158.0	-51.6	32.0	3.9	13.8
86.3	-23.5	-23.6	-38.2	-88.3	-80.8	-30.5	47.6	-158.0	-51.6	32.0	3.9	13.8
87.3	-40.3	-31.9	-38.2	-88.3	-80.8	-30.5	47.6	-158.0	-51.6	32.0	3.9	13.8

MIN-272.3-272.0-164.9-158.7-187.0-194.7-174.3-158.0 -75.0 -95.0-190.4 -25.1
 MAX 922.3 866.1 886.0 885.0 886.0 891.8 828.7 784.8 720.4 670.9 498.6 266.9

-B13-

PILE DYNAMICS, INC.

WD 58A, TP3, ECD
BLOW NO. 4

STATIC ANALYSIS

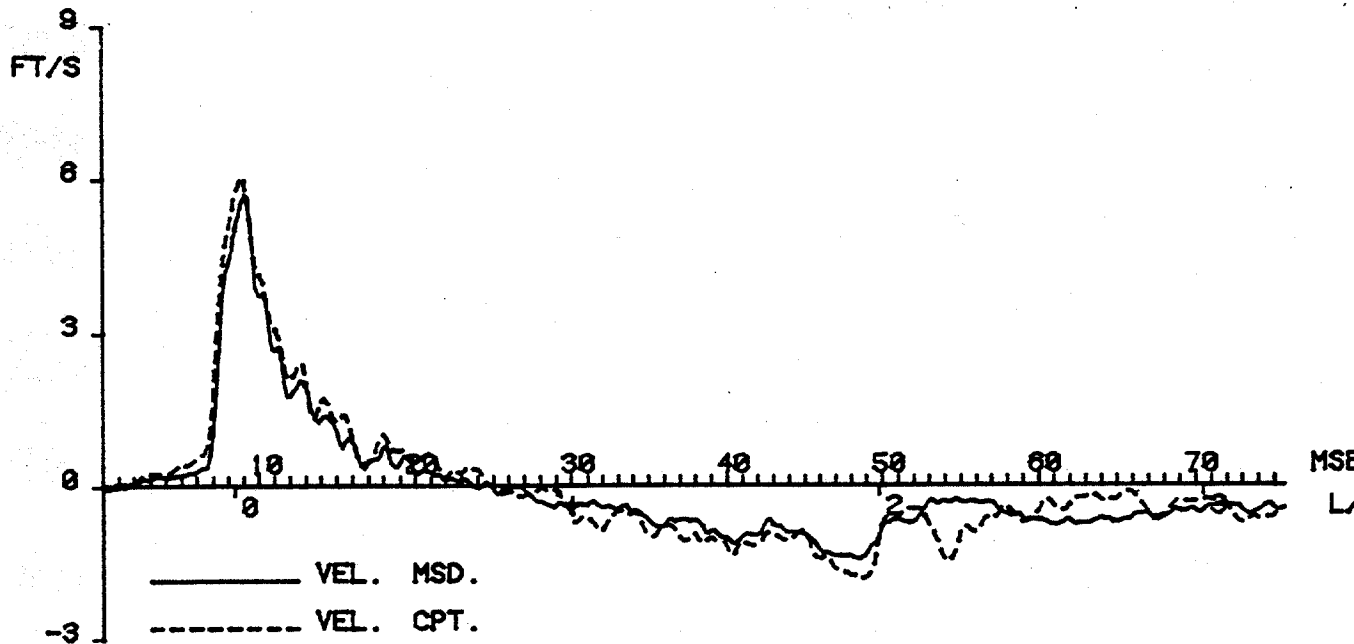
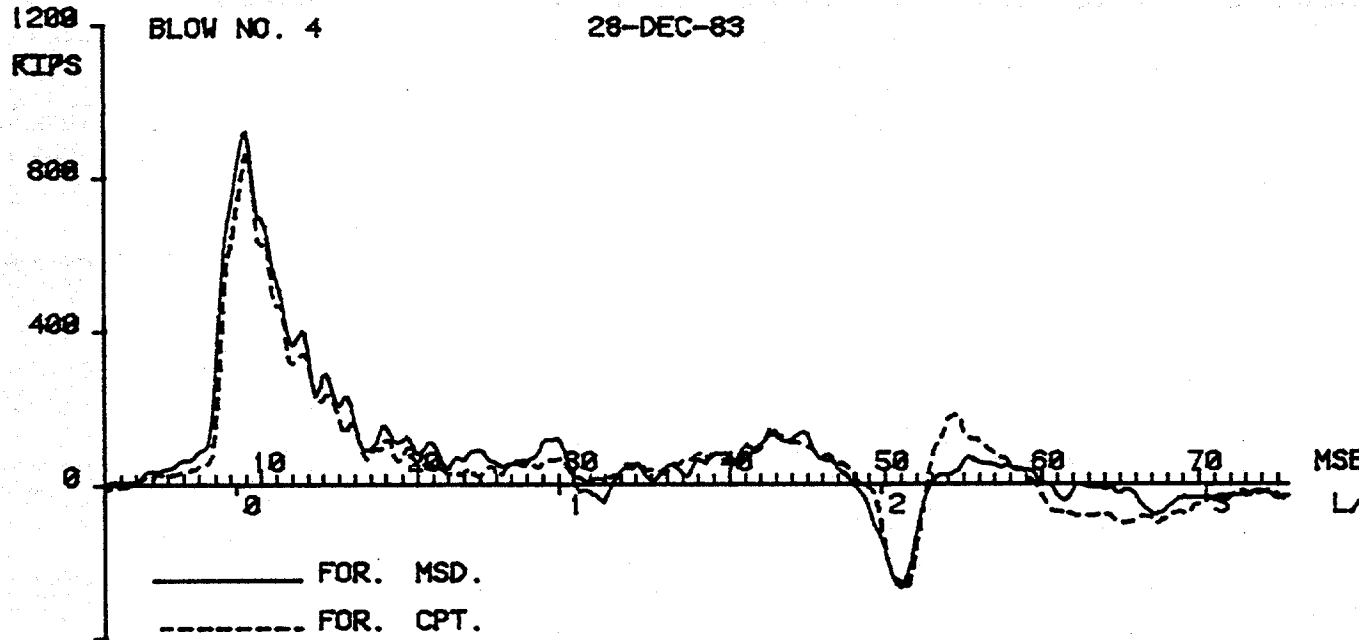
QAD(IN) = 0.000, EFAC = 1.000, CUT(FT) = 0.0

I	LOAD KIPS	SET IN	BCT. LOAD KIPS
1	0.0	0.000	0.0
2	26.7	0.027	0.3
3	33.4	0.054	0.6
4	80.1	0.081	0.9
5	106.8	0.108	1.2
6	133.5	0.135	1.5
7	146.2	0.148	1.6
8	168.9	0.173	1.9
9	197.7	0.206	2.4
10	222.4	0.237	2.8
11	244.3	0.264	3.3
12	270.5	0.299	3.9
13	294.6	0.331	4.5
14	316.8	0.362	5.1
15	342.1	0.397	5.8
16	363.0	0.430	6.6
17	386.1	0.461	7.3
18	411.8	0.500	8.3
19	437.2	0.539	9.3
20	459.2	0.574	10.7
21	482.5	0.613	12.2
22	506.8	0.655	14.2
23	531.5	0.701	16.6
24	554.9	0.769	27.4
25	578.9	0.878	51.4

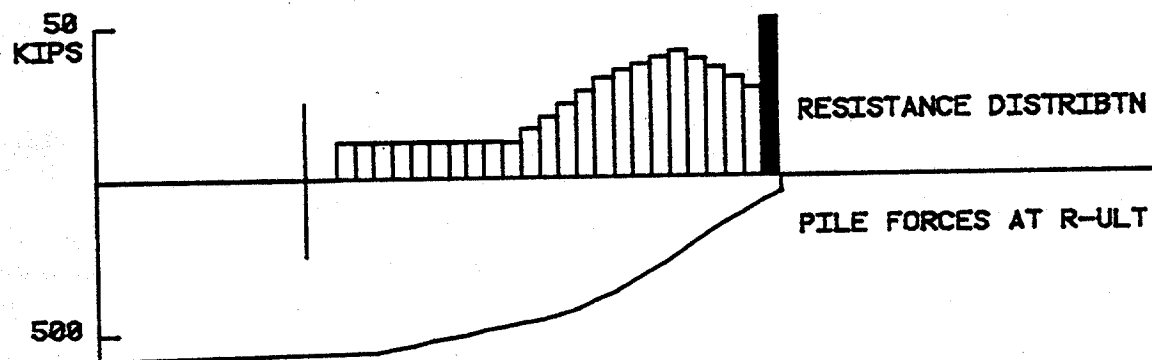
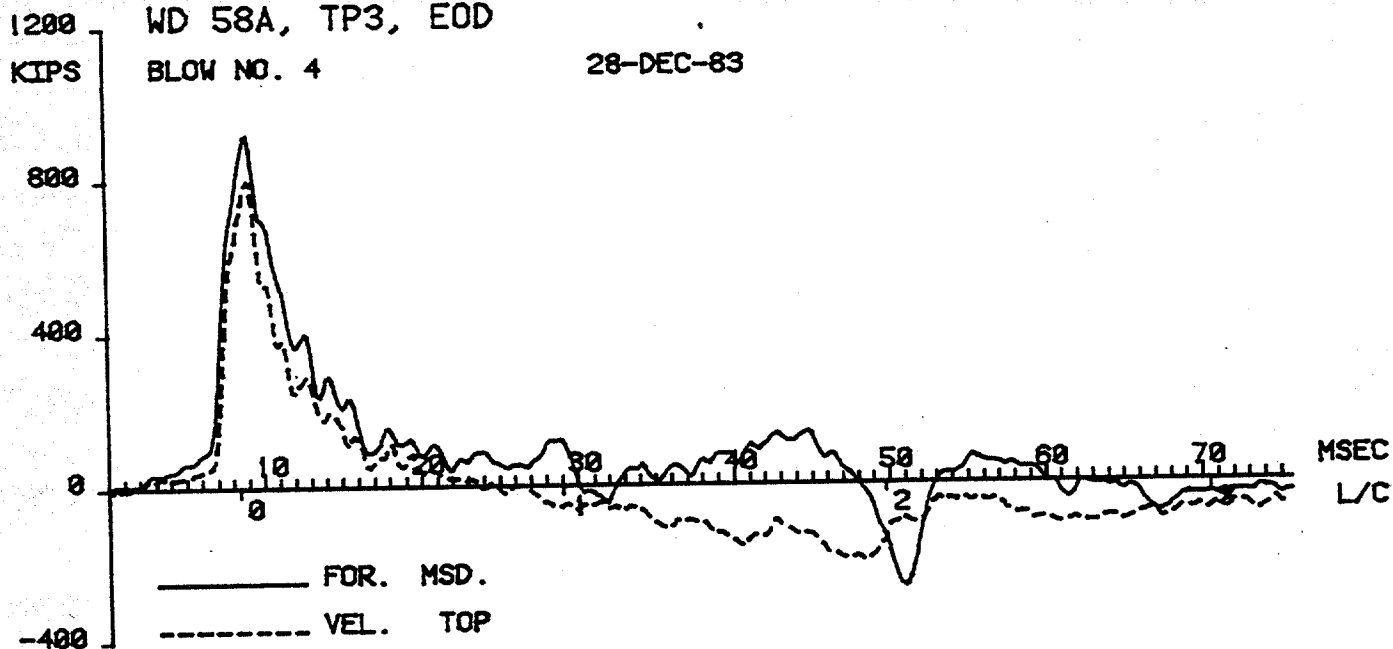
G & A PROGRAMS: CAPWAP/C RESULTS
WD 58A, TP3, EOD

BLOW NO. 4

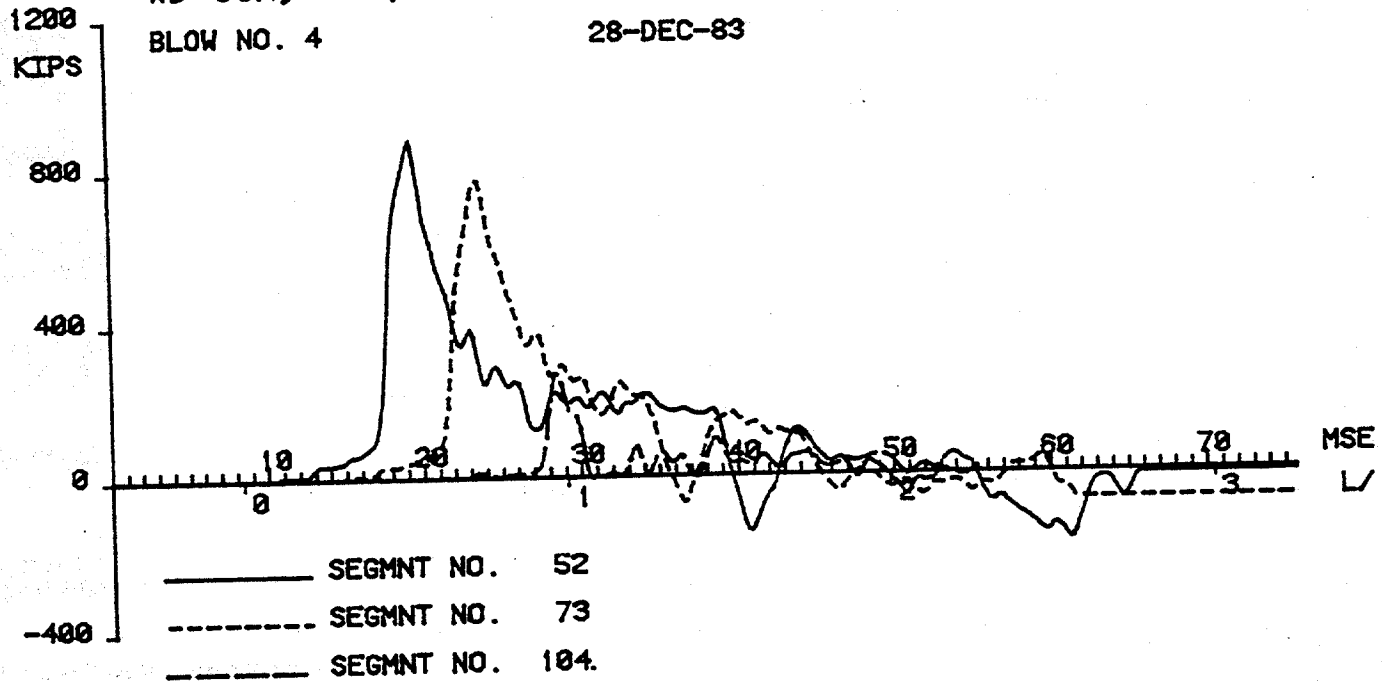
28-DEC-83



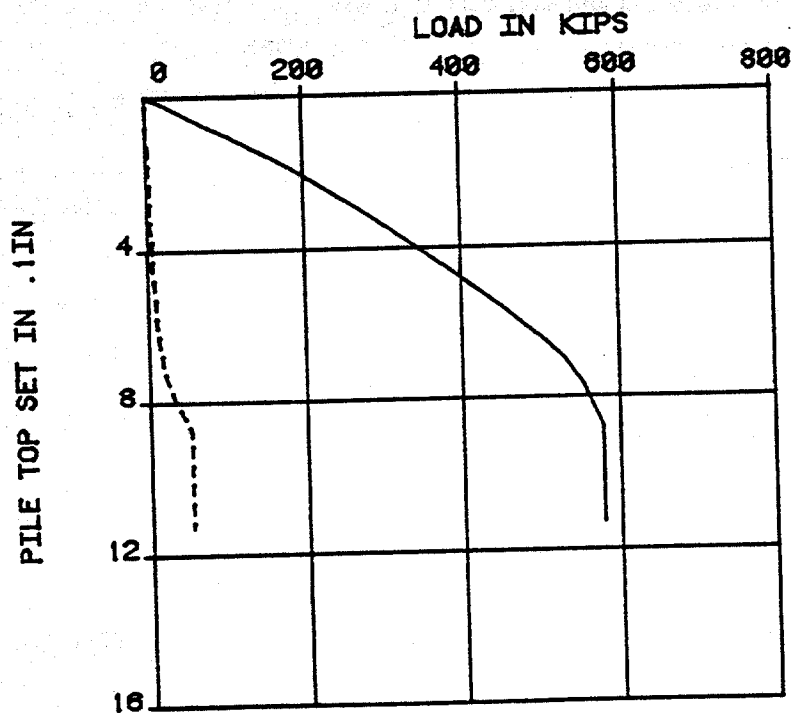
G & A PROGRAMS: CAPWAP/C RESULTS
 WD 58A, TP3, EOD
 BLOW NO. 4 28-DEC-83



G & A PROGRAMS: CAPWAP/C RESULTS
 WD 58A, TP3, EOD
 BLOW NO. 4 28-DEC-83



STATIC RESULTS
 WD 58A, TP3, EOD
 BLOW NO. 4
 ——— TOP LOAD ——— BOTTOM LOAD



IS	DEPTH FT	QUAKE IN	RES KIPS	SUM RES KIPS	VISC. J KIPS/F/S	IMPDNCE KIPS/F/S	T-SLACK IN	C-SLACK IN	IP
0	0.0	0.000	0.0	600.0					1
0	3.3	0.000	0.0	600.0	0.0	140.1	0.0000	0.0000	4
0	13.1	0.000	0.0	600.0	0.0	147.4	0.0000	0.0000	5
0	16.4	0.000	0.0	600.0	0.0	161.0	0.0000	0.0000	11
0	36.1	0.000	0.0	600.0	0.0	161.0	0.0000	0.0000	39
1	128.1	0.060	11.4	588.5	2.1	161.0	0.0000	0.0000	42
2	138.0	0.060	11.4	577.1	2.1	161.0	0.0000	0.0000	45
3	147.9	0.060	11.4	565.7	2.1	161.0	0.0000	0.0000	48
4	157.7	0.060	11.4	554.3	2.1	161.0	0.0000	0.0000	51
5	167.6	0.060	11.4	542.8	2.1	161.0	0.0000	0.0000	52
0	170.9	0.000	0.0	542.8	0.0	164.7	0.0000	0.0000	53
0	174.1	0.000	0.0	542.8	0.0	175.2	0.0000	0.0000	54
6	177.4	0.060	11.4	531.4	2.1	175.2	0.0000	0.0000	55
0	180.7	0.000	0.0	531.4	0.0	170.3	0.0000	0.0000	56
0	184.0	0.000	0.0	531.4	0.0	152.7	0.0000	0.0000	57
7	187.3	0.060	11.4	520.0	2.1	152.7	0.0000	0.0000	60
8	197.1	0.060	11.4	508.6	2.1	152.7	0.0000	0.0000	63
9	207.0	0.060	11.4	497.1	2.1	152.7	0.0000	0.0000	66
10	216.9	0.060	11.4	485.7	2.1	152.7	0.0000	0.0000	69
11	226.7	0.060	11.4	474.3	2.1	152.7	0.0000	0.0000	72
12	236.6	0.060	22.6	451.7	4.1	150.9	0.0000	0.0000	73
0	239.9	0.000	0.0	451.7	0.0	149.0	0.0000	0.0000	75
13	246.4	0.060	30.3	421.4	5.5	149.0	0.0000	0.0000	78
14	256.3	0.060	30.3	391.1	5.5	149.0	0.0000	0.0000	80
0	262.9	0.000	0.0	391.1	0.0	149.0	0.0000	0.0000	81
15	266.1	0.060	29.8	361.3	5.4	149.0	0.0000	0.0000	84
16	276.0	0.060	31.9	329.3	5.8	149.0	0.0000	0.0000	87
17	285.9	0.060	45.7	283.6	8.3	149.0	0.0000	0.0000	90
18	295.7	0.060	44.7	238.9	8.1	147.3	0.0000	0.0000	91
0	299.0	0.000	0.0	238.9	0.0	141.3	0.0000	0.0000	93
19	305.6	0.060	35.9	203.0	6.5	141.3	0.0000	0.0000	96
20	315.4	0.060	30.2	172.8	5.5	141.3	0.0000	0.0000	99
21	325.3	0.060	30.2	142.6	5.5	141.3	0.0000	0.0000	102
22	335.1	0.060	40.3	102.3	7.3	140.5	0.0000	0.0000	103
0	338.4	0.000	0.0	102.3	0.0	122.2	0.0000	0.0000	105
23	345.0	0.060	52.4	49.9	9.5	122.2	0.0000	0.0000	
PILE TOE		0.110	49.9		3.08				

RESISTANCE			CASE DAMPING		SMITH DAMPING		QUAKES	
SKIN KIPS	TOE KIPS	TOTAL KIPS	SKIN	TOE	SKIN 1/FT/S	TOE 1/FT/S	SKIN IN	TOE IN
550.1	49.9	600.0	0.648	0.020	0.181	0.061	0.060	0.110
UNLOADING QUAKES IN PERCENT:							25	100

UNLOADING TO - 0.00 OF SU, ALPHA = 1.00

ENERGY			FORCES				DISPLACEMENTS		
MAX	FIN	MAX	I	TMAX	MIN	I	TMIN	TOP	TOE
FT-KIPS	FT-KIPS	KIPS		MS	KIPS		MS	IN	IN
18.0	17.4	1001	5	22.	-212	1	64.	0.375	0.192

TIME INCR (MS) = 0.195

INT. PILE DAMPING (%) = 3.7
PILE DYNAMICS, INC.

WD 58A, TP3, BOR

BLOW NO. 4

ND 58A, TP3, BUR			FORCES IN PILE									
TIME	FM	F/VC,	10	21	31	42	52	63	73	84	94	104
MS	KIPS		KIPS	KIPS	KIPS	KIPS	KIPS	KIPS	KIPS	KIPS	KIPS	KIPS
10.6	-2.	-1.	-2.	-2.	-2.	-2.	-2.	-2.	-2.	-2.	-2.	-2.
11.5	2.	4.	-2.	-2.	-2.	-2.	-2.	-2.	-2.	-2.	-2.	-2.
12.5	5.	7.	-1.	-2.	-2.	-2.	-2.	-2.	-2.	-2.	-2.	-2.
13.5	6.	5.	4.	-2.	-2.	-2.	-2.	-2.	-2.	-2.	-2.	-2.
14.5	6.	9.	8.	-2.	-2.	-2.	-2.	-2.	-2.	-2.	-2.	-2.
15.4	16.	17.	6.	1.	-2.	-2.	-2.	-2.	-2.	-2.	-2.	-2.
16.4	15.	19.	9.	7.	-2.	-2.	-2.	-2.	-2.	-2.	-2.	-2.
17.4	20.	31.	17.	9.	0.	-2.	-2.	-2.	-2.	-2.	-2.	-2.
18.4	29.	38.	19.	8.	7.	-2.	-2.	-2.	-2.	-2.	-2.	-2.
19.4	171.	94.	31.	14.	9.	-1.	-2.	-2.	-2.	-2.	-2.	-2.
20.3	722.	650.	37.	17.	8.	6.	-2.	-2.	-2.	-2.	-2.	-2.
21.3	1008.	963.	84.	28.	15.	8.	-1.	-2.	-2.	-2.	-2.	-2.
22.3	773.	723.	681.	30.	17.	6.	5.	-2.	-2.	-2.	-2.	-2.
23.3	601.	534.	974.	42.	27.	14.	8.	-1.	-2.	-2.	-2.	-2.
24.2	423.	365.	727.	580.	29.	18.	5.	3.	-2.	-2.	-2.	-2.
25.2	439.	373.	527.	867.	42.	23.	12.	7.	-1.	-2.	-2.	-2.
26.2	267.	248.	359.	803.	527.	27.	16.	5.	2.	-2.	-2.	-2.
27.2	289.	301.	358.	613.	839.	39.	19.	9.	6.	-2.	-2.	-2.
28.2	226.	206.	246.	432.	836.	324.	24.	14.	5.	0.	-2.	-2.
29.1	99.	97.	300.	334.	643.	746.	34.	16.	7.	5.	-2.	-2.
30.1	144.	94.	196.	278.	464.	940.	271.	24.	12.	5.	-0.	-2.
31.1	128.	81.	96.	289.	352.	729.	703.	30.	14.	5.	3.	-2.
32.1	134.	102.	85.	191.	321.	546.	888.	116.	21.	10.	3.	-1.
33.0	94.	51.	94.	144.	314.	386.	660.	584.	26.	11.	2.	0.
34.0	51.	54.	109.	98.	232.	373.	478.	840.	91.	17.	5.	-1.
35.0	37.	-5.	70.	162.	202.	274.	320.	689.	522.	19.	4.	0.
36.0	96.	47.	81.	137.	125.	247.	342.	509.	764.	38.	7.	2.
36.9	80.	32.	25.	130.	164.	210.	260.	350.	664.	393.	10.	1.
37.9	51.	40.	80.	116.	124.	135.	249.	343.	507.	639.	21.	4.
38.9	45.	38.	76.	43.	113.	185.	198.	280.	360.	653.	294.	3.
39.9	70.	10.	74.	69.	120.	146.	123.	307.	337.	503.	481.	11.
40.9	129.	49.	45.	64.	78.	148.	184.	245.	285.	364.	496.	150.
41.8	102.	35.	4.	73.	105.	137.	161.	177.	305.	293.	358.	136.
42.8	9.	1.	28.	74.	99.	130.	174.	190.	245.	265.	164.	123.
43.8	-75.	-26.	35.	74.	101.	123.	159.	203.	188.	254.	-86.	90.
44.8	-68.	-20.	22.	57.	111.	149.	155.	208.	192.	147.	-124.	75.
45.7	48.	20.	14.	84.	118.	134.	146.	188.	208.	-50.	-62.	85.
46.7	47.	49.	14.	53.	96.	142.	179.	184.	174.	-83.	-4.	75.
47.7	22.	18.	48.	54.	119.	147.	163.	144.	1.	41.	48.	78.
48.7	39.	39.	81.	52.	78.	113.	163.	151.	-38.	115.	41.	32.
49.7	-2.	53.	56.	74.	73.	140.	157.	-4.	-21.	153.	109.	25.
50.6	40.	60.	79.	108.	74.	103.	99.	-50.	104.	113.	69.	34.
51.6	102.	80.	90.	75.	92.	87.	14.	-9.	147.	84.	74.	49.
52.6	81.	68.	87.	100.	124.	58.	-105.	48.	127.	79.	88.	33.
53.6	57.	50.	98.	105.	86.	-29.	-94.	101.	92.	85.	39.	32.
54.5	84.	65.	93.	108.	85.	-96.	-16.	89.	41.	84.	42.	40.
55.5	99.	94.	71.	108.	28.	-89.	54.	39.	37.	49.	45.	28.
56.5	117.	130.	82.	94.	-92.	-13.	95.	8.	43.	19.	42.	45.
57.5	154.	150.	108.	9.	-95.	60.	43.	-1.	10.	-2.	33.	33.
58.5	129.	123.	125.	-122.	-25.	87.	18.	21.	-33.	16.	29.	36.
59.4	82.	93.	110.	-97.	21.	42.	12.	23.	-34.	-14.	-9.	35.
60.4	11.	66.	-40.	-13.	48.	30.	22.	-37.	-17.	-17.	15.	30.
61.4	-36.	-6.	-118.	89.	52.	-15.	19.	-21.	-5.	-41.	-4.	26.
62.4	-129.	-148.	-85.	112.	50.	-26.	-17.	-14.	-26.	-23.	-8.	33.
63.3	-188.	-219.	-37.	46.	53.	9.	-45.	-21.	-28.	1.	-3.	18.
64.3	-83.	-136.	-20.	12.	43.	-9.	-60.	-13.	-19.	-20.	1.	20.
65.3	21.	65.	-54.	-35.	11.	11.	-28.	-39.	-17.	-4.	21.	17.
66.3	25.	160.	-54.	-70.	-29.	15.	-9.	-60.	-12.	1.	13.	20.
67.3	29.	159.	61.	-98.	-70.	-14.	9.	-41.	-18.	1.	19.	23.
68.2	22.	98.	103.	-128.	-105.	-32.	8.	-15.	-33.	11.	22.	17.
69.2	-8.	56.	108.	-15.	-133.	-57.	-16.	10.	-31.	11.	11.	17.
70.2	46.	33.	66.	54.	-147.	-103.	-32.	34.	5.	-14.	5.	17.
71.2	38.	30.	11.	75.	-21.	-133.	-49.	5.	26.	-29.	5.	17.
72.1	17.	-21.	-7.	49.	42.	-156.	-75.	-11.	44.	-22.	5.	17.
73.1	-38.	-73.	-5.	21.	66.	-60.	-113.	-23.	17.	-22.	5.	17.
74.1	-84.	-93.	-46.	-16.	46.	52.	-132.	-54.	-9.	-22.	5.	17.
75.1	-53.	-86.	-72.	-11.	20.	80.	-43.	-92.	-9.	-22.	5.	17.
76.0	-35.	-73.	-99.	-36.	4.	72.	64.	-114.	-9.	-22.	5.	17.
77.0	-1.	-70.	-97.	-71.	5.	52.	88.	-114.	-9.	-22.	5.	17.
78.0	-31.	-75.	-80.	-80.	-17.	29.	70.	-114.	-9.	-22.	5.	17.
79.0	-72.	-71.	-73.	-80.	-46.	11.	70.	-114.	-9.	-22.	5.	17.
80.0	-86.	-73.	-66.	-66.	-58.	-5.	70.	-114.	-9.	-22.	5.	17.
80.9	-77.	-57.	-50.	-47.	-68.	-5.	70.	-114.	-9.	-22.	5.	17.
81.9	-62.	-40.	-59.	-45.	-69.	-5.	70.	-114.	-9.	-22.	5.	17.
82.9	-33.	-29.	-36.	-38.	-69.	-5.	70.	-114.	-9.	-22.	5.	17.
83.9	-35.	-17.	-56.	-69.	-69.	-5.	70.	-114.	-9.	-22.	5.	17.
84.8	-54.	3.	-16.	-56.	-69.	-5.	70.	-114.	-9.	-22.	5.	17.
85.8	-23.	15.	-12.	-56.	-69.	-5.	70.	-114.	-9.	-22.	5.	17.
86.8	-27.	34.	-12.	-56.	-69.	-5.	70.	-114.	-9.	-22.	5.	17.
MIN	-195.	-225.	-118.	-131.	-154.	-156.	-132.	-114.	-47.	-89.	-131.	-2.
MAX	1008.	974.	996.	983.	968.	970.	902.	846.	784.	713.	533.	157.

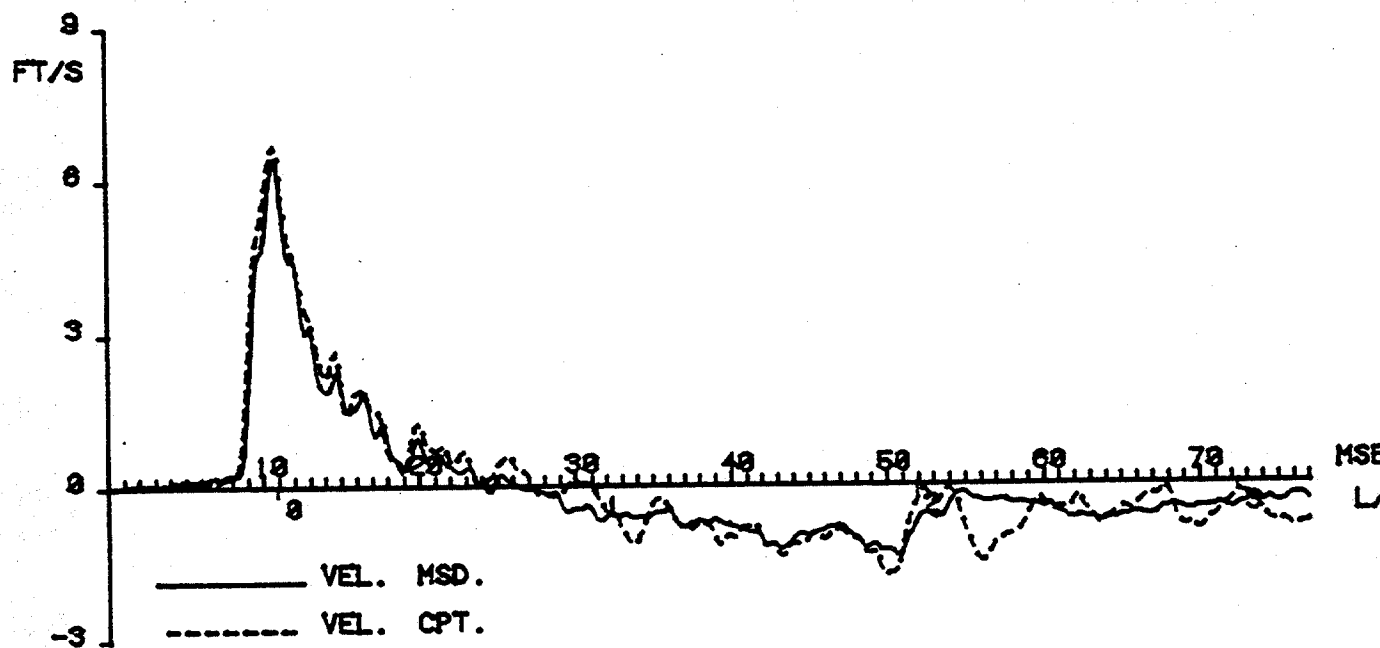
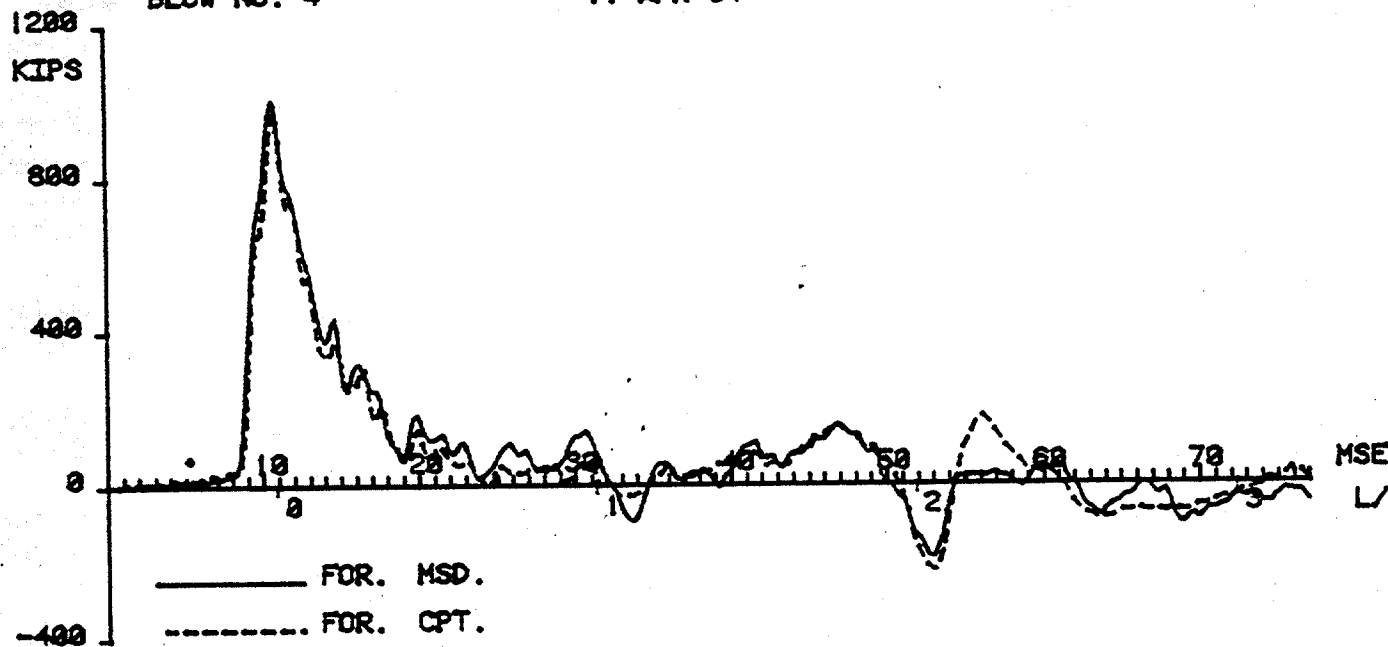
WD 58A, TP3, BOR
BLOW NO. 4

STATIC ANALYSIS

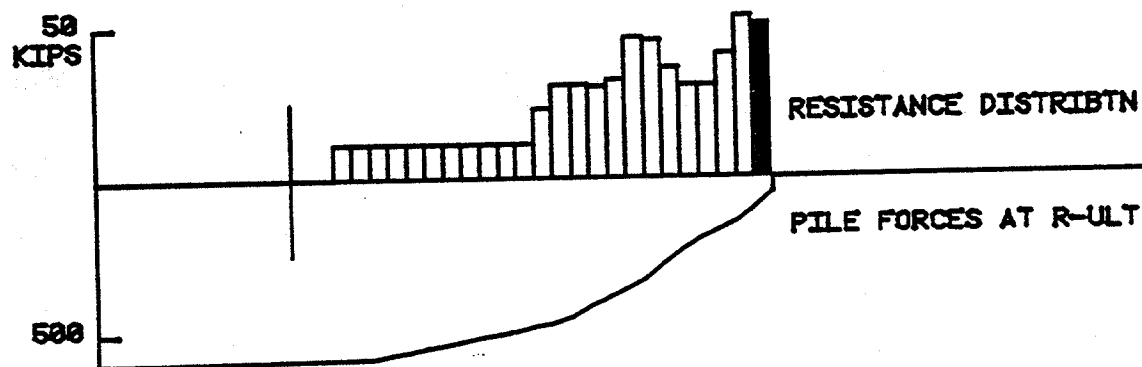
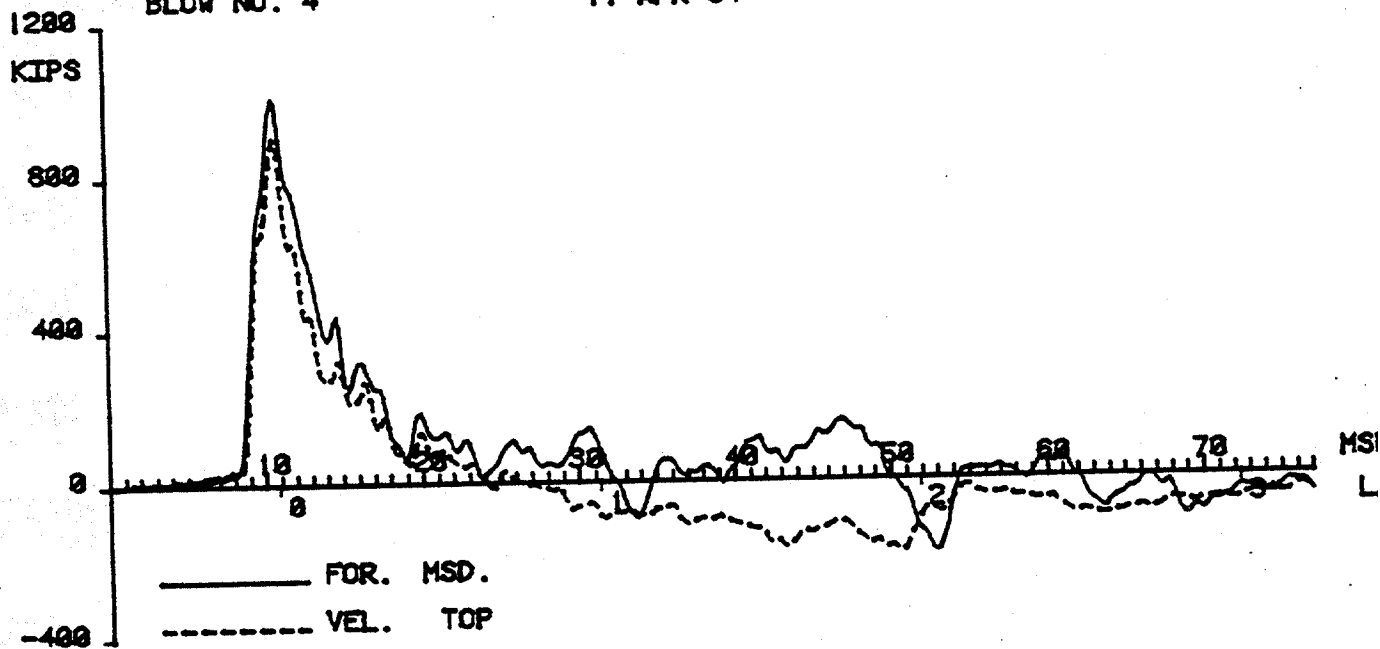
QAD(IN)= 0.000, EFAC= 1.000, CUT(FT)= 0.0

I	LOAD KIPS	SET IN	BOT. LOAD KIPS
1	0.0	0.000	0.0
2	32.4	0.033	0.4
3	53.9	0.054	0.7
4	75.5	0.076	1.0
5	107.9	0.109	1.4
6	129.4	0.131	1.7
7	159.1	0.162	2.2
8	176.3	0.181	2.5
9	206.0	0.216	3.0
10	225.4	0.240	3.5
11	254.5	0.277	4.2
12	275.6	0.305	4.8
13	300.3	0.338	5.5
14	328.1	0.375	6.4
15	352.9	0.410	7.2
16	375.1	0.442	8.1
17	401.6	0.480	9.2
18	425.2	0.515	10.4
19	451.2	0.555	11.8
20	475.8	0.594	13.4
21	500.2	0.634	15.3
22	525.2	0.677	17.8
23	550.2	0.723	21.1
24	575.1	0.774	26.4
25	600.0	0.865	49.9

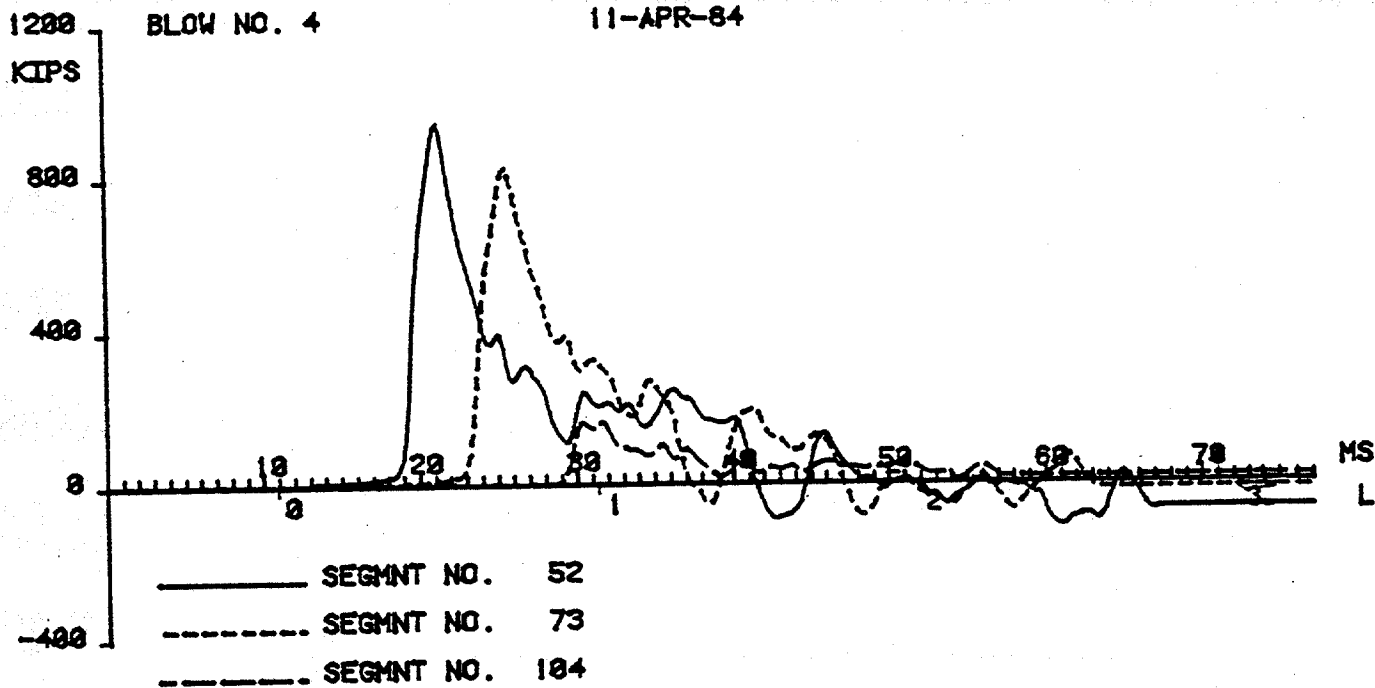
G & A PROGRAMS: CAPWAP/C RESULTS
WD 58A, TP3, BOR
BLOW NO. 4 11-APR-84



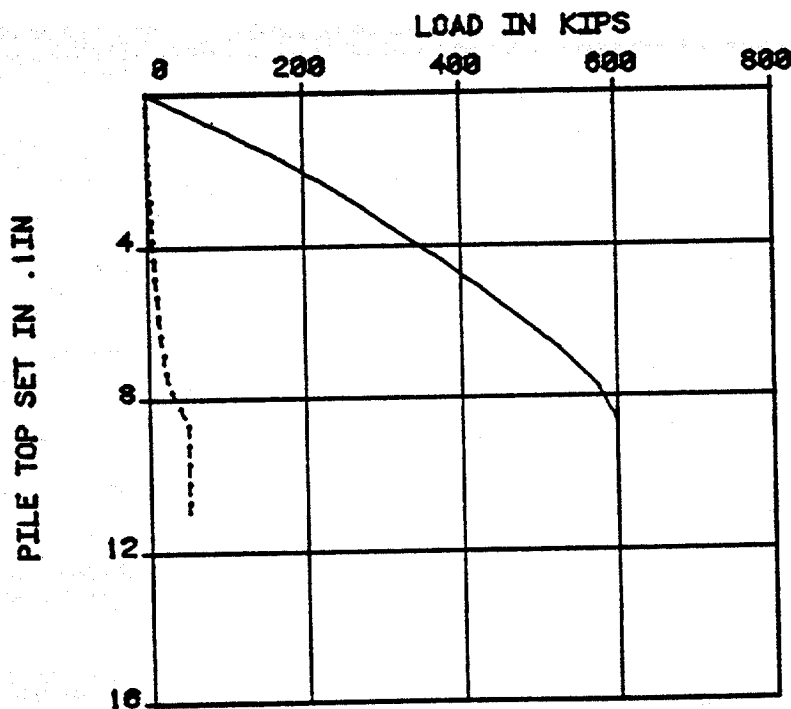
G & A PROGRAMS: CAPWAP/C RESULTS
 WD 58A, TP3, BOR
 BLOW NO. 4 11-APR-84



G & A PROGRAMS: CAPWAP/C RESULTS
 WD 58A, TP3, BOR
 BLOW NO. 4 11-APR-84



STATIC CAPWAP/C RESULTS
 WD 58A, TP3, BOR
 BLOW NO. 4
 ——— TOP LOAD - - - - - BOTTOM LOAD



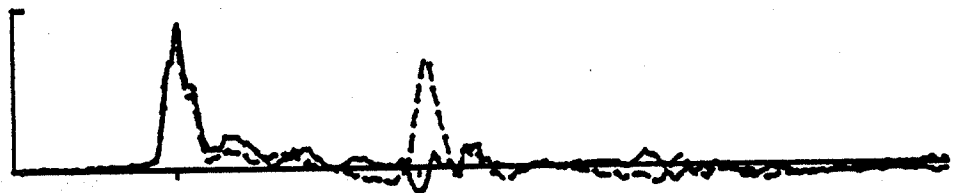
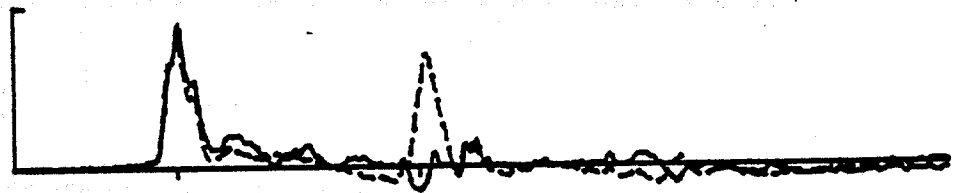
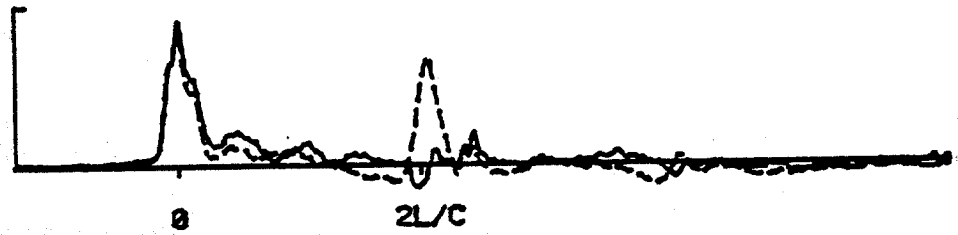
APPENDIX C

PLOTS OF FORCE (SOLID) AND VELOCITY (DASHED)
FROM PROCESSING/DIGITIZING

WD 58A, TP2, EOD

20 MS

57FS.1
828KIPS



-C1-

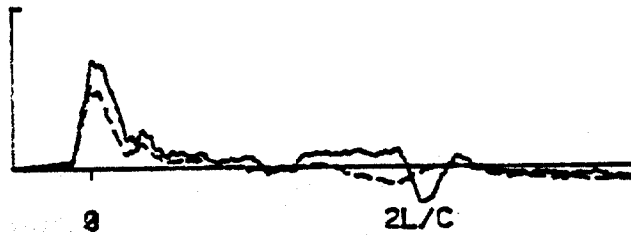
PILE DYNAMICS, INC.

ND 58A, TP3, BOD WITH 2 DAY WAIT

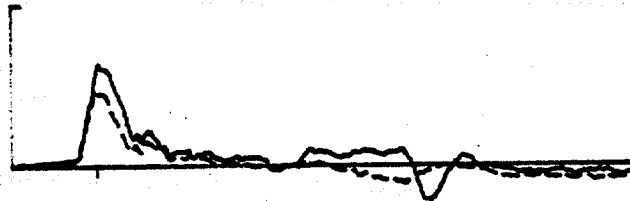
20 MS

57FS.1
800KIPS

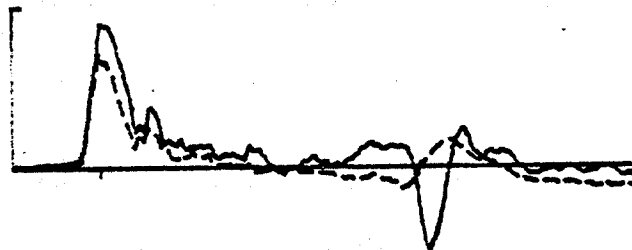
1 HS 1



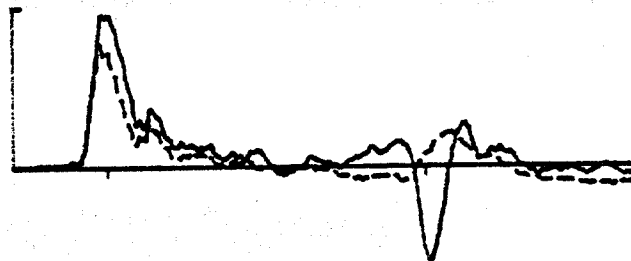
2



3 HS 2



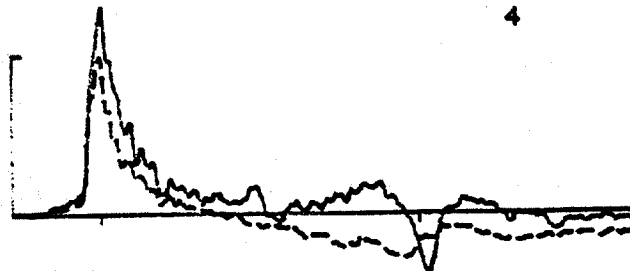
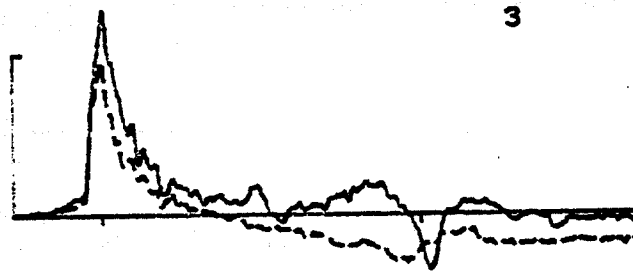
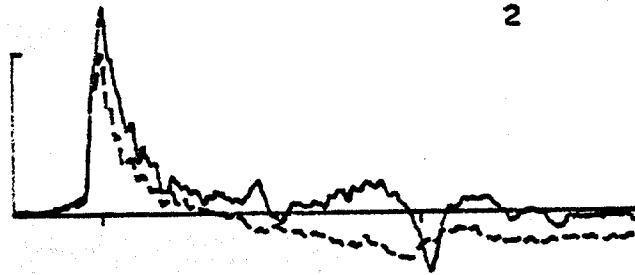
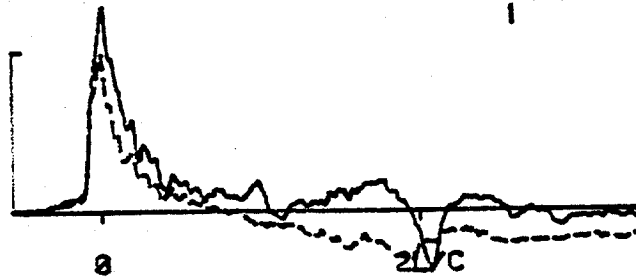
4



NO 58A, TP3, EOD

20 MS

57FS.1
800KIPS



ND 58A, TP3, BCR

20 MS

57FS.1
800KIPS

